Role of electrical synapses in information processing within a canonical feed-forward microcircuit

Andréas Hoehne

SORBONNE UNIVERSITÉ

Ecole doctorale "Cerveau, Cognition, Comportement"

Laboratoire "Gènes, Synapses et Cognition", CNRS UMR-3571

Equipe "Unité d'Imagerie Dynamique du Neurone", Institut Pasteur

Role of electrical synapses in information processing within a canonical feed-forward microcircuit

Thèse de doctorat en neurosciences par Andréas HOEHNE,

Dirigée et encadrée par David DIGREGORIO,

Soutenue publiquement le 25 Septembre 2019, devant le jury composé de:

Dr. Ann LOHOF	Examinatrice et présidente du jury
Dr. Marlene BARTOS	Examinatrice
Dr. Angus SILVER	Rapporteur
Dr. Andreas FRICK	Rapporteur
Dr. David DIGREGORIO	Directeur de thèse

Table of contents

Preface:

The brain is composed of electrically excitable cells, called neurons, which communicate with each other at specialized points of contacts, called synapses. They organize into circuits which mediate specific functional operations. By studying gene expression, neuronal development, synapse formation and plasticity, and transmission of signals between and within neurons, neurophysiologists aim to unravel these operations, to understand how they ultimately guide behaviour. At the single cell level, excitatory and inhibitory synaptic potentials combine in time and space to determine whether or not an Action Potential (AP) - the hallmark electrical signal of neurons - will be emitted, and further relay information to downstream neurons. Therefore, describing how neurons are connected to each other, and whether these connections convey excitation or inhibition is of critical importance to understand circuits' computation.

GABAergic inhibitory interneurons are frequently interconnected by electrical synapses, and form cell-type specific networks controlling the excitability of principal cells. Electrical synapses help in synchronizing interneurons activity, by equalizing membrane potentials of connected cells, and enabling spikelet transmission (*i.e.*, filtered version of presynaptic AP). Additionally, being opened at rest, they fundamentally alter the passive properties of the cells in which they are expressed. Their role in neural circuits is therefore far from being clear.

In this thesis, I propose that spikelet transmission in cerebellar basket cells (inhibitory interneurons of the cerebellar cortex) mediate a form of Feed-Forward Inhibition (FFI), albeit with a short-lasting excitation prior to inhibition onset, which results in temporal contrast enhancement and coincidence detection mechanisms.

Chapter I is the introduction of my thesis, where I will summarize the current state of the knowledge regarding biophysical properties of electrical signalling in neurons, as well as synaptic transmission, with a particular focus on electrical synapses and dendritic integration. I will also describe the cerebellum, and more specifically the cerebellar cortex, with a particular focus on basket cells. Chapter II will describe the methods I employed during my PhD, namely whole-cell patch-clamp electrophysiology *in vitro*, and 2-photon laser scanning microscopy. Chapter III is the draft of a manuscript describing the prevalence, biophysical determinants and the functional implication of spikelet transmission between cerebellar basket cells. Chapter IV is a summary of preliminary data concerning neuronal communication through electrical synapses in general, and further details concerning spikelet signalling. Chapter V is a summary of preliminary morphological and electrophysiological data suggesting that somatic-targeting basket cells and dendritic-targeting stellate cells have different dendritic integration of their common excitatory inputs, the parallel fibers.

Chapter I - Introduction:

My PhD thesis has mainly consisted in examining the role of electrical synapses in dendritic integration properties of cerebellar basket cells. Therefore, in this introduction, I would like to first summarize how neurons were historically identified as independent nerve cells, endowed with ions channels rendering them electrically excitable and able to generate action potentials, and communicating with each other at specialized points of contacts called synapses. Then, I will describe how chemical transmission was long thought to be the exclusive and only meaningful form of neuronal communication in mammals, to later introduce synaptic communication through electrical synapses. I will present how both modes of communication differ, and emphasize the most documented physiological roles of electrical synapses.

I will then describe cases of interactions between chemical and electrical inputs, and how electrical synapses can shape the dendritic integration properties of single neurons. There, I will present general features of dendritic integration properties in neurons, and how they depend on passive and active properties of individual cell types, and further describe documented cases of the unique impact of electrical synapses on dendritic integration properties. Indeed, electrical synapses are simultaneously a source of current inputs (*i.e.*, synapses), and able to shape the electrotonic structure of neurons (*i.e.*, influence dendritic integration properties).

Finally, I will present the cerebellar cortex, the model microcircuit in which cerebellar basket cells are found. I will describe its architecture and proposed functional role in sensory-motor coordination. In order to present how the cell-type diversity and connectivity combine to perform specific circuit operations, I will briefly describe cerebellum-like structures, in which non-motor roles have been described, and cease this opportunity to suggest what may be a unifying cerebellar computation. As I will summarize, the role of cerebellum in motor control has been largely documented for decades, but despite a wealth of anatomical and functional evidence that it receives connections from many non-motor areas of the brain, only recently have theories been proposed for a unifying cerebellar computations, beyond sensorimotor control.

I) Neurons as individual, electrically excitable, nerve cells, communicating through synapses:

I - 1) Historical overview of the neuron hypothesis:

Until the end of the 19th century, most physiologists thought that the nervous system was a continuous tissue, and not a network of connected cells, as we know nowadays. The reticular theory, as it was called, declined progressively between 1870s and 1890s, and the neuron theory (that is, the theory according to which the brain is made of individual cells - called neurons - connected to each other) emerged gradually. This was mostly due to the discovery of a novel technique at that time - called Golgi staining, or Golgi method - which allowed a random and relatively sparse staining of brain preparation, by a chemical reaction between potassium dichromate and silver nitrate. The crystals of silver chromate were opaque to light, and thus allowed to observe discrete cells (sometimes including their dendritic and axonal processes) under a light microscope. Using this method, numerous physiologists reported observations of individual cells in brain tissues, and the most notable ones are Camillo Golgi and Ramon y Cajal. Interestingly, the two scientists drew opposite conclusions from their observations: Camillo Golgi reported a continuous network (in support of the reticular theory), but Ramon y Cajal described individual cells (in support of the neuron theory). They were finally jointly awarded the Nobel Prize of Physiology and medicine in 1906, in recognition of their work concerning the structure of the nervous system, but a long-lasting dispute kept opposing them for many years.

Nowadays, it is clearly established that individual nerve cells do exist, and the reticular theory has been falsified. Only the discovery of direct electrical communication in the second half of the 20th century (which I will describe later) has been used to reinstate the reticular theory, but since this mode of communication between nerve cells was not observed in most instances, the "neuron doctrine" is not debated any longer. Knowledge about the physiology of neurons has been impressively refined during the 20th century. From a histological point of view, we now know that neurons possess not only a cell body, but also neurites (*i.e.*, extensions of the cell membrane) which can be classified in two general categories: dendrites, where most synaptic inputs are received; and axons, where output electrical signals are sent to downstream neurons. A large variety of neuronal morphology has been described, ranging from "adendritic" dorsal root ganglion cells to "fan radiation" Purkinje cells (Stuart, Spruston and Häusser, 2008). We also know that brain circuits are composed of large principal cells, with very long dendrites,

small local interneurons with short neurites, and even relay neurons whose somata are small, but their axons can be up to one meter-long.

Therefore, the brain is not only made of individual nerve cells, but these cells display an extraordinary diversity of morphologies. As suggested by the famous quote from Francis Crick, "If you want to understand function, study structure", diversity of morphology of the dendritic trees and axonal projections of neurons are thought to be of key importance in understanding how information is processed by neurons and neural circuits. I will come back to this point, and in particular the role of the morphology of dendrites in dendritic integration properties, in a later section of this introduction.

I - 2) Electrical excitability, and action potential generation:

Neurons, as we know now, are electrically excitable cells, communicating with each other (or with other cells) by points of contact called synapses. Classically, neurons are composed of a soma (also called cell-body), a dendritic arbour - where most synaptic inputs are received - and an axon - the structure along which output electrical signals are sent out to downstream neurons. A significant part of the information *within* neurons is carried by electrical currents originating from synaptic contacts, which propagate along the dendritic branches down to the cell-body where they are integrated. If these electrical currents (unitary or compound) are sufficiently high in amplitude, they depolarize the cell-body and the Axon Initial Segment (AIS) above a threshold value, giving birth to an all-or-none event called Action Potential (AP), the hallmark electrical signal of nerve cells required for chemical communication. APs are high amplitude, short-lasting depolarizing electrical signals, usually followed by a lower amplitude and longer-lasting hyperpolarizing signal called After Hyperpolarisation (AHP).

The precise nature of this key electrical signal, and its relationship with ionic gradients (notably sodium and potassium) across the cell's membrane, was established in (Hodgkin and Huxley, 1952). Along with John Eccles, they received the Nobel Prize in Physiology and Medicine in 1963 for their discovery. Their work notably revealed that the initial depolarizing peak of APs was mediated by sodium ions, and that the AHP was mostly mediated by potassium ions. The mathematical models they proposed to explain AP generation and waveform were based on the hypothesis that "ion channels" should be present inside the membrane of nerve cells (1); that each type of channel would be differentially permeable to each ion species (2); and that the gating properties (closed or opened) of these channels depend on the voltage difference across the cell's membrane (3).

It was between the 1970s and 1980s that the demonstration of the ion channels was established, when Erwin Neher and Bert Sakmann developed the patch-clamp technique (Neher and Sakmann, 1976), which allowed the resolution of ionic currents caused by single channels. Their electrical recordings confirmed that the amplitude of these currents depended on the ionic gradients on either side of the membrane (1); that single channels could be in different states (closed, opened, inactivated, ... - 2); and that the likelihood of observing a given state depended on the voltage across the membrane of the cell (3). For their discovery, they received the Nobel Prize in Physiology and Medicine in 1991.

Therefore, neurons are discrete cells displaying a remarkable diversity of morphologies, and they all share the fundamental property to be electrically excitable and generate action potentials. This remarkable electrical phenomenon is necessary for most cases of synaptic communication, and thus for processing of information in forms of electrical signals.

I - 3) Historical overview on the mode of communication between neurons:

Most of the uncited references in the following section are reported in (Cowan *et al.*, 2001).

The demonstration that neurons were individual, excitable cells, naturally raised the question as to how they would be able to share "electrical information" with each other. Synapses are, nowadays, defined as "specialized junctions at which a neuron communicates with a target cell" (from the Medical Subject Headings - MeSH). But such a definition as a long history, like all definitions of terms we think of on a daily basis without really wondering what their definition may be. The meaning of some words just appears so obvious that a definition would seem pointless. But it appears, more often than not, that most of the words *do have* a definition which does not necessarily relate to the *exact* idea one has in mind. Such used to be the case for "synapse", at a time where synaptic transmission was thought to be purely and exclusively mediated by what we name nowadays "chemical synapses". In the next paragraph, I briefly review the long-lasting debate about how neurons communicate with each other.

In 1897, before the acceptance of the neuron doctrine by the scientific community, Sir Charles Scott Sherrington proposed the word "synapse" to name the points of contact between (putative) individual neurons. Sherrington was lead to coin the term "synapse" after having met Cajal, who had already collected sufficient histological evidence that nerve cells were individual cells. Two different (although non-exclusive) hypotheses were proposed for synaptic transmission: "synaptic transmission is electrical" or "synaptic transmission is chemical". It was

during the 20th century that improvement in recording apparatus, and preparation of brain tissues, combined together to resolve this conundrum.

Back in the 18th century, works from Luigi Galvani (Galvani, 1791) and Alessandro Volta (Volta, 1792) had revealed that organic tissues could not only behave as conductors (*i.e.*, currents injected at one point can spread to another point, at least partly), but also *react* to electrical impulses (*e.g.*, with high current loads, muscle cells contract), suggesting that electrical communication was a plausible phenomenon. However, owing to the lack of the neuron theory, it was not possible to make any claim at that time about electrical communication as a mean for two *separate neurons* to communicate. In the second part of the 19th century, Carl Friedrich Wilhelm Ludwig developed techniques to study isolated organs, which required an appropriate medium to survive for a time; later, Sidney Ringer improved these "perfusion" techniques by testing new compounds in the solution. He notably found that an isolated heart would beat at different frequencies, depending on the content of the perfusion solution. This observation suggested that chemical agents (ions, molecules, or proteins) in the bathing solution could alter the rhythmic beating (*i.e.*, an electrical response) of the heart. These observations were fully consistent with Nernst equation (developed in 1897), which gave the relationship between the ionic flux and gradient across a biological membrane. In the meantime, Claude Bernard had observed that in a nerve-muscle preparation, electrical impulse to the nerve could force the muscle to contract, but this response was abolished in presence of curare (a poison). The muscle, however, could still be forced to contract by direct electrical stimulation. Synaptic transmission (from nerve to muscle, at least), could therefore be impaired by a chemical agent (curare). Earlier experiments from Langley published in 1905 had already revealed that chemical agents (such as curare, nicotine or atropine) could alter the excitability of neurons and/or muscles.

It was in 1921 that Otto Loewi published the results of a historical experiment. He prepared two isolated frog hearts in a similar Ringer solution, one with its afferent nerve (the vagus nerve); and the other one without. Each heart was put into a different recipient, containing the same Ringer solution. He first stimulated the vagus nerve in the first preparation, and observed a decrease in the frequency of beating of the heart. He then replaced the first heart with the second one, and observed that the second heart, in the first Ringer solution, would also beat more slowly. He therefore concluded that a chemical substance, released by the vagus nerve in the first preparation, had remained in the Ringer solution. This experiment was key in testing the hypotheses of "chemical versus electrical communication", as it demonstrated an effect of a chemical agent (undefined, but present in the bathing solution) on the rhythmic

beating of the heart, in *absence* of electrical stimulation. Otto Loewi and Henry Dale were awarded the Nobel Prize in Physiology and Medicine in 1936 "for their discoveries relating to chemical transmission of nerve impulses".

Later on, in the middle of the 20th century, Bernard Katz (along with John Eccles) established that between motor neurons and muscles, a very specific molecule (called acetylcholine) was required for the proper transmission of an electrical impulse in the motor neuron to a contraction of the muscle. Along with Ulf van Euler and Julius Axelrod, they were awarded the Nobel Prize of Physiology and Medicine in 1970 for their discoveries concerning "the humoral transmitters in the nerve terminals and the mechanism for their storage, release and inactivation". Of note, works from J. del Castillo and Bernard Katz (del Castillo and Katz, 1954) revealed that neurotransmitter release is *quantal* (*i.e.*, chemical signals can be released from a presynaptic element by packets, and any recorded post-synaptic current caused by this release is an integral number of the smallest one). During the early 50s, John Eccles (a student of Sherrington, and one of Katz's main collaborator), who had long been in favour of electrical communication, observed Inhibitory Post-Synaptic Potentials (IPSPs) in motoneurons (Brock *et al*., 1952). He reckoned that electrical communication would have been unable to display such hyperpolarizing responses, and thus admitted that if inhibition could be explained by chemical transmission, then by analogy, excitation should also be explainable by chemical transmission (even though different molecules would likely be involved in each instance).

Nowadays, our knowledge about chemical synaptic transmission has increased extensively. We now know that neurotransmitters (the chemical signals) are filled in synaptic vesicles (usually found in axon terminals), and that presynaptic APs trigger a cascade of events causing the opening of calcium channels, diffusion of calcium to the release machinery, fusion of docked vesicles, and release of neurotransmitters in the synaptic cleft. These signalling molecules diffuse rapidly in this restricted space, and rapidly bind to post-synaptic receptors to trigger their opening. During the open time of the receptors, a passive flow of ions between the extra- and intra-cellular spaces causes a current entry in the post-synaptic neuron, of positive (inhibitory) or negative (excitatory) polarity, depending on the type of receptors opened and their ionic selectivity. Neurotransmitters are very diverse, and can be classified in different groups, such as amino acids (L-glutamate, D-serine) monoamines (Dopamine, Serotonin) or peptides (somatostatin, oxytocin). Further details about chemical synaptic transmission will be provided in the next section, for a comparison with electrical synaptic transmission.

II) Electrical synaptic communication:

II - 1) History of electrical communication:

Paul Fatt (who had mainly worked on chemical communication), wisely recognized that the hypothesis of electrical communication had not been disproved by the works conducted up to the years 1950s. According to him, it was totally possible to observe an electrical (*i.e.*, "NOT chemical") form of communication between neurons. It *simply* remained to be demonstrated.

II - 1 - a) Historical experiment revealing electrical coupling:

Between the years 1957 and 1959, Edwin Furshpan and David Potter observed three phenomena of synaptic transmission between the giant axon and the motor axon of the crayfish nerve cord that could not be accounted for by the hypothesis of chemical transmission: post-synaptic responses and pre-synaptic impulses appeared concomitant (*e.g.*, no delay in synaptic transmission), albeit with different rates of rise (1); subthreshold events in the pre-synaptic element could be passed to the post-synaptic one, in a graded manner (2); and communication at this synapse was systematically bidirectional, albeit stronger in one direction than the other depending on the polarity of the input signal (3) - Figure I-1, from Furshpan and Potter, 1959).

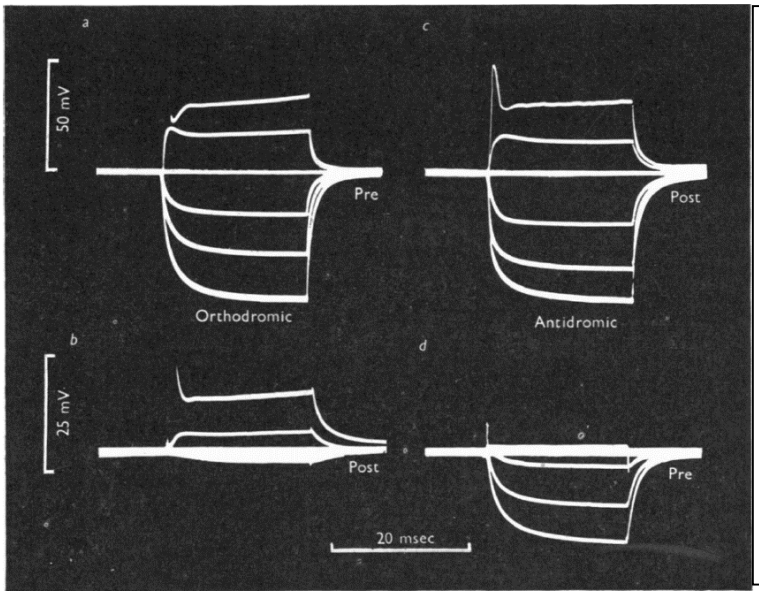

Figure I - 1: Ortho- and anti-dromic communication between the giant axon (Pre) and the motor axon (Post) of the crayfish nerve cord:

Currents are injected either in the pre-synaptic element **(top left)**, or the post-synaptic one **(top right)**, and corresponding membrane potentials are recorded in the post-synaptic **(bottom left)** and pre-synaptic element **(bottom right)**, respectively.

From Furshpan and Potter, 1959

Later on, during the 1960s, Bennett confirmed that in most cases, electrical synapses could pass current in either direction, sometimes associated with a *rectification* - a differential ability to transmit current in one direction or the other. He also found the structural correlates of these "electrotonic coupling" (one of the early names of electrical synapses) using light and electron microscopy in the spinal electromotor neurons of the mormyrid fish (Bennett *et al.*, 1967).

II - 1 - b) Slow acceptance of electrical coupling by the scientific community:

It was initially thought that these early observations about electrical communication, albeit novel, could be ignored to some extent, because fish are "lower invertebrates" (a term I wish to write with quotes, since the terminology of "higher" and "lower" is highly anthropomorphic and unwise). Such a result would start to deserve some more attention if it was observed in the brain of "higher vertebrates". It is explicitly reported by Hormudzi *et al.*, 2004 that:

"Electrical communication has been regarded for a long time as a property of the invertebrate brain where faster transmission is needed to accomplish simple, reactive tasks. [...] electrical synaptic transmission - it was argued - would not be well-suited for the more complex integrative processes of higher organisms, which would benefit from the higher diversity and fine-tuning provided by chemical synapses."

With regard to expression of electrical synapses in the CNS of vertebrates, Shepherd (Shepherd, 1994) proposed that their apparent absence in "higher vertebrates" could, I quote:

"... reflect a mechanism to increase the metabolic and functional independence of neurons, in order to permit more complex information processing."

It appears that the debate on the mechanisms of synaptic communication had favoured chemical transmission, simply because it had been demonstrated first (Loewi and Dale received a Nobel prize in 1936 for discovering the existence of chemical substances mediating communication between neurons). It then led the neuroscientific community to investigate and document chemical synapses, which were thought to be "synapses" without the preceding adjective of *chemical*, reflecting the generally accepted idea that all synapses were of chemical nature. And if not *all* synapses, maybe only the *relevant* ones. A historically interesting case is related by Bennett (Bennett, 2000), where he reports the definition of *synapse* in the Medical Subjects Headings (MeSH) of the PubMed data base (in year 2000, I insist):

"SYNAPSES: Specialized junctions at which a neuron communicates with a target cell. At classical synapses, a neuron's presynaptic terminal releases a chemical transmitter

stored in synaptic vesicles which diffuses across a narrow synaptic cleft and activates receptors on the postsynaptic membrane of the target cell. The target may be a dendrite, cell body, or axon of another neuron, or a specialized region of a muscle or secretory cell. Neurons may also communicate through direct electrical connections which are sometimes called electrical synapses; these are not included here but rather in GAP JUNCTIONS."

A careful reader would have noted in this definition that there might exist "non-classical synapses", and that the term "electrical synapses" was, at that time, not generally accepted. The current definition of synapse proposed by the MeSH, added in 2008, is:

"Specialized junctions at which a neuron communicates with a target cell. At classical synapses, a neuron's presynaptic terminal releases a chemical transmitter stored in synaptic vesicles which diffuses across a narrow synaptic cleft and activates receptors on the postsynaptic membrane of the target cell. The target may be a dendrite, cell body, or axon of another neuron, or a specialized region of a muscle or secretory cell. Neurons may also communicate via direct electrical coupling with ELECTRICAL SYNAPSES. Several other non-synaptic chemical or electric signal transmitting processes occur via extracellular mediated interactions"

This definition is not ideal, because it mainly describes features of chemical transmission only (which, again, are described as "classical"); and ends up with a consideration on "non-synaptic signal". Nevertheless, the first sentence does capture common features of synaptic transmission through both chemical and electrical synapses.

The point of these first paragraphs was to indicate that the very concept of "electrical synapse" was not obvious and generally accepted in the neuroscientific community not even twenty years ago. Once again, interesting cases and discussions on that matter are related in Bennett, 2000.

II - 1 - c) Electrical synapses as the molecular basis of electrical coupling:

In Nagy *et al.*, 2018, similar comments as those from Bennett are drawn, but the review then expands onto the reasons of why electrical synapses have gradually started to gather more attention in the last twenty years. The main reasons were the discovery of Cx-36 in 1998 (the first gap junction protein exclusively expressed in neurons - Condorelli *et al.*, 1998); the

generation of Cx-36 $^{-/-}$ genetic lines and revelation of corresponding functional deficits (Frisch *et al.*, 2005); and correlation between dye-coupling, spikelet transmission and long current pulses propagation in paired recordings of neighbouring interneurons expressing Cx-36, which I will comment in more details in the next sections

II - 1 - d) Definition of electrical synapses:

In this thesis, I will use the term electrical synapses to refer to "specialized junctions between neurons which [*directly*] connect the cytoplasm of one neuron to another, allowing a direct passage of an ion current". This is the definition from the MeSH, introduced in 2008, where I only took the liberty to add the term indicated in brackets. The reason for that will be explicitly presented in this thesis, and the reader will be invited to debate on this point. I shall however give a hint about my idea: if three neurons are connected by such synapses in a chain configuration, is there an electrical synapse between the first and the third neuron? Is the neuron in the middle a "specialized junction between the two others, connecting their cytoplasms, and allowing a direct passage of an ion current"? I will later examine, in Chapter III, how this almost trivial nuance may be of key importance in examining the electrical connectivity within a network of interneurons.

II - 2) Molecular composition of electrical synapses, and plasticity:

II - 2 - a) Molecular composition of gap junctions:

Electrical synapses are comprised of gap junction proteins that conduct ions between neurons. Gap junctions are formed by the apposition of two structures called connexons, each from two adjacent cells. Connexons, in turn, are hemichannels made of six connexin proteins. A functional gap junction therefore requires twelve connexin molecules. Twenty-one different connexin genes have been identified so far in the human genome, and twenty in mice (Nagy *et al.*, 2018). Since gap junctions are expressed almost ubiquitously in solid tissues in multicellular organisms, different isoforms can be co-expressed in a given cell-type to form homomeric or heteromeric channels (reviewed in Nielsen *et al.*, 2012). However, in neurons, connexin-36 (Cx36) is the most prevalent one (Nielsen *et al.*, 2012), and is preferentially expressed in population of interneurons rather than principal cells (reviewed in Nagy *et al.*, 2018; see also Mercer *et al.*, 2007 for electrical coupling between hippocampal pyramidal cells, and Apostollides and Trussel, 2013 and 2014 for electrical coupling between interneurons and

principal cells in the dorsal cochlear nucleus). It should be noted, nonetheless, that mRNA expression for Cx45, Cx50 and Cx57 have also been reported in neurons, and that elimination of Cx-36 protein by genetic knock-out is not always sufficient to eliminate electrical coupling between neurons (Curti *et al.*, 2012; Zolnik and Connors, 2016), suggesting that other isoforms of connexins can support electrical transmission in some populations of neurons.

I wish to mention here that molecular layers interneurons (MLIs) of the cerebellar cortex do not form electrical synapses with their closest neighbours in Cx-36$^{-/-}$ mice (Figure I-2, from Alcami and Marty, 2013). This was shown by the inability to observe passive current flow between two neighbouring cells, and suggests that only Cx-36 can form functional electrical synapses, as is the case in Wild-Type (WT) animals. This point is emphasized here because this thesis is about electrical communication between cerebellar basket cells, one of the two types of MLIs.

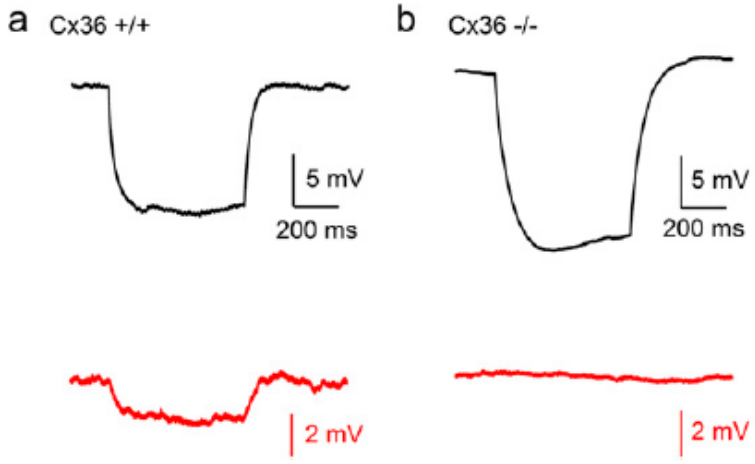

Figure I-2: Connexin-36 is required for functional electrical synapses in Molecular Layer Interneurons in the cerebellar cortex:

a) Paired recordings between neighbouring MLIs reveal direct coupling between an injected neuron (black traces) and its neighbour (red traces) in Wild-Type animals; **b)** No direct coupling is observed in Cx36 $^{-/-}$ animals. Note the differences in membrane polarizations of the injected cell in each condition.

From Alcami and Marty, 2013

II - 2 - b) Plasticity of electrical synapses:

It is generally thought that the brain can store memories by adjusting the weights of synapses between neurons (Hebb, 1949; Kandel and Spencer, 1968; Takeuchi *et al.*, 2014). In contrast, it was initially assumed that electrical synapses were static and rigid, and incapable of undergoing synaptic plasticity in vertebrates. Most of the early evidence on plasticity of electrical synapses came from work at the club endings on the goldfish Mauthner cell, where synaptic communication is enabled by adjacent chemical and electrical synapses (Furshpan, 1964; Lin and Faber, 1988), and electrical synapses are strengthened by glutamatergic transmission from the neighbouring chemical synapses (Pereda and Faber, 1996; Smith and Pereda, 2003), suggesting that electrical synaptic plasticity is supported by chemical transmission, and therefore that electrical synapses are not intrinsically plastic.

However, studies have later shown in vertebrates that electrical synapses are linked to scaffolding proteins (Flores *et al.*, 2008) or plasticity-inducing proteins (such as CaMKII - see Alev *et al.*, 2008), and that the strength of electrical synapses (relating to the number of gap junction channels located in one given plaque, their unitary conductance, and their open probability) can be increased or decreased, depending on: the electrical activity in the two connected cells (Haas *et al.*, 2011; Mathy *et al.*, 2014); metabotropic receptors activation (Landismann and Connors, 2005; Patel *et al.*, 2006; Wang *et al.*, 2015); or NMDA receptors activation (Turecek *et al.*, 2014). Furthermore, intracellular domains of connexin-36 display different phosphorylated states due to synaptically-induced activation of Protein Kinase A, which affect their unitary conductance (Urschel *et al.*, 2006).

Therefore, there is now a large amount of scientific evidence that electrical synapses are also capable of undergoing plasticity as chemical synapses. Consequently, there's no objective reason to disregard the role of electrical synapses in normal physiology of the nervous system in that regard.

II - 3) Structural and functional differences between electrical and chemical synapses:

Chemical and electrical synapses are the most prevalent forms of communication between neurons, in the current state of our knowledge. Other forms of communication, such as ephaptic transmission (Blot and Barbour, 2014), or spillover-mediated volumic transmission (DiGregorio *et al.*, 2002; Szapiro and Barbour, 2007) do exist, but they are quite rare. I wish to compare in this section some of the key aspects in which electrical and chemical synapses differ. My intention is not to describe which of the two is "better" than the other (such terminology can be found in some reviews - see Pereda, 2014), but rather to show, trait by trait, how both types of synapses radically differ in their structure, while still enabling communication between nerve cells (Figure I-3, from Pereda, 2014).

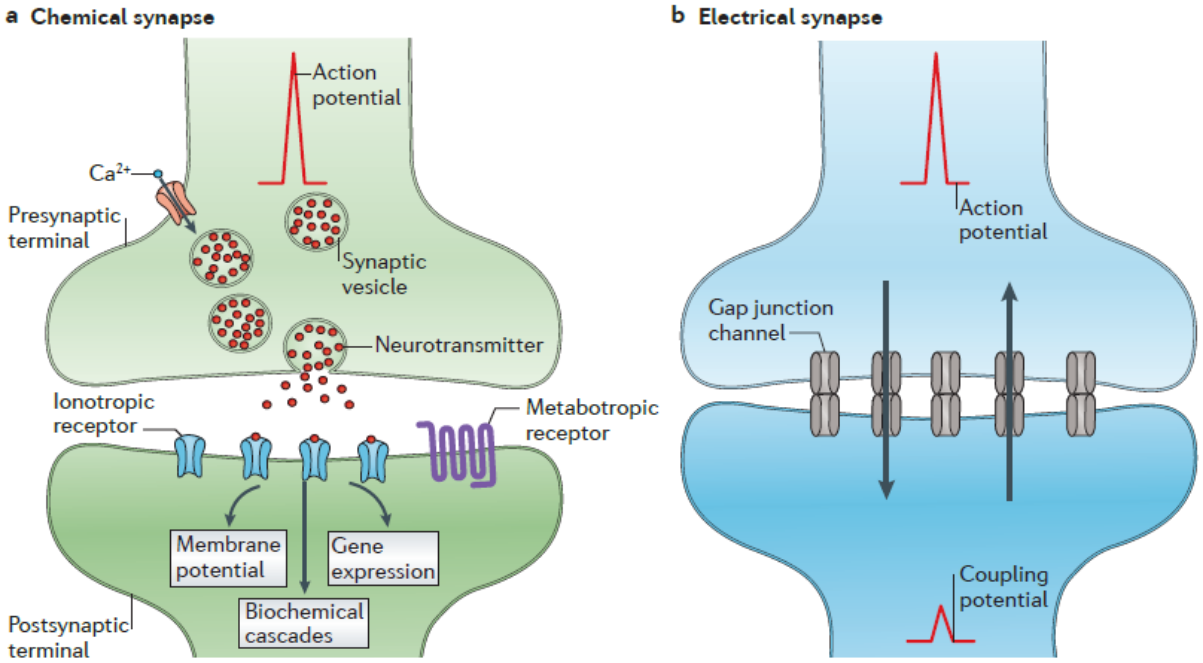

Figure I-3: Structural and functional differences between chemical and electrical synapses:

a) Chemical transmission relies on a Pre-synaptic AP to open Voltage-Gated Calcium Channels (VGCCs). Calcium diffuses in the presynaptic terminal and triggers the fusion of synaptic vesicles with the plasma membrane, which release neurotransmitters in the synaptic cleft. These chemical signals bind to post-synaptic receptors, provoking their opening and (among others things) the passive flow of current between the extra- and intra- cellular spaces. b) Electrical synapses are made of plaques of Gap Junctions (GJs), which allow a direct, passive flow of current between the two connected cells. Note here the absence of pre- and post-synaptic elements, reflecting the notion that electrical synapses are bidirectional.

Adapted from Pereda, 2014

First of all, chemical transmission relies on a very specific **suprathreshold** pre-synaptic signal, the action potential, to bring the presynaptic neuron to a high enough membrane potential, which triggers opening of calcium channels, necessary for the release of synaptic vesicles. These vesicles will then allow the transient opening of post-synaptic receptors. Cx-36 based electrical synapses, on the other hand, are opened at rest, with very little voltage-dependent gating mechanism (supposedly irrelevant in the range of physiological values; Srivinas *et al.*, 1999), and even **subthreshold** currents can cross them (first described in Furshpan and Potter, 1959 for long current pulses; but see Zsiros *et al.*, 2007 for the passive flow of GABAergic IPSCs; and Vervaeke *et al.*, 2012 for the passive flow of AMPAergic EPSCs across electrical synapses). As I will discuss later, this unique property of electrical synapses to be opened at all times can be of critical importance in shaping passive properties of neurons expressing them.

Secondly, chemical synapses allow signal transmission between neurons by a cascade of mechanisms which only work in one direction, as a causal chain. That is, an action potential is required to allow calcium entry in the presynaptic element, and the consequence is the release of neurotransmitters in the synaptic cleft (the extracellular space in between the pre- and the post-synaptic elements). These neurotransmitters bind to post-synaptic receptors, finally resulting in current entry in the post-synaptic cell (in the case of ionotropic receptors) or downstream activation of intracellular mechanisms (in the case of metabotropic receptors). But this chain reaction cannot be reverted: should a post-synaptic receptor stochastically open, it will not end up generating an action potential in a causal manner in the presynaptic element. Therefore, **chemical transmission is unidirectional**. On the other hand, electrical synapses are made of intercellular hemichannels, which by apposition create a pore in between two neighbouring cells, physically linking their cytoplasms. The symmetrical nature of this molecular construction therefore makes **electrical transmission bidirectional**.

It should be noted, however, that bidirectional communication through electrical synapses doesn't imply *symmetrical current flow*. Indeed, rectifying properties of electrical synapses themselves (Harris *et al.*, 1981; Phelan *et al.*, 2008) or differences in electronic structure of connected cells (Fortier and Bagna, 2006, Apostollides and Trussel, 2013), can cause an asymmetry in the ability of electrical currents to flow in one direction versus the other.

Thirdly, chemical synapses are often associated with a **time delay** (up to a 1 ms) between the presynaptic AP and the post synaptic potential, because the cascade of mechanisms for release of synaptic vesicles is not instantaneous. In contrast, electrical communication is considered **instantaneous**, because the electrical impulse in a pre-synaptic neuron does not need to be converted into a chemical signal to produce a post-synaptic electrical response. Moreover, chemical communication is **stochastic** in nature (*i.e.*, post-synaptic responses to a given AP in the presynaptic cell can be different, due to the variability in the number of vesicles released, along with their neurotransmitter content), whereas electrical communication is considered **reliable**, because the post-synaptic potential is merely a filtered version of the presynaptic one.

Fourthly, chemical transmission relies on **specific ion** entry in the post-synaptic element, dictated by the structure and the permeability of post-synaptic receptors (for example, Cl^-/HCO_3^- through $GABA_AR$, or Na^+/Ca^{2+} through AMPAR). Electrical synapses, on the other hand, do not display charge restriction features, and therefore allow positive and negative ions

to cross them. The size of ions is even less of a concern, as the single channels of electrical synapses are so large that they allow small metabolites (a few hundreds of Da) to flow from one cell to another (Srivinas *et al.*, 1999; Meier and Dermietzel, 2006). Therefore, electrical synapses are, in principle, **permeable to all ions** (reviewed in Spray and Bennett, 1985).

One important consequence of the specificity of ion flowing through either type of synapses is the polarity of the post-synaptic currents. Chemical synapses, because of the selective nature of the post-synaptic receptors, allow only some specific ions to flow inside the post-synaptic cells. As a consequence, the **polarity of the current is dictated by the reversal potential of the ions** involved, and the membrane potential of the cell ($\mathbf{I_{chem}(t) = g_{chem}(t)(Vm_{post}(t)-E_{rev})}$ - see Table I-1)**.** For example, AMPARs cause inward currents, because of the net entry of Na^+/Ca^{2+} ions at a resting membrane potential of -70mV. Electrical synapses, however, allow equilibration of membrane potentials by passive flow of ionic currents. The direction of current flow is therefore dictated by the difference in membrane potentials between the two connected cells ($\mathbf{I(t)=g_{gap}.(Vm_{post}(t) - Vm_{pre}(t))}$ - see Table I-1). Notably, when an action potential is triggered in a presynaptic cell, the postsynaptic one will experience a sequence of a fast inward current (the filtered version of the sodium current causing the peak of the AP) followed by a slow outward current (the filtered version of the After Hyper-Polarization (AHP)). This synaptic response is often referred to as a "spikelet".

One last consequence of this particular feature of electrical transmission is that, *a priori*, it is not possible to say if spikelet transmission has a net excitatory or inhibitory effect in a given cell-type. Figure I-4 shows that spikelet transmission can produce a net inhibition in cerebellar Golgi cells (inhibitory interneurons found in the granular layer of the cerebellar cortex), or net excitation in somatostatin-expressing interneurons of layers 2 and 3 of the cerebral cortex (Dugué *et al.*, 2009; Hu and Agmon, 2015).

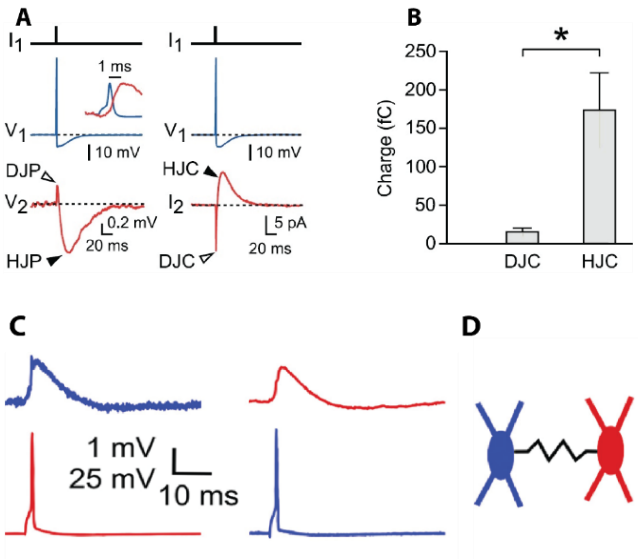

Figure I-4: Spikelet transmission causes either net inhibition or net excitation:

A) Paired recordings of cerebellar Golgi cells showing that spike initiation in one cell (blue) causes a spikelet in the second cell (red), with a prominent inhibition. **B)** Hyperpolarizing Junction Currents (HJC) carry more charge than their depolarizing counterparts (DJC).

From Dugué *et al.*, 2009

C and D) L2/3 somatostatin-positive interneurons of the cerebral cortex also form electrical synapses, but spikelets here appear mostly excitatory.

From Hu and Agmon, 2015

It is sometimes reported that the differential effect of spikelet transmission is cell-type dependent, but some studies have also reported different spikelet waveforms within the same cell-type (see Otsuka and Kawaguchi, 2013 for fast-spiking cortical interneurons; and compare spikelet waveforms between (Alcami and Marty, 2013; Rieubland *et al.*, 2014) and (Alcami; 2018) for cerebellar interneurons). During my PhD, I addressed explicitly what could be some biophysical determinants underlying these qualitative differences, in cerebellar basket cells.

In different sections of this thesis, I will employ the word "spikelet", which has been used in different contexts, to reflect different phenomena (*e.g.*, dendritic spikes - Spencer and Kandel, 1961 - or ectopic axonal spikes - Stasheff *et al.*, 1993). For my purpose, I will define a spikelet as the "filtered version of an action potential, transmitted through an electrical synapse". Spikelets can be recorded as synaptic currents, or synaptic potentials using either voltage or current clamp, respectively.

Table I-1 summarizes some of the key differences between electrical and chemical synapses that I mentioned above. Highlighted are the features that will be exploited in my analysis, later on in this thesis.

Table I-1	Electrical synapses	Chemical synapses
Ionic selectivity	neither size, nor charge	size AND charge
Gating	**always opened (at least for a fraction of the channels)**	**neurotransmitter-dependent**
Direction of current flow	**bidirectional**	**unidirectional**
Post synaptic current	**positive AND/OR negative (time dependent)**	**positive OR negative (ion dependent)**
Small molecule exchange	possible	not possible
Current flow equation	$\mathbf{I_{elec}(t) = g_{gap}\,(Vm_{post}(t)-Vm_{pre}(t))}$	$\mathbf{I_{chem}(t) = g_{chem}(t)\,(Vm_{post}(t)-E_{rev})}$

II - 4) Physiological roles of gap junctions and electrical synapses:

II - 4 - a) Physiological roles of gap junctions:

Because of the relatively large diameter of their inner pore, gap junctions allow a unique mode of communication between connected cells, by enabling the transfer of ions, metabolites and second messengers having a molecular weight up to 1kDa. Connected cells therefore tend to equilibrate their membrane potentials, and their cytoplasmic composition. These properties combine in different systems to synchronize and homogenize cells' activity.

For example, the heart expresses a very large number of gap junctions of different isoforms (mostly Cx40, Cx43 and Cx45 - Davis *et al.*, 1994; Davis *et al.*, 1995), and these gap junctions are required for the synchronous contraction of cardiomyocytes. In the vascular system, homogeneous metabolic state between smooth muscles, enabled by gap junctions, ensures a homogeneous resistance of the tissue, ultimately participating in the regulation of blood pressure. Numerous reports indicate changes in connexin regulation and expression in this tissue, in pathological conditions such as diabetes or hypertension (Zhang and Hill, 2005; Hamelin *et al.*, 2009). I would also like to mention the interesting case of gap junctions in the lens, an avascular organ within the eye. In this case, gap junctions between the exterior epithelium and the inner fibers create a syncytium-like tissue, and allow the epithelial cells to literally feed the fibers with nutrients (reviewed in Mathias *et al.*, 2007).

In the next section, I will focus on the physiological roles of electrical synapses, which are gap junctions expressed in neurons.

II - 4 - b) Physiological role of electrical synapses:

Since electrical synapses allow a passive spread of current between two connected neurons, one of their first attributed physiological role was to mediate synchrony (*i.e.*, correlated spiking) in population of neurons (Beirlein *et al.*, 2000; Landisman *et al.*, 2002; Long *et al.*, 2004), either because of subthreshold membrane potentials equilibration or spikelet transmission. The role of electrical synapses in synchrony was first demonstrated in hippocampal slices *in vitro* (Draguhn *et al.*, 1998 - Figure I-5), when extracellular recordings in the dentate gyrus, CA1 and CA3, revealed brief bursts of spontaneous high-frequency oscillations (150-200Hz) which were *not* abolished in presence of gabazine (blocker of $GABA_A$ receptors), NBQX (blocker of AMPA receptors), or in absence of extracellular Ca^{2+} (aiming to block all forms of chemical synaptic transmission). However, the use of gap junction antagonists (either Octanol, halothane or carbenoxolone) was sufficient to reversibly block these correlated discharges.

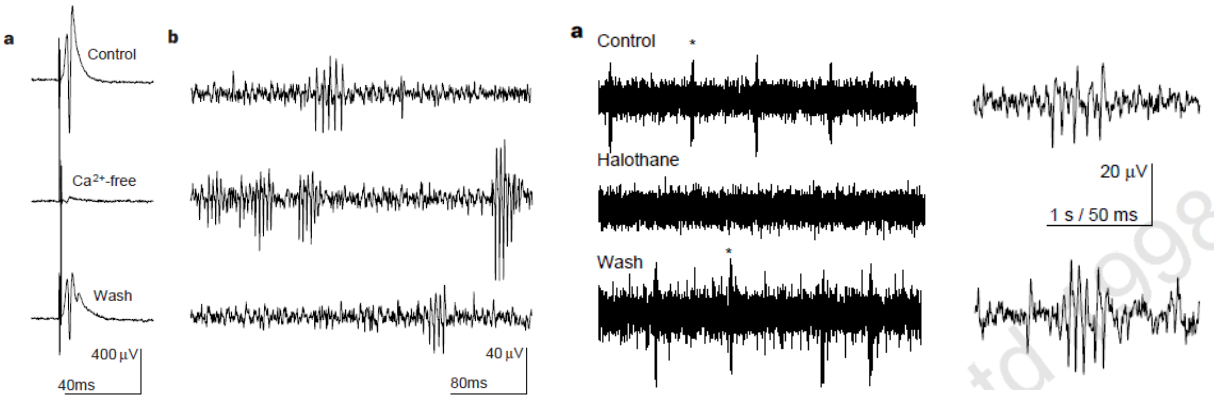

Figure I-5: High-frequency oscillations in hippocampal slices are mediated by electrical synapses:

Left panels: a) stimulation of the perforant path in CA1 region of hippocampus in Ca^{2+}-free medium confirms the block of chemical transmission. Yet, in **b)**, high-frequency oscillations are still detected. **Right panels:** application of Halothane (a blocker of electrical synapses) blocks high-frequency oscillations, in a reversible manner.

Adapted from Draguhn *et al.*, 1998

It was later shown by Deans *et al.*, 2001 that Low-Threshold Spiking (LTS) neurons of the cerebral cortex (already known at that time to generate synchronous activity), displayed impaired synchronicity (in time, but also in space) in $Cx36^{-/-}$ mice. Similar observations as those from (Draguhn *et al.*, 1998) were drawn from Mann-Metzer and Yarom, in 1999: in Molecular Layer Interneurons (MLIs) of the cerebellar cortex, spike synchrony between two interneurons was observed in Ca^{2+}-free ACSF, and positively correlated with the presence of an electrical synapse between them.

Finally, to conclude on the link between neuronal synchrony and presence of electrical synapses, I wish to highlight recent works in electrically-connected Golgi cells, found in the cerebellar cortex. It was first demonstrated by Dugué *et al.*, 2009 that electrical synapses promote synchrony in Golgi cells (GoCs), *in vitro* and *in silico*, during homogeneous input activation, with evidence that they also underlie low-frequency oscillations (~50Hz) *in vivo*. However, it was later demonstrated by Vervaeke *et al.*, 2010 that asynchronous excitatory inputs onto synchronized Golgi cells can cause rapid and prominent desynchronization of the network, due to spikelet-mediated surround inhibition and heterogeneity in electrical couplings. Finally, in Van Welie *et al.*, in 2016, the authors investigated with *in vivo* recordings and modelling approaches how spikelets influence spike synchrony between electrically-connected GoCs. They found that the spikelet-mediated depolarizations led to correlated spiking on short time scales (1-2ms), while spikelet-mediated hyperpolarization led to anti-correlated spiking on longer time scales (few tens of milliseconds). Correlated spiking was shown to be further enhanced by slow depolarizations of connected cells, prior to spike initiation.

Altogether, these studies reveal that correlated spiking at the network level depends on the spikelets waveform, the spatial distribution and dynamics of incoming excitatory inputs onto electrically-connected cells, and slow membrane fluctuations mediated by electrical synapses.

Before concluding on the link between electrical synapses and synchrony, it should also be noted that spike synchrony between neurons does not necessarily require electrical synapses: shared common presynaptic excitatory inputs (Otsuka and Kawaguchi, 2013) or GABAergic communication between interneurons (Gibson *et al.*, 2005; Hu and Agmon, 2011), are two potent mechanisms which can be sufficient to generate synchrony.

In the previous paragraphs, I presented some cases showing the involvement of electrical synapses in synchronization of cell assemblies. However, electrical synapses have been shown to confer other properties in neural networks. In the next paragraphs, I will present two studies in some details, because they highlight other roles of electrical synapses in neural networks, and start to address their contribution to dendritic integration properties, which I will examine more deeply in the next section of this introduction.

In 2016, Kuo *et al.* investigated *in vitro*, with flat retina preparations, how ON retinal ganglion cells (RGCs) are recruited by their excitatory afferents, the ON bipolar cells (Figure I-6, from Kuo *et al.*, 2016). They found that light inputs, initially processed by rod bipolar cells,

relayed to AII amacrine cells, and further relayed to ON bipolar cells by electrical synapses, are integrated in a non-linear fashion by ON ganglion cells. This non-linearity is shown on panel C, D and E: the currents recorded in ON RGCs, in response to two coincident stimuli (1 and 2) is different from the algebraic sum of responses to stimulus 1 and 2, presented separately. The authors showed that the stage of non-linear integration was downstream of AII amacrine cells (and of course, upstream of ON RGCs), and the conclusion of their article is as follows: electrical synapses between AII amacrine cells and ON cone bipolar cells allow a lateral spread of excitatory electrical currents in the ON cone bipolar cells (that is, ON cone bipolar cells not lying in the region were light stimuli are presented *still* receive excitatory currents by electrical synapses from their laterally-positioned neighbours). These excitatory currents then help in engaging a non-linear mechanism between presynaptic resting membrane potential of ON cone bipolar cells and vesicular release of glutamate onto ON RGCs (see Jarsky *et al.*, 2011).

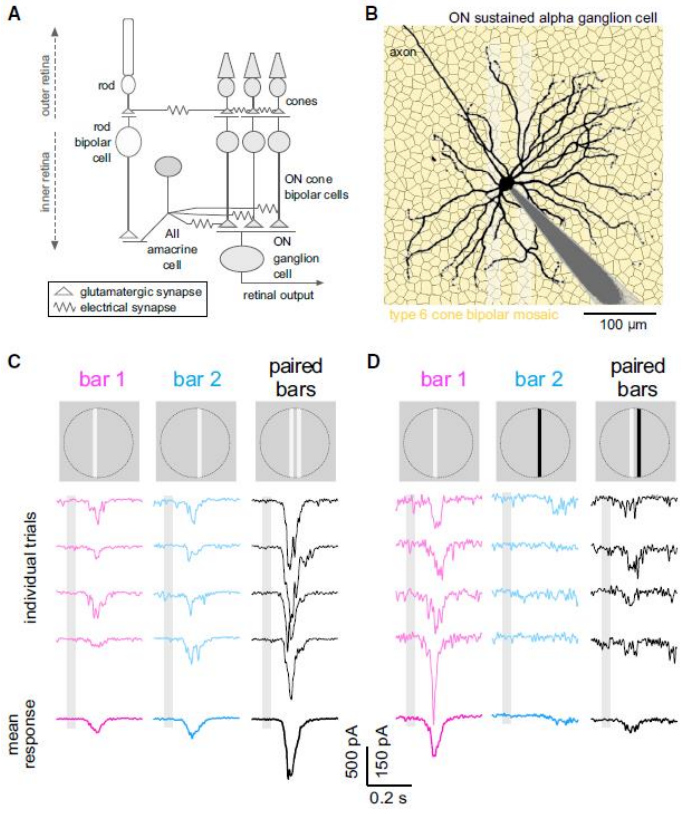

Figure I-6: Nonlinear spatiotemporal integration by electrical and chemical synapses in the retina:

A) Simplified circuit diagram of the retina; **B)** ON ganglion cell (black cell) lying over a mosaic of cone bipolar cells (yellow cells), with white rectangles representing paired light stimuli; **C)** Individual responses of the ON-ganglion cell to presentation of either of the two bars (pink and blue traces), or when both bars are presented simultaneously (black); **D)** same as in C, but for negative contrast stimuli. In both cases, the responses recorded during presentation of paired bars is different from the linear sum of the individual responses (significant differences were shown in another figure of the article).

Adapted from Kuo *et al.*, 2016

This study therefore presents an interesting case of an interplay between the spread of subthreshold electrical currents through electrical synapses, and a non-linear mechanism in chemical synaptic transmission, which ultimately increases ON RGCs sensitivity to spatiotemporally correlated inputs.

Vervaeke *et al.* (2012) described how GoGs display a distance-dependent sublinear integration behaviour for excitatory chemical synaptic inputs (*i.e.*, for distal synapses, the relationship between the amount of glutamate released from the presynaptic excitatory afferents and the postsynaptic currents amplitude is sublinear, because the local dendritic depolarization reduces the driving force for synaptic currents - I will further detail this point in a later section of my introduction). However, GoCs express electrical synapses, and thanks to experimentally-constrained network modelling, the authors showed that, at the network level, these synapses compensate for the sublinear dendritic integration behaviour at the network level (Figure I-7, from Vervaeke *et al.*, 2012), by allowing a passive spread of excitatory currents from innervated to non-innervated GoCs. This phenomenon was more prominent in distal dendritic compartments, because of the large local depolarization of the dendritic branches caused by the incoming EPSCs.

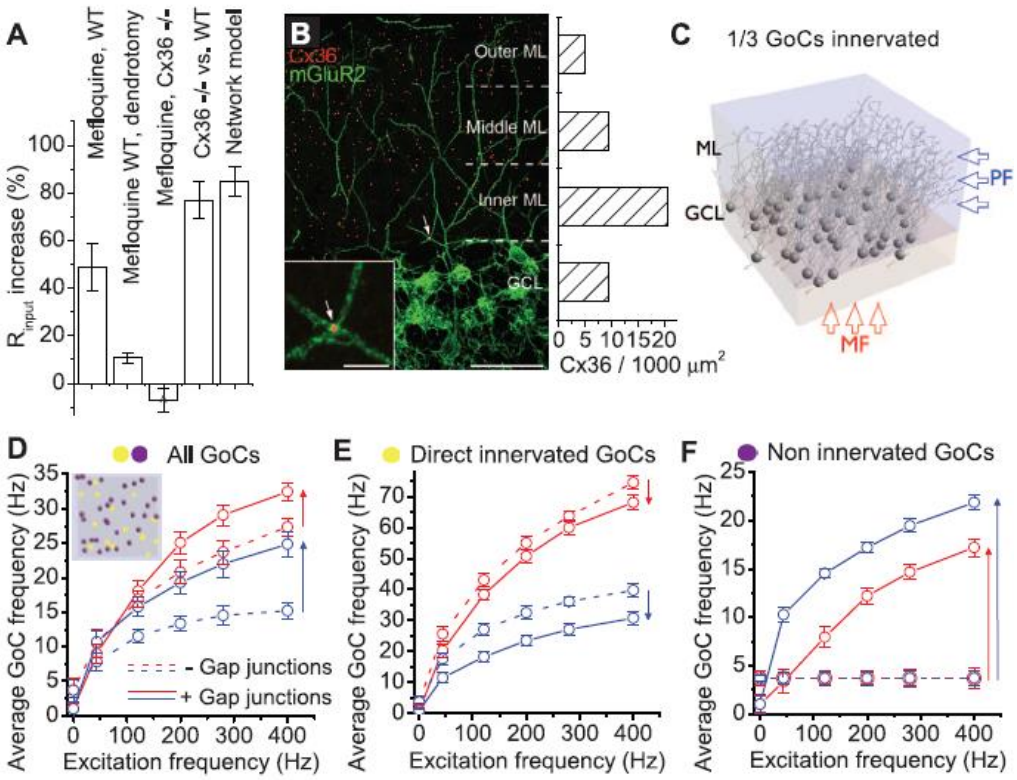

Figure I-7: Gap junctions compensate for sublinear integration in an inhibitory network:

A) Effect of mefloquine (GJ blocker), dendrotomy, knock-out of Cx36 and GJ removal from the modelled network (described in C to F), on the input resistance of Golgi cells. **B)** Immunostaining revealing the dendritic location of GJs. **C)** Network model of 45 GoCs, 15 of which receive mossy and parallel fibers excitatory inputs; **D)** GoC firing frequency in the network, when driven by PF inputs (blue) or MF inputs (red), with GJs (solid lines) or without GJs (dashed lines). **E)** and **F)** reveal the differential effect of excitatory inputs, with and without GJs, in innervated and non-innervated GoCs, respectively.

From Vervaeke *et al.*, 2012

One important note has to be made here: in an article published in 2009 by Dugué *et al.* (and later confirmed in Vervaeke *et al.*, 2010), it was shown that in GoCs, the net effect of spikelet transmission is inhibitory (Figure I-4, from Dugué *et al.*, 2009). When this result is put in relationship with the study of Vervaeke *et al.*, 2012, it indicates that a given network of GoCs fires more APs on average when "inhibitory synapses" connect them. It therefore appears that the passive spread of EPSCs enabled by electrical synapses is more important than the additional inhibitory action conveyed by spikelet transmission. This further exemplifies the unique ability of electrical synapses to mediate electrical currents from different sources, of either positive or negative polarities.

In both studies mentioned in the last paragraphs, it can be observed that electrical synapses allow the spread of subthreshold synaptic currents from innervated to non-innervated cells. This already indicates that electrical synapses can expand the receptive field of electrically-connected cells, which may be of high importance in dendritic integration, because indirect inputs have to be considered in the Input/output relationship.

To conclude on this section, electrical synapses are expressed mostly (but not exclusively) in specific populations of inhibitory interneurons of the CNS (reviewed in Nagy *et al.*, 2018), and they play a role not only in synchronizing population assemblies to create oscillations, but also in more elaborated functions in dendritic integration of single cells, or network computations. However, their contribution to the latter mechanisms have been less investigated, which raises the possibility that they could serve as a basis for other type of neuronal and network computations which have not been elucidated yet.

III) Dendritic and synaptic integration:

As neuroscientists, we are interested in understanding how computations performed by the brain can guide behaviour. The neural substrates for these operations have been probed and investigated in great details over the last decades. It was initially thought that neurons would behave as "simple" devices, linearly summing excitation and inhibition from synaptic inputs, and compare this sum to a threshold value to generate an AP, or not. In that view, most of the "interesting" computations performed by the brain would be due to how these simple elements are connected in a complex manner, and how synaptic weights can be adjusted by learning through different plasticity mechanisms. Here, I would like to quote (London and Häusser, 2005):

"Brains compute. This means that they process information, creating abstract representations of physical entities and performing operations on this information in order to execute tasks. One of the main goals of computational neuroscience is to describe these transformations as a sequence of simple elementary steps organized in an algorithmic way. The mechanistic substrate for these computations has long been debated. Traditionally, relatively simple computational properties have been attributed to the individual neuron, with the complex computations that are the hallmark of brains being performed by the network of these simple elements. In this framework, the neuron (often called a "Perceptron," "Spin," or "Unit") sums up the synaptic input and, by comparing this sum against a threshold, "decides" whether to initiate an action potential. In computational terms this process includes only one nonlinear term (thresholding), which is usually counted as a single operation. Thus, the neuron operates as a device where analog computations are at some decision point transformed into a digital output signal. Such a design forms the backbone of many artificial neuronal networks, starting from the original work of McCullough & Pitts (1943) to the present day. In this review we argue that this model is oversimplified in view of the properties of real neurons and the computations they perform. Rather, additional linear and nonlinear mechanisms in the dendritic tree are likely to serve as computational building blocks, which combined together play a key role in the overall computation performed by the neuron."

In this section, I will describe how morphological features and electrophysiological properties can shape how individual neurons transform a set of presynaptic inputs into certain outputs, what is called the input/output relationship. These mechanisms relate to an interplay

between elementary features of nerve cells which I have described in the first two sections of this introduction: individual nerve cells have a wide variety of morphologies, and are also known to express voltage-gated channels which render them excitable.

III - 1) Dendritic integration:

Dendritic integration is the process by which excitatory/inhibitory post-synaptic potentials (E/IPSPs), activated over time and space, are summed in order for the axo-somatic membrane potential to depolarize above threshold for action potential generation. It is therefore a compound effect of dendritic cable filtering - the differential attenuation of amplitude and speed of electrical events arising in different cellular locations (*Rall*, 1989); and recruitment of active mechanisms, which can amplify (through synaptic scaling, subthreshold boosting, and dendritic spiking) or compress synaptic inputs (London and Häusser, 2005).

Classically, cable filtering and active mechanisms are presented sequentially, for multiple reasons:

- cable filtering is caused by passive electrical properties of the cell membrane *(i.e.*, properties which do not vary in time, and do not depend on the transmembrane voltage), and for this reason, it is a phenomenon present in all neurons, at least qualitatively.

- active mechanisms rely on the recruitment of ion channels during synaptic activation. These mechanisms are neuron-type specific, because all of them do not display the same diversity, density, and subcellular localization of voltage-gated channels.

A good starting point, for didactic reasons, is therefore to understand how passive properties are shaped by morphological features and non-voltage-gated ion channels; and then consider how this passive neuronal system can be enriched with a variety of active properties - and notably, voltage-gated channels - which are the hallmark of neuronal diversity.

III - 1 - a) Passive properties and cable filtering:

Cable filtering can be understood intuitively because of the analogy of the cell membrane with a low-pass filter (*i.e.*, the cell membrane having both channels responsible for its resistivity (R), and lipids arranged in a bilayer fashion acting like capacitors (C), their combination in parallel of each other constitutes an RC filter in electrical terms). As a consequence, a passive membrane is expected to dampen high frequency signals. This means that any electrical current flowing between two points in a neuron will experience a decrease in

its peak amplitude, and a slowdown of its kinetics. This phenomenon will be more pronounced for rapid signals (*e.g.*, AMPAergic currents in interneurons), and for signals travelling over long distances in the neuron (*e.g.*, a synaptic event in a remote dendritic compartment spreading to the soma).

This qualitative behaviour has been extensively described in mathematical forms, notably by Wilfrid Rall (tens of articles published between 1953 and 1968), and Guy Major. I also wish to mention two excellent text books (Jack, Noble and Tsien, 1975; Johnston and Wu, 1995), which provide not only an extensive and comprehensive understanding of these phenomena, but also rich repertoires of references for scientific articles related to this topic.

The starting point is usually to consider the analogy of the cell membrane with electrical circuits. In this framework, a single neuron is represented as a "ball" (representing the somatic compartment), onto which are attached "sticks" (representing the dendritic branches). These branches are modelled as cylinders displaying three electrical components:

- an internal resistance (r_i), representing how the voltage drops along branches when electrical currents flow;

- a membrane resistance (r_m), representing how electrical currents “leak out” of the cell through ion channels opened at rest, without voltage- or ligand-gating mechanisms;

- and a membrane capacitance (c_m), representing how charge accumulate on both sides of the cell membrane.

Each of these parameters is expressed in units of impedance, with units of length of dendritic cables (r_i in Ω/cm, r_m in Ω.cm, and c_m in F/cm). These parameters are referred to as "passive", because none of them varies with the voltage drop across the membrane. The general equation describing membrane potential evolution along such cylindrical structures is known as “the cable equation”, generally expressed as follows:

$$\lambda_{DC}{}^2 \frac{\partial^2 V}{\partial x^2} = \tau_m \frac{\partial V}{\partial t} + V \quad (1),$$

where V is the voltage difference across the cell membrane, and varies in time and space; λ_{DC} is the steady-state length constant; and τ_m the membrane time constant. The last two parameters are of key importance in neurophysiology, and may be described as follows:

- the steady-state length constant refers to the distance a constant (*i.e.*, infinitely long) pulse of current has to travel in a dendritic process to experience a 63% decrease in its initial

amplitude. The higher this value, the less electrical currents are filtered along a dendritic process of a given length.

- the membrane time constant refers to the time taken by a uniform current input (*i.e.*, with an ideal device allowing to inject current, simultaneously and homogeneously, in a neuron) to charge a neuron to 63% of the steady-state response. The higher this value, the longer it takes for a neuron to "convert" a current input into a membrane potential difference with the extracellular space.

These two parameters are related to the resistances and capacitance described above by:

$$\lambda_{DC} = \sqrt{\frac{r_m}{r_i}} \text{ (2)} \qquad \text{and} \qquad \tau_m = r_m c_m \text{ (3).}$$

A final set of equation has to be introduced to link morphological parameters (such as cable diameter, denoted *d* hereafter) and specific cable parameters:

$$r_m = \frac{R_m}{\pi d} \text{ (4)} \qquad c_m = C_m \pi d \text{ (5)} \qquad \text{and } r_i = \frac{4R_i}{\pi d^2} \text{ (6)}$$

where, R_m, C_m and R_i are the specific membrane resistance, capacitance, and internal resistivity, respectively. They are expressed in impedance units (that is, Ohms and Farads). By combining equations (2), (4) and (6), it is possible to write a second equation for λ_{DC}:

$$\lambda_{DC} = \sqrt{\frac{R_m d}{4R_l}} \text{ (7)}$$

Equation (7) shows that passive equilibration of voltage along a dendritic branch depends on the diameter of this very branch. Complete mathematical development of these equations and their interpretations can be found in Jack, Noble and Tsien (1975). Figure I-8, from Johnston and Wu (1995), shows qualitatively how a constant current input applied at one point along a dendritic branch charges the cell membrane at different levels, and with different kinetics and delays.

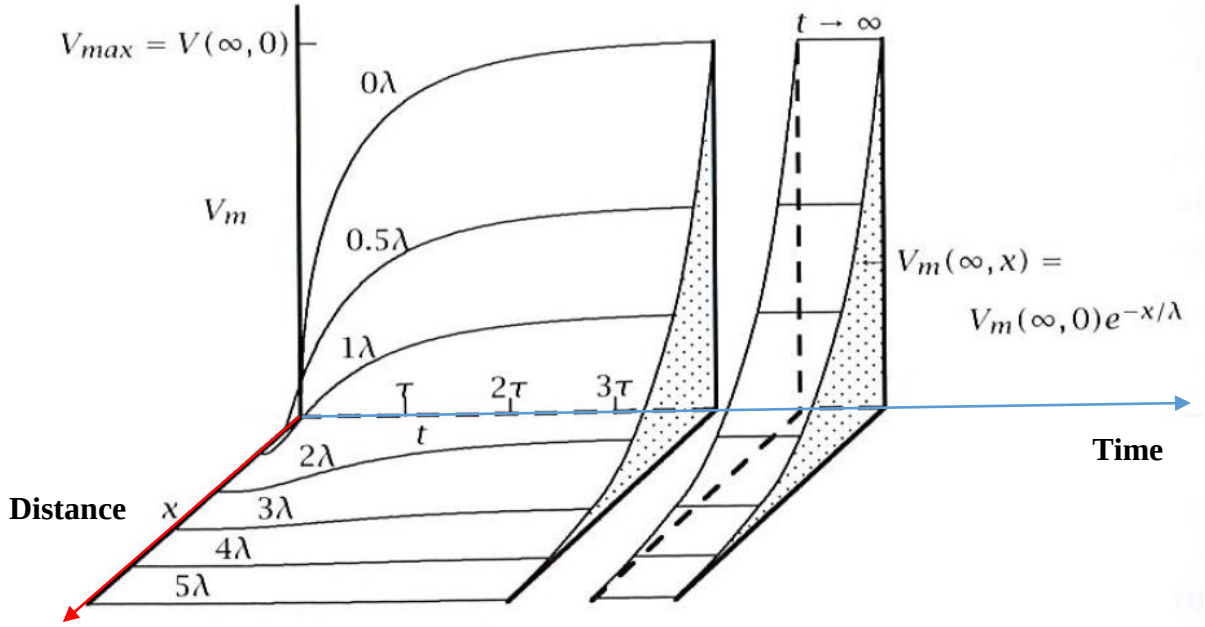

Figure I-8: Membrane polarisation during a constant current input along a cylindrical cable (*e.g.*, a dendritic branch):

The blue axis represents the temporal evolution of the charging of the cell membrane, in units of time constants (τ), while the red axis represents the spatial evolution of the charging, in units of steady-state length constants (λ).

Adapted from Johnston and Wu, 1995

With this scheme and the above equations, I wish to show that the passive spread of current along dendritic branches depends on the diameter of the branch (morphological parameter), and resistances along the branch (R_i) and across the membrane of the branch (R_m), and that virtually all neurons will have their own length constant (so long as they have dendritic processes).

III - 1 - b) Active conductances:

Nerve cells express a remarkable diversity of transmembrane ion channels. They have evolved simultaneously with the formation of lipid bilayers to constitute the membrane of living organisms, presumably to allow a specific control of metabolites and ions exchanges between the intracellular and extracellular spaces, along with specific ion transporters which are critical to create ionic gradients across the cell's membrane (Hille, 2001). While the latter mostly rely on the consumption of ATP to set-up chemical gradients for ion species, ion channels only allow a passive diffusion of ions when they are opened. Therefore, when we talk about active

conductances, we only refer to ion channels, even though they require ion gradients to be set by transporters (or "pumps") to carry any significant ion currents across the cell's membrane.

In the next paragraphs, I will focus on how specific types of voltage-gated channels usually operate to mediate ion currents, and later on explain how the expression of such channels in neurons can further expand the ability of nerve cells to process information in the form of electrical currents. The specific examples presented below were chosen because they will be referred to explicitly, later on in this thesis.

- Na^+ and K^+ channels:

In most neurons (and cells in general), there are gradients of ion species across the membrane. For example, there is a high concentration of sodium outside, and a low concentration inside. For potassium, it is the opposite. These gradients are notably set by the Na^+/K^+ exchanger, which consumes ATP to take sodium from inside and potassium from outside, and pump them in the opposite compartment. Once a gradient has been established, ions can flow across the cell's membrane mainly through ion channels of the proper kind. Hence, sodium can flow inside the cell if Na^+-channels are opened, while potassium can flow outside only if K^+-channels are opened. Relevant to neurophysiology is the observation that the ability of channels to open or close relies on many factors (time, regulation by metabolites, voltage), and transmembrane voltage *may be* considered the most important in this context, because nerve cells experience a lot of voltage changes, notably during synaptic activity.

The relative contribution of Na^+ and K^+ in the excitability of nerve cells was notably examined in (Hodgkin and Huxley, 1952 - Figure I-9). Their work revealed that g_{Na} and g_K varied with v, and their model could reproduce the voltage trajectory of an AP in the giant squid axon (numerical simulations). Importantly, they proposed that the initial positive peak of APs is caused by the rapid opening of Na^+ channels (which provide a depolarizing current), while the secondary, longer-lasting negative peak of the AP (*i.e.*, the AHP) is caused the opening of K^+ channels (which provide a hyperpolarizing current), along with a rapid closing of Na^+ channels. Remember that, at their time, ion channels had not been discovered yet, so the word "channel" carried the meaning of "proposed gating mechanism"

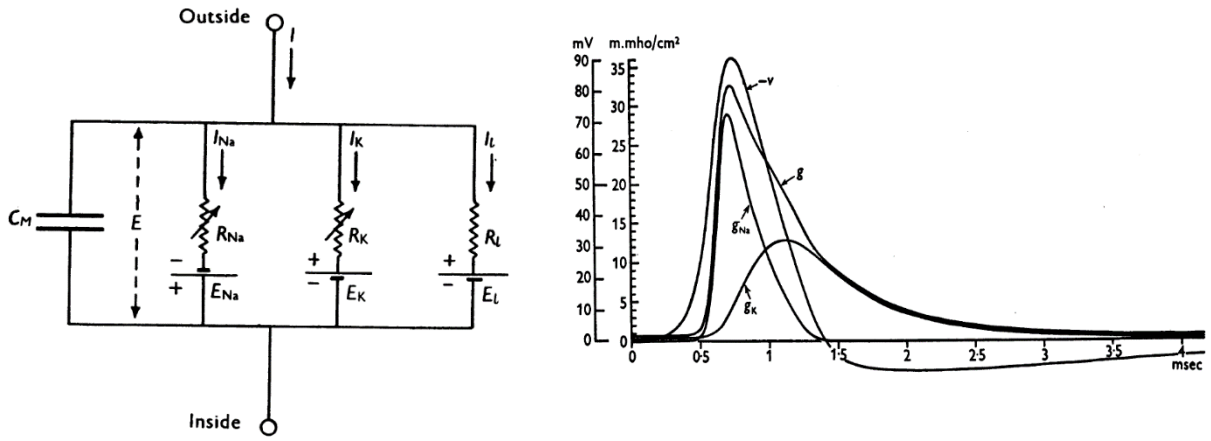

Figure I-9: Voltage-dependent gating of Na^+- and K^+-channels:

A) The transmembrane voltage between the inside and outside of a neuron (E) is set at all time by the current I flowing in the circuit. C_M is the membrane capacitance, I_i, R_i and E_i are the current, channel conductance and reversal potential of the i^{th} ion species (L stands for "leakage"); **B)** Time evolution of g_{Na} (=$1/R_{Na}$), g_K (=$1/R_K$), g (g_{Na} + g_K) and v, the transmembrane voltage during an AP.

Adapted from Hodgkin and Huxley, 1952

- Hyperpolarisation-activated cation channels:

These channels are quite unique, because they are permeable to both Na^+ and K^+. Their opening causes a net inward current called I_h (associated to a reversal potential between -20 and 0mV), and this opening is enhanced by hyperpolarization (Yanagihara and Irisawa, 1980). They can therefore cause rebound activity after strong inhibition (Lüthi and McCormick, 1998). They also display a cytoplasmic domain typical of cyclic-nucleotide-bindind domains. Binding of cytoplasmic cAMP to this domain shifts the voltage-dependent activation curve of HCN channels towards more depolarized values, which can ultimately lead to a significant steady-state I_h current in nerve cells when they are at rest (Maccaferri *et al.*, 1993).

- NMDA receptors:

NMDA (N-methyl-D-Aspartate) receptors are ligand- and voltage-gated channels. At rest, they are closed, and require two concomittant phenomena to open: binding of neurotransmitters (usually, glutamate and glycine/D-serine) onto their extracellular domains; and local depolarization of the cell membrane, to remove Mg^{2+} and/or Zn^{2+} ions which obstruct the inside of the pore and block the passage of cations (Na^+, K^+ and Ca^{2+}). Futher information about NMDA receptors can be found in (Vyklicky *et al.*, 2014)

Having briefly reviewed how different types of channels can be activated or inactivated by changes in membrane potential, I will now described how they can shape the dendritic integration properties of neurons.

III - 2) Non-linear dendritic integration:

In contrast to cable filtering, dendritic integration can be a non-linear process far more delicate to apprehend. Indeed, if one considers only EPSPs and disregards IPSPs (for the time being), the amplitude and shape of two or more EPSPs occurring within a small time window (compound EPSP), and in proximity of each other (same electrical compartment) may be different from their expected arithmetic sum (Tran-Van-Minh *et al.*, 2015). Dendritic integration can therefore be classified in three groups: linear, supralinear or sublinear, depending on if the compound EPSP is equal to, larger than or smaller than, respectively, the arithmetic sum of the individual EPSPs (Figure I-10, from Tran-Van-Minh *et al.*, 2015). Common dendritic features which endow neurons with non-linear dendritic integration properties are passive cable properties (Abrahamsson *et al.*, 2012) and ligand or voltage-gated ion channel expression (reviewed in Tran-Van-Minh *et al.*, 2015). Non-linear dendritic integration can increase the computational power of neurons (*i.e.*, increase the number of implementable functions which would transform a given number of inputs into different outputs - Cazé *et al.*, 2013), and confer pattern separation properties (Poirazi and Mel, 2001).

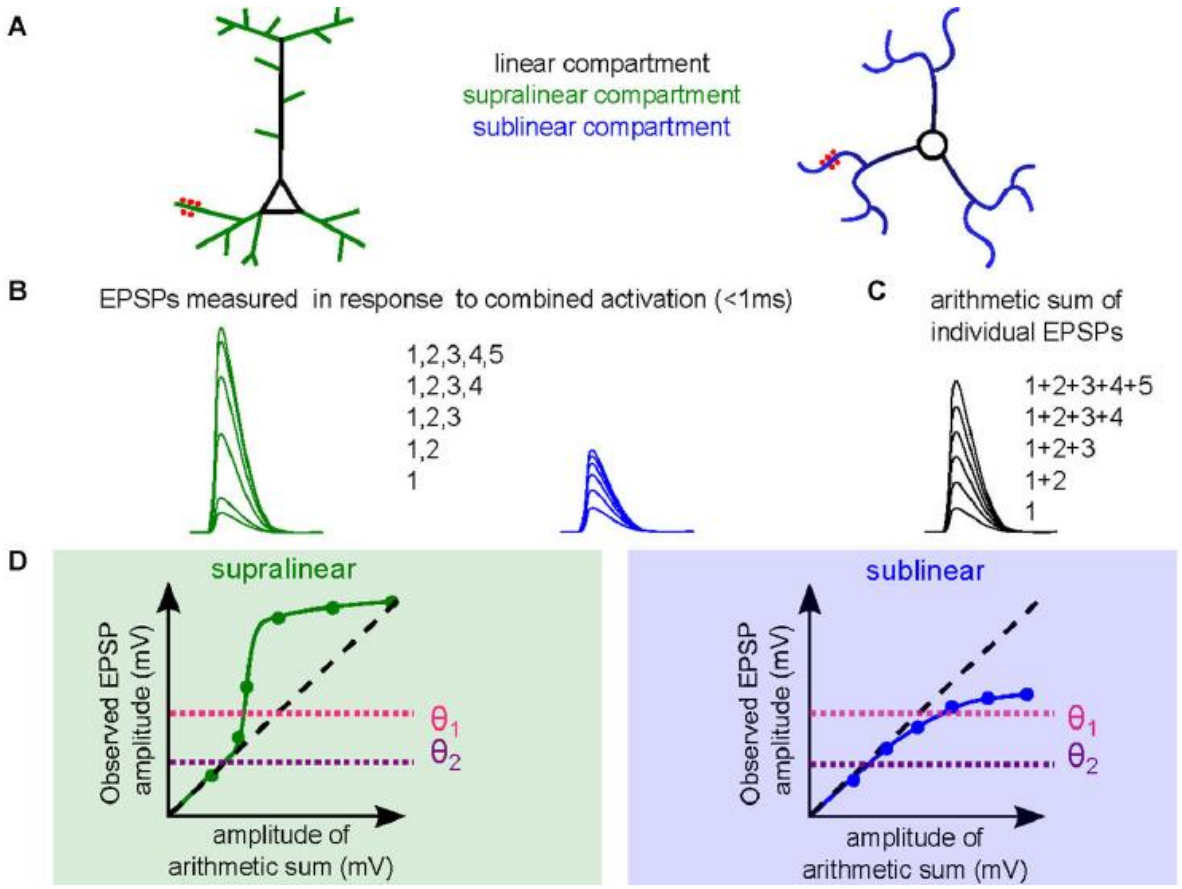

Figure I-10: Supra- and sub-linearity in dendritic integration:

A) Schematic diagrams of a pyramidal cell (left) endowed with a linear compartment (soma, in black) and supralinear compartments (dendritic branches, in green) or a stellate cell endowed with a linear compartment (soma, in black) and sublinear compartments (dendritic branches, in blue). Red dots represent the site of synaptic activation; **B)** Somatic voltage responses evoked by an increasing amount of co-activated synapses (same color code as in A); **C)** Arithmetic sum of individual responses recorded during synaptic activation; **D)** Input-output relationships of either type of dendritic integration, showing how the compound somatic EPSP amplitude (Observed EPSP - Y-axis) can differ from the expected sum of individual EPSPs (arithmetic sum - X-axis). Adjustment of the spike initiation threshold (θ_1 and θ_2) can switch a given neuron from a linear behaviour (θ_2) to a non-linear behaviour (θ_1).

Adapted from Tran-Van-Minh *et al.*, 2015

A critical consequence of these potential non-linear summations of post-synaptic potentials is that dendrites are inherently a stage of information processing within neurons, and do not simply serve as extensions of the cell membrane to increase the surface area over which synapses can be built (Poirazi *et al.*, 2003; London and Häusser, 2005). Consequently, some neurons are best represented by "two-layer models" (Figure I-11, from Poirazi *et al.*, 2003), where synaptic inputs are first (non-linearly) summed in quasi-independent sub-units representing different dendrites, and their outputs are then (linearly) summed in the somatic compartment, which ultimately determines action potential firing or not.

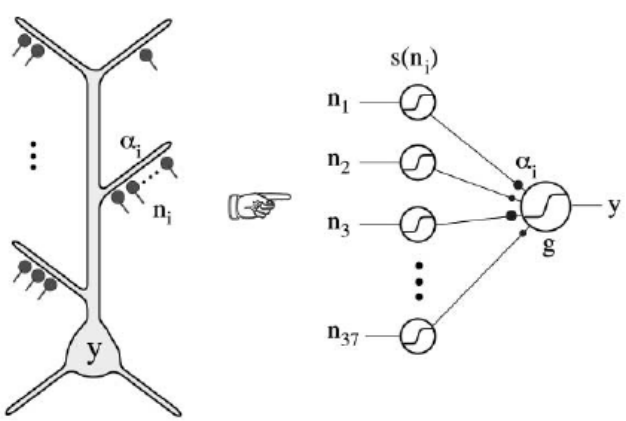

Figure I-11: Pyramidal neuron as two-layer neural networks:

A schematic pyramidal neurons (y) receives synaptic inputs distributed over n dendritic branches, each of them associated with a non-linear function ($s(n_i)$) and a functional weight over the cell body (a_i), itself associated with a threshold function g.

From Poirazi *et al.*, 2003

It should be noted that the two-layer model is conceptually very interesting, as it raises the possibility that some neurons could actually be best modelled by an "n-layer model". Notably, Häusser and Mel, in 2003, proposed a 3-layer model to describe CA1 pyramidal cells (Häusser and Mel, 2003). As is always the case with modelling approaches, the right balance to employ is to capture the most salient features of a given system with a minimal description (Major *et al.*, 2013).

In the next sections, I will present some examples of non-linear dendritic integration properties, and for this purpose, I will consider some documented cases from the literature.

III - 2 - a) Active conductances can counteract electrical filtering:

In a first example (Magee, 2000 - Figure I-12), CA1 pyramidal cells were shown to display two specific features counterbalancing the effects of electrical filtering. While passive properties of dendrites filter high frequency signals out, causing a decrease in amplitude and kinetics of electrical currents as they propagate to the soma, it was shown that, in CA1 pyramidal cells, local EPSPs in dendrites have increasingly higher amplitudes as they are more and more distal, which compensates for the decrease in amplitude they will experience while propagating to the soma. The process of increasing the number of post-synaptic receptors to increase the amplitude of the post-synaptic current *seems to serve the purpose* (such phrasing has to be written, and therefore read, with high caution: observing a correlation between two parameters A and B is not sufficient to prove any form of causality between them) of normalizing the peak amplitude of synaptic currents arriving in the soma, no matter where they originate from in the dendritic tree. It should be noted, however, that this phenomenon is not, strictly speaking, an active process: the fact that more current is delivered in distal dendritic

compartments is due to the fact that the synapses of distal compartments display more receptors, and not because a voltage-dependent phenomenon causes these receptors to deliver more current.

Additionally, there exists a gradient of HCN channels along these dendrites, which are opened at rest and deactivated by local changes in membrane potential. The "virtual" outward currents (and local changes in input resistance) produced by their closure leads to a faster repolarization of the cell membrane, which counterbalances temporal widening of distal inputs due to electrical filtering. Ultimately, this phenomenon makes distal input as equal as proximal ones to summate over time.

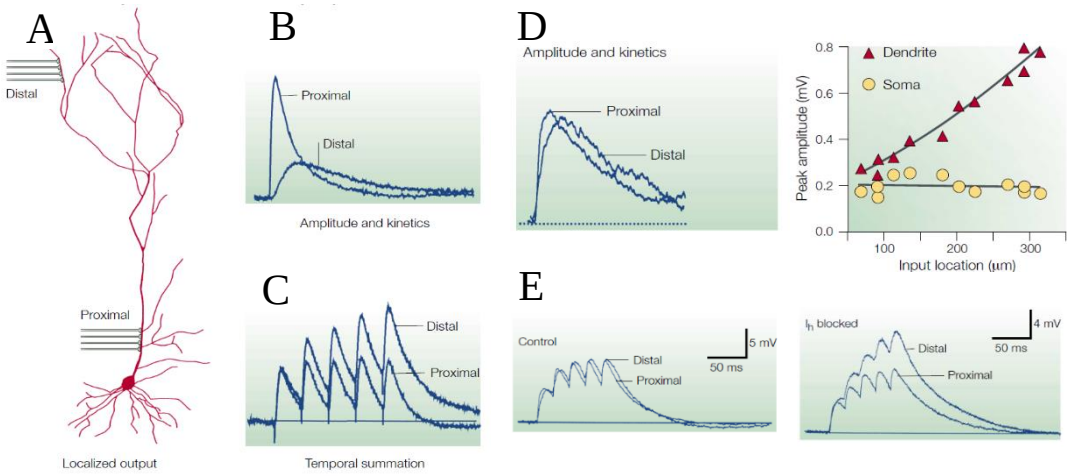

Figure I-12: Dendritic integration of excitatory inputs in CA1 pyramidal cells:

A) Scheme of a CA1 pyramidal cell, receiving excitatory inputs onto proximal of distal compartments of the dendritic tree; **B)** Due to passive properties, distal inputs are ***expected*** to have smaller amplitude and slower kinetics than proximal inputs, when recorded at the soma; **C)** Slower kinetics of distal inputs ***should*** in turn lead to stronger temporal summation, compared to proximal inputs; **D)** Surprisingly, proximal and distal inputs have similar amplitude at the soma (left panel). This is caused by stronger local depolarisations caused by distal inputs (right panel); **E)** Temporal summation is also comparable for both type of inputs (left panel), due to a compensation mechanism produced by a gradient of HCN channels along the dendrites (right panel).

Adapted from Magee, 2000

The main conclusion of this particular review is that CA1 pyramidal cells are endowed with specific mechanisms, which normalize the amplitude of somatic EPSPs (through increase in local synaptic conductance) and their ability to summate temporally (through an I_h gradient along their dendrites), no matter the distance between the synaptic site and the soma. Here, the **active component** is the **gradient of HCN channels**.

III - 2 - b) Active conductances in non-linear dendritic integration:

In this paragraph, I will show one example, among many, where synaptic inputs were shown to summate non-linearly. In layer 2/3 CA3 pyramidal cells of the somatosensory cortex, it was demonstrated that co-activation of clustered synaptic sites in the basal dendrites leads to compound EPSPs having a peak amplitude systematically higher than the peak amplitude of the arithmetic sum of the individual responses (Branco and Haüsser, 2011 - Figure I-12), a phenomenon known as supralinearity. By performing glutamate uncaging experiments in diffraction limited spots onto dendritic spines (an experimental manipulation which aims at mimicking synaptic transmission with high spatial and temporal resolution), the authors recorded synaptic responses when a single synapse was photo-stimulated at a time, or when multiple synapses were co-activated, and found that the non-linearity observed in control conditions was dampened by blocking L-type Voltage-Gated Calcium Channels (VGCCs), and abolished by blocking NMDA receptors with D-AP5. Their results indicate that photo-uncaging onto single synaptic sites mostly triggers the opening of AMPA receptors, and little activation of VGCCs and NMDA receptors; however, co-activation of multiples synaptic sites causes a local depolarization sufficiently strong to remove Mg^{2+} ions from the interior of NMDA receptors in individual spines, which then become available for opening by photo-released glutamate. Consequently, synaptic currents in the co-activation regime are now a sum of individual AMPA currents already present in single stimulation responses, along with NMDA- and VGCC-mediated currents recruited exclusively in the co-activation regime. The supralinearity observed is then due to the fact that NMDA/VGCC currents and AMPA currents are all inward currents (*i.e.*, if they had an opposite polarity, a sublinearity would be observed instead).

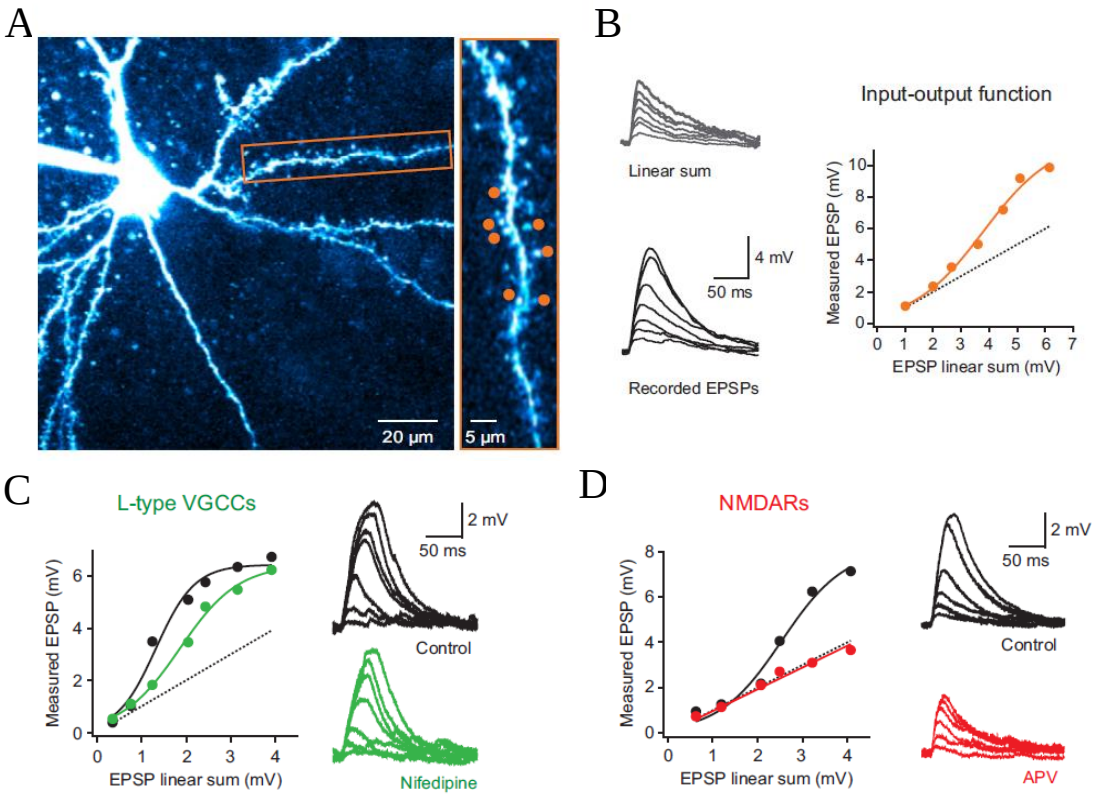

Figure I-13: Supralinear integration of clustered excitatory inputs in L2/3 pyramidal cells:

A) Image of a pyramidal cell filled with a fluorescent dye. Inset shows a specific dendritic branch with its spines, onto which glutamate uncaging was performed to mimic synaptic activation (orange dots); **B)** Comparison between the linear sum of the 7 individual responses (top) and the recorded responses during simultaneous activation (bottom). The corresponding I/O function is characteristic of supralinearity; **C)** Similar as in B, but before (black) and after (green) blockade of L-type VGCCs; **D)** Same as in B, but before (black) and after (red) blockade of NMDA receptors.

Adapted from Branco and Häusser, 2011

Put in a more general context, a non-linearity is observed in CA3 pyramidal cells because of the additional recruitment of an **active** mechanism (voltage- and ligand-gated NMDA receptors + VGCCs) in a specific regime of activation (**clustered activation**).

III - 2 - c) Role of neuronal morphology in non-linear dendritic integration:

In another article (Abrahamsson *et al.*, 2012), it was shown that inhibitory stellate cells in the cerebellar cortex display a gradient of Paired-Pulse Ratio (PPR) along the somato-dendritic axis (*i.e.*, at 50Hz, PPR = 2 in the soma and 1.4 in the dendrites). The origin of this difference was shown not to lie in the pre-synaptic element, but rather in the post-synaptic one. Indeed, the dendrites of SCs are very thin, and represent small electrical compartments. As a

consequence, EPSCs cause a significant local decrease in driving force (even if SCs are recorded from in the voltage-clamp configuration), which leads to smaller subsequent entry of current. This dynamic phenomenon (excitatory currents decreasing the driving force *during* the entry of current) causes a local saturation, where the release of more and more synaptic vesicles from the pre-synaptic element doesn't lead to a linear increase in EPSC amplitude (as hypothesized in Rall *et al.*, 1967). Consequently, while the PPR is close to 2 in the somatic (linear) compartment, this ratio is smaller in dendrites because the second facilitated pulse enters a sublinear, saturating regime. Here again, the demonstration of sublinearity was done by photo-releasing glutamate onto clustered synaptic sites, and comparing the arithmetic sum of individual responses to the compound response when the same number of inputs are co-activated (Figure I-14, from Abrahamsson *et al.*, 2012).

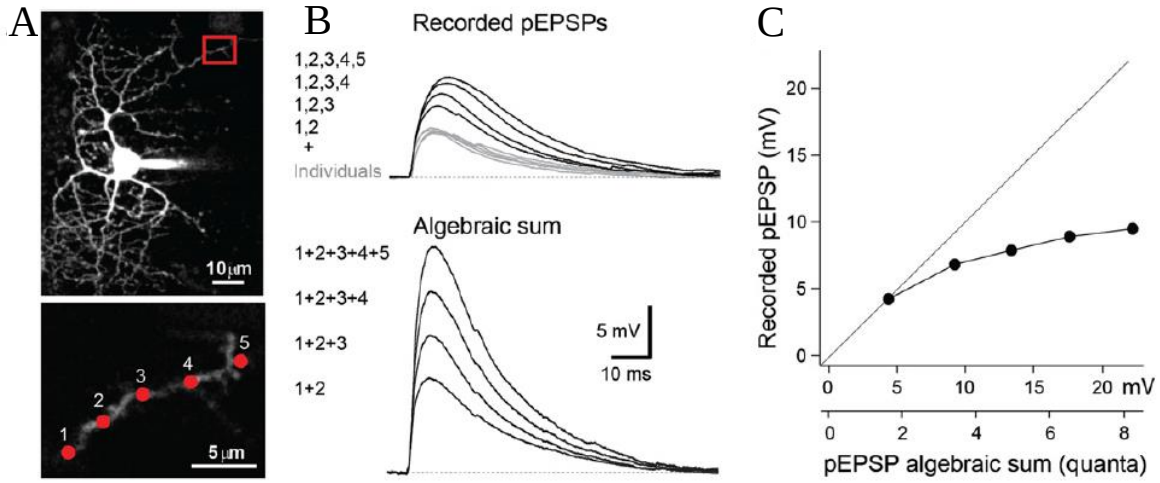

Figure I-14: Sublinear integration of clustered excitatory inputs in cerebellar stellate cells:

A) Image of a stellate cell filled with a fluorescent dye. Inset shows a specific dendritic branch onto which glutamate uncaging was performed to mimic synaptic activation (red dots); **B)** Comparison between the recorded sum of the 5 individual responses (grey traces - top), the compound synaptic responses (black traces), and the algebraic sum of the individual responses (bottom). **C)** The corresponding I/O function is characteristic of sublinearity;

Adapted from Abrahamsson *et al.*, 2012

The important conclusion of this third study is that **passive** morphological features *alone* (thin dendrites) can cause non-linear interaction of post-synaptic potentials. Here again, the non-linearity is observed in case of **clustered activation of synaptic events**.

III - 3) Integration of excitatory and inhibitory inputs:

III - 3 - a) Subcellular compartment targeting, and input/output relationship:

Since this thesis is about somatic-targeting interneurons of the cerebellar cortex, I would like to show here one example of the differential influence of dendritic- versus somatic-targeted inhibition onto principal cells in neural networks. In CA1 pyramidal cells it was shown that if inhibition is delivered to the dendrites, more excitation in the dendrites is required to reach a given firing rate (Figure I-15, from Pouille *et al.*, 2013). However, when inhibition is delivered to the soma, increasing excitation in the dendrites is not sufficient to reach similar firing frequencies. Therefore, dendritic inhibition acts as a rightward shift (subtractive operation) in the injected current/ firing rate curve of these neurons, while somatic inhibition causes a rightward shift and a decrease of maximal firing rate (subtractive and divisive operation).

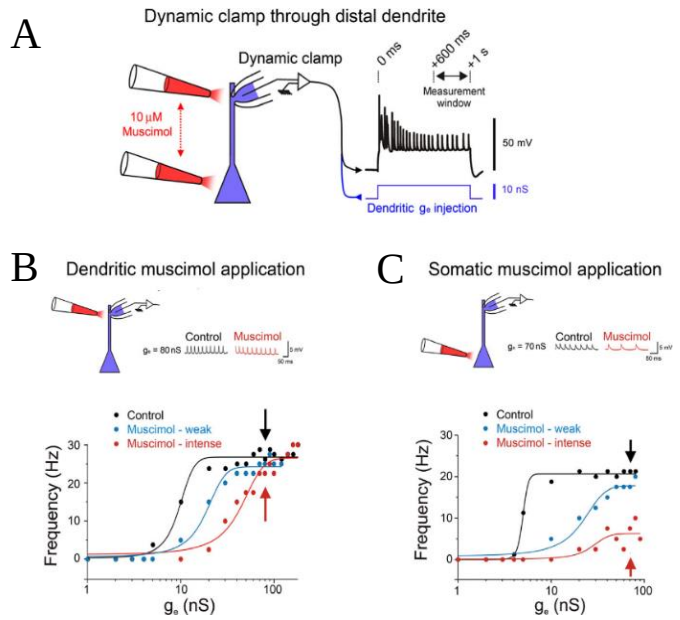

Figure I-15: Differential impact of somatic and dendritic inhibition:

A) Single cell patch-clamp recordings of CA1 pyramidal cells. The patch pipette is located in the dendrites, and dynamic clamp is employed to mimic excitatory inputs, while muscimol (agonist of $GABA_A$ receptors) is applied at the dendrites, or at the soma; **B)** firing rate is determined by the net balance between inhibitory and excitatory inputs received in the dendritic compartment; **C)** increasing dendritic excitation doesn't overcome somatic inhibition, and maximal firing rate is reduced.

Adapted from Pouille *et al.*, 2013

The explanation is that in dendrites, a given sum of excitatory and inhibitory currents flows down to the soma and axon initial segment, and the relative amplitude of this sum compared to the membrane resistance of the soma dictates the direction and magnitude of the voltage deflection, which ultimately underlies the generation of one or multiple AP(s). However, providing inhibition to the soma not only leads to an inhibitory current, but also to a reduction of somatic membrane resistance because of the opening of $GABA_A$ receptors. Therefore, if more excitation is delivered to the soma, it may overcome the amplitude of inhibitory currents to provide a net depolarizing current, but the sum of currents has now to polarize the local membrane resistance (rendered low by opening of $GABA_AR$). The somatic compartment is now “leaky”, and the maximal firing rate which can be reached is lowered. In

terms of electrical circuit, excitation and inhibition dictate the polarity of current reaching the soma (I), and delivering inhibition into dendrites only affects the net current I, while somatic application of inhibition affects both I and R, the membrane resistance. Ohm's law U = RI is therefore differentially affected whether inhibition is applied in dendrites (I only) or onto the soma (I and R).

This single example, among many, is indicative that dendritic-targeting stellate cells and somatic-targeting basket cells might play a different role in inhibiting their common post-synaptic targets, the Purkinje cells. Understanding the differential role of the two types of interneurons in shaping Purkinje cells output is a goal in itself, and would require a dense amount of work, but it would give powerful insights as to why many other brain circuits rely on different interneuron subtypes to deliver inhibition to the dendrites or the soma of the targeted cells.

III - 3 - b) Temporal integration of excitatory and inhibitory inputs: example of feed-forward inhibition:

In this thesis, I examined how the feed-forward recruitment of spikelets transmission in cerebellar basket cells could shape their spiking output. The mechanism, as I will show in Chapter III, is reminiscent of classical feed-forward inhibition (FFI) mediated by GABAergic synapses. In this section, I would like to present what is known about FFI as a general mechanism for information processing in the brain, with an emphasis on the FFI mediated by interneurons in the cerebellar cortex.

Feed-forward inhibition is a connectivity motif where a given set of excitatory synapses directly targets a principal cell, but also an inhibitory interneuron which also targets the principal cell. First demonstrated in the hippocampus, FFI was shown to be critical to minimize temporal summation of excitatory inputs (1), and increase temporal precision of spike output (2) in pyramidal cells (Figure I-16, from Pouille and Scanziani, 2001).

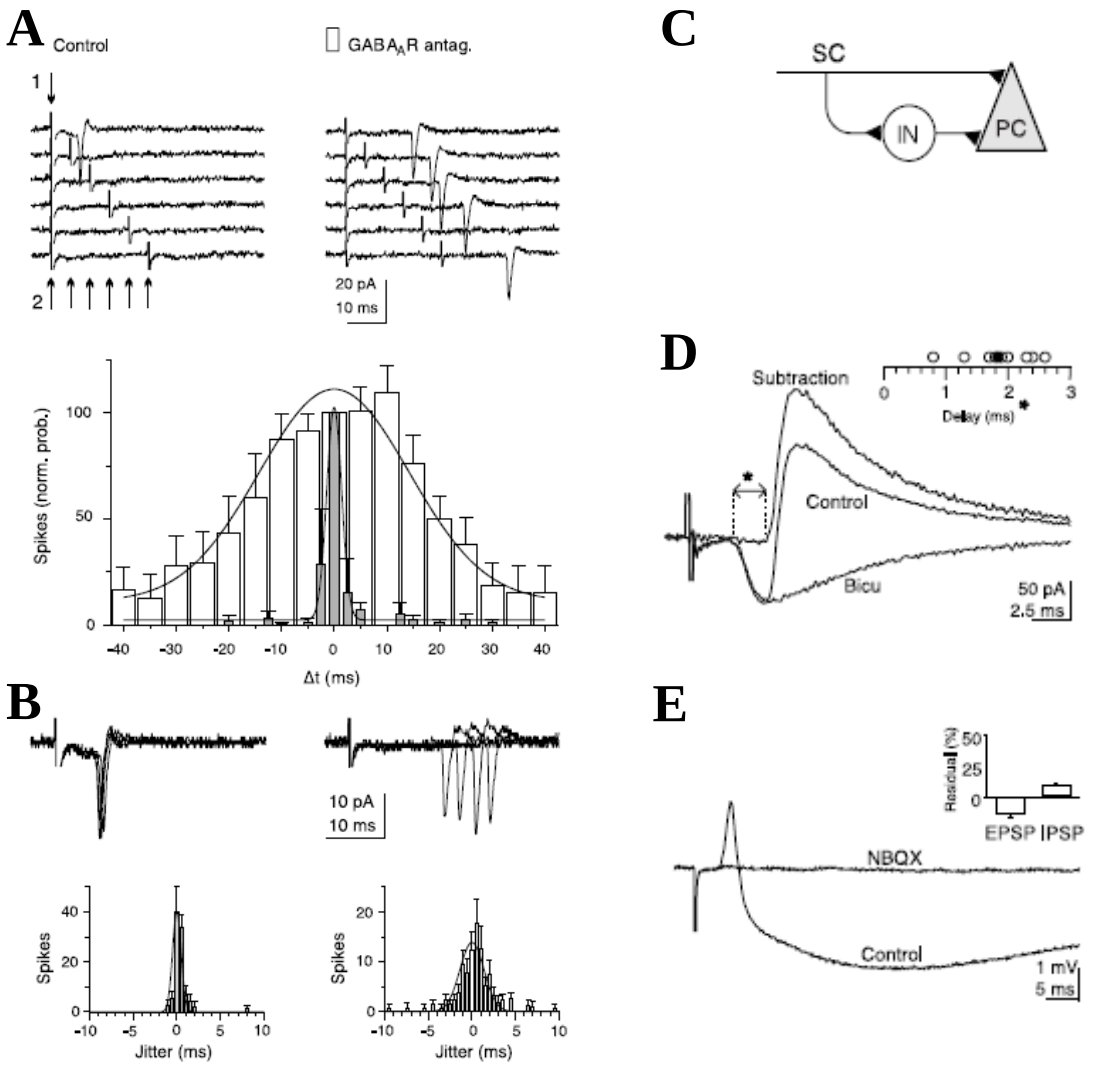

Figure I-16: Feed-forward inhibition in the hippocampus:

A) top panels: Stimulation of two independent Schaeffer Collaterals (SC - the excitatory inputs) with different time delays (arrows) produces different spike output probabilities in Pyramidal Cells (PC - the principal cell), in control conditions (grey bars) or absence of GABAergic inhibition (white bars). **Lower panel:** Blocking inhibition dramatically increases the time window for EPSP summation and spiking; **B)** During coincident stimulation of the two set of SCs, spike precision is lowered when inhibition is blocked; **C)** Schematic circuit diagram showing how SCs directly excite PC, but also interneurons (IN) which inhibit the PC; **D)** Voltage-clamp recordings in PC reveal that single SC stimulation produces a sequence of direct excitatory current, followed by a GABAergic current (blocked by bicuculline), recruited within a time delay of ~2ms; **E)** NBQX application (which blocks excitatory transmission from SC), blocks both the direct inward current and the secondary outward current, revealing that the latter is recruited by SC inputs and not direct electrical stimulation from the electrode.

Adapted from Pouille and Scanziani, 2001

A similar connectivity motif was later shown to promote a qualitatively similar effect on neuronal processing within the cerebellar cortex. In the latter case, FFI was not only demonstrated on the principal cells of the circuit (the Purkinje Cells), but also between the interneurons themselves (Figure I-17, from Mittman *et al.*, 2005).

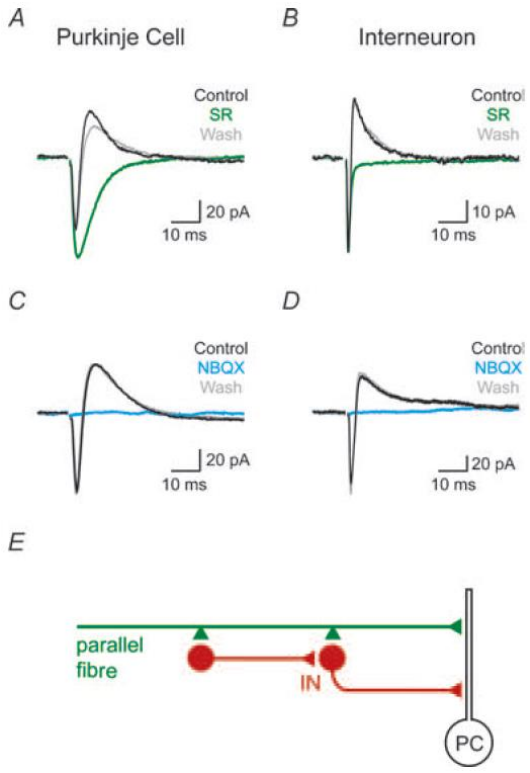

Figure I-17: Feed-forward inhibition in the cerebellar cortex:

A) Voltage-clamp recordings of a Purkinje cell after stimulation of Parallel Fibers (PFs), in control condition (black trace), and when GABAergic inhibition is blocked (green trace); **B)** Similar as in A), but for inhibitory interneurons patch-clamp recordings; **C)** Blocking excitatory transmission from PFs blocks both inward and outward currents in Purkinje cells; **D)** Same as in C), but for interneurons; **E)** Schematic FFI diagram explaining the recordings from A) to D): PFs synapse onto interneurons and PCs, so that recordings in PC show direct inward currents from PFs, and indirect outward current from disynaptically recruited interneurons; similarly, interneurons display direct inward currents from PF, and indirect outward currents from other interneurons.

Adapted from Mittman *et al.*, 2005

Therefore, FFI is a canonical connectivity motif which limits temporal summation of excitatory inputs by the disynaptic recruitment of inhibitory interneurons which "cut" the tail of the direct EPSPs. FFI thus allows neurons to process excitatory inputs faster than what their membrane time constant would suggest. These examples highlight the importance of temporal recruitment of multiple inputs in the dendritic integration behaviour to understand their input/output relationship in the time domain.

III - 4) Electrical synapses in the context of dendritic integration:

I wish to present here one article describing the role of electrical synapses in dendritic integration. The reason for this particular focus is two-fold. Firstly, because a large portion of the work presented in this thesis will deal explicitly with electrical synapses; and secondly, because electrical synapses are quite unique in the context of dendritic integration, in the sense that they are both a source of inputs for a given neuron (hence their name "synapse"), but also a key determinant of passive properties. Indeed, being always opened at rest, they fundamentally alter the electrotonic behaviour of neurons expressing them (Hjorth *et al.*, 2009; Vervaeke *et al.*, 2012; Maex and Gutkin, 2017).

The group of Idan Segev recently published an article (Amsalem *et al.*, 2016) where they quantitatively examined the passive role of electrical synapses in dendritic integration of L2/3 Large Basket Cells (LBCs). Here, passive role means "without contribution of suprathreshold event", such as AP-generated spikelets. They combined electrophysiological recordings of single cells and network modelling of electrically-connected cells, to systematically examine the influence of electrical synapses on passive parameters such as input resistance and membrane time constant.

First of all, they performed *in vitro* recordings of LBCs along with 3D morphological reconstruction and modelling of passive parameters in the NEURON environment (Hines and Carnevale, 1997). They used templates of morphologically-reconstructed cells to create a network of electrically-connected cells, and systematically varied the electrical synaptic conductance and the number of electrical partners for each cell, in a range of values consistent with previous findings. The key point of their method is to model a network of electrically-connected cells, and provide them with intrinsic passive properties (*i.e.*, R_m, C_m and R_i) so that, in the end, the modelled cells display an electrophysiological response coherent with *in vitro* observations (that is, when modelled data match a set of recordings obtained when the cells *were* connected to their electrical partners). And once the modelled cells reproduce single cell *in vitro* observations, it is possible to set, in the model, a null synaptic conductance for electrical synapses, and directly examine the electrophysiological behaviour of both the individual cells and the network when electrical synapses are virtually absent.

Their analysis reveals how much electrical synapses (unitary strength and mean number) influence estimates of passive properties such as input resistance and membrane time-constant. They notably showed that, depending on the different modelling parameters, L2/3 LBCs can have, in reality, input resistance and membrane time constants between two and four times higher than what would be estimated when neglecting the influence of electrical synapses. However, most of the errors they describe are, in reality, related to semantics and ill-defined concepts, and their main conclusion is to show how big can be the errors in estimating passive properties in a cell-type forming electrical synapses. The very problem in studying passive properties in electrically-connected cells is that models employed to fit the data are mostly inadequate by nature: they are usually designed with inherent assumptions, and one of them is that "dendritic branches can be regarded as cylindrical cables". However, the very presence of electrical synapses allows electrical currents to spread into electrical neighbours, and not only down or across the dendrites of the cell under study. The model employed to fit the experimental data is therefore ill-suited by essence, as one of its assumptions is not supported by the system

under study. Nevertheless, in such a scenario, the authors did provide an excellent method and modelling approach to correctly treat cell-types forming electrical synapses.

Finally, in the context of dendritic integration, and the passive role of electrical synapses, this study provided further evidence that these synapses, being opened at rest, can passively shape synaptic responses. The authors notably showed that, by a mechanism closely mimicking GABAergic tonic inhibition, postsynaptic potentials have smaller amplitude and shorter time constants when electrical synapses are present, due to a reduction in *apparent* input resistance and membrane time constant (Figure I-18, from Amsalem *et al.*, 2016).

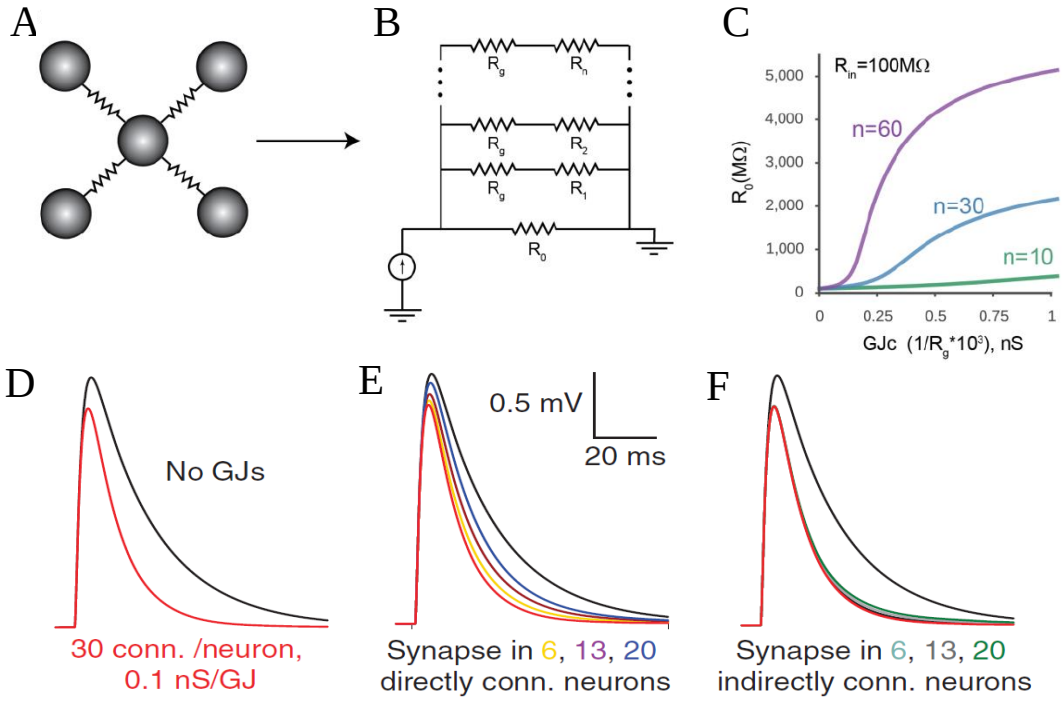

Figure I-18: Passive role of electrical synapses in intrinsic properties of neurons:

A) Scheme of a network of point neurons, where the neuron in the centre (neuron 0) is connected by electrical synapses to 4 partners; **B)** Corresponding electrical circuit, where the number of electrical partners varies from 1 to n; R_g denotes the (uniform) resistance associated to electrical synapses, while R_0, R_1, R_2, ... R_n are all considered equal, and refer to the *intrinsic* input resistance of the cells; **C)** In order to obtain an *apparent* input resistance of R_{in} = 100MΩ for a given cell, the number of electrical partners (n=10, 30 or 60), and the conductance of the GJs (GJc) allow to estimate the *intrinsic* input resistance of the cell (R_0); **D)** Addition of electrical synapses reduces the peak amplitude of excitatory inputs, and shorten their half-width, either through direct **(E)** or indirect coupling **(F)**.

Adapted from Amsalem *et al.*, 2016

IV) The cerebellum as a canonical microcircuit:

My PhD project aimed to examine how cerebellar basket cells process their excitatory inputs, with the long-term goal of comparing how their dendritic integration behaviour could be different from stellate cells, the second type of interneurons found in the cerebellar cortex which the host laboratory has already studied (Abrahamsson *et al.*, 2012; Tran-Van-Minh *et al.*, 2016). In order to set the context for the comparison between both cell-types, and their role in physiology, I will now describe the cerebellum in general, and more specifically the cerebellar cortex. I will later present models and experimental evidence of the nature of cerebellar computations, and how learning takes place in the cerebellar cortex. Some insights on the link between cyto-architecture (structure) and physiological role (function) will be brought by examining cerebellum-like structures, where such links have already been established, at least partially.

IV - 1) Anatomy of the cerebellum:

The *cerebellum* is a specific part of the brain, located in the dorsal part of the nervous system, in vertebrates. Its name derives as a diminutive of the Latin word *cerebrum*, and can therefore be translated as "small *cerebrum*". It is divided into two anatomically-defined regions (Figure I-19, from D'Angelo and Casali, 2013): the cerebellar nuclei, located in the centre; and the cerebellar cortex, located on the outer surface. Mossy Fibers (MFs), originating from many brain regions, enter the cerebellum via three peduncles (called inferior, middle, and superior peduncles), and make excitatory connections with up to four types of post-synaptic targets: deep cerebellar nuclei neurons; Golgi Cells; unipolar brush cells (which are mainly found in the vestibular cerebellum); and granule cells, which constitute the input layer of the cerebellar cortex. The inferior olive (a structure found in the medulla) also provides an important set of excitatory inputs (called the climbing fibers) to the deep cerebellar nuclei neurons, as well as to the Purkinje cells located in the cerebellar cortex.

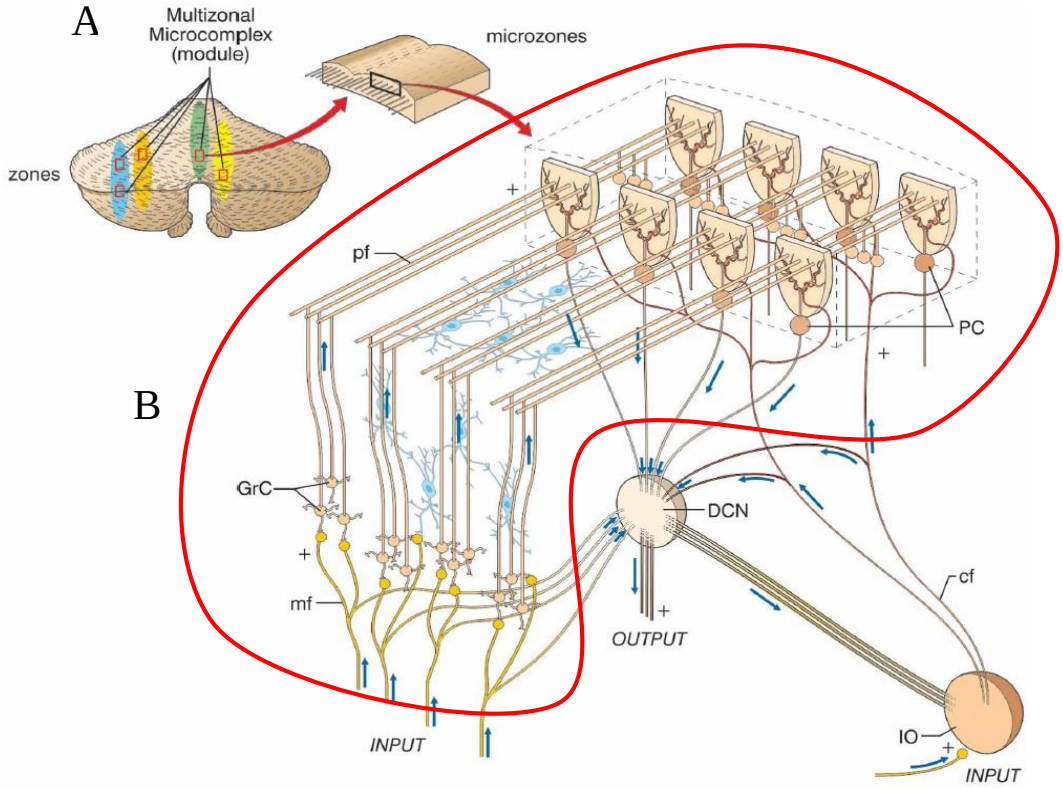

Figure I-19: Modular organization of the cerebellum:

A) flattened view of the cerebellum, with highlighted regions representing four ideal zones, further divided into microzones aligned along the parasagittal axis; **B)** Each microzone is composed of mossy fiber inputs (mf), going to the cerebellar cortex (in red), and also to the deep cerebellar nuclei (DCN). DCN neurons communicate with neurons from the inferior olive (IO). Purkinje cells from the cerebellar cortex receive climbing fiber inputs from the IO, and send inhibitory projections to the DCN neurons.

Adapted from D'Angelo and Casali, 2013

From a functional point of view, the MFs which project to a specific microzone of the cerebellar cortex also project to output cells in the deep cerebellar nuclei which receive inhibitory inputs from Purkinje cells of the same microzone. Neurons from the inferior olive project onto the Purkinje cells which inhibit the same subset of neurons in the deep cerebellar nuclei. Altogether, MFs, specific Purkinje cells in the cerebellar cortex, neurons from the inferior olive and deep cerebellar neurons are strongly interconnected, and form a functional module. Multiple modules are spread along the coronal axis, and show very little intrinsic variability between each other. However, they mostly differ by the set of afferent inputs they receive, and their main projection sites. I will now focus on the cerebellar cortex, as it is the main component of these modules.

IV - 2) The cerebellar cortex:

The cerebellar cortex, displaying very few different cell-types organized in a quasi-crystalline structure, has long been regarded as a canonical microcircuit. It can be decomposed into three layers: the granular layer (1); the molecular layer (2); and the Purkinje Cells layer (3), as shown on Figure I-20 (from Apps and Garwicz; 2005), and described in the next sections.

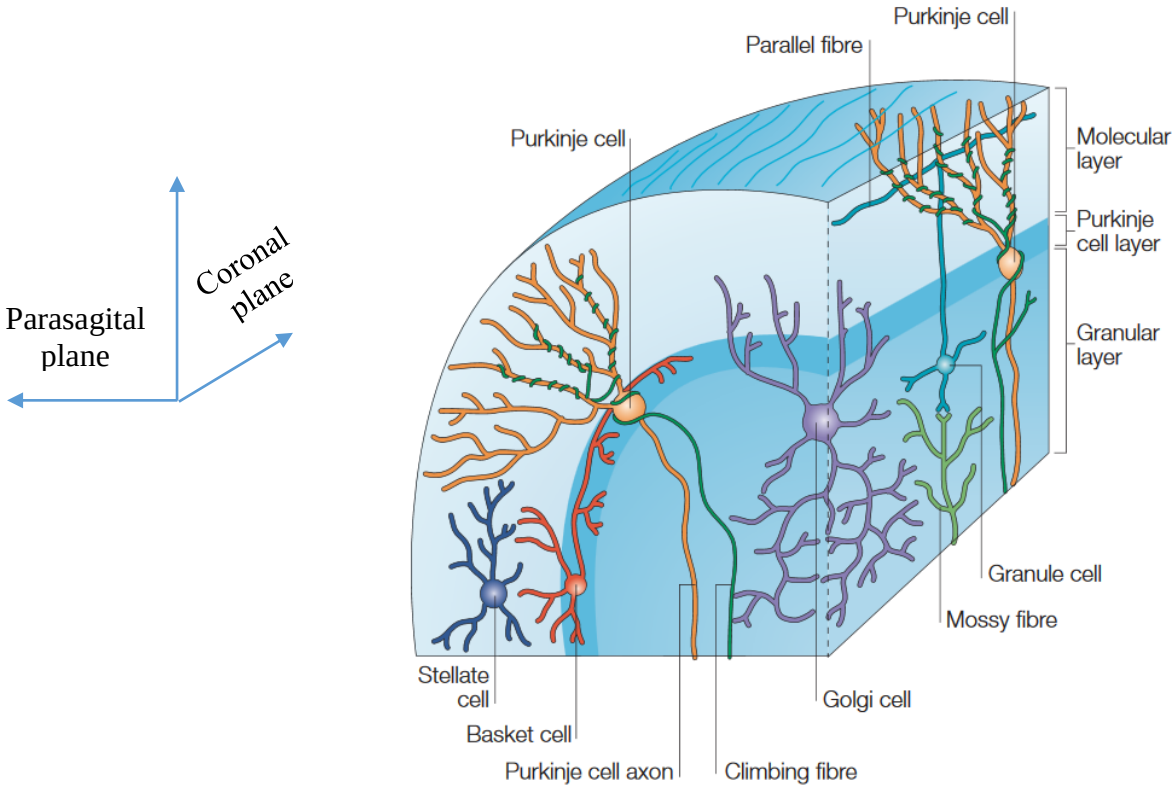

Figure I-20: Cell-type diversity and connectivity of the cerebellar cortex:

A detailed description of the circuit is provided in the main text. Unfortunately, this scheme represents basket cells in the Purkinje cell layer (PCL), but in reality, these cells are located in the molecular layer, close to the PCL

Adapted from Apps and Garwicz, 2005

IV - 2 - a) Cell-type diversity and cytoarchitecture:

- The granular layer:

The Granule Cells (GCs), which represent one of two types of excitatory inputs of the cerebellar cortex, represent at least half of the neurons in the whole CNS (Ito, 1984). They receive excitatory inputs from mossy fibers (MFs), which convey information from numerous brain regions (spinal cord, peripheral nerves, and the brainstem - Shepherd and Grillner, 2010). GCs relay this information through their axons, classically decomposed into two different sections: an initial ascending axon – which goes through the Purkinje cells layer to the

molecular layer - and the subsequent Parallel Fibre (PFs), running through the molecular layer in the coronal plane after a "T-shaped" bifurcation from the ascending axon. These parallel fibers are extremely numerous (it is estimated that ~175,000 PF synapses onto a single PC, although most of them are silent - Napper and Harvey, 1988; Isope and Barbour, 2002), and they can extend up to 2.5 mm in the coronal plane (Harvey and Napper, 1991). Therefore, they constitute (potential) functional bridges between different modules of the cerebellar cortex, in the sense that a Purkinje cell from a given microzone can receive excitatory inputs from GCs from a different microzone.

The second type of neurons found in the granular layer are the inhibitory Golgi Cells (GoCs). Their soma and proximal dendrites lie in the granular layer, and their main dendritic tree extends in the molecular layer, while their axonal projections target GCs. Therefore, they receive excitatory inputs from MFs as well as PFs, and consequently, they can deliver both feed-forward and feed-back inhibition onto GCs, through MF and PF recruitment, respectively. Additionally, they express electrical synapses with neighbouring GoCs, which tend to synchronize (Dugué *et al.*, 2009; Van Welie *et al.*, 2016) or desynchronize (Vervaeke *et al.*, 2010) their activity, depending on the dynamics of the incoming excitatory inputs.

It should also be noted that, in the vestibulo-cerebellum, there exists another cell-type called the unipolar brush cells (UBCs), which is not found in all parts of the cerebellar cortex. However, some cerebellum-like structures (which I will present later) present UBC-like cells. UBCs are excitatory interneurons, excited by MFs, and projecting onto GCs.

- The molecular layer:

In the molecular layer, PFs contact the dendritic trees of Purkinje cells (PCs), Golgi Cells (GoCs), as well as basket cells (BCs) and stellate cells (SCs). Altogether, BCs and SCs form the population of molecular layer interneurons (MLIs). PCs, GoCs, and MLIs are all inhibitory neurons. The second type of excitatory inputs found in the molecular layer are the CFs (originating from the inferior olive). During development, multiple CFs synapses onto one given PC, but during maturation of the circuit, most of these connections are pruned, and in adulthood, each PCs is contacted by a single CF (Crepel *et al.*, 1981), which wraps around the main trunk of its dendritic tree. It is reported that the CF-PC synapse is among the strongest excitatory synapse found all throughout the CNS (Eccles *et al.*, 1966; Harting, 1997). CFs also provide a potent excitatory action onto MLIs by spillover of glutamate, which notably allows multiple CFs to excite a given MLI (Szapiro and Barbour, 2007).

Finally, MLIs are connected via GABAergic and electrical synapses to each other (Rieubland *et al.*, 2014), and deliver GABAergic FFI onto PCs (Mittman *et al.*, 2005). I will further detail the connectivity between interneurons in the next section of this introduction.

- The Purkinje cell layer:

The cell bodies of PCs are located in the Purkinje cell layer. They constitute the sole output of the cerebellar cortex, by sending their axons to neurons in the deep cerebellar nuclei. In contrast to what is shown in Figure I-20, BCs somata do not lie in the Purkinje cell layer, but rather in the molecular layer.

IV - 2 - b) Differences between stellate cells and basket cells:

Investigation of MLIs has revealed that they are connected by both GABAergic and electrical synapses (Mann-Metzer and Yarom, 1999, Alcami and Marty, 2013, Rieubland *et al.*, 2014). Multiple studies have now shown that stellate-type cells and basket-type cells are not randomly distributed inside the molecular layer, and that each cell type features specific properties. The general idea is as follows: stellate-type cells are close to the pia (outer third of the molecular layer), have a thin axon projecting onto other MLIs or dendritic compartments of Purkinje cells; rather short dendrites, radiating in all directions around the soma; with few and relatively weak electrical synapses. On the other hand, basket-type cells have their somata usually lying close the Purkinje cell layer (inner third of the molecular layer); display long axons forming the so-called “basket” and “pinceau” structures wrapping around Purkinje cell’s somata; their dendrites are very long, often reach the pia, and are arranged in a “fan” shape; finally, they form frequent and relatively strong electrical synapses with each other (Sultan and Bower 1998, Rieubland *et al.*, 2014). Moreover, one study has revealed differential mRNA expression levels (notably for genes coding for ion channels) in MLIs, according to their position along the molecular layer (Schilling and Oberdick, 2009), suggesting that SCs and BCs may have different electrophysiological properties on top of different morphological properties and patterns of synaptic connections. There exists *in vitro* and *in vivo* evidence that SCs have a weaker inhibitory impact on PCs than BCs (Vincent and Marty 1996; Chu *et al.*, 2012), but these differences may be due to a differential recruitment of each type of MLIs along the coronal extension of PFs (Santamaria *et al.*, 2007). Furthermore, SCs are more likely to only produce a local clamp of the membrane voltage in the dendritic tree of PCs (Jaegger *et al.*, 1999), suggesting that the weak inhibitory action of SCs recorded at the soma of PCs may

underestimate their role in circuit function. It should also be noted that ephaptic transmission has been demonstrated at the BC-PC synapse specifically (Blot and Barbour, 2014). The authors showed that the presynaptic AP in BC produces a significant voltage change of the local extracellular space, which influences PC spike output. This significant influence is primarily caused by the very morphology of the synapse, where the characteristic pinceau structure of BC terminals wraps around the Axon Initial Segment (AIS) of the PC. BCs, through ephaptic transmission, can therefore mediate near-instantaneous inhibition of PCs, and virtually create a "negative weight GC-PC synapse", functionally different from a GC-MLI-PC synapse recruiting classical inhibition with a 1-2ms time delay associated to the disynaptic recruitment of the MLI (Mittman *et al.*, 2005).

Finally, it should be noted that studies conducted on MLIs usually agree on one particular point: the distinction between “stellate-type” and “basket-type” cells is not always clear, as the features described above more likely represent extreme cases and idealized properties of either type, but a gradient of morphological and electrophysiological properties along the molecular layer is closer to the reality (Figure I-21, from Rieubland *et al.*, 2014).

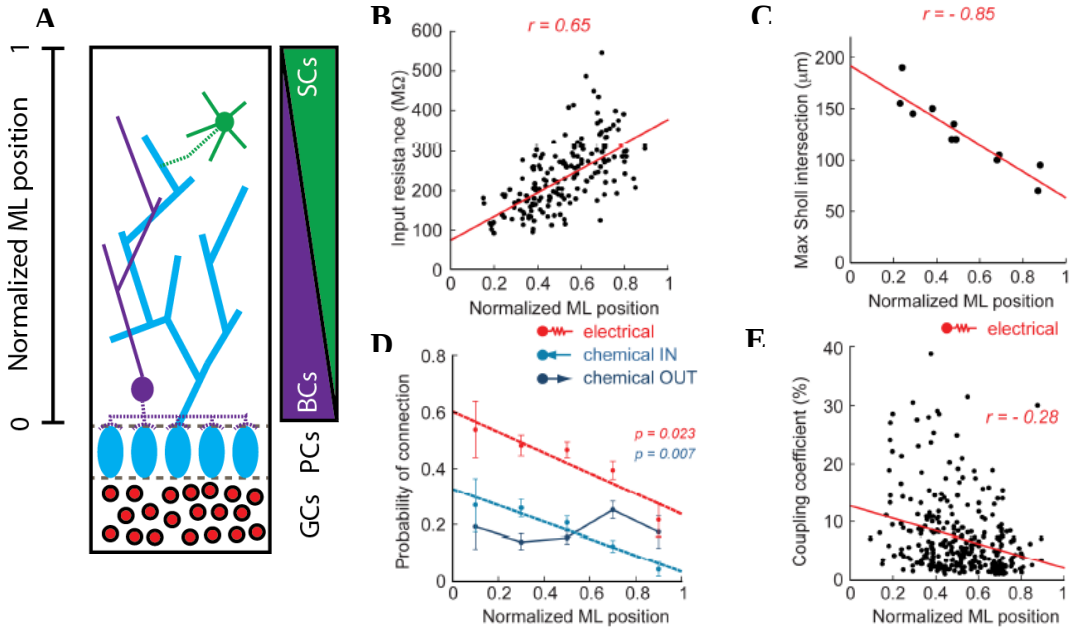

Figure I-21: Gradients of morphological, electrophysiological, and connectivity features of MLIs, along the molecular layer:

A) Diagram of the cerebellar cortex, showing that BCs are more numerous in the lower part of the molecular layer ("0" normalized ML position), while SCs are more numerous in the upper part ("1" normalized position); **B)** Input resistance increases with somatic position of the MLI along the ML; **C)** Maximal dendritic length decreases with ML position; **D)** For a given MLI, the likelihood that it forms an electrical synapse with a neighbouring MLI decreases with its position along the ML; **E)** When an electrical synapses is found between two MLIs, the coupling coefficient (a proxy for electrical synaptic strength) decreases with ML position.

Adapted from Rieubland *et al.*, 2014

Because electrical connectivity is more prevalent and stronger between BCs than SCs, it suggests that BCs are a better model to investigate the biophysical properties of spikelet transmission in the MLI population. Moreover, differences between dendritic length, input resistance, and electrical connectivity strongly suggest that BCs and SCs may have different passive properties, which would be critical in influencing their dendritic integration properties.

IV - 2 - c) Synaptic plasticity in the cerebellar cortex:

One way for the brain to keep track of the passage of time, or store memories about past experiences, is to induce synaptic plasticity at the appropriate connections between neurons. In the cerebellar cortex, multiple forms of synaptic plasticity have been demonstrated. For example, repetitive activation of PFs on short time scales (tens of millisecond) leads to a gradual increase in post-synaptic potential peak amplitude in MLIs (Bao *et al.*, 2010; Abrahamsson *et al.*, 2012), a phenomenon called short-term potentiation (STP). In contrast, most MF-GCs synapses in lobule X of the cerebellar vermis display a gradual decrease of post-synaptic responses on short time scales (short-term depression, STD - Chabrol *et al.*, 2015). Synaptic facilitation and depression (*i.e.*, increase or decrease in synaptic weights, respectively) can also be observed on longer time scales (hours, days), under certain conditions. For example, repeated stimulation of PFs alone classically induces long-term potentiation (LTP) of PF-PCs synapses, and long-term depression (LTD) of PF-MLI synapses (Lev-Ram *et al.*, 2002; Jörntell and Ekerot, 2002), while pairing PFs stimulation with CFs stimulation induces LTD at the PF-PC synapse and LTP at the PF-MLI synapses (Ito and Kano, 1982; Sakurai, 1987; Jörntell and Ekerot, 2002; but see Bouvier *et al.*, 2018). PCs display a potentiation of MLI-PC GABAergic synapses when these inputs are paired with CF stimulation (Kano *et al.*, 1992; He *et al.*, 2014), and PF-MLIs synapses can further experience LTP or LTD depending on the frequency of PF activation (Soler-Llavina and Sabatini, 2006; Bender *et al.*, 2009).

In a future section of this introduction, I will present how these different forms of synaptic plasticity underlie different aspects of cerebellar learning.

IV - 3) Cerebellum-like structures:

In terms of cell-types diversity, and connections between them, the cerebellum as a lot in common with other brain regions found in vertebrates, such as the auditory and electro-sensory systems. The similarities are so salient that these structures are often referred to as "cerebellum-like structures". The common cell-types are the granule cells (and their associated parallel fibers), stellate-like inhibitory interneurons, principal cells resembling Purkinje cells, DCN-like neurons and IO-like neurons (Warren and Sawtell, 2016; Roberts and Portfors, 2008 - Figure I-22). The connectivity between these cells is remarkably similar to that found in the cerebellum, and some plasticity rules seem to be shared by homologous synapses in each structure. Notably, co-activation of PFs and Purkinje-like cells induces Long-Term Depression (LTD) of PF-PCs synapses (Bell *et al.*, 1993; Tzounopoulos *et al.*, 2004).

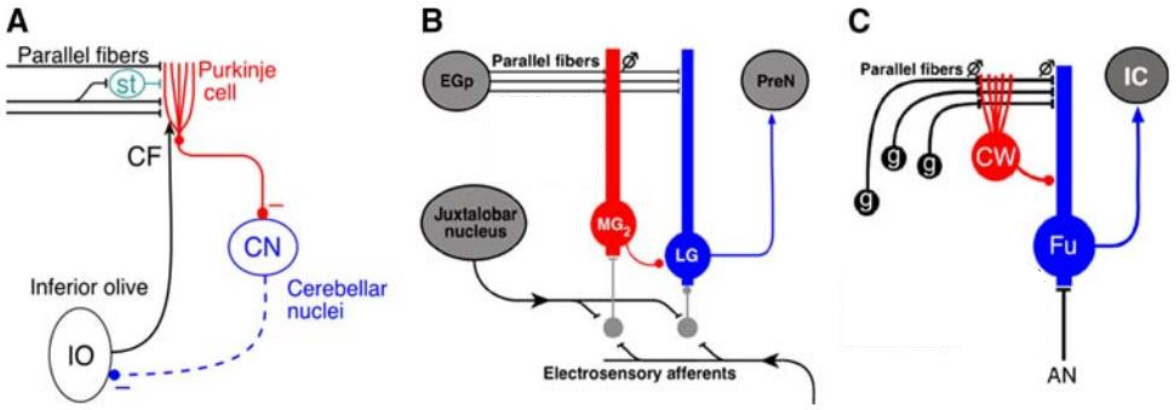

Figure I-22: Cerebellum-like structures:

A) simplified circuit diagram of the cerebellum; st: stellate cells; CF: Climbing Fibers **B)** Electrosensory lateral line lobe (ELL) of the mormyrid electric fish; EGp: eminentia granularis posterior; MG: medium ganglion cells; LG: large ganglion; **C)** Dorsal Cochlear Nucleus (DCN); g: granule cells; CW: cartwheel cell; Fu: fusiform cell; IC: Inferior Colliculus.

Adapted from Roberts and Portfors, 2008

These similarities further support the idea that the cerebellum - and more particularly, the cerebellar cortex - is a canonical microcircuit, and studying cerebellum-like structures can provide valuable insights about the internal computation performed by the cerebellum itself (a point I will address in a future section).

IV - 4) Role of the cerebellum in physiology:

Given its repeated and stereotyped organization, the cerebellar cortex has long been regarded as a canonical microcircuit (Eccles, Ito and Szentagothai, 1967). The low diversity of

the cell types it contains, along with their precise geometrical arrangements, and the stereotyped connections between them, has set a biological ground to make testable predictions about the computation it performs. It was initially thought that the cerebellum is key in motor coordination and learning, but experimental and medical observations over the last decades have sufficiently accumulated to indicate that the cerebellum plays a role in very diverse cognitive functions.

In the next section, I will review models and experimental observations of cerebellar computations. Given that most of these computations have been considered in the context of sensory motor learning, I will also try to describe how they can be thought of in more abstract terms, in order to present higher order functions of the cerebellar cortex.

IV - 4 - a) Early models of pattern separation in the cerebellar cortex:

In 1969, David Marr proposed a theory of the cerebellar cortex (Marr, 1969), where CF signalling in PC would induce changes at PF-PC synapses in order to learn specific movements. In his theory, after repetitive training by CF inputs, PCs could "learn" to fire when activated by a certain set of coactive PF inputs, those which were active at the time of CF input during the training. His theory, however, proposed that co-activation of CF and PFs would cause LTP at PF-PC synapses (this hypothesis has been largely falsified since then; but again, see Bouvier *et al.*, 2018), and that molecular layer interneurons would mainly serve as threshold adjusters for spike initiation in PCs.

In 1971, James Albus proposed a second theory of the cerebellar cortex, where he postulated that co-activation of CF and PFs would rather induce LTD of PF-PCs synapses. He also proposed two different computational roles for stellate and basket cells: basket cells could serve to assign a "virtual negative weight of PF-PC", by being recruited by PFs and projecting rapid inhibition onto PCs, while stellate cells could serve to speed up membrane repolarization after PF inputs in PCs (*i.e.*, provide FFI in local dendritic compartments).

Despite a few points of disagreement, both theories converged on some key aspects:

1) expansion recoding at MF-GC synapses helps in transforming similar MF input patterns into highly different GC output patterns, owing to the massive divergence of inputs at MF-GC synapses (tens of millions of MFs mapping onto tens of billions of GCs);

2) sparse activity in the GC layer is a fundamental requirement to avoid saturation of PF activity in the molecular layer (as it would otherwise impair pattern separation in downstream

PCs), and feed-forward and/or feed-back inhibition from GoCs to GCs could provide a threshold adjustment of GCs' recruitment, depending on the global level of activity in MFs.

3) CFs signalling onto PCs acts as a teaching signal to guide PF-PC synaptic weight adjustment, so that after repeated pairing of contextual information (relayed through the MF-PF pathway) with a teaching signal (relayed through the CF pathway), the sensory context is sufficient to induce an adequate PC firing, and does not require the "teaching signal" from CF any longer.

4) Combination of expansion recoding at MF-GC and sparse activity in GCs amplify PF pattern diversity, and the main role of PCs is to learn the appropriate PF patterns when an error is signalled.

Although these models were proposed in the 70s, and further refined since then, experimental evidence that the cerebellum performs pattern separation is still lacking, notably because of technical difficulties in recording the activity of small, densely packed GCs in vivo (reviewed in Cayco-Gajic and Silver, 2019).

Therefore, whether or not the cerebellum performs pattern separation is still undemonstrated. However, as I will briefly describe in the next section, the cerebellum has been shown to be of critical importance in other aspects of learning, and notably temporally specific learning. Whereas pattern separation was shown to be implementable by the very circuitry of the cerebellar cortex with modelling approaches, temporal specific learning has been experimentally demonstrated, but the underlying mechanisms are still not clear, and multiple models have been proposed to explain it.

IV - 4 - b) Eye-blink conditioning - a classical example of cerebellar temporal learning:

Historically, delayed eye-blink conditioning (a temporally controlled Pavlovian conditioning task) has been used to investigate certain forms of cerebellar learning. When an aversive unconditioned stimulus (US - like an air puff to the eye) is presented to a rabbit, the animal blinks instinctively to protect its eye (the unconditioned response, UR). If a neutral tone (serving as a conditioned stimulus, CS) is consistently presented shortly (hundreds of milliseconds to a few seconds - Schneiderman and Gormezano, 1964) before the air puff, then the animal learns to blink in anticipation of the air puff, thus acquiring a conditioned response

(CR). In 1984, McCormick and Thompson reported that lesion of the cerebellum abolishes the CR, while sparing the UR (Figure I-23; Medina *et al.*, 2000; Bracha, 2004).

It was later shown that information about the CS (*e.g.*, the tone) is relayed along the MF-GC pathway, while information about the US (*e.g.*, the air puff) is relayed through the CF pathway (Steinmetz *et al.*, 1989; Thompson and Steinmetz, 2009; Rasmussen *et al.*, 2014).

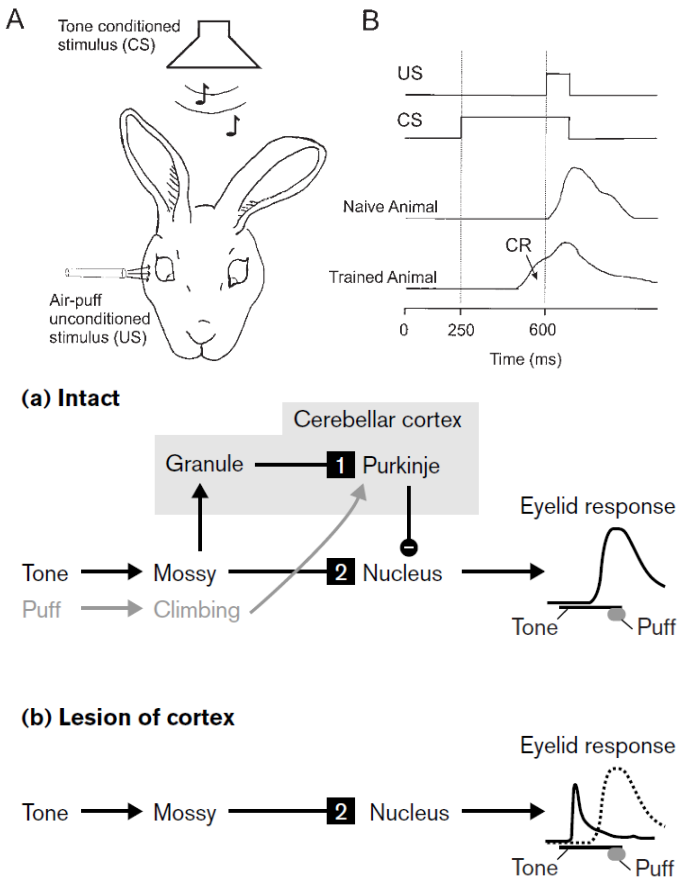

Figure I-23: Role of the cerebellum in eye-blink conditioning:

A) Scheme of the experimental paradigm; **B)** Timing onsets of air puff (US), tone (CS), and eye-blink response (CR), before and after training (naive and trained animal, respectively).

From Bracha, 2004

a) After training (*i.e.*, consistent pairing of contextual information relayed by MF and teaching signal relayed by CF), PC reduce their firing prior to the air puff, and relieve the cerebellar nuclei from inhibition, thus allowing the initiation of a motor command.

b) After cerebellar cortex lesion, the motor command is initiated at the time of tone onset, and the temporal match with puff onset is lost

From Medina *et al.*, 2000

Therefore, as a preliminary conclusion on this part, we can say that the cerebellum is at least known to be involved in introducing an adapted time-delay between the initiation of a motor command and a given sensory context.

IV - 4 - c) Implication of the cerebellum in sensory motor control:

From a historical point of view, the cerebellum has mainly been investigated in the context of motor learning. This focus may have been caused by different factors, such as the early report that cerebellar dysfunction is only manifested in motor deficits (Flourens, 1824); the influential models developed by Marr and Albus, which were concerned with optimizing motor control; the observation that acute cerebellar injuries in adult humans, more often than

not, cause motor deficits (reported in Wang *et al.*, 2014); or the fact that, by conducting experiments on animal models, probing involvement of the cerebellum in motor control is easier than probing its function in more cognitive aspects. Notably, among the most documented cerebellar functions in basic research, one can find: adaptation in vestibulo-ocular and optokinetic reflexes, and ocular saccades (see Ito, 1984), posture maintenance and balance (Crawley *et al.*, 2007); and eyeblink conditioning (described above).

Therefore, the involvement of the cerebellum in controlling movement precision and timing is largely accepted. However, this doesn't exclude that the cerebellum may be involved in non-motor functions.

IV - 4 - d) Implication of the cerebellum in non-motor tasks:

Towards the end of the 20th century, a growing amount of evidence has started to reveal cerebellar implication in non-motor behaviours, such has "mental skills" in general (Leiner *et al.*, 1986); attention, working memory, pain perception and addiction (reviewed in Strick *et al.*, 2009), or even Autism Spectrum Disorders (ASD - Wang *et al.*, 2014). There are also indirect evidence that the cerebellum is involved in spatial map elaboration in the hippocampus (Shiroma *et al.*, 2016).

This list could be further extended, but my intention here was to emphasize that the cerebellum is not exclusively involved in motor control. As reported in Moberget and Ivry, 2016:

"Meta-analyses of the neuroimaging literature reveal consistent cerebellar activation patterns related to working memory, executive function, emotional processing, and across a range of linguistic tasks. Of note, these reviews likely underestimate the extent of cerebellar "cognitive" activations since cerebellar coverage is often incomplete in functional imaging studies."

It not should not be surprising to observe activation of the cerebellum in so diverse functions of the brain. Indeed, the cerebellum receives information from motor as well as non-motor areas (Bostan *et al.*, 2013). One of the main question in cerebellar research nowadays is therefore to identify what could be the common internal computation performed in this structure. Because of its stereotyped structure, it is thought that the computation performed within the cerebellar cortex would be uniform. Its diversity of functions would however be

related to the diversity of input sources and output regions to which each module of the cerebellum is connected (Medina and Mauk, 2000).

In trying to address what could be the uniform computations of the cerebellum (D'Angelo and Casali, 2013), one should therefore think in terms of general computations (*i.e.*, "multi-sensory integration" should be replaced by "multi-modal integration", so that it doesn't convey the idea that only sensory inputs are integrated, but more generally, any "type" of inputs). The next section aims to present some candidates for these unifying cerebellar computations.

IV - 5) Proposed unifying theories of the role of cerebellum and cerebellar-like structures:

Recent theories about the cerebellum propose that it encodes forward or inverse internal models (Ito, 2008; Medina, 2011; Moberget and Ivry, 2016). Basically, microzones in the cerebellar cortex would learn over time the dynamics of a controlled object (*e.g.*, moving one arm in one direction) in a certain sensory context, and therefore store its *expected* behaviour in the AP firing profiles of PCs (the "expectation" is obtained thanks to learning, and doesn't imply a conscious process, but rather a "learnt habit to pair a sensory context with a motor command, separated by a fixed time delay"). In that case, the firing profile of PCs would correlate with movement kinematics, and instruct downstream motor neurons with information as to when the command should be executed. Such models (applied to motor control) offer the benefit to be able to manipulate objects and coordinate movements without the need of sensory feedback, with immediate gain on the ability to execute rapidly and accurately a motor command (Ohyama *et al.*, 2003). The cost would however be that (very) long, repeated training, may be required to optimize circuit output.

A wealth of experimental data support this type of models. First of all, PC activity correlates with movement parameters, such as direction, speed and acceleration (reviewed in Medina, 2011 - see Figure I-24, from Medina and Lisberger, 2007). Secondly, it is well-established that PC activity changes in parallel with motor output reponses in sensori-motor learning tasks, only in presence of CF activity (Medina and Lisberger, 2007). Different bottom-up models are now proposing that the proper temporal pairing of sensory inputs (relayed by MFs) and a teaching signal (relayed by CFs) rely on the ability of the cerebellar cortex to establish a "temporal basis", where GCs activity could change over time during a constant MF

input, so that different subsets of GC-PC synapses can be up- or down-regulated over learning by CF activity.

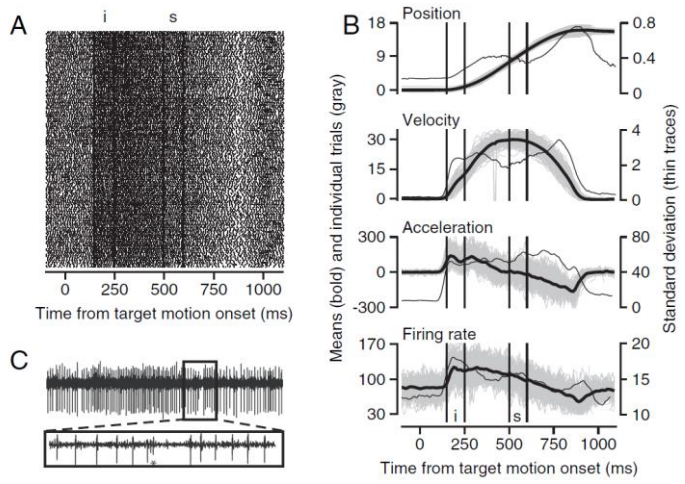

Figure I-24: PC activity in the flocullus correlates with eye movement parameters:

A) Raster plot of a PC to 200 repetitions of eye pursuit trials with a moving target; i: initiation of movement, s: steady state movement; **B)** Position, velocity and acceleration of the eye (top three plots) with PC firing rate (bottom plot); **C)** Time course of a representative PC recording, showing complex spike (*) activity.

From Medina and Lisberger, 2007

IV - 5 - a) Temporal specific learning:

A uniform network computation performed by the cerebellar cortex could be to lower (or suppress) PCs firing during constant MFs input trains (representing contextual information), precisely at the time of CFs activation (representing an error), and this computation could be learnt by repeated trials and errors. Modelling approaches have suggested different mechanisms by which PCs could achieve this learning (reviewed in Medina and Mauk, 2000). Most of them require that a constant set of MF input induces temporally-spread activity in the GC population (Yamazaki and Tanaka, 2007; Rössert *et al.*, 2015; Südhakar *et al.*, 2015). PCs receiving excitatory inputs from GCs would then learn to decrease the weight of GC-PC synapses, only for those which are active at the time of CF activity (Figure I-25, from Medina *et al.*, 2000)). After learning, the sensory context (provided by MFs, and relayed by GCs) would be sufficient to produce the appropriate decrease in PCs activity, without the requirement of a CF input (because, when the appropriate response is achieved, no error signal appears any longer in PCs).

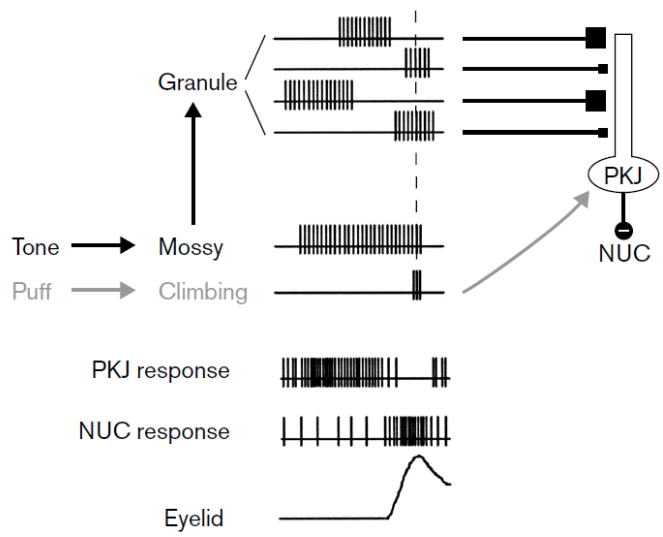

Figure I-25: Cerebellar cortex mechanisms involved in temporal specific learning:

Consider a tone presented to an animal, producing a constant MF input. A "temporal basis" is ***proposed*** to be set-up between MF and GC, producing temporally-diverse activity in the GC population, with different time-delays for first AP generation, and temporal window for AP firing. During training, climbing fiber activity induces plasticity at GC-PC synapses, only for those synapses which are active at the time of CF input. After learning, PCs don't fire at the time where an error signal used to be present, because the sensory context, relayed by GC, has been learnt.

Adapted from Medina *et al.*, 2000

IV - 5 - b) Multisensory integration:

The content of the "sensory context" relayed by the MF-GC pathway introduced above could, at least in principle, be a combination of any type of unimodal sensory stimulus, so long as GCs integrating MF inputs from different sensory modalities can be found in the appropriate lobule of the cerebellum. Recent *in vitro* work of the host laboratory (Chabrol *et al.*, 2015) has revealed that single GCs in lobule X of the cerebellum integrate inputs from different sensory modalities, while other groups have reported multimodal integration at the single cell level in GCs *in vivo* (Huang *et al.*, 2013; Ishikawa *et al.*, 2015).

IV - 5 - c) Multisensory integration and temporal specific learning in cerebellum-like structures:

In the electrosensory lobe of the mormyrid fish, it has been shown that GCs also integrate inputs from MFs conveying proprioceptive and self-generated electrical stimuli information (Sawtell, 2010). Moreover, individual GCs respond with a wide variety of firing profiles, notably due to the time delays introduced by unipolar brush cells (Kenedy *et al.*, 2014). This phenomenon has been coined "temporal basis", and closely mimics theoretical work proposing a delay-line model to account for temporal diversity in the GC population of the cerebellum during constant MF activation (Medina and Mauk, 2000).

Therefore, at least in the ELL, two important transformations happen between MFs and GCs: multimodal integration, and establishment of a temporal basis

Similarly, in the DCN, parallel fibers relay information from different sensory modalities and brain regions (Kanold and Young, 2001; Widgerson *et al.*, 2016; Kanold *et al.*, 2011; Koehler *et al.*, 2011), which are able to modulate the average firing frequency, spike timing and temporal representation of sound in the principal cells (Kanold *et al.*, 2011; Koehler *et al.*, 2013). However, no study so far seems to have explicitly demonstrated the existence of a temporal basis in the input layer of the DCN.

IV - 5 - d) Long- and short-term plasticity as bases for temporal learning:

In the cerebellum, long-term forms of plasticity at MF-GC are thought to act in a synergistic way with GoC-mediated feed-back inhibition, and intrinsic properties of GCs, to improve expansion recoding of MFs inputs onto GCs (reviewed in D'Angelo and De Zeeuw, 2009). Additional forms of long-term plasticity in the molecular layer further optimize the storage capacity of PF input patterns in PCs and MLIs (reviewed in Gao *et al.*, 2012; Mapelli *et al.*, 2015).

Short-term forms of plasticity in the granular layer, on the other hand, is one of the proposed mechanism by which constant MF firing rates can be translated into dynamic GC firing rates (Medina and Mauk, 2000), and *in vitro* evidence of this mechanism have recently been reported (Chabrol *et al.*, 2015).

IV - 5 - e) Inhibitory interneurons and time processing:

The hypothesis that a temporal basis is set-up in the cerebellar cortex at MF-GC synapses is currently being tested in the laboratory, and preliminary evidence of its existence can be found in (Chabrol *et al.*, 2015). The current model examines how STP rules between MF-GC synapses, along with long-term adjustment of GC-PC synaptic weights induced by CF activity, combine to induce changes in PC firing output with different time delays after MF activation onset. For simplicity, the role of STP at GC-MLI and MLI-PC synapses is not examined. However, experimental and theoretical studies (reviewed in Motanis *et al.*, 2018) suggest that such additional sites of STP can enrich the repertoire of time processing functions in feed-forward circuits, notably by creating interval- or frequency-specific filters. These filters,

which include inhibitory interneurons, could ultimately expand and refine the temporal basis set-up in the input layer (*i.e.*, the GCs in the cerebellar cortex - see Figure I-26, from Motanis *et al.*, 2018).

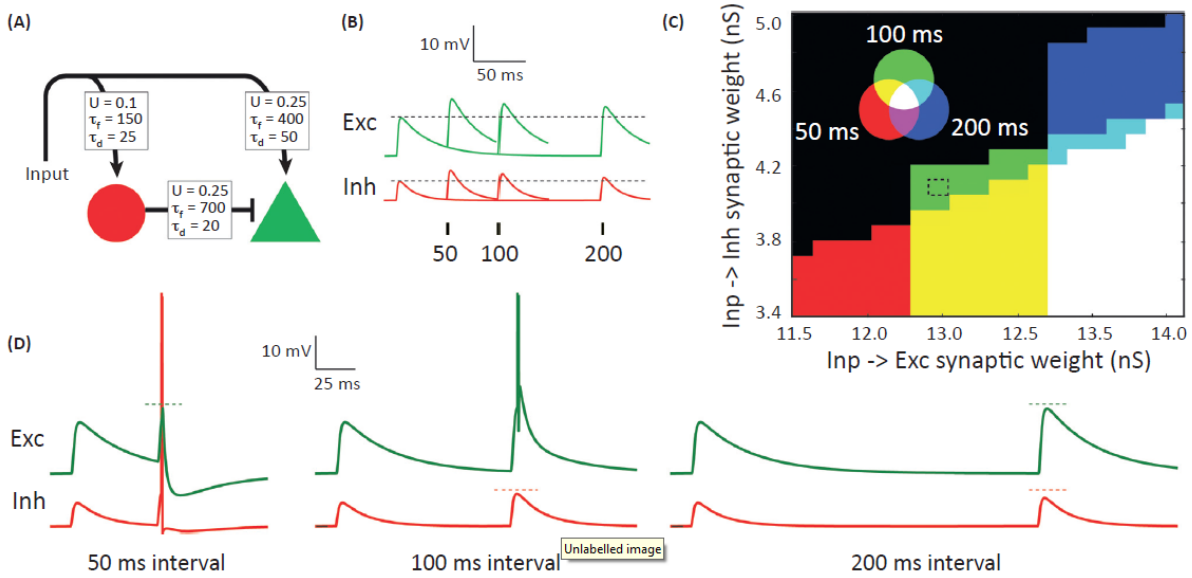

Figure I-26: Interval selectivity simulated in a simple feed-forward circuit with STP:

A) Simple feed-forward circuit composed of an excitatory input, an inhibitory interneuron (Red) and a principal cell (green). Each synapse is endowed with an initial release probability (U), and time constants of facilitation (τ_F) and depression (τ_D); **B)** Modelled behaviours of input-> principal cell and input-> inhibitory interneurons synapses, depending on the time interval between Input activation: **C)** Varying the initial synaptic weights makes the excitatory neuron fire an AP only for certain time delays between the two input stimulations; **D)** the excitatory neuron fires an AP only for 100ms time delays, for initial weights indicated by the dashed box in C). Changing the weight of Inp->Inh and/or Inp->Exc changes the interval selctivity of the Exc neuron.

Adapted from Motanis *et al.*, 2018

In the cerebellar cortex, recent *in vitro* studies (Grangeray-Vilmint *et al.*, 2018; Dorgans *et al.*, 2019) have notably revealed that the firing profile of PCs is highly sensitive to the firing frequency and number of APs emitted by presynaptic GCs. The authors showed that different STP rules at GC-MLI synapses underlie differences in mean firing rate and first spike latency of MLIs, which can then translate into a net gain or loss in emitted spikes, at the single PC level.

General question, and summary of results:

The initial purpose of this thesis was to investigate how basket cells (somatic-targeting interneurons) process their excitatory inputs coming from parallel fibers, and establish their input-output relationship. We had the long-term goal of comparing basket cells to dendritic-targeting stellate cells, which have already been studied in details by the laboratory (Abrahamsson *et al.*, 2012; Tran-Van-Minh *et al.*, 2016). Furthermore, because the cerebellar cortex is a canonical microcircuit, we aimed to provide some more general insights as to how somatic-targeting interneurons found in the CNS could share common features in their input/output relationships.

I discovered that, *in vitro*, parallel fiber stimulation produces a sequence of fast inward current and slow outward current in BCs, reminiscent of classical GABAergic FFI, and despite the presence of supramaximal concentration of gabazine in the ACSF. I later found that the secondary outward current was the inhibitory component of spikelets delivered by electrical neighbours, brought to threshold by parallel fibers stimulation. Therefore, I examined what could be the biophysical determinants of the excitation/inhibition balance of spikelet signalling, and how prevalent this mode of communication was in mature animals, compared to the well-known and documented GABAergic inhibition that interneurons project onto each other. Finally, I examined how spikelet recruitment could shape information processing of PF-mediated direct EPSPs, and influence EPSP-spike coupling. These results are summarized in Chapter III, presented in the format of a manuscript in preparation.

Later, I examined in more details electrical communication within the basket cell population, first by examining if subthreshold EPSCs could be transferred through electrical synapses; then if HCN channels expressed in basket terminals could shape presynaptic APs and transmitted spikelets; and finally how temporal summation of spikelet signalling depends on the firing frequency of the presynaptic cell. These results are summarized in Chapter IV.

Finally, I examined how different morphological features and electrophysiological properties between stellate and basket cells indicate that they have different dendritic integration rules of PF-mediated inputs. These results are summarized in Chapter V.

Chapter II - Materials and Methods:

I - 1) Slice preparation:

Animal experiments were performed in accordance with the guidelines of Institut Pasteur, France, and all protocols were approved by the ethics committee CEEA-Ile de France-Paris 1. Acute parasagittal slices (200 µm) of cerebellar vermis were prepared from postnatal day 30-60 (~44 days on average) mice (F1 cross of BalbC and C57Bl/6J). Mice were rapidly killed by decapitation, after which the brains were removed and placed in an ice-cold solution containing (in mM): 2.5 KCl, 0.5 $CaCl_2$, 4 $MgCl_2$, 1.25 NaH_2PO_4, 24 $NaHCO_3$, 25 glucose, 230 sucrose, and 0.5 ascorbic acid. The solution was bubbled with 95% O_2 and 5% CO_2. Slices were cut from the dissected cerebellar vermis using a vibratome (Leica VT1200S), and incubated at 32°C for 30 minutes in an solution containing (in mM): 85 NaCl, 2.5 KCl, 0.5 $CaCl_2$, 4 $MgCl_2$, 1.25 NaH_2PO_4, 24 $NaHCO_3$, 25 glucose, 75 sucrose and 0.5 ascorbic acid. Slices were then transferred to an external recording solution containing (in mM): 125 NaCl, 2.5 KCl, 1.5 $CaCl_2$, 1.5 $MgCl_2$, 1.25 NaH_2PO_4, 24 $NaHCO_3$, 25 glucose and 0.5 ascorbic acid, and maintained at room temperature for up to 6 hours.

I - 2) Electrophysiology:

Whole-cell patch-clamp recordings were performed from basket cells (BCs), located in the inner-third of the molecular layer of acute parasagittal slices (200µm thick) of cerebellar vermis. Unless otherwise stated (Figures 3 and 4), 10 µM of SR-95531 was added to the Artificial Cerebrol-Spinal Fluid (ACSF), to block $GABA_A$ receptors. Recordings were performed at holding membrane potentials as indicated in the text, and near physiological temperature (32°C) using a Multiclamp 700B amplifier (Molecular Devices). To achieve whole-cell recordings, we used fire-polished thick-walled glass patch-electrodes (tip resistances of 4-6 MΩ). Patch pipettes were backfilled with the following internal solution (in mM): 115 $KMeSO_3$, 40 HEPES, 1 EGTA, 6 NaOH, 4.5$MgCl_2$, 0.49 $CaCl_2$, 0.3 NaGTP, 4 NaATP, 1 K_2-phospocreatine and 0.02 Alexa-594 or 0.04 Alexa-488 (adjusted to 300-305 mOsm, pH = 7.3, referred to as K^+-based internal solution); 115 $CsMeSO_3$, 40 HEPES, 1 EGTA, 6 NaOH, 4.5$MgCl_2$, 0.49 $CaCl_2$, 0.3 NaGTP, 4 NaATP, 1 Tris-phospocreatine and 0.02 Alexa-594 (adjusted to 300-305 mOsm, pH = 7.3, referred to as Cs^+-based internal solution). Series resistance was 14.0 ± 5.8 (mean ± SD, estimated from n=160 cells) and always under 30 MΩ. For current-clamp recordings, a bias current was injected to maintain the membrane potential at values reported in the text, and series resistance was compensated by balancing the bridge and compensating pipette capacitance. All values of membrane potential were corrected for

liquid junction potential, estimated to be -8mV for K^+-based internal solution and -11mV for Cs^+-based internal solutions (Abrahamsson *et al.*, 2012).

In experiments described in Figure 1 and 5, internal solutions were further complemented with 1mM QX-314 to prevent AP generation after entry of PF-mediated EPSCs.

I - 3) Transmitted light and fluorescence imaging:

BC somata in the inner third of the molecular layer were identified and whole-cell patched using infrared Dodt contrast (Luigs and Neumann, Germany) and a Q1Click digital CCD camera (QImaging, Surrey, BC, Canada) mounted on an Ultima multiphoton microscopy system (Prairie Technologies, USA) based on an Olympus BX61W1 microscope, equipped with a water-immersion objective (60X, 1.1 NA, Olympus Optical, Tokyo, Japan). Two-photon excitation of Alexa-488 and Alexa-594 was performed at 780 for pairs of BCs. When Alexa-594 alone was used (single-cell patch-clamp), it was excited at 840nm. A transmitted light PMT after the Dodt tube was used to acquire a laser-illuminated contrast image simultaneously with the 2P-LSM image.

I - 4) Image analysis:

All images were analysed using ImageJ and Fiji. To stitch images for BCs, the pairwise stitching plugin (*Preibisch et al.*, 2009) was used. To assess the distance dependency of PPR and rise time along BC dendritic tree, the freehand line drawing function of the software was used to measure distances between stimulated dendritic sites and somata, and Z differences between dendrites and soma locations were accounted for. To measure maximal radial extension of dendrites in BCs and SCs, the straight line function of the Fiji software was used on Z-projection images.

I - 5) Pharmacological agents:

D-AP5 (D-(-)-2-Amino-5-phosphopentanoic acid) and SR 95531 (2-3-Carboxyprobyl)-3-amino-6(4-methoxyphenyl)pyridazinium bromide) were purchased from Abcam, UK. NBQX (2,3-Dioxo-6nitro-1,2,3,4-tetrahydrobenzo[f]quinoxaline-7-sulfonamide) was purchased from Tocris Bioscience, UK. Alexa Fluor 488 and 594 were purchased from Life Technologies, USA. Mefloquine hydrochloride was bought from Sigma Aldrich, France.

I - 6) Parallel fibre-mediated responses:

Stable EPSC responses from parallel fibers (On-beam stimulation) was performed by positioning the stimulation electrode (filled with ACSF, and visualized by Dodt contrast) on top of the slices, above the dendrites of the patched MLIs (visualized by 2PLSM fluorescence of Alexa 594, introduced through the patch pipette). Stimulus intensities were set to 5-10 V above threshold for detecting an EPSC (Abrahamsson et al. 2012), referred to as low stimulation. To trigger spikelet responses (Off-beam stimulation and direct stimulation), the stimulation pipette was positioned intentionally outside of the dendritic tree, and the relationship between electrical stimulation intensity and spikelet recruitment was systematically examined (Figure 2). In the experiments shown in Figure 1, the external ACSF contained 2mM $CaCl_2$, 1mM $MgCl_2$, 10µM gabazine (SR-95531) and 50µM D-AP5 to block $GABA_AR$ and NMDAR, respectively. In our attempt to block the PF-mediated outward current (Figure 1), we also added in the ACSF either 20µM mefloquine + 0.1% DMSO, or simply 0.1% DMSO. In all other experiments, we used 1.5 mM $CaCl_2$ and 1.5 mM $MgCl_2$, values, which are closer to the physiological ones (Silver and Erecinska, 1990; Bouvier *et al.*, 2018).

I - 7) Detecting electrical and/or chemical synapses in paired recordings:

The presence of an electrical synapse was assessed by analysing CCs, and post-synaptic inward currents after pre-synaptic AP firing. Inward currents following presynaptic AP stimulation can only be due to spikelets, while outward currents can be caused by either spikelets and/or GABAergic currents. If inward currents are not detected (*i.e.*, distribution of peak amplitude not significantly different from baseline distribution), then outward currents in the postsynaptic responses are used to infer the presence of a GABAergic synapse. However, when an electrical synapse is detected, the outward current in post-synaptic responses can be caused by a mix of electrical and chemical inputs. In that case, peak amplitude of post-synaptic outward currents were compared at different holding membrane potentials of the post-synaptic cell (to change the electromotive force for GABAergic inputs), and/or before and after application of gabazine. The presence of a GABAergic synapse was inferred when the peak amplitude distribution of outward current in these different conditions were significantly different from each other. When an electrical connection was present, bias current in the pre-synaptic cell was manually adjusted, to compensate for passive flow of different holding currents from the post-synaptic cell.

I - 8) Data analysis and statistics:

Electrophysiological data were analysed in the Neuromatic analysis package (www.neuromatic.thinkrandom.com) written within the Igor Pro environment (Wavemetrics, USA). Peak amplitude of synaptic responses recorded in voltage-clamp or current-clamp were measured as the difference between the baseline level immediately preceding the stimulation artifact, and the mean amplitude over 200 µs window centred around the peak of the mean response. Due to the long-lasting nature of the fAHP component of spikelets, the peak amplitude of the inhibitory component was averaged in a time widow of 3ms, centred on the peak amplitude of the mean response. When electrical artefact of the stimulating pipette did not reach baseline before synaptic responses occurrence (Direct stimulation, Figure 2), single or double exponential fits of the decay were subtracted from the recordings. All traces displayed are averages of 20 to 30 sweeps, filtered off-line using a binomial smoothing equivalent to 4 kHz filtering.

Measurement of distances between synaptic activation and soma (Figure 1) or between the somata of two neighbouring cells (Figure 4) was performed on 2P-LSM images in ImageJ with a freehand line in maximal intensity projection images, and compensated for differences in z offsets.

Data are expressed as averages ± SEM, unless otherwise indicated. Statistical tests were performed using a non-parametric Mann-Whitney two-sample rank test routine for unpaired comparisons, or Wicoxon matched-pairs signed rank test for paired comparisons. Kruskal-Wallis tests, followed by Dunn's multiple comparison tests, were employed to compare multiple groups inside a single experiment. For one-way multiple groups comparison with pairing information, we employed Friedman tests, and regular one-way ANOVA when samples size were above $n = 30$. Linear correlations were determined using a Pearson test. Statistical significance was defined as $p < 0.05$. All statistical tests were two-sided, and performed in GraphPad Prism 6.

Chapter III: Electrical synapses within a feed-forward electrical circuit generate temporal contrast enhancement:

This chapter is the current state of a manuscript summarizing most of the work of my PhD. It will be presented in the classical format of a manuscript, exception made for the materials and methods section, which has already been presented in Chapter II; and the reference section, which will be incorporated in the general reference section of this thesis.

I) Abstract:

In the cerebellar cortex, molecular layer interneurons are connected by both chemical and electrical synapses, with the precise control of postsynaptic spiking being driven by the ratio of excitatory and inhibitory chemical transmission. While electrical synapses have been proposed to be important in entraining neuronal firing to be synchronized, whether they can be used to fine-tune information flow, particularly within feed-forward circuits, is less well explored. By combining whole-cell patch-clamp and 2-Photon laser scanning microscopy of basket cells, we found that classical EPSCs are followed by a GABAergic-independent outward current. These hyperpolarizing currents are due to passive propagation of an EPSP-evoked action potential from gap junction coupled neighbour(s). The depolarized resting membrane potential of basket cells ensures that spikelets result in a net inhibition, which curtails the time window and dampens the temporal summation of concomitant EPSPs. But during coincident arrival with an EPSP, basket cells experience higher amplitude synaptic responses, due to the transient depolarizing component of the spikelets, ultimately enhancing AP firing for a few millisecond. Therefore, spikelet transmission contributes to a temporal contrast enhancement of excitatory inputs, and provides a precise coincidence mechanism for temporally coded information without any loss in excitatory drive.

II) Introduction:

GABAergic interneurons play important, but diverse, roles in gating, routing and modulating excitatory information flow within neural circuits, through inhibitory chemical synapses. These different computational functions are classified according to canonical wiring motifs (Isaacson and Scanziani, 2011; Feldmeyer *et al.*, 2018). Feed-back inhibition supports rate-based modulation of excitation through gain modulation and increased dynamic range of the levels of excitatory input that can be encoded within a circuit, while feed-forward (FF) inhibition permits precise regulation of post-synaptic spike-timing by sharpening EPSP-spike coupling (Pouille and Scanziani, 2001; Mittman *et al.*, 2005; Blot, 2016). FF motifs can also expand the dynamic range of inputs which can be represented by principal cells (Pouille *et al.*, 2009). However, how FF inhibitory motifs can be used to regulate interneuron firing is less well studied.

Interneurons communicate with each other through both chemical and electrical synapses. While chemical synapses can regulate interneuron firing in the same way as for principal neurons (Mittman *et al.*, 2005), the presence of gap junctions that couple neurons directly as resistive elements, are thought to generate emergent properties such as oscillations and synchronized firing within neuronal assemblies (Draguhn *et al.*, 1998; Beierlein *et al.*, 2000; Bennett and Zukin, 2004; Maex and De Schutter, 2007; Ostojic *et al.*, 2009; Van Welie *et al.*, 2016; Gutierrez *et al.*,. 2013). Electrical synapses between molecular layer interneurons within the cerebellum have been shown to mediate synchronized firing (Mann-Metzer and Yarom, 1999) and coincidence detection (Alcami, 2018), while those between Golgi cells act to synchronize or desynchronize cerebellar cortical network activity (Dugué *et al.*, 2009; Vervaeke, 2010; Van Welie *et al.*, 2016). Finally, electrical synapses modulate passive properties in interneurons (Hjorth *et al.*, 2009; Amsalem *et al.*, 2016; Alcami, 2018). However, despite theoretical studies showing the influence of electrical synapses in information processing within FF circuits (Pham and Haas, 2019), experimental demonstration that electrical synapses modify temporally coded information within FF neural circuits has not been examined.

Owing to the low-pass filtering properties of the cell membrane, presynaptic APs are heavily filtered, and consequently detected as "spikelets" in post-synaptic cells (Dugué *et al.*, 2009; Pereda *et al.*, 2013). However, whether the spikelet conveys mostly the depolarizing component of the AP (Hu and Agmon, 2015; Mann-Metzer and Yarom, 1999), or the after-hyperpolarization component (Dugué *et al.*, 2009; Vervaeke et al. 2010) can vary, and thus

determines whether the electrical synapses can mediate a net excitation or inhibition. Alterations in the spikelet waveform can arise from alterations in presynaptic AP waveforms, which are modulated by differences in the resting membrane potential (Mann-Metzer and Yarom, 1999; Dugué *et al.*, 2009; Russo *et al.*, 2013). Theoretical studies show that net depolarizing spikelets will drive synchronization within neuronal networks, while hyperpolarizing spikelets will generate bistable networks either oscillate synchronously or remain in asynchronous states (Ostojic *et al.*, 2009). Thus, the contribution of electrical synapses network computations depends on the precise polarity of the spikelet.

In the cerebellar cortex, molecular layer interneurons (MLIs) are known to mediate feed-forward inhibition (FFI) onto each other and Purkinje Cells (PCs) by the means of GABAergic synapses (Mittman *et al.*, 2005; Blot *et al.*, 2016). MLIs have also been shown to be electrically coupled via the gap-junction protein, Cx36, likely located in the dendrites (Alcami, 2013). Given the gradients of both prevalence and strength of electrical connectivity along the molecular layer in favour of lower-third MLIs (Rieubland *et al.*, 2014), which are usually basket cells (Sultan and Bower, 1998), we investigated if electrical connectivity could be recruited in a feed-forward manner in the BC population, and how it could modulate EPSP-spike coupling. We found that electrical stimulation of parallel fibre (PFs) excitatory inputs reliably elicited EPSCs, followed rapidly by an outward current that was blocked by gap junction antagonists, consistent with suprathreshold synaptic recruitment of an electrically coupled neuron. Paired whole-cell recordings from electrically coupled BCs showed that the spikelets were predominantly inhibitory due to the depolarized presynaptic resting potential. Thus, the synaptic recruitment of an electrically coupled MLI neighbour displays some of the characteristic features of FFI: temporal shortening of single EPSPs, and dampening of temporal summation. However, unlike chemical FFI, we demonstrate that EPSP-evoked spikelets can amplify synchronous compound synaptic responses, and consequently increase the probability of AP firing over a brief time window. Thus, synapse-evoked spikelet recruitment in a feed forward motif can act as a mechanism for temporal contrast enhancement of information flow within neural circuits.

III) Results:

III - 1) PF-triggered outward current mediated by electrical synapses in cerebellar basket cells:

Molecular layer interneurons (MLIs) found in the inner third of the molecular layer of the cerebellar cortex are more likely to be basket cells, defined by their basket-like axonal projection targeting Purkinje cell (PC) somata and axon initial segment (Sultan and Bower, 1998). Because inner MLIs have been shown to form stronger and more frequent electrical synapses (Rieubland *et al.*, 2014), we examined whether electrical synapses could be recruited in a feed-forward manner between electrically coupled basket cells. Two photon laser scanning microscopy (2P-LSM) of whole-cell patch clamped inner MLIs revealed that more than 95% of cells with basket collaterals also presented a dendritic that traversed nearly the entire molecular layer (174±4.9 µm, n=30 cells - Figure 1A). All subsequent recordings were made from inner MLIs with either a characteristic dendritic or axonal morphologies of basket cells (Sultan and Bower, 1998).

Simultaneous Dodt contrast imaging and 2P-LSM was used to target stimulation of PFs at different locations along the dendritic tree (Figure 1A-C). Stimulation intensity was adjusted to obtain stable EPSCs and 50Hz PPR (generally 5-10 V above threshold; Abrahamsson *et al.*, 2012) in the presence of saturating concentrations of the $GABA_A$ receptor blocker, gabazine (10 µM - Ueno *et al.*, 1997). All stimulus locations in this cell evoked currents with a conventional fast EPSC component and outward component, except when targeting the soma. The gabazine-insensitive outward current was detected in approximately 60% of stimulation locations (Figure 1G, red circles) across 24 cells. Twenty-one cells displayed significant outward currents in at least one stimulation site (see Methods). The outward current was detected all along the dendritic tree, with an amplitude independent of the distance from stimulation site to the soma (Figure 1D). Bath application of 10µM of the AMPA receptor (AMPAR) antagonist, NBQX, eliminated both the EPSC and the subsequent outward current (Figure 1E, n=6/6 experiments). Increasing the stimulation voltage increased the amplitude of the inward current, but EPSC amplitude did not correlate with the outward current amplitude (Supplementary Figure 1), which suggested that voltage-dependent potassium conductance recruitment by unclamped dendritic EPSCs (Tran-Van-Minh *et al.*, 2016) did not contribute to the outward current. Replacement of internal potassium by cesium to block potassium conductances, did not alter the frequency or amplitude of outward currents (Figure 1F-I). However, 20 µM mefloquine, a potent blocker of gap junctions (Cruikshank *et al.*, 2004)

reduced the prevalence of observing an outward current to 22±2% (Ordinary one-way ANOVA, F = 57.13, P-value < 0.0001; followed by Tukey's multiple comparisons tests), with those detected currents being 2.8 fold smaller (Figure 1I - Kruskal-Wallis test, p < 0.0001, followed by Dunn's multiple comparison tests). In conditions where only 0.1% DMSO was added to the ACSF, neither the prevalence nor the amplitude of the outward current was significantly different to control conditions (Figure 1H and I, pink group; ordinary one-way ANOVA followed by Tukey's multiple comparison's test). In all groups, EPSC amplitude was comparable (Figure 1G, Ordinary one-way ANOVA, F = 0.5676, P-value = 0.6368), indicating that PF synaptic transmission was not impaired by any of the pharmacological agents. These observations are consistent with feed-forward AMPAR-mediated recruitment of an inhibitory current via electrical synapses, analogous to classical, GABAergic-mediated, FFI (Scanziani *et al.*, 2001; Mitmann *et al.*, 2005).

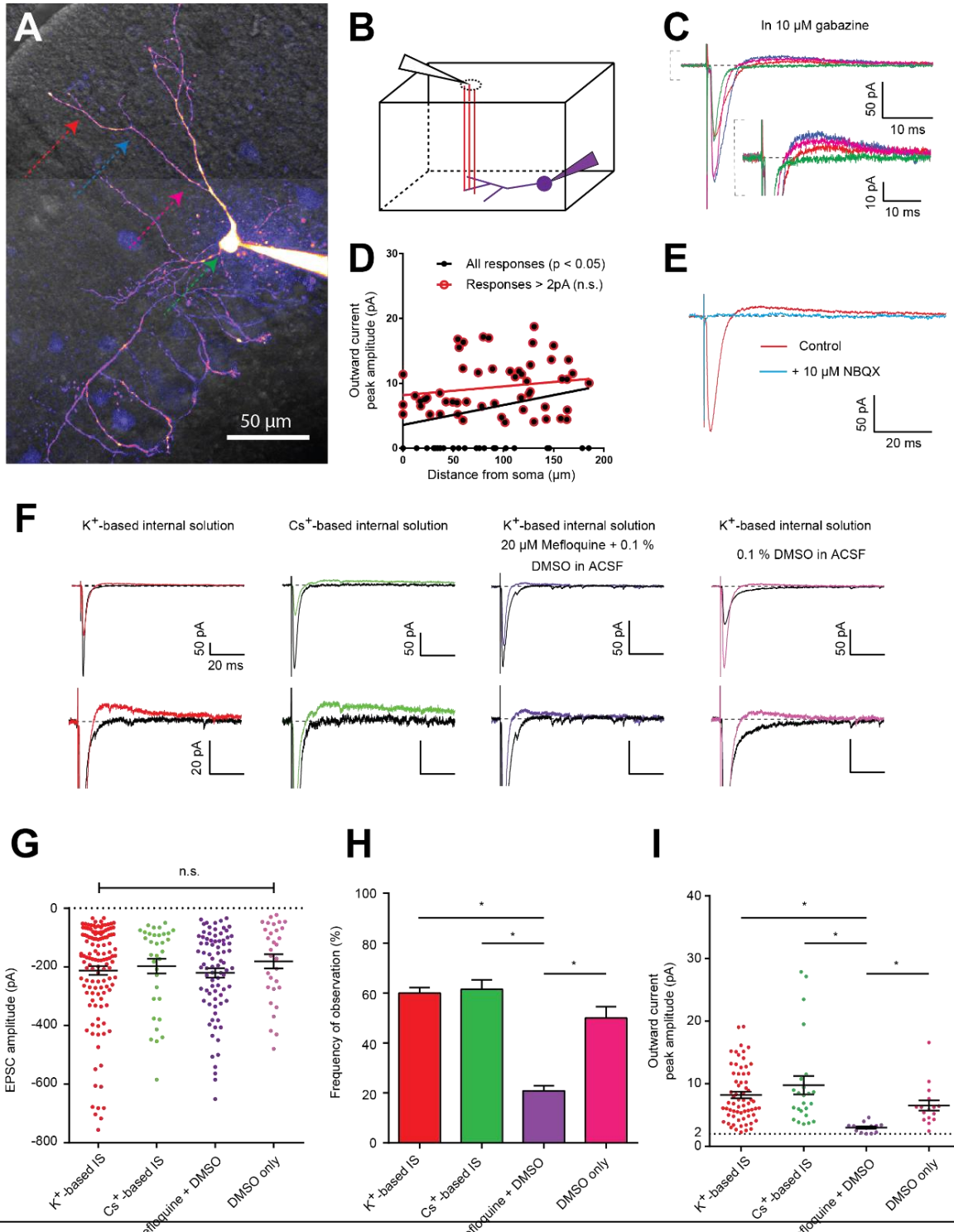

Figure III-1: PF-induced inhibitory current mediated by electrical synapses in cerebellar basket cells:

A) 2P-LSM image (maximal intensity projection) of a BC loaded with 20µM Alexa-594. Color arrows indicate the positions of the stimulating pipette. **B)** Block diagram of parasagittal slices showing the stimulation pipette (black triangle), parallel fibers (PFs - red lines), and the patched cell loaded with Alexa-594 (purple). **C)** Averaged EPSCs in response to a single stimulation of PFs in 10µM gabazine (same color code as in A). **D)** Average peak amplitude of the outward current versus distance between synaptic current entry and somatic compartment. **E)** Representative experiment of application of 10µM NBQX, revealing the disappearance of both inward and outward currents (n=6/6 experiments). **F)** Representative traces of PF-mediated synaptic responses recorded in four different pharmacological conditions. Two traces, recorded within the same cell for each group, reveal either the presence (color) or the absence (black) of the outward current. **G)** EPSC amplitude following PF stimulation is not significantly different in any of the four groups. **H)** Frequency of detection of the outward current in each group. **I)** Outward current peak amplitude (in cases where it can be detected) in each group.

III - 2) PF-evoked and direct recruitment of MLI's spikelets

Spikelets transmission through electrical synapses has been shown to exhibit a long-lasting inhibitory current (Mann-Metzer and Yarom, 1999; Alcami and Marty, 2013; Rieubland *et al.*, 2014). We therefore hypothesized that the outward current reflects the filtered after-hyperpolarisation (fAHP) of presynaptic AP of electrically coupled neighbours, generated by PF-evoked AMPAR mediated EPSPs. To test this hypothesis we reasoned that stimulation of PF beams, in the presence of gabazine, outside the dendritic tree of the recorded BC (Figure 2A, 2B; off-beam stimulation) would depolarize a coupled neighbour to threshold, thereby generating a spikelet-only waveform, without the direct EPSC observed previously. Indeed, rapid and small inward currents were invariably observed prior to large relative outward currents (Figure 2C, 2D). Both current components increased with increasing extracellular stimulus intensity (from 20-50V), consistent with recruitment of at least one additional electrically coupled MLI (Figure 2E). In 12/12 locations from 9 cells, we never observed an outward current exceeding 2*SD of the baseline noise without being preceded by an inward current, as one would expect for exclusive spikelet transmission.

Our hypothesis that BCs exhibit FF recruitment of spikelets also predicts that in the presence of AMPAR antagonists, direct stimulation of a neighbouring MLI soma should also elicit a single spikelet (Figure 2F and G). Figure 2H shows a representative example where, at 10V, no post-synaptic response is detected, but at 20V, some trials elicited small inward currents concomitant with outward current. Increasing the stimulation intensity increased the number of successes, but did not alter the amplitudes (p-value > 0.05 for two-by-two comparisons of inward and outward currents - Figure 2I and 2J). In n=12/12 experiments from 11 cells, we found that each time an outward current was detected, it was preceded by a detectable inward current.

Taken together, these experiments confirmed that all outward currents detected were systematically preceded by an inward current, which is the electrophysiological signature of spikelet signalling in MLIs, and provide further evidence that inhibitory currents described in Figure 1 are the fAHP associated with FF recruitment of spikelet signalling.

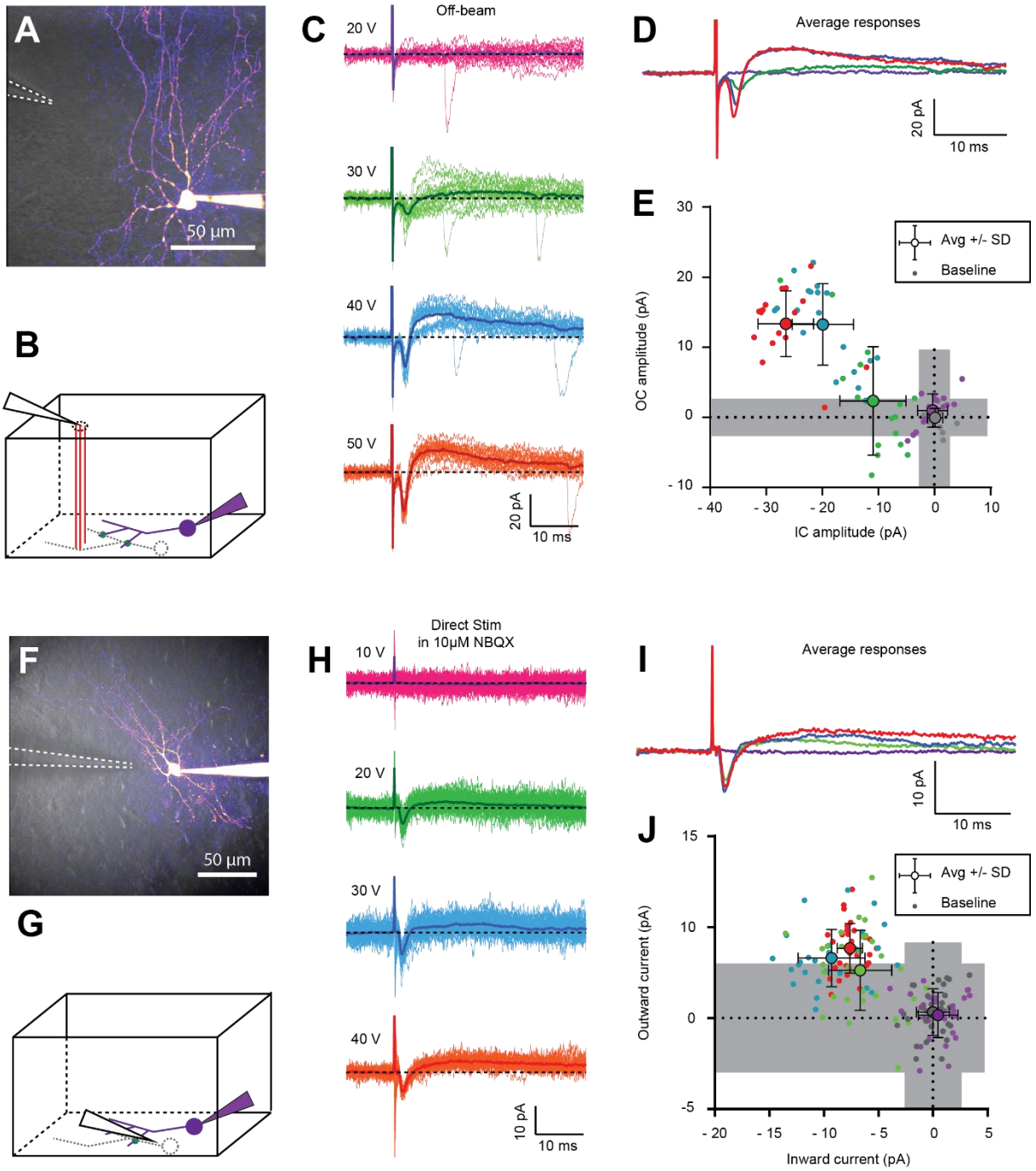

Figure III- 2: Recruitment of spikelet through PF recruitment or direct stimulation A) 2P-LSM image (maximal intensity projection) of a BC loaded with Alexa-594. Dashed white lines indicate the position of the stimulating pipette on top of the slice (off-beam stimulation). **B)** Block diagram of parasagittal slices showing stimulating pipette (Black triangle), parallel fibers (PFs - red lines), a neighbouring MLI (dashed grey lines) forming an electrical synapse (green dots) with the patched cell (purple). **C)** Post-synaptic responses recorded in the patched cell, with respect to the stimulation intensity. Dark lines represent averages of 15-20 single sweeps, shown in lighter colors. **D)** Superimposition of average responses, shown for visual comparison of the differences in mean peak amplitude of inward and outward currents. **E)** Summary plot of peak amplitudes of inward and outward currents shown in C, with corresponding averages +/- SD represented by larger dots. **F-J)** Similar as in A-E, but for a direct stimulation protocol, with 10µM NBQX in the bath.

III - 3) Modulation of spikelet polarity by presynaptic membrane potential:

Spikelets recorded from different cell-types throughout the brain have been shown to differ in their waveforms, and notably in the balance between excitation and inhibition (Galaretta and Hestrin, 2002; Dugué *et al.*, 2009; Hu and Agmon, 2015). In immature BCs, a predominant depolarizing components was reported (Alcami and Marty, 2013; Alcami, 2018). Because we showed above that outward current component of the spikelet was prominent as well, we more closely investigated the net polarity of spikelets and the influence of membrane potential. Pairs of BCs were whole-cell patch clamped and a hyperpolarizing current pulse (400 ms duration) was used to confirm the presence of electrical synapses and estimate unidirectional coupling coefficients (CCs). In order to examine spikelet transmission in isolation, GABAergic inhibition was blocked with gabazine, which did not affect CCs (Figure 3B and 3C - n=16 cells from 8 pairs, Wilcoxon matched-pairs signed rank test, $p > 0.05$). APs were then triggered when varying the membrane potential of either the transmitting or receiving neuron (Figure 3D-G). The peak amplitude of the inward and outward currents, as well as the charge transfer of the spikelet response, were unaffected when altering the holding membrane potential of the post-synaptic neuron (Figure 3E, n=12 cells from 6 pairs, 3 independent Friedman tests, with p-values > 0.05 for each of them). When adjusting the holding current to alter the membrane potential of the presynaptic neuron between approximately -80, -70 or -60 mV, the inward current reduced in amplitude and the outward current increased (Figure 3F and 3G; n=12 cells from 6 pairs, 3 independent Friedman tests, with all p-values < 0.001). Because of the slower outward component, the compound effect of inward and outward current changes led to an inversion of charge transfer from net excitation to net inhibition as the presynaptic neuron was depolarized. These results imply that net polarity of spikelets changes significantly with the presynaptic membrane potential, and that spikelet waveforms can be used to estimate resting membrane potential of unperturbed (*i.e.*, no whole-cell dialysis) presynaptic neurons.

In order to estimate the membrane potential of unperturbed electrical partners, we compared peak inward and outward current amplitudes of spikelets from paired recordings to those of spikelets evoked by off-beam stimulation and direct stimulation (from Fig. 2). Linear regression analysis of each of the five groups showed a similarity between direct and OFF-beam stimulations data (Figure 3H). These two regression lines were significantly different from those of -80mV and -70mV, but not significantly different from the -60mV group. These data indicate that unpatched MLIs have a resting membrane potential of at least -60mV (and perhaps greater). Figure 3G shows that spikelet responses from -60 mV holding potentials

should carry a net inhibition, as the total charge integral was positive. Because we were not certain to have only single neuron spikelet responses by direct or off-beam stimulation, we first normalized spikelets to the peak of the inward current before integration (over 50 ms), and then compared the net relative charge to that from spikelets from paired recordings when holding the presynaptic neuron at -60 mV. Consistent with a net inhibitory effect, the charge integral for directly stimulated and off-beam recruited spikelets were positive (Figure 3I). Off-beam spikelets were similar in the net relative charge transfer as those arising from presynaptic neurons held a -60 mV, but directly recruited spikelets displayed a significantly higher normalized charge transfer, possibly because of dialysis effect in paired recordings (ordinary one-way ANOVA followed by Dunn's multiple comparisons test). The difference between the off-beam elicited and direct spikelets could be due to the passage of subthreshold EPSP transmitted from the presynaptic neuron that contribute an additional inward current.

Altogether, these results indicate that the resting membrane potential of MLIs forming electrical synapses is critical in setting the net excitatory/inhibitory impact of spikelet transmission. Moreover, we determined that MLIs from mature mice have a depolarized resting membrane potential (-60mV) in agreement with previous estimates (Chavas and Marty, 2003; Kim *et al.*, 2014). This depolarized membrane potential ensures that spikelets deliver a net inhibition and thus could act to provide FFI.

Figure III-3: Modulation of spikelet polarity by presynaptic membrane potential: A) 2P-LSM image of two BCs loaded with 20µM Alexa 594 (red), or 20µM Alexa 488 (green). **B)** Membrane potential of both cells (same color code as in A), when either of them is injected with a long hyperpolarizing current pulse. Solid lines indicate responses in control conditions, while dashed lines correspond to responses recorded in 10µM gabazine. **C)** Unidirectional coupling coefficients are not significantly changed by gabazine addition. **D)** Action potential from one cell of the pair, maintained in current-clamp around -70mV (upper panel), with corresponding spikelets received in the post-synaptic cell, held in voltage-clamp at different membrane potentials (lower panel). **E)** Inward current peak amplitude (left panel), outward current peak amplitude (middle panel) and charge transfer (right panel) do not vary with post-synaptic membrane potential. **F)** Action potential from the same cell, maintained in current-clamp at three different resting membrane potential (upper panel), with corresponding spikelets recorded in the post-synaptic cell, held at -70mV in voltage-clamp (lower panel). **G)** Inward current peak amplitude (left panel), outward current peak amplitude (middle panel) and charge transfer (right panel) are all significantly altered by changing the resting membrane potential of the pre-synaptic cell. **H)** X-Y plot of outward versus inward current peak amplitudes of spikelets recorded in pairs (-60, -70, -80mV) and in the conditions described in Figure 2 (Direct stimulation and Off-beam stimulation). **I)** Spikelet charge transfer, normalized to the peak amplitude of the inward currents

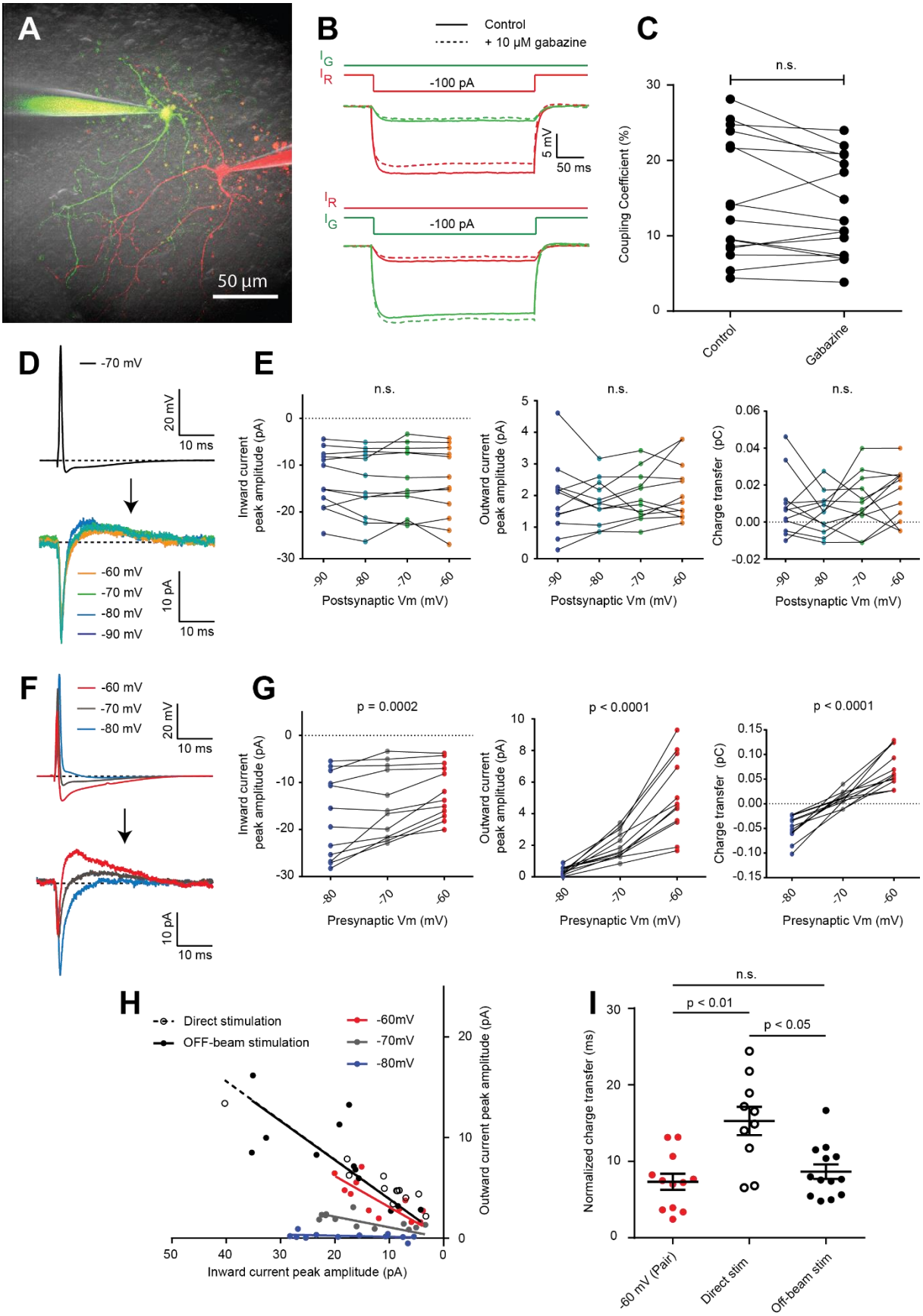
A
50 µm
B
Control
+ 10 µM gabazine
I_G
I_R
-100 pA
5 mV
50 ms
I_R
I_G
-100 pA
C
n.s.
Coupling Coefficient (%)
30
20
10
0
Control
Gabazine
D
-70 mV
20 mV
10 ms
-60 mV
-70 mV
-80 mV
-90 mV
10 pA
10 ms
E
n.s.
Inward current peak amplitude (pA)
0
-10
-20
-30
-90
-80
-70
-60
Postsynaptic Vm (mV)
n.s.
Outward current peak amplitude (pA)
5
4
3
2
1
0
Postsynaptic Vm (mV)
n.s.
Charge transfer (pC)
0.06
0.04
0.02
0.00
-0.02
Postsynaptic Vm (mV)
F
-60 mV
-70 mV
-80 mV
20 mV
10 ms
10 pA
10 ms
G
p = 0.0002
Inward current peak amplitude (pA)
Presynaptic Vm (mV)
p < 0.0001
Outward current peak amplitude (pA)
10
8
6
4
2
0
Presynaptic Vm (mV)
p < 0.0001
Charge transfer (pC)
0.15
0.10
0.05
0.00
-0.05
-0.10
-0.15
Presynaptic Vm (mV)
H
Direct stimulation
OFF-beam stimulation
-60mV
-70mV
-80mV
Outward current peak amplitude (pA)
20
10
0
50
40
30
20
10
0
Inward current peak amplitude (pA)
I
n.s.
p < 0.01
p < 0.05
Normalized charge transfer (ms)
30
20
10
0
-60 mV (Pair)
Direct stim
Off-beam stim

III - 4) Electrical synapses form the majority of inhibitory connections between BCs in adult animals:

In young rats, electrical synapses have been shown to be more prevalent than chemical ones in the inner-third MLI population (Rieubland *et al.*, 2014). Here, we re-examined the relative impact of electrical synapse-mediated FFI and classical chemical FFI in mature mice, as developmental changes have been described in other circuits (Peinado *et al.*, 1994; Hormuzdi *et al.*, 2001). Previous studies used multi-electrode whole cell recordings to establish the fraction of synapses that were chemical and electrical, albeit using long current step injections and a coupling coefficient >1% for electrical coupling (Rieubland *et al.*, 2014). Here electrical coupling was examined using both long hyperpolarizing current pulses (Figure 4B; see Methods) and brief current injections to elicit APs in the presynaptic neuron and monitor the post-synaptic currents. Electrical connectivity was estimated based on CCs, and detection of inward current peak amplitude of spikelets significantly different from baseline (Figure 4C). To probe chemical connectivity, we compared the post-synaptic responses to presynaptic AP generation, before and after application of gabazine; or at different holding membrane potential of the post-synaptic cells (held at -70mV or -60mV, Figure 4C), in order to increase the driving force for GABAergic currents. As shown above, this manipulation does not influence the waveform of potential superimposed spikelets (Figure 3D and E).

Figures 4A to C show an example paired recording in which bidirectional voltage deflections were observed in the unstimulated neuron (Figure 4B) and post-synaptic inward currents were observed after generating a presynaptic AP (Figure 4C, left), together indicating the presence of an electrical synapse. Comparison of post-synaptic responses before and after gabazine addition, or at two holding membrane potentials of the post-synaptic cells, revealed significantly different outward currents in each condition, indicating the presence of two unidirectional GABAergic synapses, with a stronger one going from cell 1 to cell 2. Examples of recordings from two other pairs, where a pure chemical synapse or a pure electrical synapse were observed, are shown in Figure 4D and 4E, respectively.

In order to compare the prevalence of chemical and electrical synapses, we only considered AP-triggered post-synaptic responses, as coupling coefficients below 5% are not systematically correlated with detection of spikelets (Supplementary Figure 2), suggesting indirect coupling. For CCs above 5% however, peak amplitude of inward and outward currents of spikelets are linearly correlated with CC (Supplementary Figure 2). Consistently, a coupling coefficient of 5% more accurately predicts spikelet detection (Figure 4F). Bidirectional spikelet transmission was significantly higher than unidirectional GABAergic connection (p(spikelet) =

51±3.4% vs p(GABA) = 40±2.7%, $p < 0.05$, Unpaired t-test with Welch's correction). Our data therefore indicate that, within the BC population of adult animals, inhibition is more often carried by electrical synapses than chemical synapses.

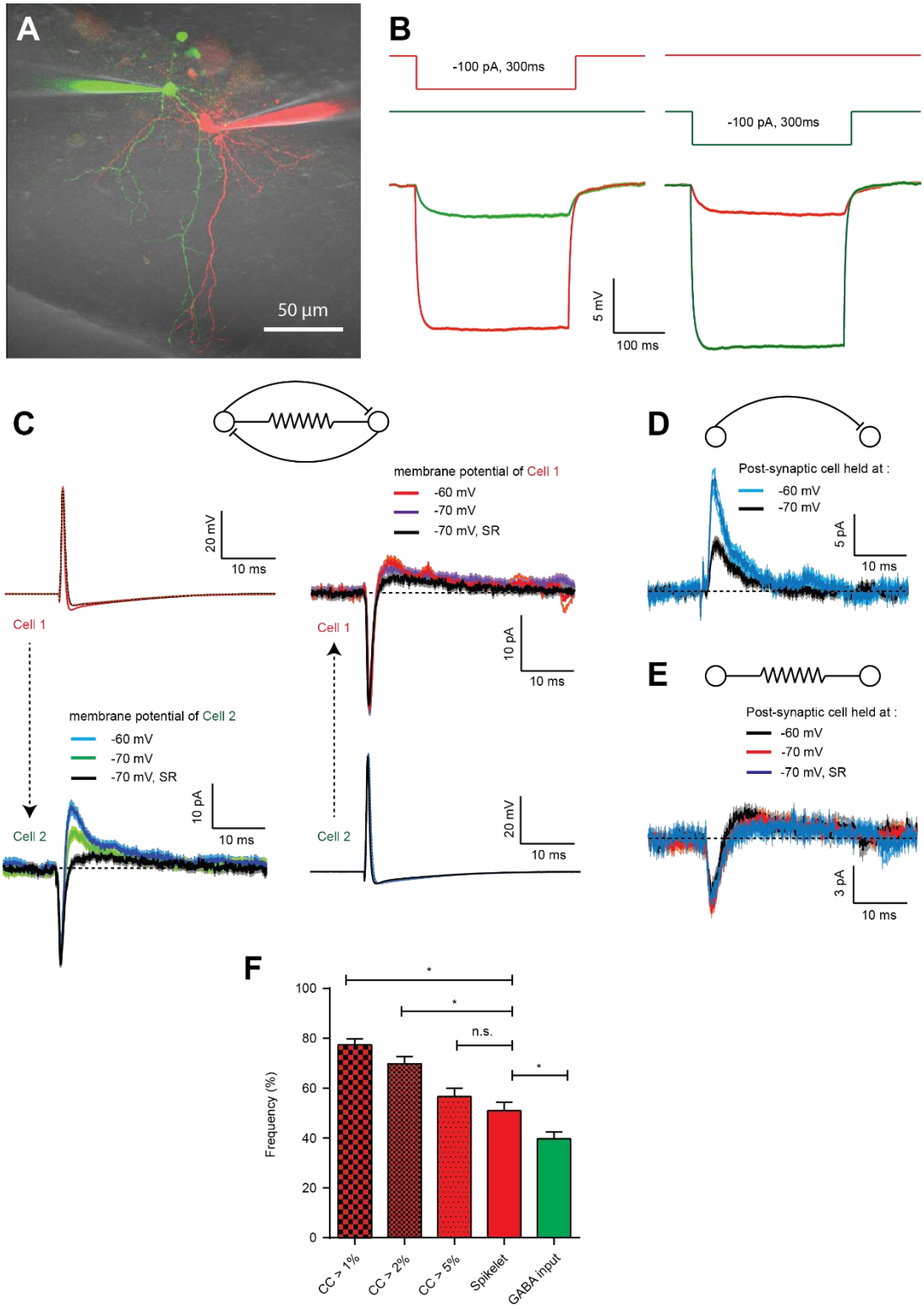

Figure III-4: Electrical synapses form the majority of inhibitory connections between BCs in mature animals. A) 2P-LSM image of two BCs loaded with 20µM Alexa 594 (red), or 20µM Alexa 488 (green). **B)** Membrane potential of both cells (same color code as in A), when the red cell is injected with a hyperpolarizing current pulse (left panel), or when the green cell is injected with the same current pulse (right panel), in absence of gabazine. **C)** Examples of dual electrical/chemical connections; left panels: AP waveforms from cell 1 (red cell), and corresponding post-synaptic responses in cell 2 (green cell), when cell 2 is held at different potentials, or in presence of gabazine (left panels). Right panels: similar recordings when the same protocols are applied in the reverse direction (AP triggered in cell 2, and post-synaptic responses recorded in cell 1). **D and E)** Example of a chemical synapse only, and of an electrical synapse only, recorded in two different cells. **F)** Frequency of electrical synapses (in n = 53 bidirectional connections) based on bidirectional CCs above 1%, 2%, 5%, or significant spikelet-induced inward current (red bars), compared to frequency of chemical synapses (in n = 78 unidirectional connections – green bar).

III - 5) Feed-forward recruitment of spikelets narrows single EPSP time-window, and dampens temporal summation:

Having observed that electrical synapses are a prominent source of inhibitory inputs in BCs, we investigated if the FF recruitment of spikelets could influence EPSP kinetics and temporal summation as for classical chemical FFI. Because mefloquine is known to alter input resistance by blocking electrical synapses (Vervaeke *et al.*, 2012), and displays the side-effect to increase membrane capacitance (Szoboszlay *et al.* 2016), we took advantage of the fact that some stimulation locations along the dendrite did not recruit a spikelet when stimulating 5-10 V above threshold (θ) for eliciting an EPSC (Low stimulation - Figure 1). We then increased the stimulus intensity another 15V (High stimulation), which in some cases only increased the EPSC amplitude (Figure 5A), and in others recruited AP firing of a neighbour, and thus a spikelet in the recorded cell (Figure 5B). For those cases where an outward current was *not* recruited, current clamp recordings of the same cells showed no differences in the half width of the EPSPs, despite an increase in the amplitude (Figure 5A - n=15 EPSPs, Wilcoxon matched-pairs signed rank test, $p = 0.1876$). For the cases where additional stimulation intensity elicited a detectable outward current, the half-width in current clamp conditions was decreased by 19.6 ± 1.2 % (n=10, $p = 0.002$; Figure 5B). These results support the notion that FF recruitment of spikelets sharpen the temporal precision of EPSPs, as is the case for classical chemical FFI.

To examine the influence of FF recruitment of spikelets on the temporal summation of EPSPs, we applied high frequency train stimuli at dendritic locations, with or without detectable outward currents. Example EPSPs show that spikelets produce rapid compound EPSPs followed by a hyperpolarizing component, as compared to the case without spikelets (Figure 5C). Temporal summation of EPSPs in response to five stimuli at 50Hz was significantly reduced at stimulus locations that recruited spikelets (Figure 5C; Two-way repeated measure ANOVA). This difference could not be attributed to differences in peak amplitude of the first EPSP, nor to uneven sampling of PF-mediated responses along the dendritic tree (Supplementary Figure 3A and B). Together, these data indicate that spikelets can act like chemical FFI by reducing the half-width and dampening temporal summation of EPSPs.

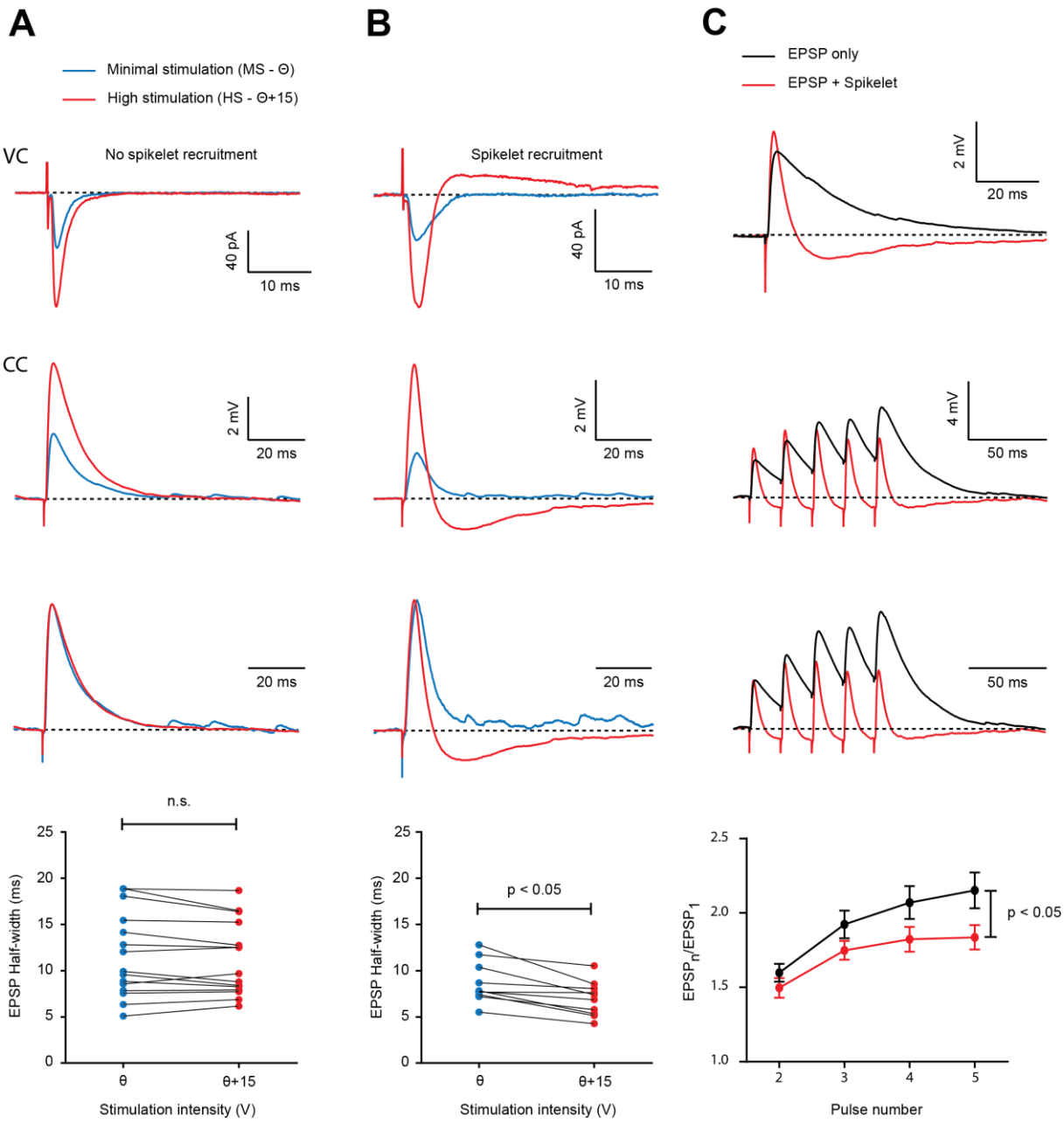

Figure III-5: Feed-forward recruitment of spikelets narrows single EPSP time-window, and dampens temporal summation. A) Voltage-clamp recordings of PF-mediated synaptic responses in low (LS – blue traces) and high stimulation intensity (HS – red traces). Recordings here show no outward current in either stimulation regime. CC recordings show no change in EPSP half-width when stimulation intensity is increased **B)** same as in A, but for cases where stimulation intensity increase caused a significant outward current after the EPSC. Here, a significant decrease in EPSP half-width is observed in HS. **C)** Superimposed post-synaptic responses from two different cells, recorded in LS, when the direct EPSP is followed by a spikelet-induced hyperpolarisation (red), or when it is not (black) - upper panel. Post-synaptic responses to a train of five stimulations at 50Hz (middle panel), corresponding to the traces shown in upper panel. Normalized peak amplitudes of EPSPs in the train reveal a significant decrease in temporal summation in the group where a spikelet-induced hyperpolarisation was present.

III - 6) Spikelet signalling enables temporal contrast enhancement of temporally coded excitation:

Because spikelets are also comprised of a brief depolarization component, we considered the possibility that spikelets could contribute to enhanced firing rates over a brief window, in contrast to classical chemical FFI where peak firing rates are reduced. We therefore performed patch-clamp recordings of single BCs, but stimulated two independent sets of PFs: one location within the dendritic tree (on-beam) to recruit EPSPs, and another positioned to stimulate off-beam, so as only to recruit spikelets in the recorded cell (Figure 6A-C). Stimulation intensity was adjusted independently for each location: low stimulation for on-beam stimulation (see Figure 5), and high stimulation intensity for off-beam responses (Figure 2). Stimulation pipette positions were always displaced by at least 100µm, to ensure the recruitment of two different beams of PFs. BCs were initially held between -75 and -70mV, in order to examine the amplitude of the compound subthreshold synaptic response with respect to the time delay between the two stimulations (Figure 6D). Coincident stimulation of spikelets and on-beam stimulation over a 4-6 ms window significantly increased the EPSP depolarization by 21.6 ± 2.6 % (n=12, p = 0.0005, Wilcoxon matched-pairs - Figure 6D and 6E). However, if spikelet recruitment preceded the EPSP (by 5 to 75 ms), the peak amplitude of the EPSP was significantly reduced, with a peak reduction of 20 ± 2.7% occurring for a time delay of 20ms (n=12, p = 0.0005, Wilcoxon matched-pairs - Figure 6D and 6E). We also confirmed that spikelet concomitant with EPSP reduced their half-width by 16.7 ± 1.8 %, consistent with previous results (Figure 5B).

Finally, we examined if these changes in peak amplitude of compound synaptic responses could translate into differences in spike probability. We maintained the patched cells between -65 and -60mV, to achieve EPSP-induced AP firing in around 50% of the trials (Figure 6F). We then examined AP firing probability versus time delay between on- and off-beam stimulations (Figure 6G). We found that the relative spike probability was significantly increased by 52 ± 8.5 % for coincidental arrival of both inputs (n=11 cells, p = 0.002), and significantly decreased by 55.4 ± 6.7 % if EPSPs were triggered 20 ms after the spikelets (p = 0.001). We also observed an improvement in spike timing initiation, which was reduced by 12.2 ± 1.2 % during the brief window of increased spike probability (Figure 6H). Thus, a unique property of spikelet-mediated FF modulation is the ability to enhance spike probability and accelerate spike-timing, a form of temporal contrast enhancement. Moreover, for independent PF beams, the BC network can detect coincident excitation that will in turn generate a global precise inhibition of downstream Purkinje cells.

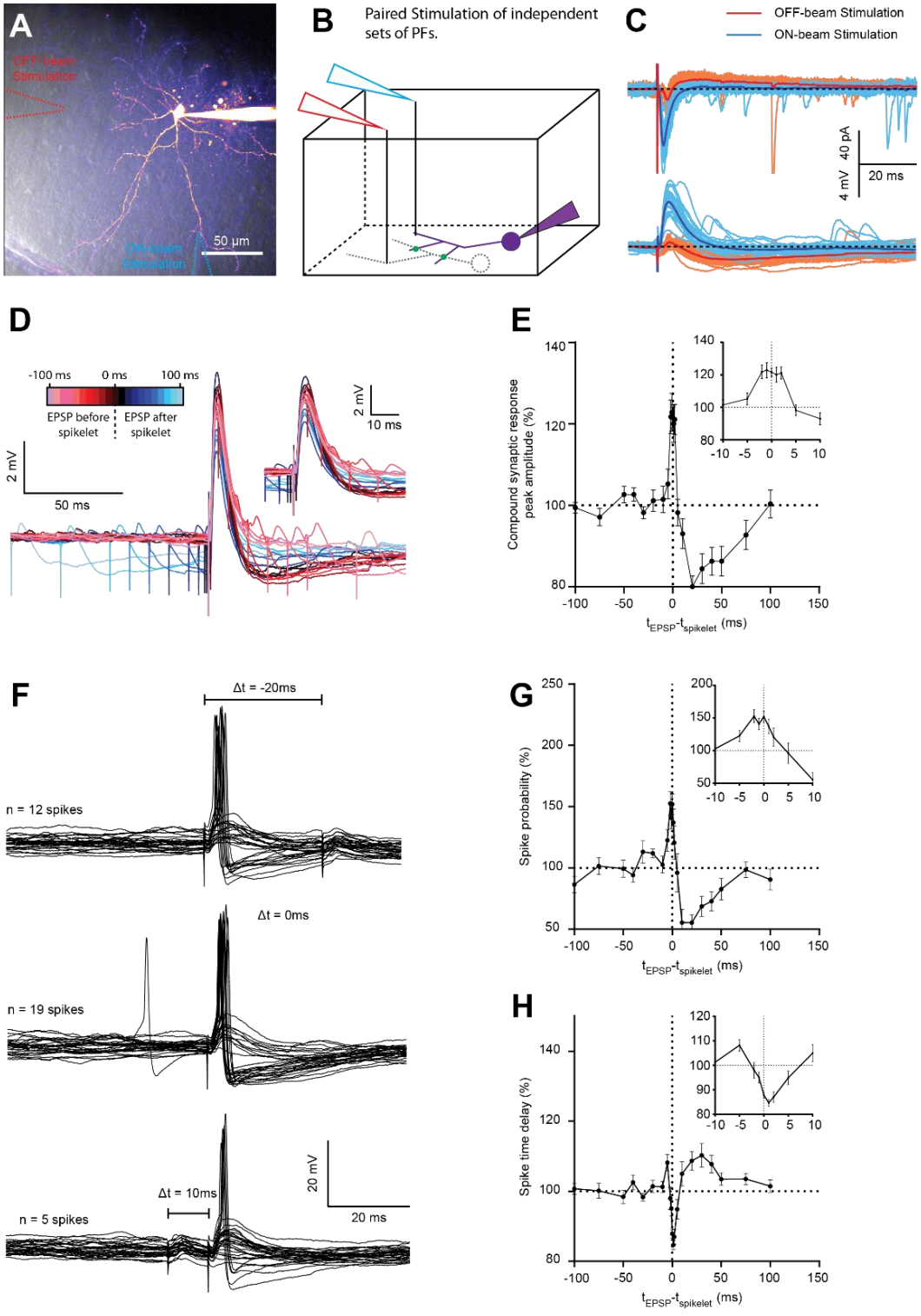

Figure III-6: Spikelet signalling enables temporal contrast enhancement of temporally coded excitation. A) 2P-LSM image of a BC loaded with Alexa 594. Dashed lines indicate the position of the stimulating pipettes on top of the slice (Off-beam stimulation in red, On-beam stimulation in blue). **B)** Block diagram of the experiment. **C)** Superimposed voltage-clamp recordings (upper panel) and corresponding current-clamp recordings (lower panel) of post-synaptic responses to On-beam stimulation (blue) or Off-beam stimulation (red). **D)** Superimposed compound synaptic responses, with different time delays between On- and Off-beam stimulations, aligned on On-beam stimulation time. For clarity, positive time-delays (*i.e.*, Off-beam stimulation prior to On-beam stimulation) are shown in blue shades; Coincident stimulations are shown in dark colors; and negative time-delays in red shades. **E)** Peak amplitude of the compound synaptic responses (normalized to the mean amplitude of the single EPSPs alone) versus the time-delay between EPSP and spikelet recruitment. **F)** Single-sweep responses of On-beam-induced AP firing, depending on the onset of Off-beam stimulation, for three representative cases: spikelet recruited 20ms after EPSPs (top panel), coincidentally with EPSPs (middle panel), or 10ms before the EPSP (lower panel). In each instance, 30 sweeps are shown. **G)** Probability that an AP is fired after On-beam stimulation (normalized to the mean probability of AP firing by On-beam stimulation alone), versus the time-delay between On- and Off-beam stimulation (n=11 cells). **H)** Same as in G, but for spike time-delay.

IV) Discussion:

MLIs within the cerebellar cortex have been shown to provide FFI onto Purkinje cells *in vitro* (Mittman et al. 2005; Dizon and Khodakhah, 2011; Valera *et al.*, 2016) and *in vivo* (Blot *et al.*, 2016). Interneurons of the cerebellar cortex are known to communicate through both chemical and electrical synapses (Kondo and Marty, 1998; Mann-Metzer and Yarom, 1999, Rieubland *et al.*, 2014). GABAergic chemical synapses have been shown to mediate inhibition between MLIs (Mittman *et al.*, 2005) and has been suggested to mediate a disinhibition of PCs (Blot *et al.*, 2016), but whether or not electrical connectivity could be recruited in a similar manner, and influence EPSP-spike coupling, had not been studied.

Here, we demonstrate and describe the functional implication of feed-forward recruitment of spikelet signalling in cerebellar basket cells, an MLI subtype that has strong bias towards electrical synapses (Alcami and Mary 2013; Rieubland *et al.*, 2014). Our results indicate that low stimulation intensity of small PF beams lead to the recruitment of APs in electrical neighbours that generate spikelets in the postsynaptic cell (Figures 1 and 2). We show that the polarity of spikelet responses, a parameter regulating excitation and inhibition balance, is net inhibition and can be influenced by the presynaptic neuron membrane potential (Figure 3). This form of inhibition is more prominent than cFFI (Figure 4). Nevertheless, the brief depolarizing component of the spikelet provides a distinct advantage over cFFI, because postsynaptic output firing is briefly enhanced, providing a temporal contrast enhancement mechanism (Figure 6). Such a mechanism could provide strong synchronized inhibition that temporally entrains PCs, an efficient strategy for driving deep cerebellar nuclei (Person and Raman 2012; Brown and Raman; 2018).

IV - 1) Spikelets dynamically modulate BC EPSP-spike coupling

cFFI is characterized by its ability to shorten EPSPs and thus narrow the time window for spike generation, generally at the cost of decreasing the spike probability. Spikelet transmission via gap-junctions can regulate spike probability bi-directionally, depending on the time integral of depolarization and hyperpolarization. Depolarizing spikelets would tend to provide FF excitation and thus synchronize electrically coupled interneurons (Alcami 2018; Mann-Metzer and Yarom, 1999), whereas hyperpolarization favouring spikelets could generate low frequency resonance in a resting state of the network (Dugué *et al.*, 2009) and/or desynchronize network activity upon synaptic stimulation (Vervaeke *et al.*, 2010).

Spikelet waveforms have been shown to depend on a variety of physiological parameters across different cell-types, including resting membrane potential (Mann-Metzer and Yarom, 1999; Otsuka and Kawaguchi, 2013), active conductances in the pre-synaptic (Curti and Pereda, 2004; Russo *et al.*, 2013) or the post-synaptic cell (Mann-Metzer and Yarom, 1999; Dugué *et al.*, 2009). By systematically examining the role of both the pre- and post-synaptic resting membrane potentials, we found that the latter had no detectable influence on spikelet waveform (Figure 3). However, the presynaptic membrane potential critical in shaping the triggered AP, and therefore the corresponding spikelet. A hyperpolarized resting state leads to a net excitatory spikelet, while a depolarized resting state revealed a prominent AHP, causing the corresponding spikelets to carry a net inhibition. We used these experiments to calibrate spikelets from unperturbed electrically coupled neighbours, and determined the resting membrane potential to be > -60 mV, favouring net inhibition. It is likely that differences in holding potential accounted for the mostly depolarizing spikelets recorded previously in MLIs (Alcami, 2018).

By stimulating single beams of PFs, we were able to examine the influence of spikelets on kinetics and temporal summation of PF-mediated EPSPs. We found that spikelets narrow the half-width of concomitant EPSPs, and dampen their temporal summation, consistent with their net inhibitory action identified earlier. These first results indicated that feed-forward recruitment of spikelet shows a functional equivalence with classical GABA-mediated FFI. However, because the spikelets comprised a significant depolarizing component, perhaps due to the strong average coupling coefficient (11.3 +/- 1%; n=33 pairs displaying a mean CC > 5%), we also considered the temporal influence of the spikelet. When stimulating PFs within the dendritic tree of BCs, recruited we were not able to reliably detect the inward component, suggesting it was masked by the peak of EPSC (Figure 1). This led to the notion that perhaps FF modulation by spikelets could provide a brief excitation (Figure 6). We found that the transient excitatory drive of spikelets significantly increased the peak amplitude of the compound synaptic response, when both signals were coincident (within a 4-6 ms window). Thus, unlike cFFI, electrical feed-forward modulation (eFFM) can both shorten the temporal window for EPSP-spike coupling, thus improving spike precision, while simultaneously enhancing spike probability. The degree of such temporal contrast enhancement could be regulated by factors that adjust presynaptic spike shape, in particular the relative size of the AHP, and thus regulate temporal balance of excitation and inhibition.

IV - 2) Electrical connectivity of cerebellar cortex is tuned for rapid output synchrony

We observed that 60% of PF stimulus pipette locations within the BC dendritic tree produced sufficient excitatory drive in electrically coupled neighbours to produce an AP, and thus generating a spikelet in the postsynaptic cell. This robust recruitment can be accounted for by 3 factors: 1) overlap of MLI dendritic trees in order to more likely receive common synaptic input (See Figure 3A); 2) resting membrane potential close to threshold, which we established (Figure 3H); and 3) a strong coupling coefficient sufficient to transmit detectable spikelets (>5% - Figure 4F). Strong coupling coefficient are most certainly mediated by Cx36 (Alcami et al. 2013), and could be due to a large number of gap junctions formed between dendrites of MLIs, as shown for Golgi cells (mean CC_{Golgi} = 12% - Szoboszlay *et al.*, 2016).

This high degree of connectivity can provide global network mechanism spanning > 100 µm in the sagittal plane (Rieubland *et al.*, 2014) for generating simultaneous FF modulation of PC spiking patterns through synchronous inhibition (*i.e.*, excitation of MLIs) followed by a rapid disinhibition (*i.e.*, MLI self-inhibition). In support of this sagittal extension we find no correlation in CC over soma displacements up to 60 µm (Supplementary Figure 2A). Moreover, *in vitro* experiments have revealed that electrical connectivity in the MLI population increases convergence from MLI to PCs (Kim *et al.*, 2014). Finally, the lateral spread of PF activity through electrical synapses (as observed in Vervaeke *et al.*, 2012), along with spikelet transmission, would also contribute to increasing the effective convergence between MLI and PC.

Within this extended plane of coupled MLIs any PF activity pattern impinging on PCs would receive a network amplified, highly synchronous inhibition. Whereas the relative amount of excitation and inhibition depends on the intersectional overlap between the active PF pattern recruiting the MLI network and that exciting a particular Purkinje cell, which could in part account for the diversity of PC responses to sensory stimuli *in vivo* (Bosman *et al.*, 2010; Brown and Raman. 2018), in addition to module-specific mechanisms (Valera *et al.*, 2016). In one of the few studies examining activity of BCs and Purkinje cells, a biphasic correlogram suggested an initial excitation of PCs followed by a brief 8 ms inhibition PC firing (Blot *et al.*, 2016). This very narrow and powerful inhibition could indeed be the result of precisely synchronized BC activity followed by self-inhibition, both mediated by eFFM. Such a network-wide synchronization would be less efficient, via chemical inhibition, which does not propagate beyond one synapse. Interestingly, voltage clamped recordings of BCs *in vivo* in response to whisker pad air puffs (Chu *et al.*, 2012) showed that BC EPSCs are much faster than the PC

EPSCs, consistent with cases of predominant inhibition of PC firing in response to sensory stimuli (Bosman *et al.*, 2010; Chen *et al.*, 2016; Brown and Raman, 2018). Thus eFFM could ensure a rapid and brief BC network recruitment necessary for precise refinement of PC firing patterns.

IV - 3) Electrical synapses reinforce coincidence detection in electrically connected interneurons

PV^+-interneurons in hippocampal and cortical circuits display a wide variety of features which minimizes temporal summation of excitatory inputs. These include AMPAR with rapid kinetics (Geiger *et al.*, 1997); Kv3 channels recruited during synaptic activation (Nörenberg *et al.*, 2010), which ensure minimal temporal summation of EPSPs (Hu *et al.*, 2010); and electrical synapses, which passively alter the electrotonic structure of neurons, and notably reduce their apparent membrane time constant (Amsalem *et al.*, 2016). Altogether, these features contribute to a precise EPSP-spike coupling, in line with a proposed role of interneurons to behave as coincidence detectors (McBain and Fisahn, 2001). Cerebellar basket cells share some of these features, like fast AMPAR (Carter and Regehr, 2002) and electrical synapses to passively shape their electrotonic structure (Alcami and Marty, 2013; Maex and Gutkin, 2017), but also display specific properties supporting the same general property: axonal speeding (Mejia-Gervacio *et al.*, 2007), and classical FFI (Mittman *et al.*, 2005). Rapid eFFM is yet another mechanism sharpening EPSP-spike coupling, and may thus be regarded as a feature generalizable to other types of GABAergic interneurons throughout the CNS.

IV - 4) Implications of eFFM in fine-tuning cerebellar-dependent motor behaviours

Whisker movement kinematics can be both encoded (Chen *et al.*, 2016) and driven by precise PC firing patterns (Heiney 2014). Moreover, millisecond synchrony of PC firing is critical for synchronized inhibition in order to precisely gate deep cerebellar nuclear drive of movement (Brown and Raman, 2018). The authors propose that at initial millisecond inhibition of PC firing by sensory stimuli might disinhibit cerebellar nuclei, thus initiating motor responses. Finally in vivo evidence that BCs play an important role in refining PC firing on the millisecond scale (< 8 ms) supports their important role timing cerebellar cortical output (Blot *et al.*, 2016). We therefore propose that eFFM could be an important mechanism to achieve such robust and precisely timed control of PC firing.

V) Supplementary figures:

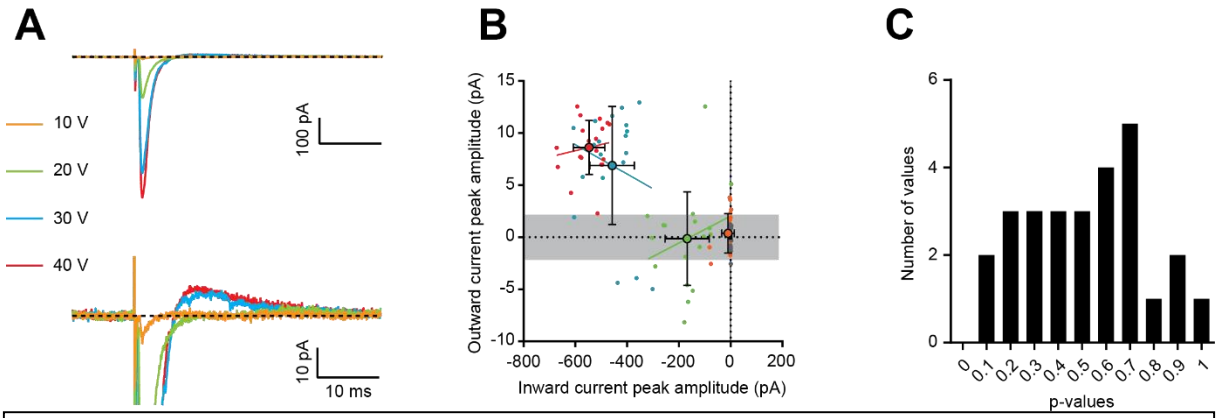

Supplementary figure 1: the amplitude of direct EPSCs and secondary outward currents are not correlated. A) Average compound synaptic responses recorded at different stimulation intensities reveal an increase in the amplitude of the direct EPSC (upper panel) and of the secondary outward current (lower panel). **B)** Outward current peak amplitude versus inward current peak amplitude of the 4 average responses shown in A (large dots), along with their underlying single sweeps (small dots). Linear regression analysis reveals that, for each stimulation intensity between 10 and 40V, no significant relationship is observed between the peak amplitude of both components of the compound synaptic response, on a single-sweep basis. **C)** P-value distribution of the analysis shown in B) (n = 27 stimulations from 9 cells, 2 to 4 stimulation intensities per cell) reveals that no significant correlation is ever observed between EPSC and outward current peak amplitudes.

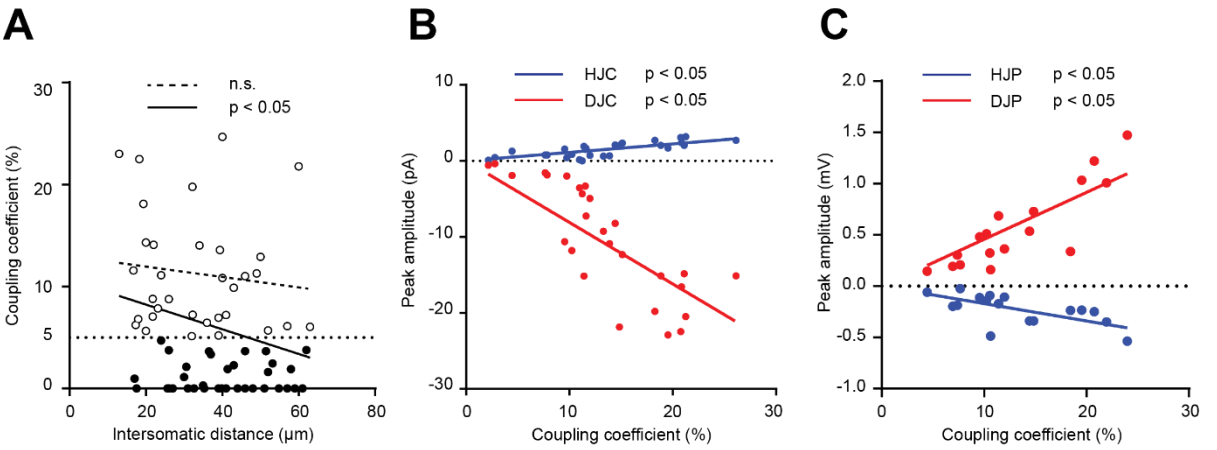

Supplementary Figure 2: Features of electrical connectivity in the BC population: A) Mean coupling coefficient versus intersomatic distance between simultaneously patched BCs. Linear regression analysis reveals that for strongly coupled pairs (CC>5%, white dots), CC doesn't significantly decrease with intersomatic distance (dashed line). However, if all pairs are considered (black + white dots), CC significantly drop down with intersomatic distance ($p < 0.05$). **B)** Expectedly, we find a significant relationship between spikelet inward currents (depolarizing junction current, DJC, red), fAHPs (hyperpolarizing junction current, HJC, blue) and coupling coefficient in paired recordings (n=27 spikelets). Note that in these recordings, the presynaptic cell was maintained around -70mV. **C)** Similar to B, but for spikelets recorded in current clamp in the post-synaptic cell (n=17 spikelets); DJP: depolarizing junction potential; HJP: hyperpolarizing junction potential.

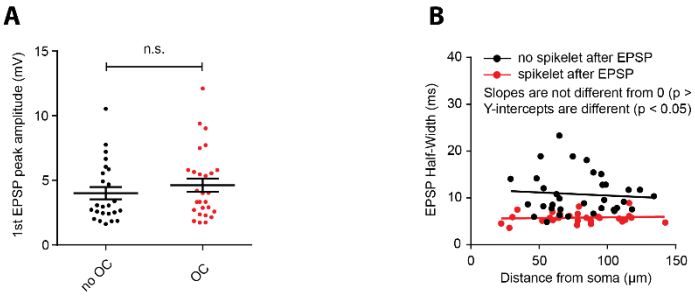

Supplementary Figure 3: controls for temporal summation. A) The amplitude of the first EPSP is not significantly different between the group where and outward current could be detected (OC, red group, n = 27 cells) and the one lacking a detectable outward current after the initial EPSP (no OC, black group, n = 24 cells - Mann-Whitney test, p = 0.4150). **B)** HW of EPSPs or compound synaptic responses is independent of distance, but EPSP with spikelets have smaller HW than pure EPSPs.

Chapter IV - Integration and modulation of electrical synapses-mediated inputs in cerebellar basket cells:

I) Evidence for transmission of subthreshold EPSCs across electrical synapses:

I - 1) Experimental results:

In Chapter III, I have mostly investigated how electrical synapses allow the transmission of spikelets, which are the filtered version of suprathreshold APs from electrical neighbours. However, as I have mentioned in the introduction, electrical synapses also allow the transmission of subthreshold EPSCs/IPSCs. Without *a priori* knowledge of these events (amplitude, kinetics, relative abundance etc...), it is not possible to tell whether or not they may have a functional and/or relevant impact on the I/O relationship of the cells receiving them. Here, I will briefly comment some preliminary results that I obtained to characterize these signals.

When I performed experiments aiming to force electrical neighbours to fire an AP, through indirect recruitment by PFs stimulation ("OFF-beam stimulation", Chapter III, Figure 2), I observed cases where only small amplitude, long-lasting inward currents could be recorded in the patched cell. Figure IV-1 shows a better example of this phenomenon than the one shown in Chapter III.

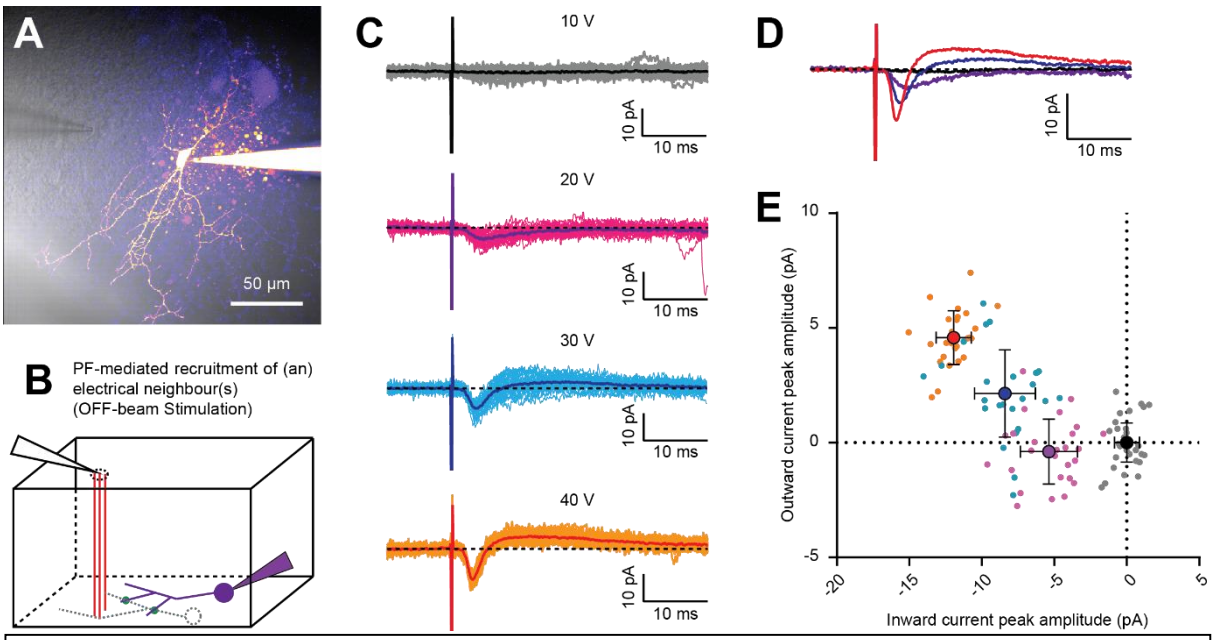

Figure IV-1: Evidence for transmission of subthreshold EPSCs through electrical synapses: A) Z-projection of a basket cell loaded with Alexa-594; **B)** Scheme of the experiment, aiming to force the recruitment of (an) electrical neighbour(s) through stimulation of afferent PFs; **C)** Average and single sweep responses, recorded in the patched cell, depending on the stimulation intensity; **D)** Average responses from C, superimposed to compare their inward and outward current peak amplitudes; **E)** Outward current versus inward current peak amplitude of all responses shown in C. Small dots represent the single sweep, and bigger dots with brackets represent average responses +/- SD.

As it can be clearly seen in this example, spikelets can be recorded on each sweep at 40V, and no response is observed a 10V. The responses observed at 20V and 30V are, however, not all spikelets. On panels C and E, it can be observed that responses recorded at 20V show, on average, a significantly higher inward current peak amplitude compared to baseline. However, their outward current peak amplitude is not significantly different from baseline. Therefore, the signal recorded in this condition is only made of an inward current. Given that these signals are not recorded when the stimulation intensity is increased to 40V, I hypothesize that they represent EPSCs experienced by the presynaptic electrical neighbour(s), but these EPSCs are not strong enough to trigger AP firing. In that case, no spikelet response is expected, and it is conceivable that a fraction of the EPSC crosses the electrical synapse.

The small amplitudes and slow kinetics of these signals is fully consistent with a heavily filtered EPSCs, and inconsistent with spikelets coming from hyperpolarized neighbours (Figure IV-2). Indeed, even though I could easily resolve only two of these cases in my data, it appears that their kinetics are slower than the most distally-triggered direct EPSCs, and their amplitude is also consistently smaller. It can also be seen that they are unlikely to be spikelets coming from hyperpolarized electrical neighbours (*i.e.*, those displaying almost none, if any, outward currents), because their half-width is dramatically higher than those of spikelets coming from neighbours held at -80mV, recorded in pair configuration (Chapter III, Figure 3).

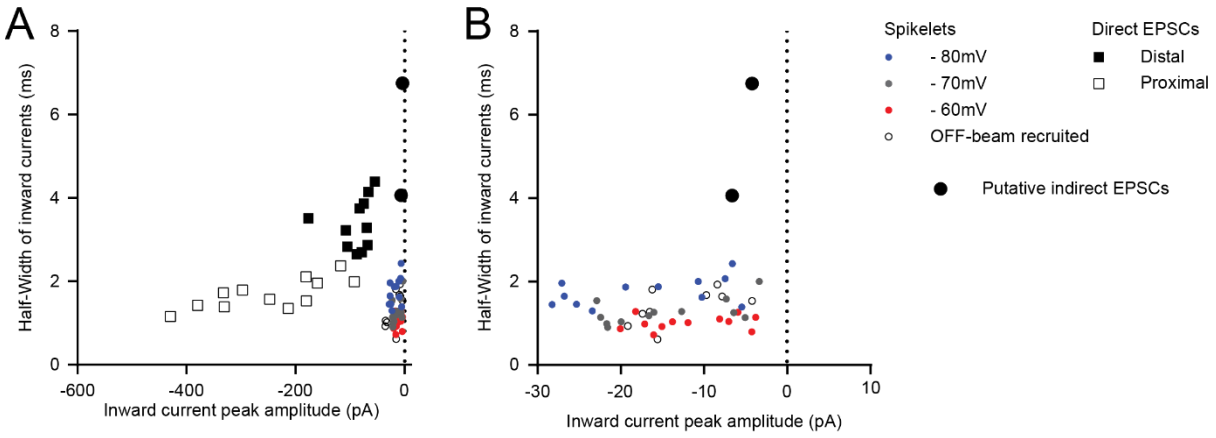

Figure IV-2: Consistent with heavily filtered EPSCs, the recorded signals have a small amplitude and slow kinetics: A and B) Relationship between inward current peak amplitudes and half-widths of seven types of responses: spikelets recorded in pairs from -80, -70 or -60mV; spikelets recorded by OFF-beam stimulation; EPSCs recorded after direct stimulation (see Figure 1 of Chapter III). Distal EPSCs come from synaptic sites at least 150µm away from the soma, while proximal EPSCs come from synaptic sites within a radius of 50µm around the soma.

I - 2) Discussion:

These preliminary data support the previous observations (and the known ability of electrical synapses) to transmit subthreshold events (Zsiros *et al.*, 2007; Apostollides and Trussel, 2014; Kuo *et al.*, 2016), which is likely to further extend the receptive field of BCs to their presynaptic inputs. Their relatively small amplitude could imply that they are unlikely to significantly influence AP firing in the post-synaptic cell, but on the other hand, their kinetics are very slow, which suggest that the charge carried by these indirect EPSCs are more likely to efficiently polarize the cell membrane. In Vervaeke *et al.*, 2012, it was notably shown that indirect EPSCs from either parallel fibers or mossy fibers can significantly influence the spiking output of electrically-connected GoCs (See Introduction).

The signals recorded in my experiments (which I will now name indirect EPSCs) should be more thoroughly examined and analysed, but this was not the main point of this thesis. In the next section, I propose an experimental paradigm better suited to study them, and propose some hypotheses as to why they could be recorded only in a subset of my recordings (1), and what could determine, at least partly, their peak amplitude and kinetics (2).

The reason why these putative filtered EPSCs were not observed in all instances when I performed OFF-beam stimulation might be that a particular arrangement of PF-MLI synapses and electrical synapses in the dendritic tree is required to record them faithfully. Figure IV-3 suggests, with schematics, that indirect EPSCs may be recorded only when the electrical synapse lies between the site of the PF-MLI synapse and the soma.

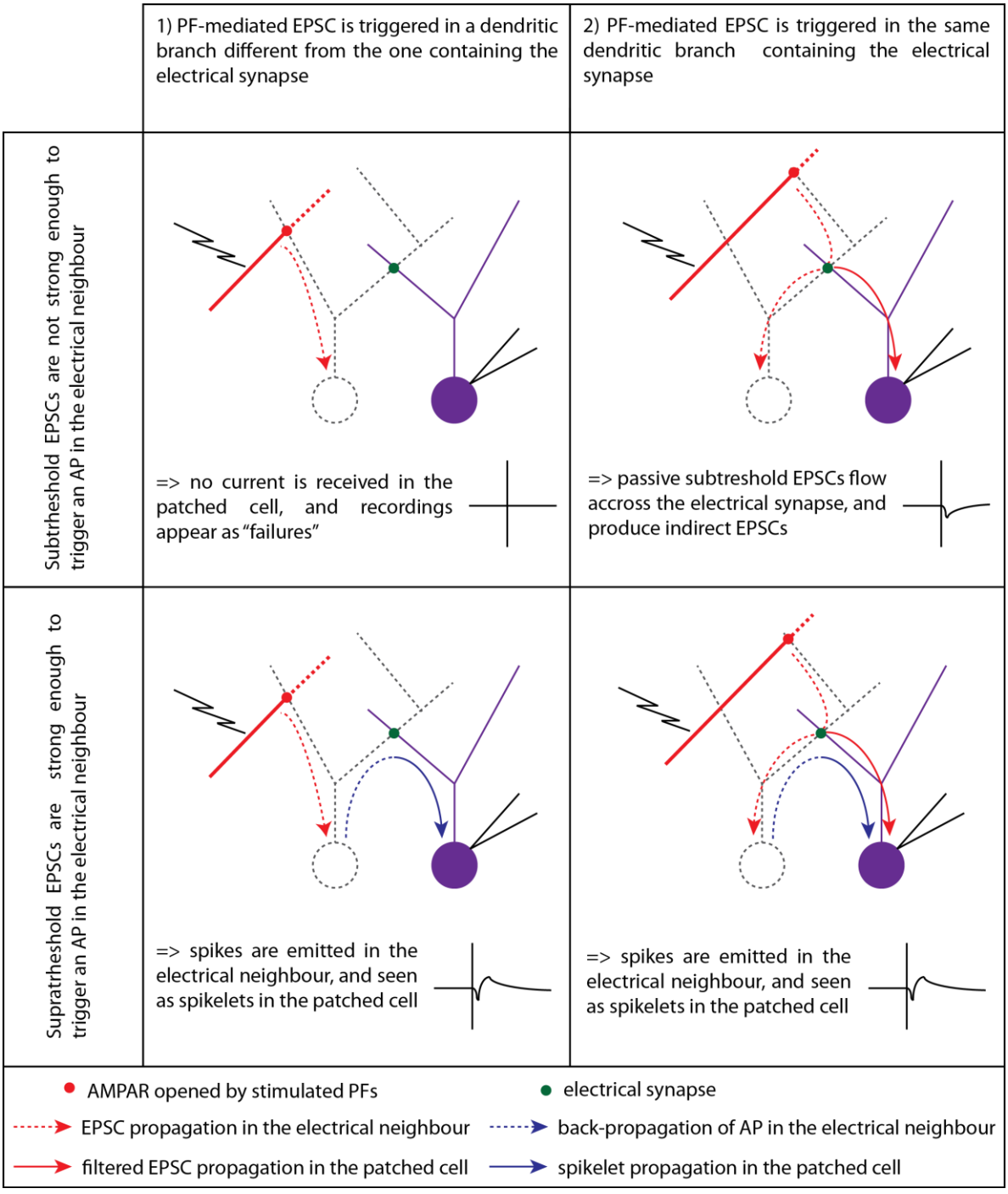

Figure IV-3: Proposed dendritic arrangements of PF-MLI synaptic inputs and electrical synapses explaining why putative filtered EPSCs are not necessarily always observed: top left) when EPSCs are subthreshold, and propagate along a branch where the electrical synapse is not located, no response is observed in the patched cell (purple); **bottom left)** by increasing stimulation intensity, EPSCs finally become strong enough to trigger an AP, and the AP back propagates in the dendritic tree, crosses the electrical synapse, and a spikelet is observed; **top right)** here, subthreshold EPSCs propagate down to the soma and don't trigger an AP, but since the electrical synapse is located along the dendritic branch where the EPSC travels, a fraction of the current crosses the electrical synapse, and an indirect EPSC would be observed; **bottom right)** in the case where the EPSC triggers an AP, it is unclear what is the exact nature of the recorded signal is: a fraction of the indirect EPSC might superimpose onto the spikelet.

It is only in the case where a fraction of the EPSC crosses the electrical synapse when travelling from PF-MLI synapse to the soma, and then triggers an AP which back-propagates in the dendritic tree, that the exact nature of the recorded signal is not clear to me, as it depends on the ability of APs to "reset" the membrane potential in the dendritic arbour of the patched cell, especially at the site where the electrical synapse is located. Indeed, it is known that the ability of APs to shunt EPSPs is cell-type dependent, and that faster EPSPs are better shunted by APs than slower EPSPs (Häusser, 2001).

In our recordings, when we examined spikelet responses between direct and off-beam stimulation (Chapter III, Figure 3H), we found a striking similarity in correlation between positive and negative peak amplitudes, suggesting that such EPSCs do not contaminate the spikelet-mediated outward current. However, we found evidence that time integral of normalized spikelet responses are significantly higher in direct stimulation compared to off-beam stimulation (Chapter III, Figure 3I), which suggests that indirect EPSCs may contaminate spikelet responses at later times, but we cannot tell if these indirect EPSCs originate from the spiking cell, or from other cells experiencing subthreshold EPSCs.

In order to directly examine the relationship between presynaptic EPSCs (sub- or supra-threshold) and post-synaptic responses across an electrical synapse, I imagined that combining dual patch-clamp recordings of electrically-connected BCs with electrical stimulation of a single set of PFs would be the ideal experiment to perform. By systematically examining the response recorded in each cell after PF stimulation onto either of their dendrites, or in a region where their dendrites cross, it might be possible to obtain the experimental results supporting or disproving the hypotheses formulated in Figure IV-3.

The results of this experiment would give valuable insights about the role of electrical synapses between basket cells, or electrically-connected cells in general. Indeed, it would allow to examine how potent indirect EPSCs/IPSCs experienced by an electrical neighbour would be in influencing AP firing in one cell. The ability of subthreshold events to cross electrical synapses and influence AP firing in a post-synaptic cell has notably been demonstrated between fusiform cells and stellate cells in the dorsal cochlear nucleus (Apostolides and Trussell, 2014) and between hippocampal interneurons (Zsiros *et al.*, 2007). Most studies of electrical communication examine how steady-state changes (*e.g.*, long current pulses) or rapid signals (*e.g.*, APs) are transmitted. However, owing to their inherent differences in kinetics, either type of signal is differentially filtered by the membrane of the connected cells. The kinetics of direct EPSCs and IPSCs fall between these two extremes, suggesting that they are likely to contribute

a significant proportion of the receptive fields of electrically connected cells. Additionally, the exact location of electrical synapses and direct chemical synaptic inputs (*e.g.*, EPSCs from PFs) onto one cell may underlie differences in magnitude and kinetics of the filtered current, due to end effect of sealed cables (Rall 1969, Tran-Van-Minh *et al.*, 2016 - Figure IV-4).

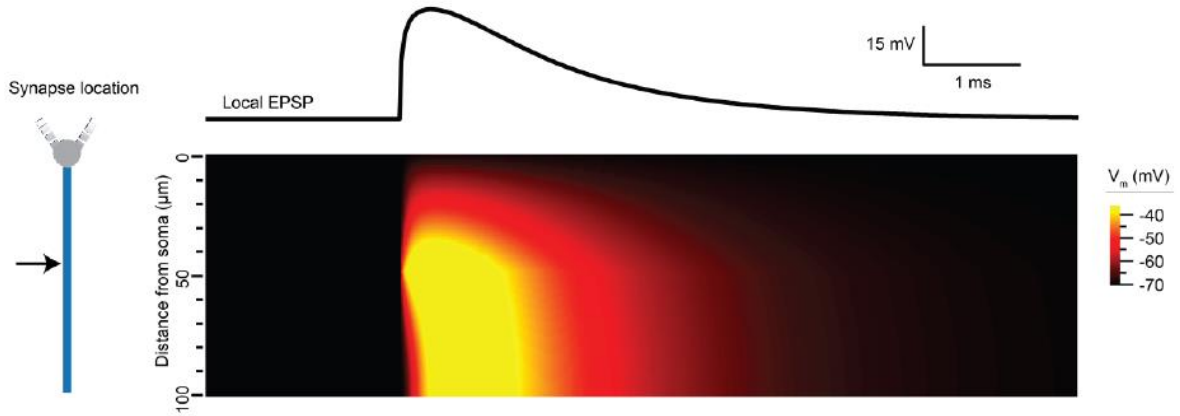

Figure IV-4: Temporal and spatial extent of PF-induced EPSP in the dendritic tree of a cylindrical branch: left) Schematic diagram of a "ball and stick" modelled cell, with a single dendritic branch. The black arrow indicates the site of synaptic location; **Top right)** Time course of the local EPSP (*i.e.*, at the site of synaptic current entry); **Bottom right)** spatio-temporal dynamics of voltage deflections induced by the EPSP in the cable. Note the difference in amplitude and dynamics between the distal and the proximal compartments, due to the end effect and the somatic current sink, respectively.

From Tran-Van Minh *et al.*, 2016.

The schematics shown in Figure IV-5, representing two different configurations of PF-BC synapse, electrical synapse, and somatic compartment ordering, may further help in clarifying this idea.

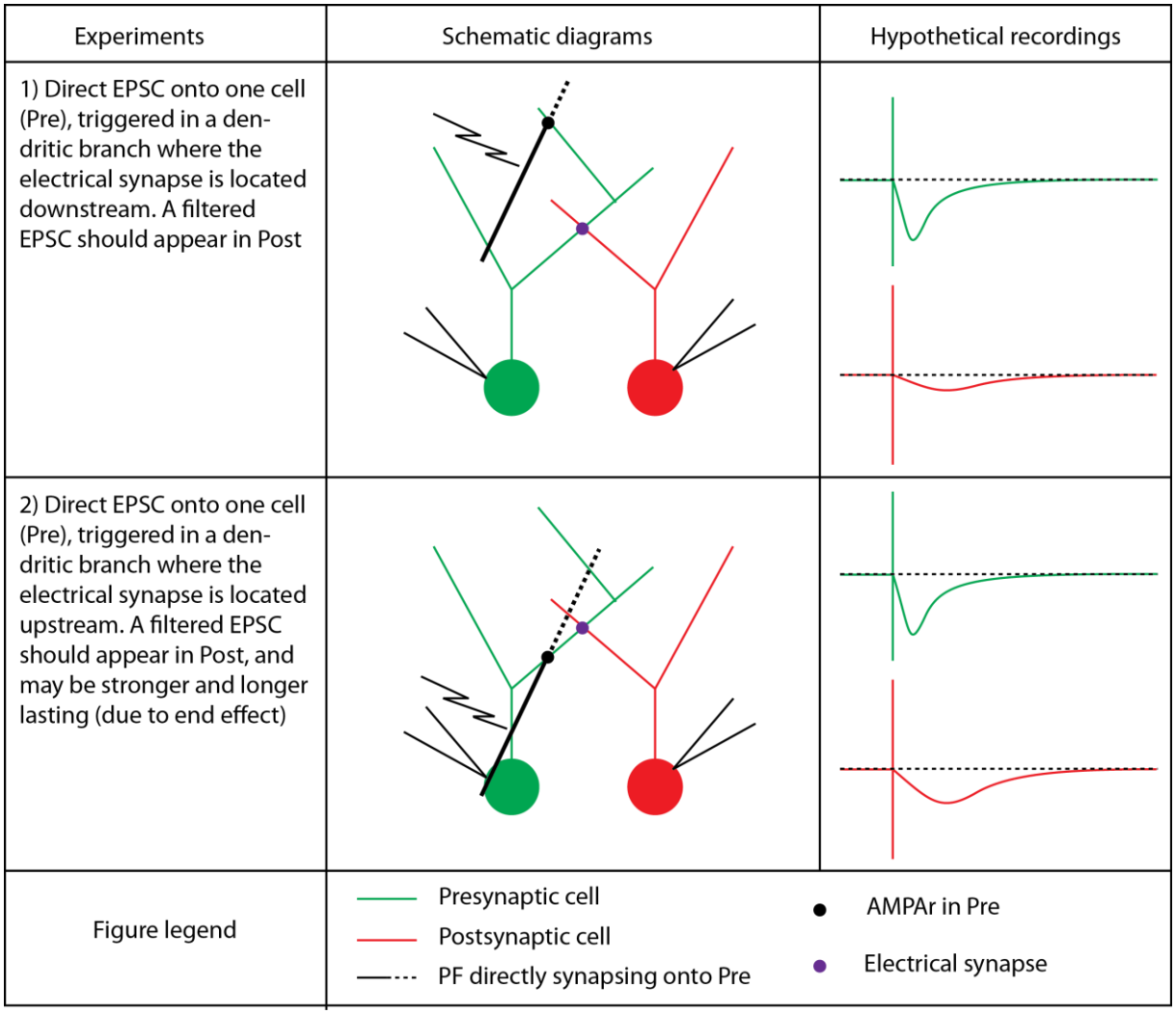

Figure IV-5: the exact relative position of synaptic inputs and electrical synapses may impact amplitude and kinetics of the filtered, subthreshold events.

It could be argued that indirect EPSCs, by being so heavily filtered, are unlikely to significantly influence the I/O relationship of basket cells. However, two features can actually be proposed to counter this argument. Firstly, the number of PFs causing indirect EPSCs is likely to be higher than the number of PFs providing direct EPSCs (*i.e.*, higher receptive field for indirect EPSCs), due to the tendancy of BCs to form electrical clusters (Alcami and Marty, 2013; Kim *et al.*, 2014; Rieubland *et al.*, 2014). For example, if one cell is electrically connected to N numbers, then N/(N+1) (upper limit) of the EPSCs received are indirect EPSCs. This estimate could be further refined by considering the equivalent number of neighbours (introduced in Alcami and Marty, 2013). Briefly, this metric compensates the physical number of electrical neighbours by the electronic coupling associated to each of them. Secondly, direct currents are very fast, and thus not fully converted to synaptic potentials, while indrect EPSCs, thanks to their much slower kinetics, are likely to be more (or fully) converted to efficient

synaptic potentials. The relatively small amplitude of indirect EPSCs alone should therefore not be considered as a good proxy for their ability to influence spiking.

II) Role of HCN channels in shaping AP waveform, and transmitted spikelets:

II - 1) Experimental results:

In Chapter III, I described how the presynaptic state critically influences the waveform of the transmitted spikelet, notably by altering the waveform of the presynaptic AP. From this observation, I hypothesized that in principle, any active conductance able to shape the presynaptic AP waveform would be able to change the transmitted spikelet. This phenomenon has already between demonstrated in electrically connected, fast-spiking, striatal neurons (Russo *et al.*, 2013). I therefore examined the literature of cerebellar basket cells, with a particular focus on the type of channels which they have been shown to express, especially in adult animals. HCN channels appeared to be a plausible candidate to test this hypothesis. Indeed, they are densely expressed in the pinceau structure of BCs in adulthood (Lujan *et al.*, 2005), and are opened at a resting membrane potential of -70mV, mediating an inward cationic current when the BCs are hyperpolarized (Southan *et al.*, 2000). By combining these observations, I reasoned that HCN channels could shape the AHP of cerebellar basket cells, and speed up the membrane repolarization by providing a depolarizing current triggered during the transient hyperpolarization caused by the AHP.

I first set out to compare spikelet waveforms recorded during OFF-beam stimulation, and later AP waveforms, before and after application of a blocker of HCN channels. This experimental approach proved to be ill-advised, because:

- even if spikelet waveforms were found different in some cases, it was not possible to conclude that the presynaptic AP had changed after drug application (with single-cell patch clamp, the recorded spikelets came from one electrical neighbour, whereas recorded APs originated from the patched cell).

- strong fluctuations in holding currents or resting membrane potentials were observed after drug application, for an unclear reason. A representative case of these experiments in shown in Appendices, along with the corresponding discussion on these experiments.

In order to better test the hypothesis that HCN channels shape APs and transmitted spikelets, I performed paired recordings of BCs, and applied 5-10µM of ZD-7288 when the connected cells displayed a relatively strong coupling coefficient, in order to examine the

changes in presynaptic AP waveform and post-synaptic spikelets. A representative example, along with population average, is shown in Figure IV-6.

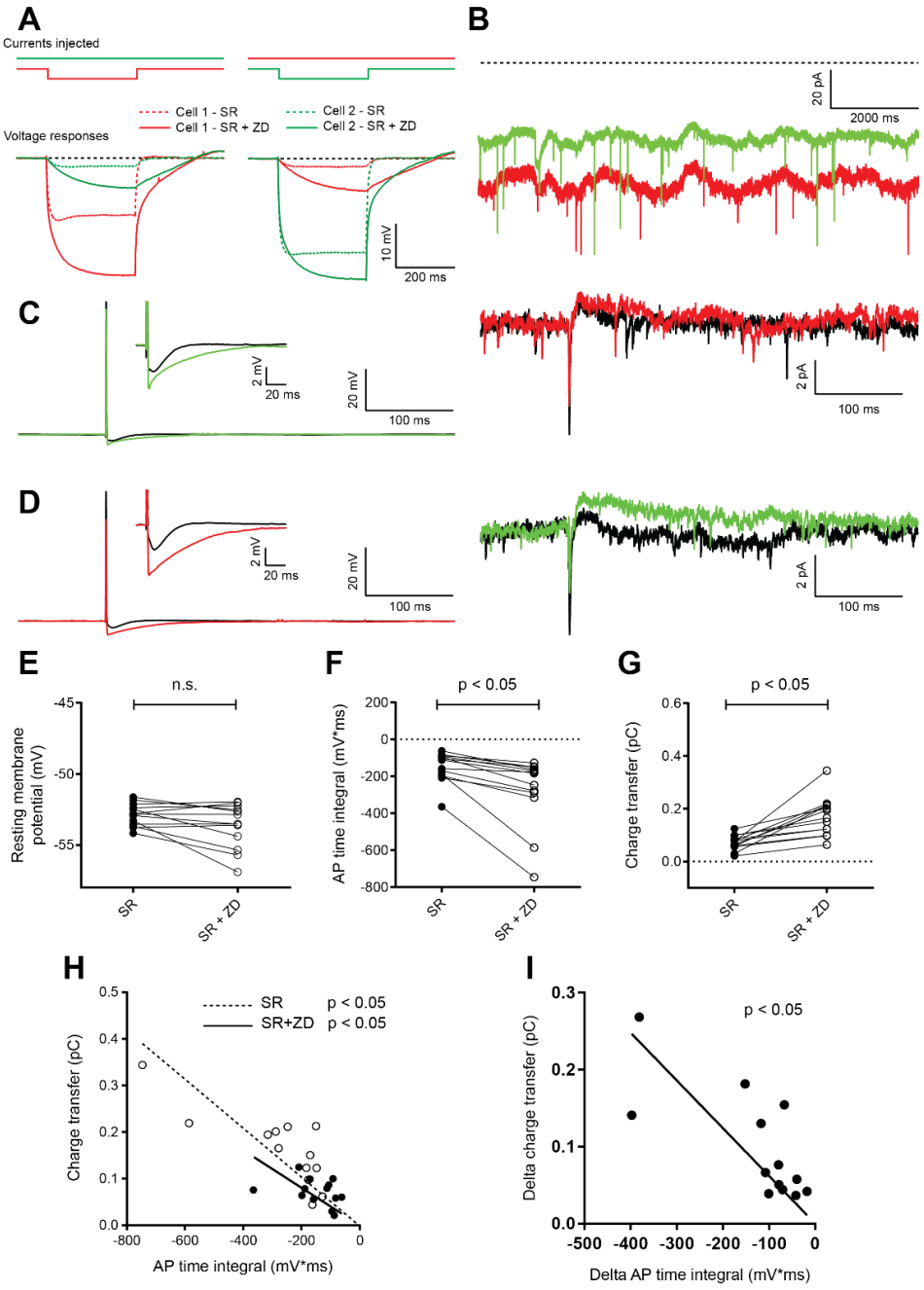

Figure IV-6: Evidence for a role of HCN channels in shaping AP waveform and their corresponding spikelets: A) Membrane hyperpolarization is different after application of ZD, even for the non-injected cell; **B)** 10s recordings of spontaneous activity between two electrically-connected cells display signs of correlations on long time scale; **C)** AP waveform in one cell of a pair, before (black) and after (green) application of 10µM ZD-7288 (left), with the corresponding spikelets recorded in the second cell of the pair (right); **D)** same as in A, but the red cell now emits APs, and the green cell receives the spikelets; **E)** The resting membrane potential is comparable in the two conditions; **F)** AP time integral is more negative after ZD-7288 application; **G)** Spikelets are more hyperpolarizing after drug application; **H)** Charge transfer of spikelets recorded in post-synaptic cells correlate with the AP time integral in the presynaptic cells; **I)** The changes in AP and spikelets waveforms before and after drug application correlate with each other.

First, I observed that during a hyperpolarizing current pulse, injected cells displayed the caracteristic feature of a "sag" response at the early phase of the pulse, which is known to be a strong indicator of HCN recruitment. This sag disappeared after application of ZD, and the same current pulses caused more pronounced hyperpolarizations than in control conditions (Figure IV-6A). This result is consistent with an increase in input resistance and blockade of feedback recruitment of inward currents, caused by HCN channels. Then, it was possible to observe correlations in holding currents of electrically connected cells on long time scales after ZD application (Figure IV-6B). These fluctuations were not present before application of ZD (not shown, but see Appendices). Furthermore, AP waveform changed after bath application of ZD, either because of a misadjustement of the bias current after drug application to keep a similar resting membrane potential, or because of changes in AHP kinetics. These changes translated into different waveforms of the post-synaptic spikelets, and changes in AP waveform and spikelets mirrored each other (Figure IV-6C and D).

In a population of n=14 cells from 7 pairs, I first confirmed that the resting membrane potential was comparable after ZD application, to ensure that further changes in AP waveforms and transmitted spikelets were not caused by a misadjustment of the resting membrane potentials. Indeed, lower resting membrane potentials will tend to decrease the time integral of the presynaptic AHP and the transmitted spikelets (Chapter III-Figure 3). I later found that the time integrals of APs (Figure IV-6F) and spikelets (Figure IV-6G) were both significantly *higher* in ZD condition (in terms of absolute amplitude). In most cases, the effects were minor (see Discussion). Finally, I found that the time integral of APs, and their corresponding spikelets, were correlated in control conditions and after drug application (Figure IV-6H), and more importantly, that the differences in AP time integral and charge transfer of spikelets before and after drug application were also significanly correlated (Figure IV-6I). Altogether, these results suggest that blockade of HCN channels lengthens presynaptic AHPs, and that consequently, the corresponding spikelets convey more inhibition.

II - 2) Discussion:

In Chapter III, I have shown how modulating the presynaptic membrane potential changes the AP waveform in BCs, and consequently the spikelets transmitted to their electrical neighbours. From this observation, I imagined that in principle, any ion channel able to shape

the presynaptic AP waveform should be equally capable to change the waveform of the transmitted spikelet. I therefore set out to examine if HCN channels blockade could change the presynaptic AP waveform, and consequently the transmitted spikelets.

I first focused on examining if the (partial) blockade of HCN channels could change AP waveform and transmitted spikelets between electrically-connected cells. Initially, I performed single-cell patch-clamp recordings, paired with OFF-beam electrical stimulation of PFs, to force electrical neighbours to fire an AP. Application of ZD-7288 caused large fluctuations in holding currents and resting membrane potentials of the patched cells, and appeared to cause longer-lasting spikelet responses. However, this second observation may have simply reflected a non-specific effect of HCN blockade in the whole slice, and these experiments appeared ill-suited to address my hypothesis (see Appendices).

The results obtained from paired recordings provide some evidence that HCN channels can indeed shape the presynaptic AP waveform, and the corresponding spikelets. However, I would suggest to interpret these results with high caution, because the effects detected are overall minor, and the two cells shown in Figure IV-6 are actually those displaying perhaps the most striking differences (both in AP and spikelet waveforms) before and after application of ZD-7288. For a reason which I have not had the time to investigate more deeply, most of the cells did not display any obvious changes in either AP or spikelet waveform after blockade of HCN channels. Moreover, some of the effects observed in spikelets may also be caused by differential ZD-induced changes in inputs resistances of each cell of a pair (See Appendices, for considerations about the link between input resistances and coupling coefficients in between two cells), and not necessarily to the block of the HCN-mediated cationic current which would repolarize the cell membranes faster during the AHP.

In the next paragraph, I propose hypotheses for the different unexplained observations encountered during these experiments, and notably the mismatch between the striking spikelet changes observed after ZD application in OFF-beam stimulation, and the minor ones observed in pairs.

First of all, HCN blockade *always* caused a significant change in voltage response during a long current pulse, and *always* made the sag disappear. This indicates that ZD-7288 *did* cause a blockade of HCN channels in the BCs I patched, without necessarily indicating where these channels are located (*e.g.*, axon, soma, dendrites). Then, large holding currents fluctuations were not necessarily observed in all instances after drug application: here again, *sometimes* they did, and *sometimes* they did not. This may relate to the fact that MLIs can form

electrical network, clustering on average four to five cells (Alcami and Marty, 2013; Kim *et al.*, 2014). In large clusters, we may expect large holding current fluctuations because many electrical partners have an erratic spiking behaviour in ZD-7288 (assuming HCN *does* play a major role in shortening the AHPs), while in smaller clusters, if two cells (*i.e.*, those from the pair) are prevented from AP generation, then the few others left in the network do not spike sufficiently to impair the recordings. The bias currents introduced by the amplifier to maintain the patched cells in a slightly hyperpolarized state may have further hyperpolarized the electrical neighbours in the network, and prevented them from spiking.

Another possibility is that the behaviour of HCN channels is significantly altered by the patching procedure itself, possibly because of dialysis. This argument is proposed because I postulated that the large holding current fluctuations which I observed could be caused by erratically spiking electrical neighbours with very long AHPs (on the order hundreds of milliseconds to seconds) after drug application, while in paired recordings, only minor effects were observed. The sole difference between spikelets from the network and those from the patched cells is, as far as I can tell, that the latter come from a dialyzed cell. Further support for this hypothesis is revealed by examination of the large changes in spikelet waveforms during OFF-beam PF stimulation, before and after drug application (See Appendices). This hypothesis is also consistent with the fact that HCN channels have a wealth of internal regulators, such as [cAMP] (Chen *et al.*, 2001), and [PIP_2] (Pian *et al.*, 2006), which are dialyzed during the patching procedure.

Finally, there's also the genuine possibility that HCN channels have a weak effect on AHP and corresponding spikelets, implying that the effect I detected in my paired recordings is real, but the effect size is weak, or even irrelevant. In that case, however, one would be left with only speculations as to why ZD-7288 addition tended to cause large fluctuations in holding currents in the patched cells.

To conclude on this section, the statistical analysis of paired recordings indicates that HCN channels accelerate AHPs and decrease the inhibitory component of spikelets. However, my personal opinion is that a deeper analysis is required to publish these data. We should ideally first characterize HCN channels in BCs, and resolve the problem of the large holding currents fluctuations; then examine how they could be regulated by internal molecules; and finally address their ability to regulate AHPs and transmitted spikelets. Moreover, when coming to the ability to shape transmitted spikelets, a proper analysis of the changes in input resistance induced by blockade of HCN channels should be performed, in order to address if the putative

changes would be caused by changes in AHP waveforms, or simply changes in input resistance in the post-synaptic cell (Fortier and Bagna, 2006).

III) Frequency-dependent temporal summation of spikelets:

III - 1) Experimental results:

In Chapter III, I showed that compound synaptic responses mixing an EPSP and a spikelet summate less than pure EPSPs, at a stimulation frequency of 50Hz (Chapter III, Figure 5). Since this value was quite arbitrary (for example, *in vivo* recordings of granule have shown that they can fire in burst, up to a few hundreds of Hz, during sensory stimulation - Chadderton *et al.*, 2004), I was interrested to examine systematically how spikelets alone (*i.e.*, without confounding EPSPs) would summate over time, depending on the frequency of stimulation of the presynaptic cell, and adress the temporal summation properties of spikelet transmission in cerebellar basket cells.

Before doing so, I changed the temperature of recordings from 32°C to 36°C, to examine if increasing the temperature to approach more physiological conditions would change spikelet signalling in cerebellar basket cells, notably by accelerating the kinetics of the potassium channels mediating the AHP. I found that the difference of 4 degrees didn't change significantly the half-width of AHPs, from APs fired at Vm= -60mV ($p=0.6673$, Mann-Whitney test; n=12 AHPs recorded at 32°C vs. n=14 AHPs at 36°C - data not shown).

Later, in order to examine the temporal summation of spikelets, I performed paired recordings of electrically connected BCs, and triggered 10 APs at different frequencies (10, 20, 50 and 100Hz) in the presynaptic cell, while monitoring the post-synaptic responses. These experiments were conducted with 10µM gabazine in the ACSF, to block GABAergic inhibition. A representative experiment, along with statistical analysis of n=10 cells from 5 pairs is shown in Figure IV-7.

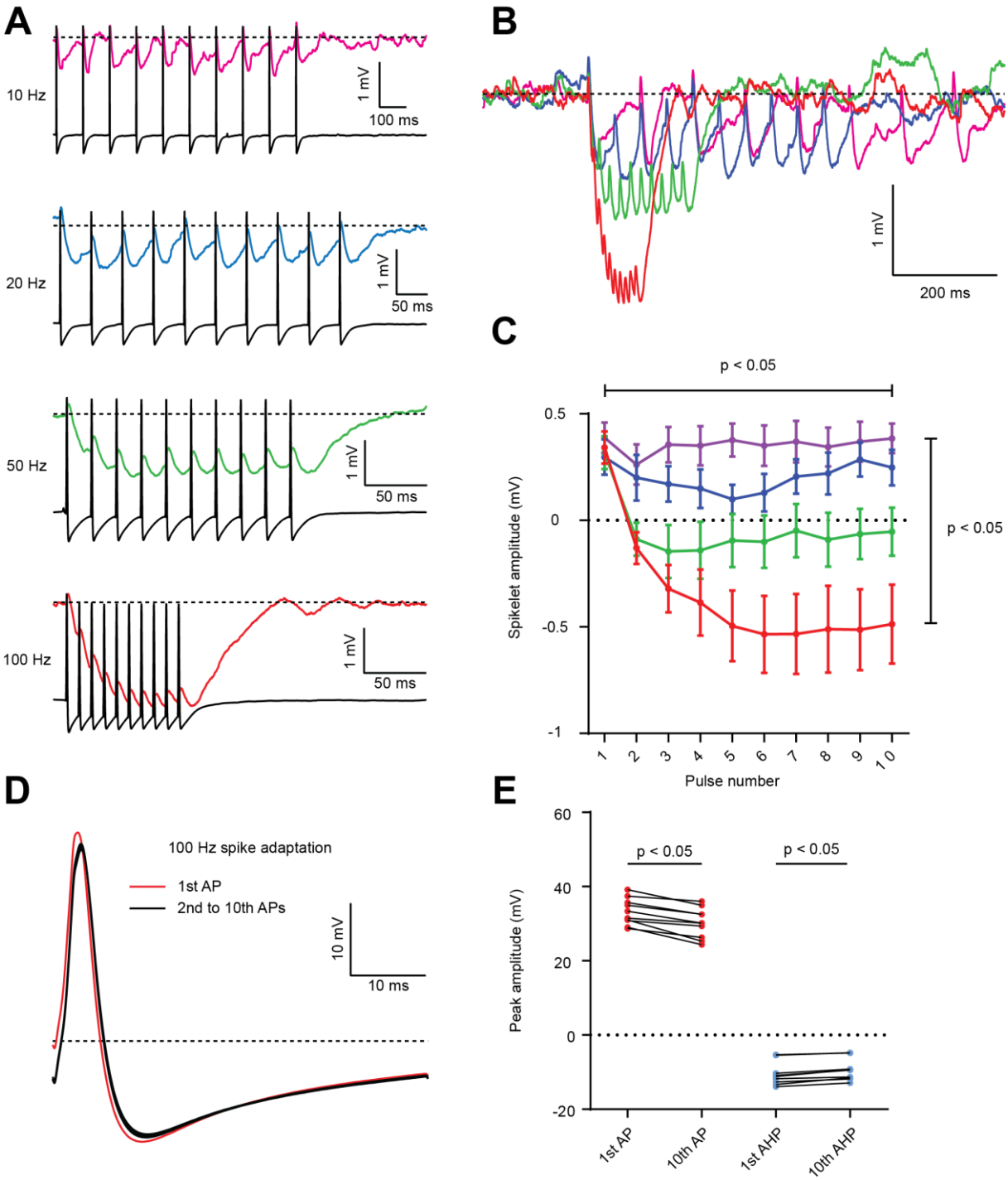

<u>Figure IV-7: Frequency-dependent temporal summation of spikelets in cerebellar basket cells:</u> A) representative examples of 10 APs fired at different frequencies (black traces), and the corresponding spikelets recorded in the post-synaptic cells (color); **B)** Color traces from A are superimposed to reveal the differences in temporal summation; **C)** Spikelet peak amplitude (from baseline before the first AP), depending on the frequency of the presynaptic APs (same color code as in A). Two-way repeated measure ANOVA test reveals a significant effect of both pulse number and frequency of AP firing (n=10 cells, from 5 pairs); **<u>D)</u>** Spike adaptation at 100Hz stimulation, showing that only the first spike (red trace) is different from the subsequent ones (black traces); **<u>E)</u>** Peak amplitude of AP and AHP are significantly different between the first and the 10th AP fired.

It can be seen that at low stimulation frequency (10Hz), the voltage trajectory of the pre-synaptic cell corresponds to the voltage trajectory of 10 independent APs, repeated accross

time. Consequently, the spikelet responses recorded in the post-synaptic cell are independent of each other, and display no detectable temporal summation, as assessed by measuring the positive peak amplitude of each spikelet response along the train (p-value > 0.05). Increasing the firing frequency to 20Hz caused a minor but significant decrease of the spikelet peak amplitude along the trains (as compared to 10Hz responses, p-value < 0.05), most likely because the resting membrane potential of the post-synaptic cell has not fully returned to baseline before each subsequent spikelets. The effect seems to be present for some cells, and absent in others (data not shown). Finally, increasing the firing frequency to 50 and later 100Hz further decreases the peak amplitude of the spikelets (compared to baseline), although this effect is again cell-dependent at 50Hz, but present in all cells at 100Hz. Two-way repeated measure ANOVA detected a significant effect of both the frequency of AP firing (1), and the pulse number (2) on temporal summation, with no interaction between the two factors. This result suggests that spikelet reponses, in each regime, reach a different steady-state behaviour, with a different number of APs. Overall, increasing the frequency of AP firing causes an increase the absolute amplitude of inhibition.

Finally, up to 50Hz firing frequency, no AP waveform adaptation occurs (data not shown), and changes in post-synaptic responses are therefore due to a difference in voltage trajectory *per se*, and do not indicate a dynamic change of gating properties of sodium and potassium channels underlying the presynaptic APs. However, at 100Hz firing frequency, small but significant decreases in peak amplitude of APs and AHPs are detected (Figure IV-7D and E), suggesting that at high frequencies, temporal summation of spikelets is a compound effect of changes in presynaptic AP waveforms, and cable filtering of the presynaptic voltage trajectory.

III - 2) Discussion:

In Chapter III, the ability of spikelets to reduce temporal summation of EPSPs was tested at an arbitrary frequency of 50Hz. However, I was interested to examine if this effect could be frequency-dependent. *A priori,* owing to the different gating properties of Na^+- and K^+-channels, along with their dependency on presynaptic voltage, it was unclear how the overall spikelet-mediated post-synaptic response could vary with the presynaptic firing frequency.

My experiments confirmed that APs show no adaptation up to 50Hz. At 100Hz, however, significant signs of spike adaptation became apparent (AP and AHP peak amplitudes decreased by ~10% between the first and the last APs). These experiments also revealed that

the amount of inhibition delivered increases with the AP firing frequency of the pre-synaptic cell. It appears that the increase in inhibition received in the post-synaptic cell is caused by a recurrent recruitment of AHP in the pre-synaptic one, which increases with firing frequency. Overall, and as to be expected from electrical transmission, the post-synaptic cell receives a filtered version of the pre-synaptic voltage trajectory. At high frequencies, the global readout in the post-synaptic compartment virtually matches what would be expected from a long hyperpolarizing current pulse (mimicking the recurrent recruitment of slow AHPs), onto which brief depolarizing currents (mimicking the rapid sodium peaks) would be superimposed.

I hypothesize that this behaviour of electrical transmission could become *even more interesting* if AP firing frequency is further increased. Indeed, at low stimulation intensity, spikelet responses show no adaptation, because APs are independent of each other and repeat their waveform over time. If AP firing frequency is progressively increased to 100Hz, a build-up of inhibition starts to be observed because of a recurrent recruitment of the AHPs in the pre-synaptic cell. This behaviour would likely be observed at higher rates, *up to a certain point*. My intuition is that at much higher firing frequencies (let's say, 500Hz and above), then an AP train will become a barrage of sodium peaks, with little (if any) AHP.

From a strictly physical point of view, and assuming an ideal case of no spike adaptation up to such high frequencies (or even in the case of adaptation, AHPs would certainly suffer from increased firing faster than the sodium peaks of the APs) I suppose that the temporal summation of the spikelets could then display a net *excitatory* behaviour: if a cell emits an AP every 2ms, and the sodium peak lasts ~0.5/1 ms, then half of the time between two APs is spent in the sodium peak, while the other half is spent in the lower amplitude potassium peak. Over repeated stimulation, the read-out in the post-synaptic cell may thus very well match a long depolarizing current step with a saw-toothed envelope (See Figure IV-8).

	Voltage trajectory in the presynaptic cell	Voltage trajectory in the postsynaptic cell	Net effect of spikelet temporal summation
Low AP firing frequencies (< 10 Hz) allows the presynaptic cell to go back to baseline before each spike. => no spikelet adaptation	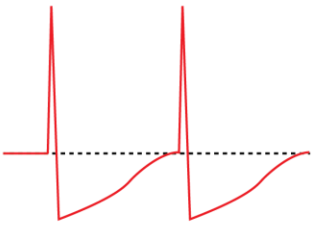		no summation
Medium AP firing frequencies (10 - ~300Hz) forces each spike to start before the AHP is over in the presynaptic cell. => inhibitory spikelet adaptation	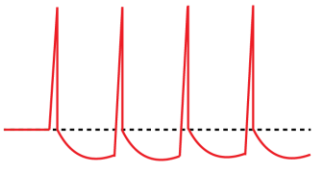	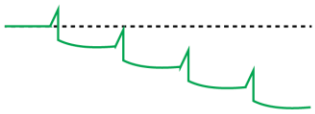	build up of inhibition
(Very) fast AP firing frequencies (> ~300Hz) forces each spike to start before the AHP has started to initiate significantly. => excitatory spikelet adaptation	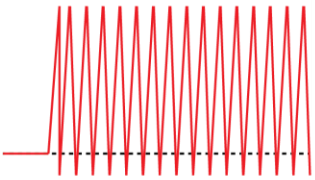		build up of excitation

Figure IV-8: Speculative relationship between AP firing frequency and net effect of spikelet summation: As firing frequency increases, spikelet summation could change from no temporal summation to net inhibitory summation, and later on to net excitatory summation. These changes should match the filtering properties of the cell membranes (passive properties) and sodium/potassium channels kinetics (input currents)

Whether or not this behaviour could be observed in basket cells is a totally open question which I did not address. Nevertheless, in 2016, Wang *et al.* reported firing frequencies of fast-spiking cortical neurons in human, monkey and mice up to 600Hz. Given that these neurons show minimal spike adaptation up to a few hundreds of Hz (Azouz *et al.*, 1997), and can form electrical synapses (Hu *et al.*, 2014), they may be a candidate system to test the hypothesis that electrical transmission can non-monotonically change their net impact on post-synaptic targets, depending on the frequency of AP firing. If such a behaviour could be demonstrated, it would elegantly show how electrical synapses can, in certain conditions, support neuronal computations that chemical synapses cannot. Indeed, chemical synapses are well-known to display short-term plasticity features, where the peak amplitude of post-synaptic currents changes according to the frequency of stimulation of the pre-synaptic site. But in these cases, the polarity of these currents cannot change. From an epistemological point of view, if electrical synapses could be shown to have a behaviour which chemical synapses cannot display, it would further help in demonstrating that electrical synapses are genuinely important in physiology.

Once again, I don't wish to raise the idea that electrical synapses are "any better" than chemical ones, but simply that they provide another mechanism for neurons to share electrical information. Rather than opposing chemical and electrical synapses in neuronal computation and circuit function, it appears wiser to me to consider them in a synergistic way: they can cooperate to further enrich the repertoire of neuronal computations, especially (but not exclusively) in interneuron populations. Stated in other words, claiming that any type of synapses is better than the other one would be as simple-minded as saying that words are better than numbers to communicate information.

IV) Conclusion:

In this Chapter, I have shown evidence that subthreshold EPSCs can cross electrical synapses, which suggests that they could influence the I/O relationship of cerebellar basket cells. Moreover, I showed that spikelet signalling (which I mostly characterized in Chapter III) can genuinely be regarded as any synaptic signal in a neuron: it can be modulated. Here, I only showed two different ways in which the presynaptic element could influence its waveform (potential role of HCN, and robust evidence of presynaptic firing frequency), but it is conceivable that other experimental manipulations, typical of chemical synaptic transmission, could be employed to test more hypotheses. For example, one fundamental question which I did not address in this thesis is how the strength of electrical synapses could be modulated in BCs.

Chapter V - Evidence for differential dendritic integration properties between SCs and BCs:

I) Differences in dendritic morphology between stellate and basket cells:

As reported in (Chu *et al.*, 2012), PF-mediated synaptic currents recorded *in vivo* during sensory stimulation tend to display faster kinetics and higher amplitudes in BCs than in SCs. Such differences could be due to differential feed-forward recruitment of spikelets (Chapter III); GABAergic FFI (Mittman *et al.*, 2005); differences in cable filtering; or differential recruitment of active conductances. In any case, these differences suggest that BCs and SCs may be differentially recruited by their common presynaptic afferents. We therefore set out to compare dendritic integration properties between the two cell-types. To do so, I reproduced in BCs a part of the experimental work and analysis which had been performed in SCs (Abrahamsson *et al.*, 2012). I started by comparing morphological features, and later examined cable filtering of PF-mediated EPSCs.

I first focused onto morphological features for three reasons: firstly, because morphological parameters constitute the backbone of passive properties, and establishing these properties is the first step in addressing the dendritic integration properties of a cell-type; secondly, because thin dendritic branches (~400nm) is the critical morphological factor responsible for a sublinear dendritic integration behaviour in SCs; thirdly, classical analytical solutions to the cable equation are derived from an ideal case of an infinitely long cylinder, but it is obvious that no real dendritic branch can satisfy this criterion. The relevance of this ideal consideration can be assessed by comparing the calculated steady-state length constant to the length of the dendrites (*i.e.*, if the dendrites are "much" longer than the steady-state length constant, then the calculation of the latter by assuming an "infinitely long cable" is justified). Additionally, the ratio of frequency-dependent length constant (λ_{AC}) over dendritic length is indicative of how cable filtering will impact synaptic events and cause space-clamp errors, depending on where they originate from in the dendritic tree (Williams and Mitchell, 2008). The equation for the frequency-dependent length constant can be approximated by:

$$\lambda_{AC} = \sqrt{\frac{d}{4\pi f R_i C_m}} \quad (8), \text{ (for f > 100Hz)}$$

where f is the characteristic frequency of the electrical signal examined; here, we considered an excitatory current mediated by AMPA receptors, and we chose f = 1kHz, as in Abrahamsson *et al.*, 2012 (the equation is taken from Johnston and Wu, 1995).

In my investigation of BCs, I first examined two of their dendritic morphological features: their diameter, and maximal radial length. I focused on these two for the following reasons:

- comparing how synaptic events could be differentially filtered by BCs and SCs (dendritic diameter values for SCs were taken from Abrahmsson *et al.*, 2012);

- considering dendritic diameter as a first indicator of sublinear readout of synaptic inputs in BCs (*i.e.*, diameters inferior/superior to those found in SCs would indicate stronger/weaker sublinear dendritic integrative behaviour, respectively - Tran-Van-Minh *et al.*, 2015);

At this step, I wish to remind the reader that the equations for calculating length constants are drawn from the assumption that dendritic branches can effectively be modelled by simple cylinders, even though I (and previous studies) have shown the presence of electrical synapses in BCs, which make such assumptions invalid. However, as it is usually the case in estimating passive properties of any cell-type, a good starting point is to derive a simple model which can be updated later on. Additionally, in the case where experimental results would not match the predictions from the simple model, one obvious candidate to explain the discrepancies will be the electrical synapses.

I - 1) BCs display longer dendritic branches than SCs:

Morphological features of MLIs have already been investigated in previous studies in young mice (Rieubland *et al.*, 2014) or adult rats (Sultan and Bower, 1998). However, none of these studies clearly distinguished between basket cells and stellate cells, but rather relied on the position of MLIs along the molecular layer. Basket cells are classically defined as displaying characteristic "pinceau" or "basket nets" axonal structures, wrapping around the Purkinje cells' somata, while stellate cells lack such structures, and their axons mainly target the dendritic trees of Purkinje cells. Moreover, inner-third MLIs (lying close to the PCL) tend to make basket collaterals, while outer third MLIs tend to be stellate cells (Palay and Chan-Palay, 1974).

To compare dendritic lengths in BCs and SCs, I patched inner-third MLIs with an internal solution containing 20 µM of Alexa-594. After a period of 20-30 minutes of loading, MLIs were imaged with a 2-Photon Laser Scanning Microscope (2-P LSM). An initial acquisition was performed to obtain the coarse morphology of each cell (512x512 pixels, pixel size of $(0.43\ \mu m)^2$) by scanning in X, Y and Z, and classify cells as being BCs or not, according to the presence or absence of their characteristic feature, the basket collaterals. Only cells displaying basket collaterals were retained for further morphological analysis.

SCs images, recorded in similar conditions (although patched in the outer third of the molecular layer, close the pia), were provided by Alexandra Tran-Van-Minh, former post-doctorate in the laboratory, for comparison of maximal radial length. Figure V-1 shows three representative cells: an outer-third MLI, lacking the basket collaterals - classified as a SC (Figure V-1A); an inner-third MLI lacking the basket collaterals - rejected form further analysis (Figure V-1B); and a second inner-third MLI presenting clear basket collaterals - classified as a BC (Figure V-1C).

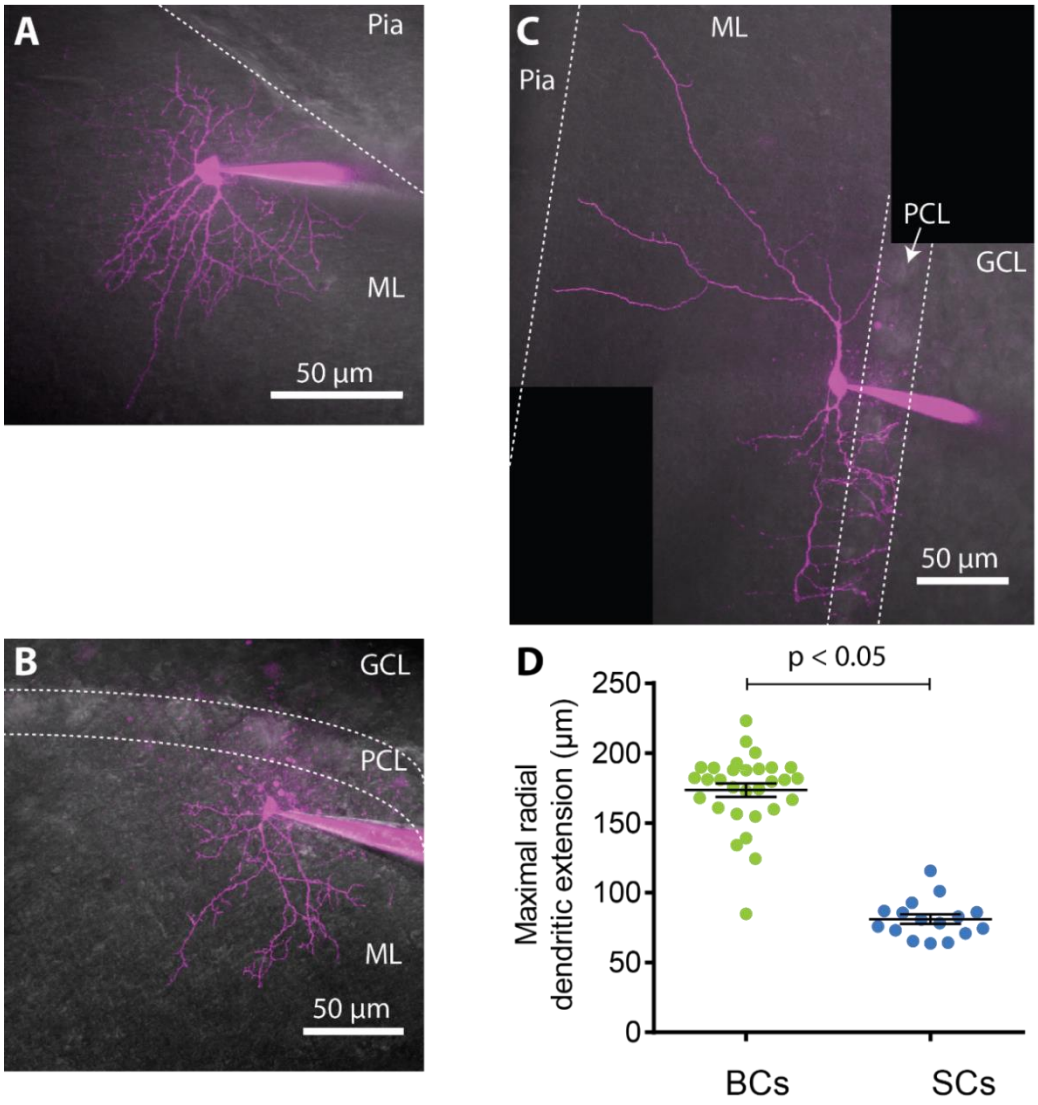

<u>Figure V-1: Basket cells' dendrites are significantly longer than those of stellate cells:</u> **A)** Representative example of a stellate cell, patched close to the pia (image provided by Alexandra Tran-Van-Minh); **B)** Representative example of a MLI patched close to the Purkinje Cell Layer, but in which no clear basket collateral was identified, and was rejected from further analysis; **C)** Representative example of a MLI classified as a basket cell, where basket collaterals can clearly be observed; in **A-B-C)** ML : Molecular Layer, PCL: Purkinje Cell Layer, GCL : Granule Cells Layer **D)** dendrites in basket cells (n=30) are significantly longer than in stellate cells (n=16);

Comparison between 30 BCs and 16 SCs revealed that BCs have significantly longer dendrites (174 ± 4.9 µm vs 81.1 ± 3.47; $p < 0.05$, Mann-Whitney test). This result suggests that EPSCs in BCs may be more affected by electrical filtering compared to SCs, because distal inputs in this population would have a longer distance to travel to reach the somatic compartment. However, as indicated in equations (2), (6) and (7) (see Introduction), dendritic diameter affects internal resistivity and therefore length constants. It was therefore necessary to measure dendritic diameters in BCs to make a proper comparison with SCs.

I - 2) BCs have larger dendrites than SCs:

To estimate the diameter of dendritic branches in BCs, I imaged BCs with a finer spatial resolution (see below). Dendrites were defined as structures extending towards the pia, without substructures extending toward the PCL (to avoid axons and basket collaterals), starting beyond a 25-30µm radius from the centre of the cell bodies. These proximal compartments were excluded from analysis for two reasons: firstly, because dendritic trees in BCs usually start from a rather large trunk, from which it is known that axons can emerge (Palay and Chan-Palay, 1974); secondly, the trunks could quite often be delicate to separate visually from the soma. To avoid confounding effects of axonal branches or slightly ambiguous shapes of the somata, all these structures were discarded from further analysis. If any bias was introduced by rejecting such structures, it would only have lowered the estimate of the mean diameter of dendritic branches in BCs, because trunks were invariably way larger than dendrites, and most dendrites tended to display an apparent tapering from soma to distal dendrites (not shown).

Averages of eight *in focus* images were recorded all along dendritic trees, by using a 10X digital zoom (pixel size of $(0.043\mu m)^2$). Figure V-2 shows a representative example of this experiment: in this case, the 6^{th} structure was rejected from analysis because of the proximity with the cell body. On each of the five remaining images, light intensity line profiles were drawn perpendicularly to each dendritic branch, and were fitted to a Gaussian function. Dendritic diameters were finally estimated by the Full-Width Half-Maximum (FWHM) of the Gaussian fits, and a histogram of FWHM distribution was obtained, yielding an average dendritic diameter in BCs of 0.58±0.09 µm (Figure V-2D). In the case of SCs, a similar protocol had yielded a value of 0.40±0.05 µm (Abrahamsson *et al.*, 2012).

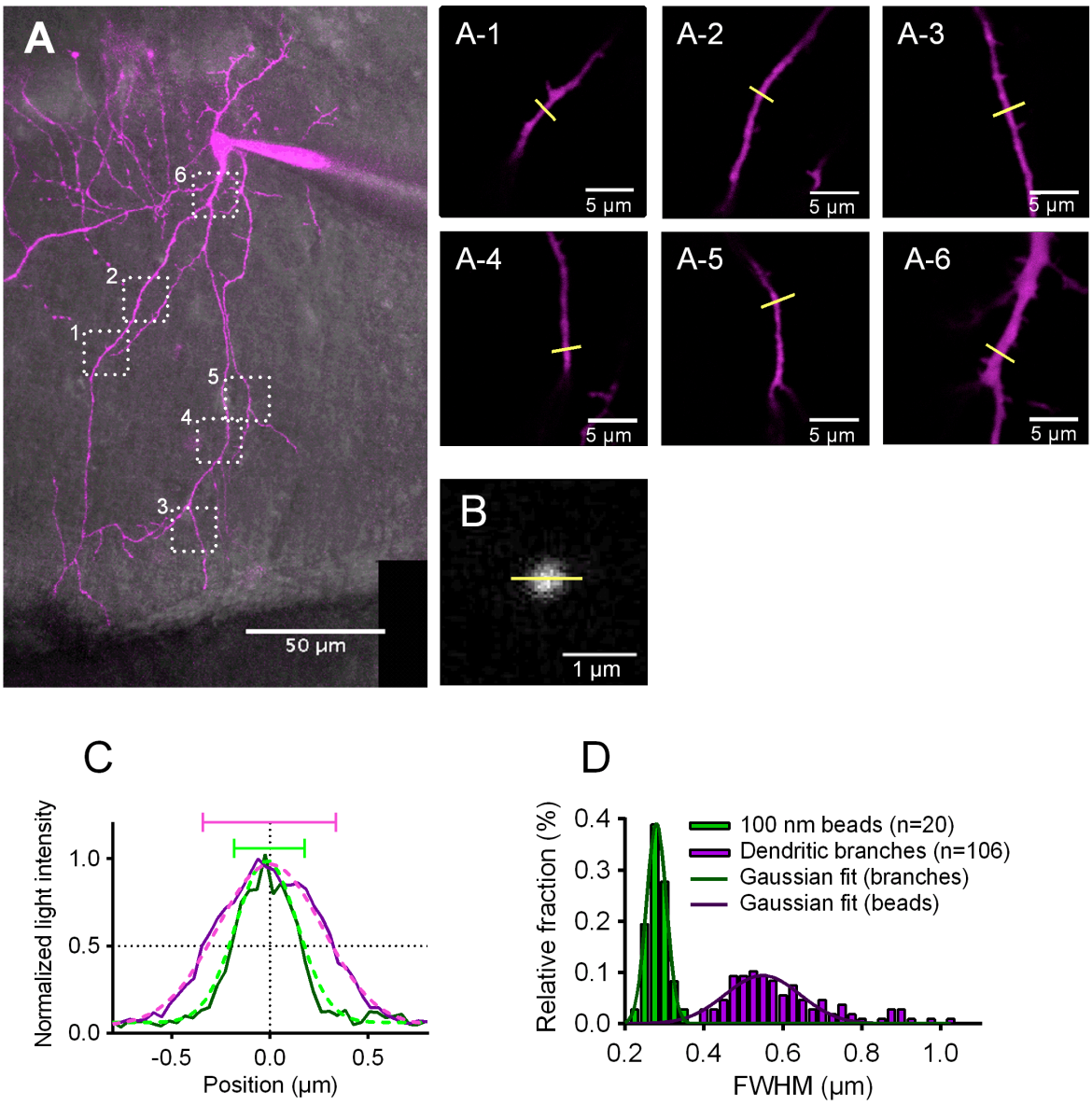

Figure IV-2: Estimating the diameter of dendritic branches in BCs: **A)** Z-projection of 2P-LSM images of a BC loaded with Alexa Fluor-594, superimposed onto a Dodt infrared contrast image. White dashed boxes indicate where images were taken along the dendritic tree; **A-1 to A-6)** Averages of 8 images from A), using a 10X digital zoom; yellow lines indicate where line profiles were taken. **B)** Average of 8 images of a 100 nm fluorescent bead. Insets A-1 to A-6 and B are displayed with an enhanced contrast. **C)** Normalized light intensities of line profiles in A-1 and B (dark purple and green solid lines, respectively) and corresponding Gaussian fits [light pink (FWHM = 0.53 µm) and green (FWHM = 0.30 µm) dashed lines, respectively]; **D)** Histogram showing the distribution of FWHM from 100 nm fluorescent beads (green bars) and BC dendritic branch diameters (purple bars), showing no overlap in the distributions. Lines indicate Gaussian fits to each distribution.

Given the small values obtained for the estimates of dendritic diameters (hundreds of nanometres), it was necessary to confirm that these measurements were not limited by diffraction. To determine the resolution limit of the 2-photon excitation system, I employed Abbe's criterion, which is defined as the minimal distance between two infinitely small objects

necessary to resolve each of them. The formula, in case of a 2-photon excitation system, is given by:

$$FWHM = 0.37\frac{\lambda}{NA} \text{ (9)},$$

where λ is the wavelength of excitation, and NA is the numerical aperture of the objective. In our system, this equation yields a theoretical value of 273nm (λ=810 nm, NA = 1.1). By imaging 100nm large fluorescent beads, and employing the same protocol and analysis as those employed for dendritic branches in BCs, I found $FWHM_X$ and $FWHM_Y$ to be 285±26 and 275±27nm (n=20 beads), respectively. These values were reasonably close to the theoretical one, meaning that the imaging system was close to its optimal state. Furthermore, as it can be seen in Figure V-2D, there was no overlap between the distributions of FWHM for fluorescent beads and BCs' dendrites. This means that the imaging system was capable of estimating the dimensions of smaller objects than the dendritic branches, and therefore that the estimated values of dendritic diameters were accurate, and not limited by diffraction.

So far, I have estimated maximal dendritic length in BCs and SCs (Figure V-1), and measured BCs dendritic diameter (Figure V-2). From (Abrahamsson *et al.*, 2012), we also know the diameter of dendritic branches in SCs. These values were employed to calculate the steady-state length constants (λ_{DC}, Equation (7)) and the frequency-dependent length constants (λ_{AC}, Equation (8)), which are summarized for each cell-type in Table V-1 (values for R_i and R_m were assumed to be equal between SCs and BCs):

Table V-1	λ_{DC} (µm)	λ_{AC} (µm)	Maximal dendritic length (µm)
Basket Cells	447	59	174
Stellate Cells	365	47	81

It is now possible to compare the two length constants relative to the maximal dendritic length, in each cell-type. The ratio between dendritic lengths and λ_{DC} yields values of 4.5 (SCs) and 2.6 (BCs). This first result reveals that, at steady-state, under voltage-clamp conditions, mature SCs are electronically compact, but for BCs, a slight voltage decay exists between the soma and the very tip of the longest dendritic branches. To a first approximation, we can say that imposing a 10mV voltage command at the soma of a BC will only lead to polarization of 9.2mV ($10*e^{-2.56} = 0.8$) at the tip of the longest dendrites. As a comparison, a similar calculation

in SCs gives a polarization of the cell membrane at the tip of the longest dendrites of 9.99 mV ($10*e^{-4.5}= 0.01$).

The higher λ_{AC} in BCs suggests that non-linearities should be harder to engage, because an EPSC of a given amplitude will distribute its charge on longer electrotonic distances. Stated in other words, the increased diameter of dendritic branches in BCs will reduce the local impedance. Therefore, for a similar distance between synaptic site and the somatic compartment, an EPSC of a given amplitude will produce a smaller EPSP in BCs than in SCs. On the other hand, the longer dendrites in BCs may cause an enhancement of non-linearity recruitment, because of end effect of dendritic cables and longer electrotonic distance between the synaptic site and the somatic current sink (Tran-Van-Minh *et al.*, 2015).

Finally, the ratio between maximal dendritic length and λ_{AC} in each cell types yields values of 34% (BCs) and 58% (SCs). This second result reveals that distal inputs have to travel approximately 3 λ_{AC} in BC before reaching the soma, while they only need to travel slightly less than 2 λ_{AC} in SCs, suggesting that cable filtering is more impactful in BCs than in SCs.

I - 3) Differences of cable filtering influence between theoretical predications and *in vivo* data:

I have performed imaging experiments aiming to extract morphological parameters of BCs (dendritic length and diameter), which I used to make two predictions: higher relative impact of cable filtering on synaptic events, and a potential gradient of non-linearity recruitment along BCs dendrites: non-linearities should be small (or inexistent) in proximal compartments, and gradually increase towards distal compartments, as observed in SCs (Abrahamsson *et al.*, 2012).

The prediction that cable filtering is more impactful in BCs is at odds with the results from (Chu *et al.*, 2012), where EPSCs recorded *in vivo* displayed faster kinetics and higher amplitudes in BCs during sensory stimulation. However, the discrepancy between our predictions and these results could be explained by:

- differential recruitment of GABAergic FFI between the two cell-types, associated with different amplitude of local EPSCs;

- differential targeting of sensory-evoked PF activity along the somato-dendritic axes of each cell-type (for example, proximal branches in BCs, and distal ones in SCs).

- differential feed-forward recruitment of spikelet-signalling (Chapter III of this thesis);

- differential passive impact of electrical synapses (Amsalem *et al.*, 2016).

Importantly, the last two points are related to one another, because they both rely on the ability of MLIs to form electrical synapses, which we know is higher in BCs than in SCs (Alcami and Marty, 2013; Rieubland *et al.*, 2014).

In order to examine the relative contribution of each point mentioned above, I performed *in vitro* electrophysiological recordings of PF-mediated synaptic responses in BCs to examine their kinetics, and later compare them to those found in SCs. This allowed us to compare de distance dependency of cable filtering between the two cell-type, and avoid the confounding effect of chemical FFI by performing recordings in presence of gabazine.

II) Impact of cable filtering on PF-mediated EPSCs in BCs and SCs:

II - 1) Longer dendrites in BCs causes stronger cable filtering of distal events:

In the study from (Abrahamsson *et al.*, 2012), it was found that paired stimulations of PF inputs at 50Hz shows a differential facilitation between the somatic and dendritic compartments. On average, the PPR is close to 2 in the somatic compartment, and 1.4 in the dendritic tree. It was further shown that the PPR decrement along SCs' dendrites was significant (*i.e.*, as PF stimulations are triggered further and further away from the soma, the PPR decreases linearly). These differences are due to a saturation of the second facilitated pulse in the dendrites, which behave as a sublinear compartment. Therefore, the PPR can be used as an indicator of sublinear dendritic integration behaviour in MLIs. In order to start examining the dendritic integration properties in BCs, I reproduced the same experiment as in Abrahamsson *et al.*, 2012.

I systematically recorded PF-mediated synaptic responses as the stimulation pipette was placed in 3 to 4 different positions along the somato-dendritic axis. The internal solution contained 1mM of QX-314 to block EPSC-induced action potential generation, and the ACSF employed to perfuse slices during the experiments was complemented with 10µM Gabazine and 50µM D-APV, to block $GABA_AR$ and NMDAR, respectively. These receptors were blocked to maximize chances of recording pure AMPAergic responses, and extract their kinetics and amplitudes with no confounding effects (exception made for unavoidable spikelets). For a fair comparison with results obtained in SCs, these experiments were performed in 2mM extracellular Ca^{2+}, and not 1.5 mM, as in Chapter III. Figure V-3 shows a representative example of such an experiment.

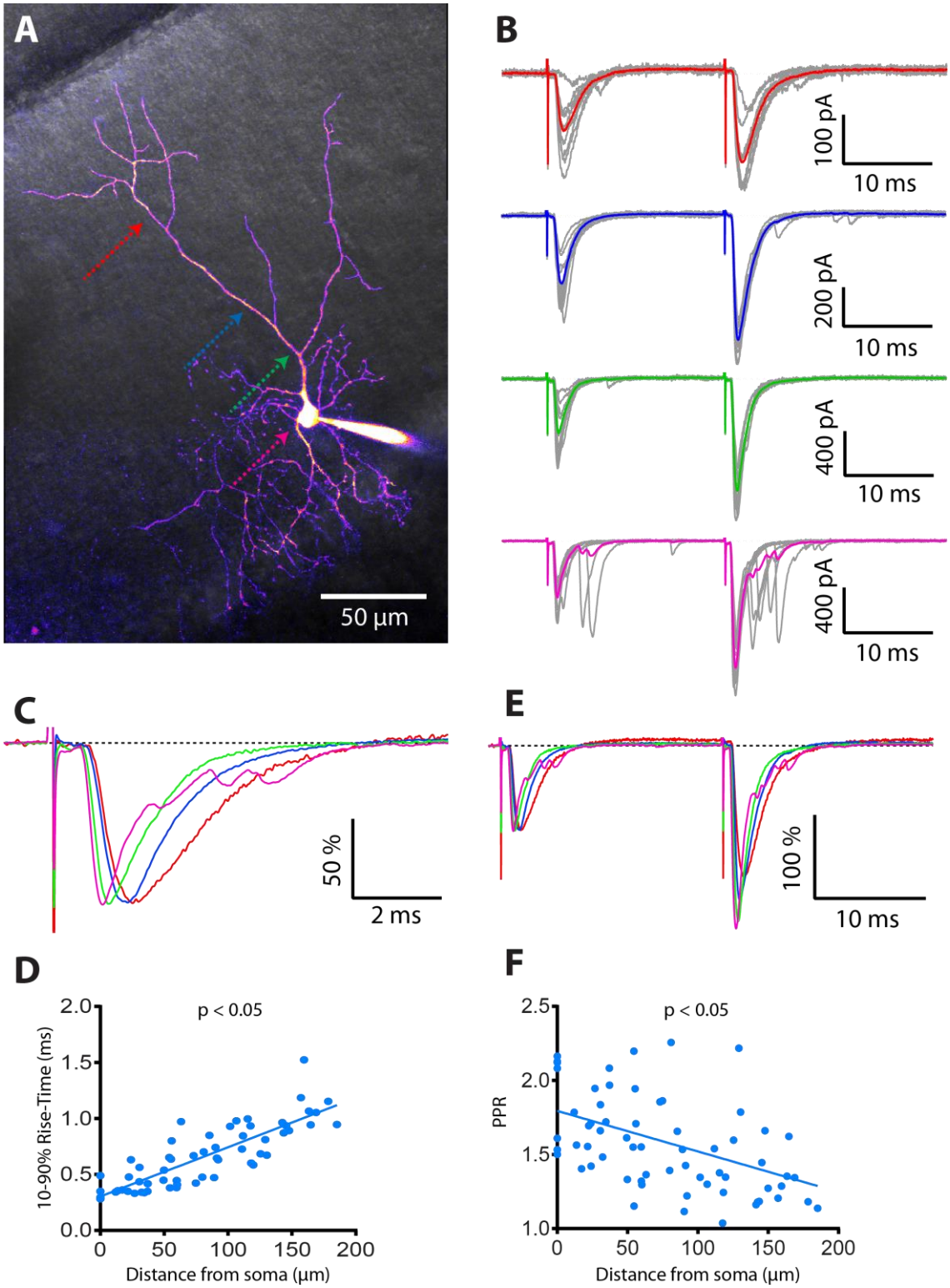

Figure V-3: Significant cable filtering and PPR decrement of PF-mediated EPSCs in BCs:
A) Z-project of 2P-LSM images of a BC loaded with Alexa Fluor-594 superimposed onto a Dodt infrared contrast image. Color lines indicate sites of electrical stimulation. **B)** Paired pulse responses to 50Hz stimulation of PF fibers along the somato-dendritic axis (same color code as in A). **C)** Initial EPSC responses normalized to their peak amplitude, revealing differences in kinetics. **D)** Population plot revealing the relationship between 10-90% rise-time of EPSCs and the distance between stimulation site and the soma. **E)** PPR responses normalized to the amplitude to the first response, revealing the differences in PPR. **F)** Plot of PPR versus distance from the soma, revealing a significant decrement of PPR along the somato-dendritic axis.

Synaptic responses were recorded from 4 locations of the stimulation pipette. Single EPSCs displayed increasingly higher 10-90% rise-times as they originated from more and more distal locations, while their corresponding PPRs decreased (Figure V-3C and E). These results manifested similarly at the population level (n=21 cells, 3 to 4 locations per cell): 10-90% rise-times significantly increased with distance (Figure V-3D - $p < 0.05$, linear regression analysis), while corresponding PPRs significantly decreased with increasing distance of synaptic stimulation from the soma (Figure V-3F - $p < 0.05$, linear regression analysis).

These results confirm that electrical filtering is a prominent phenomenon in BCs, as they are qualitatively similar to those observed in SCs. Additionally, the decrease in PPR as synaptic location is more and more distal from the soma suggest that BCs, similarly to SCs, experience synaptic saturation along the somato-dendritic axis. This may underlie a sublinear dendritic integration behaviour, but numerous control experiments are missing to make such a statement.

Electrical filtering affects amplitude kinetics of synaptic responses. For the latter, only 10-90% rise-times were examined, because the outward current due to spiking electrical neighbours could have influenced the falling phase of the EPSCs, and therefore their half-width. Furthermore, as it can be seen in the representative cell shown in figure V-3, stimulation of PF synapsing onto the soma often caused delayed release, which would have further complicated the analysis of half-width measurements.

A more elaborated protocol to demonstrate cable filtering on amplitude consists in examining the correlation between peak amplitude of the synaptic responses, and distance of the synaptic site to the soma. The stronger the cable filtering, the smaller becomes the amplitude of the responses with distance. However, in the case of electrical stimulation of PFs, it is difficult to control how many PFs are recruited at each location (1); how many of them effectively synapse onto the patched cell (2); and what is the quantal size of each of them (3). These limitations impair the classical analysis of amplitude versus distance along the somato-dendritic axis.

The most reliable way to address this question is to record synaptic responses following electrical stimulation in low concentration of external Ca^{2+}, in order to decreases the probability of vesicular release. Then, the average EPSC size (calculated from successes only, and if the failure rate is higher than 90%) well-approximates the amplitude and time course of a quantal EPSC (qEPSC; Silver, 2003). This experiment was performed in SCs, and provided another proof that electrical filtering is a prominent phenomenon in this cell-type (Abrahamsson *et al.*, 2012).

Nevertheless, in order to compare directly the impact of cable filtering on EPSCs' rise-times, and the PPR gradient along dendritic branches, we incorporated the values from (Abrahamsson *et al.*, 2012) to the graphs shown in Figure V-3. The results can be observed in Figure V-4.

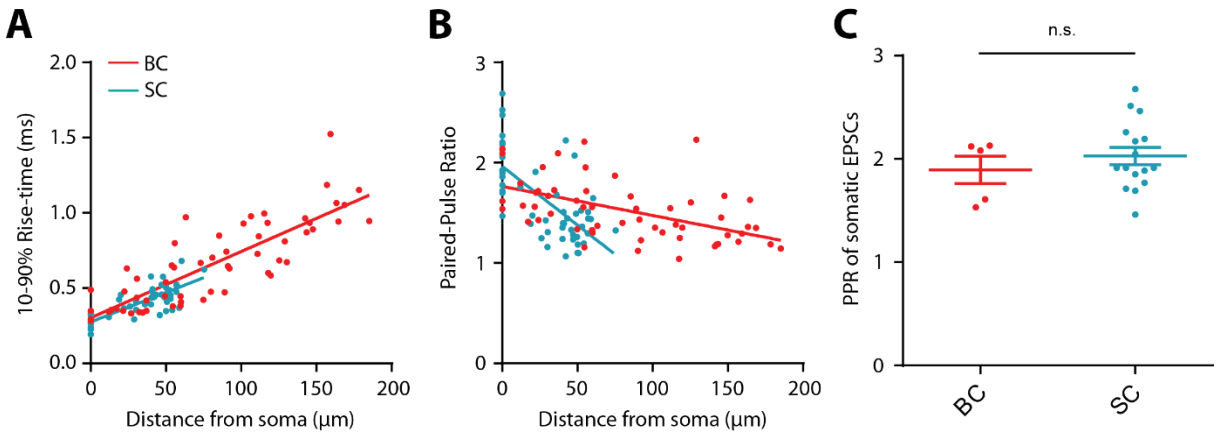

Figure V-4: Comparison of rise-time and PPR between BCs and SCs: **A)** Rise-time differences between EPSCs recorded at the soma in BCs and SCs. Slopes of regression lines are not significantly different; **B)** Paired-pulse ratio is significantly different along the somato-dendritic axis of each cell-type; **C)** PPR of somatic EPSCs are not significantly different

Statistical analysis reveals that rise-times gradients are not significantly different between the two cell-types. This indicates that for similar distances, and despite a large difference in dendritic diameters, cable filtering affects similarly the kinetics of synaptic currents. Paired-pulse ratio gradients, on the other hand, are significantly different between the two cell-types, with SCs presenting the steepest gradient, consistent with the smaller diameter of their dendritic branches. PPR of somatic EPSCs are not significantly different however, suggesting that the somatic compartments behave linearly in both cell types. These results are also consistent with previous suggestions that electrical synapses in BCs provide extra path for current flow during synaptic activation in the dendritic tree, meaning that local saturation of dendritic branches requires more current than in SCs. As a consequence, the PPR gradient is flatter in BCs, and further suggests that their dendritic integration behaviour is more linear than in SCs.

II - 2) Synaptic currents and potentials are unevenly affected by electrical filtering:

In this section, I would like to present some relatively ambiguous results concerning cable filtering of PF-mediated inputs in BCs. In Chapter III (Supplementary Figure 3), I showed that synaptic potentials recorded at the soma have a half-width independent of their dendritic

origin. However, in the last section, I showed that synaptic currents have an increasingly higher 10-90% rise times as their dendritic origin becomes more and more distal. The two results therefore suggest a different influence of cable filtering on the kinetics of synaptic events, depending if these events are considered as currents or potentials.

In order to make a clearer picture of these observations, I re-analysed VC and CC recordings of the dataset shown in Chapter III (Figure 5 and Supplementary Figure 3), and plotted the HW of both EPSCs and EPSPs against the dendritic location. This time, data recorded in each configuration were not sorted according to the presence or absence of a secondary spikelet response. Results are summarized in Figure V-5.

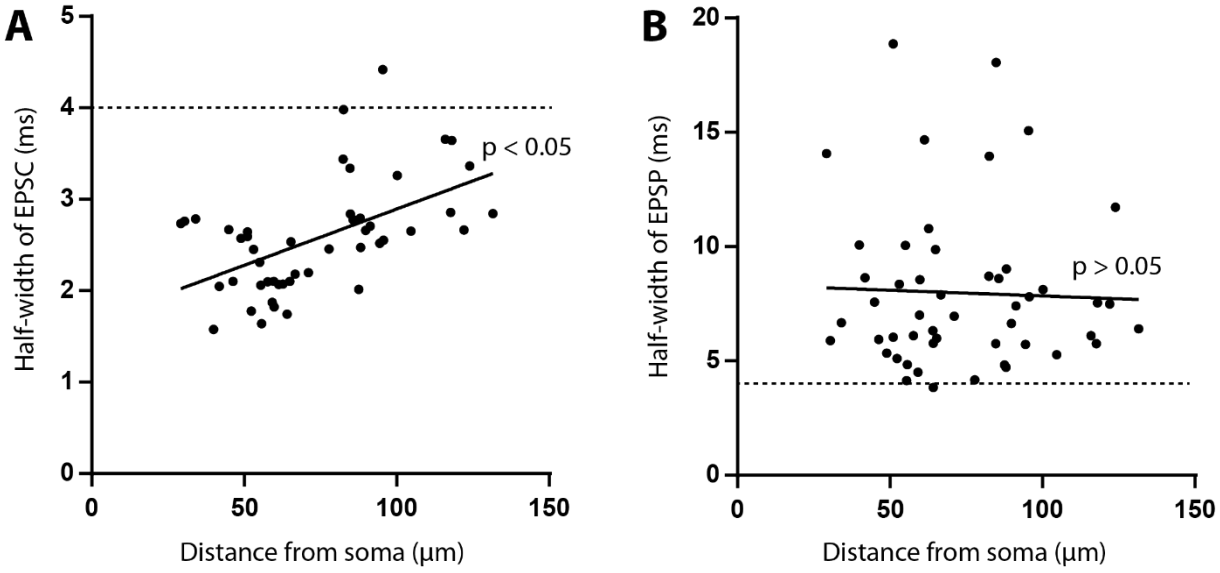

Figure V-5: Half-width of synaptic currents and their corresponding synaptic potentials: A) Half-width of EPSCs increases significantly with dendritic location; **B)** However, the corresponding EPSPs display a half-width independent of the synaptic location. Dotted lines represent a half-width of 4ms in each case.

It can be seen that, consistent with previous observations, HW of EPSCs increases with their synaptic origin in the dendritic tree, while the corresponding EPSPs still display no correlation between the same two parameters. Compared to previous observations reflected in different figures of this thesis, Figure V-5 has the advantage that the same kinetic parameter is considered (half-width), and for the same responses (each point on panel A has its match on panel B). Therefore, the ambiguity raised before about the effect of cable filtering remains: kinetics of EPSCs suggest cable filtering, while those of EPSPs do not.

The most plausible and parsimonious hypothesis to explain this discrepancy is that the kinetics of synaptic currents record at the soma are a due to a convolution between the time-

course of receptor opening, and the cable filtering of the current travelling down to the soma, while synaptic potentials are the convolution between synaptic currents arriving at the soma and the impulse response function of the cell (*i.e.*, the function converting a time-varying current (input) into a time-varying potential (output)). Because the impulse response function behaves as a RC filter in the case of a biological membrane, synaptic potentials have a finite lower limit for their half-width, which is indirectly related to the membrane time-constant of the cell. Consequently, synaptic currents displaying kinetics faster than this limit will occasion synaptic potentials displaying a HW of at least this value (all other parameters considered equal, and under the assumption that the cell-type under study behaves passively). This is why I represented on each panels of Figure V-5 a dotted line for a similar half-width (I decided to draw the lines at Y=4ms in each case, so that most of the EPSCs' HW values fall below this line, while all EPSPs' HW lie above it).

According to this logic, it should not be surprising that EPSPs display a HW unrelated to their dendritic origin, while EPSCs do: all EPSCs, even the longest ones, are too rapid compared to the transfer function of the cell membrane.

An analogy can be drawn here with the resolution power of a microscope: the impulse response function of an imaging system is set by the Point-Spread Function (PSF). If one aims to resolve an object having spatial dimensions smaller than the PSF, then these objects will produce a diffraction-limited image, where the objects are seen as large as the PSF. However, if the objects are much larger than the PSF, then their image is not limited by diffraction, and their original spatial dimensions can be retrieved from the image (see Figure V-3). The analogy would therefore be that EPSCs are equivalent to the real objects, and the EPSPs are equivalent to the image. The PSF would then be equivalent to the impulse response of the cell membrane.

The different influence of electrical filtering onto EPSCs and EPSPs may also be caused by active conductances in BCs dendrites, which would help to normalize the half-width of EPSPs regardless of their dendritic origin. Such examples have been described in CA1 pyramidal cells (Magee, 2000 - See Introduction), and in hippocampal basket cells (Hu *et al.*, 2010), where K^+-channels in the dendrites are recruited during synaptic activation, and sharpen the kinetics of the corresponding EPSPs. The passive role of electrical synapses in the dendritic compartment may also contribute to this non trivial link between somatically-recorded EPSCs and EPSPs

II - 3) Indirect evidence of the passive role of electrical synapses in sharpening EPSP kinetics:

Another point which can be addressed now is the potential passive role of electrical synapses in narrowing the half-width of EPSPs, as presented in the Introduction with the study from (Amsalem *et al.*, 2016). As a reminder, electrical synapses are permanently opened, and therefore, they change the electronic structure of neurons expressing them. In first approximation, this influence on passive properties is quite similar to tonic inhibition, in that it reduces the *apparent* input resistance and the *apparent* membrane time constant. The main difference is that this GJ-mediated tonic inhibition links the cell under observation to other cells in the network, and not to the extracellular space as is the case with tonic, GABAergic inhibition.

It is not trivial to examine the passive influence of electrical synapses without a mathematical model. Only indirect evidence can be drawn from electrophysiological recordings exclusively. Nevertheless, when I performed single-cell patch-clamp recordings of basket cells paired with dual stimulation of their PF afferent inputs (as shown in Chapter III - Figure 6), I recorded synaptic responses of different sorts: pure EPSPs, and EPSP-spikelets compound synaptic responses (Chapter III - Figure 6). However, in the category of pure EPSP, synaptic responses could be further split into two groups, according to another criterion: was it possible to find a pure spikelet response, in that cell? Indeed, I experienced cases where, within 30 to 45 minutes during an experiment, I was unable to find a spikelet response by OFF-beam stimulation (or even ON-beam stimulation), which is highly suggestive that the patched cells were, in such instances, not connected to any electrical neighbour. An interesting correlation could appear between EPSPs' HW and this additional sorting criterion (that is "can one find a spikelet response, or not?"), as shown on Figure V-6.

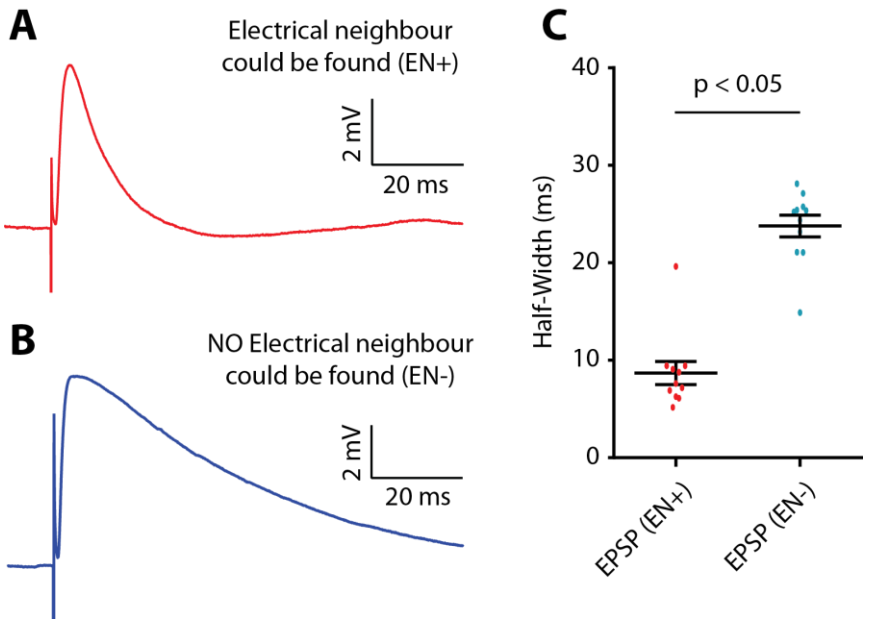

Figure V-6: Kinetics of EPSPs correlate with the ability to find at least one electrical neighbour: A) Representative EPSP from a BC where a spikelet response (indicative of the presence of an electrical neighbour) could be found; **B)** EPSP from a BC in which no spikelet response could be found after sampling both sides of its dendritic tree; **C)** EPSPs are significantly shorter-lasting when at least one electrical neighbour can be found.

It can be clearly observed that EPSPs have strikingly different kinetics in each group. They have much faster kinetics when a spikelet response can be found, consistent with the indication that there exists at least one electrical neighbour to accelerate the kinetics. Note that in the first group (shown in red), the EPSPs considered for analysis were not followed by a significant hyperpolarisation indicative of a disynaptic recruitment of a spikelet response (examined on voltage-clamp recordings - data not shown).

Therefore, these data suggest that a strong correlation exists between the kinetics of pure EPSPs recorded in a basket cell, and the presence or absence of at least one electrical neighbour. This observation is merely a correlation, but it supports the idea that electrical synapses have a passive effect on EPSP kinetics. More thorough analysis is required to make any definitive conclusion on that matter, because a genuine possibility is that there may exist a link between the presence of an electrical synapse and the expression of voltage-gated channels (like potassium ones), and the latter only could underlie the differences indicated in Figure V-6. Performing similar experiments in $Cx36^{-/-}$, or after blockade of electrical synapses with an appropriate blocker, along with modelling approaches, appear to be the most direct ways to quantify the passive role of electrical synapses in shaping the passive properties of basket cells, and their influence on dendritic integration of EPSPs.

III) Discussion:

After examination of spikelet recruitment and signalling in the BC population, I investigated if these interneurons displayed morphological features different from those of SCs, with the long-term goal of addressing if and how each type of MLI could differentially process excitatory inputs from PFs.

III - 1) Morphological differences of the dendritic branches in the MLI population:

First, I confirmed that in adult mice, the dendrites of BCs are significantly longer (around 2.5 times) than those of SCs. I also showed that their dendrites were thicker (around 50%). These results are qualitatively similar to those obtained in adult rats (Sultan and Bower, 1998), and provide further evidence that the differences observed in their study can be related to differences between stellate-type and basket-type cells.

Under the assumption that SCs and BCs' dendrites can be modelled by cylinders (and thus, neglecting the presence of electrical synapses), the combination of these two morphological differences resulted in a striking difference in cable filtering between the two cell-types. For a given 1kHz characteristic frequency of an excitatory input (mimicking the entry of a PF-mediated EPSC), I found that BCs' dendrites were around 3 times longer than their frequency-dependent length constant, while a similar calculation applied to SCs yielded the value of 1.5. These results suggests that cable filtering would be more pronounced in BCs than in SCs; however, the higher frequency-dependent length constant in BCs suggests that, for a similar PF-mediated current entry, local polarization of the cell's membrane would be smaller in BCs than in SCs. Consequently, engaging a non-linear mechanism in basket cells would require stronger EPSCs, compared to SCs.

III - 2) Differential dendritic integration behaviour of EPSCs in MLIs:

I later found that 50Hz paired stimulation of PFs in BCs displayed a significant decrease of the PPR along BCs dendrites, a result qualitatively similar to what had been reported in SCs (Abrahamsson *et al.*, 2012). However, the gradient was significantly steeper in SCs, consistent with thinner dendritic branches. An important note is that somatic PPR were comparable in both cases.

In Abrahamsson *et al.*, 2012, a systematic analysis of the relationship between sublinearity, dendritic diameter, and dendritic length in SCs was performed. It revealed that

sublinearity increased systematically with distance from dendrite to soma, and with increasingly smaller dendritic diameters. Given that BCs have relatively larger dendrites, but much longer dendrites, it is also conceivable that a gradient of sublinear summation exists along their dendritic branches. Longer dendritic branches would tend to extend this gradient, while larger diameters would tend to flatten it (Tran-Van-Minh *et al.*, 2015). Consistent with this predictions, my electrophysiological recordings confirmed that the gradient of PPR was flatter in BCs.

III - 3) Passive effect of electrical synapses:

The presence of electrical synapses in BCs' dendrites provides an extra path for passive current flow, which decreases the apparent membrane time constant (Alcami and Marty, 2013), and sharpens the kinetics of synaptic events (Amsalem *et al.*, 2016). Regarding the dendritic integration behaviour, addition of electrical synapses in the dendritic tree should counteract sublinear integration, because EPSCs would significantly flow across them to charge electrical partners (Vervaeke *et al.*, 2012). In first approximation, electrical synapses in this context behave as branching points in a dendritic tree, and increased branching in the dendrites tend to minimize non-linear dendritic integration behaviours (Tran-Van-Minh *et al.*, 2015). Consequently, a higher amount of synaptic currents would be required to drive local voltage deflections in the dendritic tree, compared to a case where electrical synapses are absent. The dendritic location of electrical synapses might also explain why synaptic potentials recorded at the soma have similar kinetics, regardless of where they originate from (Chapter III-Supplementary Figure 3), because electrical synapses would virtually act as a local current sink.

Chapter VI - Discussion, and perspectives

I) Electrical connectivity and spikelet transmission in BCs:

In this section, I will extend the discussion of the manuscript shown in Chapter III, mainly because of the lack of space imposed by the publication procedure, which doesn't allow a discussion of methodological details, or epistemological considerations.

I - 1) Feed-forward recruitment of spikelet signalling:

To my knowledge, the work presented in Chapter III is the first one to reveal the recruitment of spikelet transmission in a feed-forward manner. In our study, this recruitment was achieved by stimulating a single set of PFs, which are the main source of excitatory inputs to BCs (and MLIs in general). However, it is known that electrical stimulation recruits PFs in a beam pattern, and that this behaviour may not be a proper approximation of PF activity evoked by natural stimuli (Marcaggi and Atwell, 2005 and 2007). Moreover, it is unlikely that a single PF would activate two neighbouring, electrically connected BCs, since a single PF, extending in the coronal plane, would have to cross simultaneously the dendritic trees of two BCs, which are confined within a relatively narrow (~20µm) single parasagittal plane (Palay and Chan-Palay, 1974; Rieubland *et al.*, 2014). Consistent with this hypothesis, work in the Dorsal Cochlear Nucleus - a cerebellum-like structure - has notably shown that a single PF in this circuit is unlikely to recruit simultaneously two neighbouring MLIs (Roberts and Trussell, 2010). Furthermore, in my experiments, I found that when an EPSC and an outward current could be detected on a single sweep basis, their amplitude were uncorrelated (Chapter III, Supplementary figure 1). This suggests that, at a given stimulation site and intensity, the very PFs directly synapsing onto the patched cell were not the same as the ones causing its electrical neighbour(s) to spike. Therefore, in our case, feed-forward recruitment has to be understood in the sense that multiple parallel fibres in one beam are required: some of them directly synapse onto one MLI of interest, and others recruit at least one of its electrical neighbours.

Nevertheless, a recent *in vivo* study showed that PFs in the cerebellar cortex tend to be co-activated in clustered patterns (Wilms and Häusser, 2015), which suggest that activation of PFs in beam is not unrealistic. Furthermore, *in vitro* work using the same stimulation paradigm has concluded that MLIs deliver a form of feed-forward inhibition, mediated by GABAergic synapses, onto PCs and each other (Mittman *et al.*, 2005).

Knowing the relationship between spatio-temporal activation of PFs, and the very synaptic contacts they make with their post-synaptic targets in the molecular layer, would certainly help in addressing the physiological relevance of the *in vitro* work presented here. The

laboratory is currently recording the spatio-temporal activity from PFs *in vivo*, by imaging GCamp-reported calcium transients in PFs, or iGluSnFR-reported glutamate release from PF boutons.

I - 2) Spikelets can be used to retrieve the resting membrane potential of unperturbed, electrically-connected cells:

Spikelets have been shown to vary in waveforms and net excitatory/inhibitory balance in different cell-types. It has been shown that these differences could be due to different active conductances expressed in the post-synaptic (Mann-Metzer and Yarom, 1999; Dugué *et al.*, 2009) or presynaptic cells (Russo *et al.*, 2013); the frequency of AP firing in the pre-synaptic cell (Galaretta and Hestrin, 2001; Russo *et al.*, 2013) or by the resting membrane potential of the pre-synaptic cell (Mann-Metzer and Yarom, 1999; Dugué *et al.*, 2009; Otsuka and Kawaguchi, 2013). Consequently, spikelet transmission was reported to mediate a net excitation in some conditions (Mercer *et al.*, 2007; Hu and Agmon, 2015, Alcami 2018) and a net inhibition in others (Galaretta and Hestrin, 2001; Dugué *et al.*, 2009).

In order to address the biophysical determinants of spikelet transmission in BCs, I performed paired recordings to control simultaneously the resting membrane potential of two electrically connected cells. I found that the state of the pre-synaptic cell was critical in shaping the pre-synaptic AP waveform, and consequently the transmitted spikelets, while the state of the post-synaptic cell did not have any detectable influence.

By combining these two observations, I hypothesized that spikelet waveform could carry the information of the presynaptic membrane potential, and designed a novel method aiming to retrieve its value in electrically connected, unperturbed cells. First, I used paired recordings where the presynaptic membrane potential was known, and employed spikelet waveforms as "calibrators" for estimating the resting membrane potential. I later used the spikelets recruited by direct stimulation or OFF-beam stimulation, and ultimately retrieved the resting membrane potential of unpatched electrical neighbour, by comparing the waveform of these spikelets to those obtained in pairs. I found that spikelets from unperturbed MLIs indicate a depolarized state of at least -60mV, and perhaps slightly above this value. Additionally, because the patched cells were held at -70mV, a bias current was flowing across the electrical synapses, and therefore slightly hyperpolarized the presynaptic electrical neighbours. These results are consistent with previous findings where the resting membrane potential of MLIs in young rats was estimated to be around -58mV (Chavas and Marty, 2003). It has even been

proposed that MLIs have a resting membrane potential very close to threshold, where the spikelet-induced depolarization would be sufficient to trigger AP firing in cell(s) receiving them (Kim *et al.*, 2014).

I - 3) Technical considerations on the new method:

I propose that the method shown in (Chapter III - Figure 3G) can be applied to retrieve the resting membrane potential of any type of neurons forming electrical synapses. For this method to provide the most accurate (*i.e.*, precise and unbiased) result, I propose that the relationship between post-synaptic state and spikelets waveform is first established (by performing paired recordings), in order to ensure that in subsequent experiments, the holding membrane potential of the cell receiving the spikelets (*i.e.*, the "probe") doesn't influence the waveform of the recorded signal. Indeed, without prior knowledge of a particular cell-type, one cannot tell if spikelets can recruit active conductances in the post-synaptic cells. Secondly, the "probe" should ideally be held close to the value towards which the estimate of the resting membrane potential of unperturbed neighbours converges, in order to minimize the bias current flowing across the electrical synapse. Thirdly, I hypothesize that additional knowledge about the location of the electrical synapse in the dendritic tree could be used to estimate the extent to which the fast depolarizing component and the slower hyperpolarizing component would be differentially filtered by the two electrically-connected cells. Owing to the low-pass filtering properties of the cellular membrane, I expect that for a given coupling coefficient (which only provides an information for steady-state currents to cross the synapse - like the filtered AHP), the variability of the fast depolarizing component will be higher than that of the slow hyperpolarizing component. Fourthly, a "proper" range of coupling coefficients would be best to retrieve the resting membrane potential of unperturbed cells. Indeed, if the CC is too small, a negligible bias current is introduced to the unperturbed electrical neighbour, but the corresponding spikelet might be too small to be reliably detected. In line with this idea, I provided evidence that small CCs can be due to indirect couplings, as they correlate with an inability to observe a spikelet after AP firing in the presynaptic element. On the other hand, if the CC is too high, then a large bias current will be injected in the unpatched cell, and significantly alter its resting membrane potential. In first approximation, the "best spikelets" should ideally indicate a coupling coefficient lying between 5 and 10%, but this intuition may be further refined by considering how differences in input resistances between two connected cells differentially influences the ability of currents to cross them in either direction (Fortier

and Bagna, 2006). Finally, when aiming to trigger APs in electrically connected cells by stimulating their presynaptic afferents, being able to distinguish if a spikelets-like response comes from one, two, or even more electrical neighbours would be ideal; and one should ensure that the recorded "spikelet-like" signals are not a mixture of "pure spikelets" and indirect EPSCs/IPSCs concomitantly experienced by the presynaptic electrical partner, by using appropriate blockers.

I - 4) Electrical synapses are more frequent than chemical synapses in adult mice:

In order to start addressing the physiological relevancy of spikelet transmission in cerebellar basket cells, I performed paired recordings of neighbouring BCs, and tested how frequent electrical and GABAergic synapses would be between them. I could have relied on the estimates of (Rieubland *et al.*, 2014), but the progressive developmental decline of connexin-36 has been established in multiple brain regions, such as the thalamus, the cerebral cortex, or the CA3 region of the hippocampus (Belluardo *et al.*, 2000), and the retina (Söhl *et al.*, 1998). Recent findings even suggests that electrical synapses could serve as an early-developmental substrate to guide the formation of GABAergic synapses (Todd *et al.*, 2010; Yao *et al.*, 2016). Therefore, I found more prudent to estimate the prevalence of both electrical and chemical synapses formed by MLIs in adult animals. Moreover, it was shown in Rieubland *et al.*, 2014 that the likelihood for an MLI to make an electrical or a chemical synapse is differentially affected by the intersomatic distance between the two neurons, in both the parasagittal and coronal planes. I highly relied on their experimental procedures, and took advantage of their protocols to establish mine. It is notably thanks to their work that I restricted my paired recordings to intersomatic distances of maximum of ~70µm in the parasagittal plane, and ~15µm in the coronal plane, to maximize the probability of finding electrical and chemical connections. Finally, electrical connectivity in their study was estimated only by coupling coefficients, and such estimates can be misleading (see below).

By performing dual patch-clamp recordings of BCs, I found that electrical synapses are still highly prevalent in adult animals. I systematically compared how the amplitude of spikelets and coupling coefficients varied with one another, and observed that for low coupling coefficients (*i.e.*, a few percent), no detectable spikelet was found in the post-synaptic cell. This could be due to a difficulty in resolving small spikelets (compared to baseline noise), or to the differential ability of long current pulses to cross at least one intermediate electrical neighbour before causing a small hyperpolarization in the second cell of the pair (this indirect coupling

would cause a small CC), while spikelets would not be transmitted through this type of indirect coupling (See Appendices). My estimates for electrical connectivity therefore decreased as I increased the threshold value of CCs. This particular point is important to consider, because a lot of studies about electrical connectivity employ a threshold for CC, sometimes with relatively low values (for example, CC > 1% in Rieubland *et al.*, 2014). This implies that electrical synapses might be overestimated by simply considering CCs.

To remind the reader, I raised the question in my introduction of whether or not "if three neurons are connected by electrical synapses in a chain configuration (A-B-C), should the neuron in the middle (B) be considered an electrical synapse, by virtue of the definition of "*specialized junctions between neurons which connect the cytoplasm of one neuron to another allowing direct passage of an ion current*"? I suppose the correct answer is "no", because a whole neuron should not be considered a "specialized junction". However, such indirect couplings will be retained as "electrical synapses" in connectivity studies based solely CCs.

Ultimately, since I was interested in the ability to mediate excitation/inhibition through spikelet transmission in the BC population, I found more reasonable to base my estimates on the ability to transmit a spikelet, rather than an arbitrary threshold value for CCs. This method appeared the least bias to establish a comparison with the prevalence of GABAergic synapses, given that this chemical connectivity can only be probed by forcing AP in the presynaptic cell. Ultimately, even when I considered the most stringent criterion to estimate the prevalence of electrical synapses (*i.e.*, detectability of a reciprocal spikelet transmission after AP initiation), I still found that electrical synapses were present between 51% of the recorded cells. This estimate was significantly higher than the estimate for the prevalence of unidirectional GABAergic synapses, which was close to 42%.

I - 5) Spikelet transmission displays characteristic features of FFI:

I - 5 - a) Narrowing EPSP time window:

Classically, GABAergic-mediated FFI has been investigated by comparing EPSPs before and after blockade of GABA receptors, usually by application of picrotoxin or gabazine (Pouille and Scanziani, 2001; Mittman *et al.*, 2005; Marek *et al.*, 2018). However, in my case, the use of pharmacological agents appeared ill-suited to block spikelets. Firstly, because of their known side effects, and long-time to act (*e.g.*, 20µM mefloquine takes tens of minutes to block electrical synapses; and at this dose, the block of electrical synapses is incomplete (~70% block

- Cruikshank *et al.*, 2004), and membrane capacitance is increase 2-fold (Szoboszlay *et al.*, 2016)); secondly, I aimed to address the contribution of feed-forward recruitment of spikelets, but blocking electrical synapses with pharmacological agents would have caused two effects: 1) blocking spikelet transmission, and 2) changing the passive properties of the recorded cells, due to the influence of electrical synapses on passive properties.

In order to examine if spikelet recruitment was a potent mechanism to provide FFI in the BC population, I performed patch-clamp recordings of BCs paired with single or dual electrical stimulation of PF inputs. Multiple lines of evidence shown in this thesis converge towards the conclusion that spikelets narrow the time-window of EPSPs.

Firstly, changing the stimulation intensity at one given site of PF stimulation allowed to recruit the same set of PF inputs, and revealed that the recruitment of spikelets in high stimulation conditions does narrow the half-width of the EPSPs, while the sole increase in stimulation intensity doesn't cause any significant change in EPSP kinetics (Chapter III, Figure 5). The advantage of this method is that the same set of PF inputs (experiencing the same amount of electrical filtering when propagating to the soma) is compared between the two stimulation regimes, thus increasing the statistical power of downstream analysis (see Appendices for the importance of this particular point), but its drawback is that spikelets recruited in high stimulation intensity regime have to counter higher amplitude EPSPs (compared to minimal stimulation condition), which may underestimate their effect. Nevertheless, this protocol proved to be sufficiently efficient in narrowing the half-width of EPSPs. Secondly, I found that, surprisingly, EPSPs have a half-width virtually independent of their synaptic origin along the somato-dendritic axis (Chapter III, Supplementary figure 3). This observation allowed to compare the half-width of EPSPs alone, versus EPSPs followed by a spikelet (all of them in minimal stimulation condition), from two sets of PF-induced synaptic responses, sampled all throughout the dendritic tree. I found that EPSPs followed by a spikelet have a significantly shorter half-width than the EPSPs alone, which provide further evidence that spikelets narrows EPSPs' half-width. However, the differential impact of electrical synapses' influence on passive properties could cause confusion in interpreting these results (see Chapter VI-II-3). Finally, when I performed paired electrical stimulation of PFs to recruit independently EPSPs and spikelets, I also found that their coincident recruitment significantly reduces the half-width of the EPSPs, compared to baseline (see Appendices).

I - 5 - b) Dampening temporal summation:

To test the hypothesis that spikelets can also dampen temporal summation, I resolved to compare post-synaptic responses to a train of 50Hz stimulations, between two different populations (Chapter III, Figure 5). Indeed, in this case, the very change in stimulation intensity had a profound effect on temporal summation, regardless of the presence or absence of a spikelet response (see Appendices). At the cost of pairing information (again, see Appendices), I still found that spikelets reduce temporal summation through this approach. This required to evenly sample the dendritic tree in each group, as otherwise, it could have been argued that differences in temporal summation were due to differences in the ability of distal compartments to summate more than proximal compartments, and that paired-pulse facilitation was biased in either group for this reason (see Figure 1 in Abrahamsson *et al.*, 2012). Nevertheless, I showed that the sampling of PF stimulation sites along the somato-dendritic axes of the two populations of cells was comparable, just like the peak amplitude of the individual responses (Chapter III, Supplementary Figure 4), which provided evidence that differences in temporal summation between the two groups of recordings was not due to such biases.

I - 6) Frequency-dependent inhibitory action of spikelets:

I found that single spikelets mediate a net inhibition in resting conditions. However, I was genuinely interested to examine if this behaviour could depend on the firing frequency of the presynaptic cell, especially to dissect out by which mechanism spikelet could alter temporal summation of concomitant EPSPs (Chapter III - Figure 5). By performing paired recordings of electrically connected cells, I found that spikelet-mediated inhibition was enhanced when firing frequency was increased from 10 to 100Hz. Spike waveform adaptation started to appear between 50 and 100Hz of firing frequency, and decreased the peak amplitudes of both the sodium and the potassium peaks. Nevertheless, changes in presynaptic spike waveform, along with cable filtering of dendritic branches where electrical synapses are located (Alcami and Marty, 2013), caused an increase in net inhibition with increasing firing frequency. A similar behaviour has been reported in fast-spiking striatal neurons (Russo *et al.*, 2013).

At the microcircuit level, one functional consequence of this behaviour could be to endow MLIs with another mechanism to mediate reliable inhibition to their neighbours (the first one being the classical GABAergic inhibition), regardless of their firing frequency. Indeed, MLI-MLI GABAergic synapses display a relatively high probability of vesicular release (Arai

and Jonas, 2014; Pulido *et al.*, 2015), suggesting a depressing behaviour during high frequency AP firing. Short-term depression would therefore impair synaptic inhibition during burst activity. However, inhibition conveyed by electrical synapses would become highly potent in such regimes.

I - 7) Spikelets mediate temporal contrast enhancement and coincidence detection:

I - 7 - a) Transient excitation followed by long-lasting inhibition:

In the last experiments described in Chapter III, I paired stimulation of two independent sets of PFs to induce direct EPSPs in the patched cells (ON-beam stimulation) and the recruitment of spikelet(s) from their electrical neighbour(s) (OFF-beam stimulation). I confirmed that spikelets arriving before the EPSPs reduce their amplitude, because of the long-lasting hyperpolarizing component. I could also finally reveal that their transient depolarizing component significantly *increases* the peak amplitude of concomitant EPSPs. This observation is in marked contrast to classical GABAergic mediated FFI, where the disynaptic recruitment of inhibitory interneurons can only *reduce* the peak amplitude of the direct EPSPs, assuming they are recruited sufficiently rapidly (Mittman et al., 2005; Pouille *et al.*, 2009).

The ability of spikelets to induce a short-lasting depolarization, followed by a longer-lasting hyperpolarization, therefore acts as if a single signal causes a sequence of feed-forward excitation/inhibition, a phenomenon which has not been reported in the literature, to my knowledge. Consequently, I argue that spikelet transmission in the MLI network enhances temporal contrast enhancement of a given set of PF input, and coincidence detection of independent sets of PF inputs.

I - 7 - b) Comparison with previous studies of spikelet transmission in cerebellar basket cells:

My results contrast with those of Alcami, 2018. In his study of electrical transmission between cerebellar basket cells, spikelets only displayed a depolarizing component, and Pepe Alcami postulated that these signals may serve as a basis for sequence detection in BCs (Figure D-1).

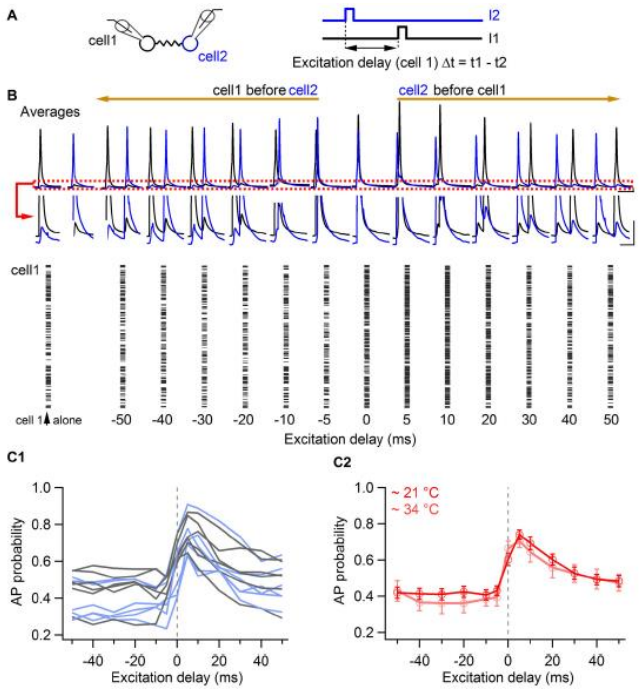

Figure D-1: Electrical synapses between cerebellar basket cells mediate a sequence detection mechanism: A) Dual-cell patch-clamp recordings of electrically connected basket cells. Each of them is injected with a short current pulse to force AP generation with an average probability of ~40% on each trial. Different delays are introduced between the two pulses; **B)** Average AP waveforms recorded in each cell, depending on the time delay between the two current pulses. ***Increase in average peak amplitude of APs indicate an increased likelihood of AP firing on each sweep***; **C1)** AP probability versus time delay between the two current pulses; **C2)** Population averages for two sets of recordings, performed at 21°C (dark red) and 34°C (light red), showing that the temperature of the recordings doesn't change the general behaviour of sequence detection.

From Alcami, 2018

However, as the author noted himself in the discussion of his article:

"*Since intrinsic properties determine the waveform of action potentials, spikelets and coupling potentials, they are likely to determine the time-window for coincidence and sequence detection. Likewise, the value of the membrane potential of coupled cells receiving coincident inputs is expected to modulate the time-window for enhanced firing. It would be interesting to explore in detail the modulation of the time-window for enhanced interneuron recruitment as a function of the membrane potential and the intrinsic properties of coupled cells.*"

Indeed, in his paired recordings of BCs, Pepe Alcami injected a bias current maintaining basket cells around -70/75mV. Consequently, as it can be seen in his figures, no AHP is present after the sodium peak of APs. It is even possible that the potassium currents, at this resting potential, are slightly depolarizing, suggesting that the long time constant for sequence

detection (Figure D-1, Panel C2) could partly be mediated by potassium currents and not sodium currents.

Given that I proposed a method to retrieve the resting membrane potential of BCs, and that my estimates converged towards an average value of at least -60mV, where AHPs are prominent, and that spikelets from unpatched electrical neighbours deliver a net inhibition (Chapter III, Figure 3), I think that my conclusion is better supported by scientific evidence. Moreover, in my study, coincidence detection was mediated by the recruitment of spikelets emitted by unpatched electrical neighbours. Any bias of injected current or dialysis due to the patching procedure itself was therefore avoided, and I can argue that the effect I observed was mediated by largely unperturbed cells emitting the spikelets, which should make my conclusion more robust, at least *in vitro*.

I - 7 - c) Implication for cerebellar processing:

As previously mentioned, a detailed information of spatio-temporal activity of PFs, along with the connectivity between PFs and the MLI network is required to make any strong hypothesis about the physiological implication(s) of these findings.

Nevertheless, connectivity studies in the cerebellar cortex indicate that electrically connected cells tend to form clusters (Alcami and Marty, 2013; Rieubland *et al.*, 2014); electrically connected MLIs increase convergence of GABAergic inhibition onto PCs (Kim *et al.*, 2014); neighbouring MLIs tend to receive excitatory inputs from the same patches of GCs (Valera *et al.*, 2016). Furthermore, *in vitro* work in the visual cortex indicates that electrical synapses may serve as a signal to orchestrate co-innervation by presynaptic excitatory inputs (Otsuka and Kawaguchi, 2013). Finally, it was recently confirmed *in vivo* that BCs deliver classical FFI onto PCs in anaesthetized animals, and the amount of FFI delivered is proportional to the strength of excitatory inputs common to BCs and PCs onto which they project (Blot *et al.*, 2016). Altogether, these observations suggest that electrical connectivity in BCs could sharpen the temporal recruitment of inhibition delivered to PCs, and also allow a proportional increase of inhibition during enhanced PF synaptic activity in the molecular layer, which may be critical for the proper functioning of the cerebellar microcircuit.

II) Addressing the dendritic integration properties of cerebellar basket cells:

Now that we have understood the importance of electrical synapses in this population of interneurons, both in their ability to transmit sub- and supra-thresold events, and their impact on passive properties, performing glutamate uncaging experiments onto BCs, along with realistic model simulation in the NEURON environment (Hines and Carnevale, 1997) would be very interesting to examine how electrical synapses impact dendritic integration properties. I hypothesize that BCs behave more linearly than SCs in general, since their larger dendrites and the presence of electrical synapses should make these compartments harder to saturate by PF inputs. One should also examine if the quantal size between PF-SC and PF-BC synapses is comparable, as it would be the first indication that they do receive similar inputs (on average) from PFs. If that was the case, then their differential dendritic integration properties would certainly translate into a differential recruitment of somatic- and dendritic-targeted inhibition onto PCs.

Given that the cerebellar cortex is a canonical microcircuit, conducting these experiments would provide some more insight as to the differential computational roles played by somatic- or dendritic-targeting interneurons population in the CNS. Additionally, a toy model of an MLI endowed with electrical synapses could serve as a model system to examine the role of these synapses in dendritic integration *per se*, and more specifically on the input/output relationship. To my knowledge, such an analysis has not been conducted yet, but given the large number of cell-types expressing electrical synapses, it would start to address more directly their role in information processing within the brain, outside of the "synchrony and oscillations" fields within which they have been studied the most.

Finally, although I could not examine the I/O relationship of cerebellar basket cells *per se*, I still found direct evidence that electrical synapses extend the input sources which are likely to influence their firing, as previously suggested in (Alcami and Marty, 2013). In the case of stellate cells, the main excitatory input comes from direct PFs contacts; however, basket cells, by forming electrical synapses, not only receive direct synaptic contacts from PFs, but also indirect excitation from their electrical neighbours (filtered EPSCs), and spikelets. Analysis of electrical transmission within the BC population was therefore important to reveal other types of inputs which would have to be considered in their I/O relationship.

III) Large scale implications:

III - 1) Implication for information processing in interneurons:

Altogether, my results indicate that feed-forward recruitment of spikelet signalling within the MLI network shows two characteristic features of GABAergic-mediated FFI (narrowing of EPSPs' time-widow, and dampening of temporal summation), along with a novel form of feed-forward or lateral excitation, mediated by the short-lasting depolarizing component of spikelets.

Put in a more general context, these results provide further evidence that BC behave as coincident detectors (McBain and Fisahn, 2001), a general role attributed to inhibitory interneurons, which tends to minimize interactions between temporally-close events. BCs display a high number of features which tend to narrow the time-window of PF-mediated EPSPs: 1) AMPA receptors in interneurons have rapid kinetics (Geiger *et al.*, 1997), and cerebellar BCs are no exception to this observation (Carter and Regehr, 2002; 2) The axon of cerebellar BCs acts as a current sink, draining the synaptic currents experienced in the dendritic tree, which further accelerates the kinetics of EPSPs (Mejia-Gervacio *et al.*, 2007); 3) they receive modest GABAergic-mediated FFI from their neighbours (Mittman et al., 2005), but these results may need to be reconsidered in the light of the resting membrane potential used in this study (-70mV), which tended to overestimate the size of PF-mediated EPSPs and underestimate the impact of the disynaptic recruitment of GABAergic inhibition; 4) electrical synapses decrease the apparent membrane time-constant, due to their impact on passive properties (Alcami and Marty, 2013; Maex and Gutkin, 2017), which further accelerates kinetics of EPSPs. All these features appear to combine to ensure a precise EPSP-spike coupling in the BC population resulting in a rapid and efficient inhibition onto PCs, either by GABAergic or ephaptic inhibition (Chu *et al.*, 2012; Blot and Barbour, 2014; Blot *et al.*, 2016).

It is interesting to note that BCs in the hippocampus and the neocortex are also parvalbumin-positive interneurons, targeting the somatic compartment of principal cells, and delivering feed-forward inhibition (along with feedback inhibition - reviewed in Hu *et al.*, 2014). They also express a high density of K^+ channels in their dendrites, which are recruited during synaptic activation, and shorten the time-window for EPSP summation (Hu *et al.*, 2010), and similarly to cerebellar basket cells, they are subject to axonal speeding (Nörenberg *et al.*. 2010). Interestingly, they also form electrical and GABAergic synapses with each other (Galaretta and Hestrin, 2001; Tamas *et al.*, 2000), which promote network oscillations. It therefore appears that somatic-targeting interneurons share a high amount of features across

different brain regions, with a convergent role towards delivering rapid and efficient inhibition to their post-synaptic targets, and minimizing temporal summation of their excitatory inputs.

III - 2) Implication for cerebellar computation:

In rodents, whisker movement kinematics can be both encoded (Chen *et al.*, 2016) and driven by precise PC firing patterns (Heiney, 2014). Moreover, millisecond synchrony of PC firing is critical for synchronized inhibition in order to precisely gate deep cerebellar nuclear drive of movement (Brown and Raman, 2018). The authors propose that at initial millisecond inhibition of PC firing by sensory stimuli might disinhibit cerebellar nuclei, thus initiating motor responses. Finally in vivo evidence that BCs play an important role in refining PC firing on the millisecond scale (< 8 ms) supports their important role timing cerebellar cortical output (Blot *et al.*, 2016). We therefore propose that eFFM could be an important mechanism to achieve such robust and precisely timed control of PC firing.

Conclusion:

During my PhD, I aimed to examine how excitatory inputs are processed by somatic-targeting interneurons in the cerebellar cortex, the basket cells. I found that this cell-type has a distinct dendritic morphology from their dendritic-targeting counterparts, the stellate cells, and that short-term facilitation was more linear throughout the dendritic tree of BCs than SCs. Moreover, BCs form relatively strong and frequent electrical synapses with each other, which plays a critical role in shaping their passive properties, and also provide another source of inputs as compared to stellate cells.

Owing to the geometrical organization of the cerebellar cortex, I was able to show with *in vitro* electrophysiological experiments that electrical connectivity can be recruited in a feed-forward manner in BCs, similarly to classical, GABAergic-mediated feed-forward inhibition. My work was focused on spikelet signalling, and revealed that in unperturbed BCs, spikelets indicate a relatively depolarized state, and deliver a net inhibition. I provided evidence that feed-forward recruitment of spikelet signalling displays some characteristic features of GABAergic FFI, albeit with a key difference: spikelets coming in coincidence with PF-mediated EPSPs increase the peak amplitude of these EPSPs, while GABAergic FFI would only be able, at best, to decrease it. Spikelet signalling in the BC population therefore appears to mediate coincidence detection and temporal contrast enhancement mechanisms, which is fully in line with the proposed role of interneurons found throughout the brain to have a sharp EPSP-spike coupling.

The results provided in this thesis could now serve as a building block from which a systematic analysis of the influence of electrical synapses in the dendritic input/output relationship could be performed, which may reveal another major role for these synapses in brain computation, aside from a generally well-accepted role in mediating synchrony and brain oscillations. The role of electrical synapses in passive properties further supports the notion that interneurons behave as coincidence detectors, and may also relate to a general different computational role in dendritic integration properties between electrical synapse-expressing or non-expressing interneurons subtypes found throughout the brain.

References:

1. Abrahamsson, T., Cathala, L., Matsui, K., Shigemoto, R. & DiGregorio, D. A. Thin Dendrites of Cerebellar Interneurons Confer Sublinear Synaptic Integration and a Gradient of Short-Term Plasticity. *Neuron* **73**, 1159–1172 (2012).

2. Albus, J. S. A theory of cerebellar function. *Mathematical Biosciences* **10**, 25–61 (1971).

3. Alcami, P. & Marty, A. Estimating functional connectivity in an electrically coupled interneuron network. *Proceedings of the National Academy of Sciences* **110**, E4798–E4807 (2013).

4. Alcami, P. Electrical Synapses Enhance and Accelerate Interneuron Recruitment in Response to Coincident and Sequential Excitation. *Frontiers in Cellular Neuroscience* **12**, 156 (2018).

5. Alev, C. *et al.* The neuronal connexin36 interacts with and is phosphorylated by CaMKII in a way similar to CaMKII interaction with glutamate receptors. *Proceedings of the National Academy of Sciences* **105**, 20964–20969 (2008).

6. Amsalem, O., Van Geit, W., Muller, E., Markram, H. & Segev, I. From Neuron Biophysics to Orientation Selectivity in Electrically Coupled Networks of Neocortical L2/3 Large Basket Cells. *Cerebral Cortex* **26**, 3655–3668 (2016).

7. Apostolides, P. F. & Trussell, L. O. Regulation of interneuron excitability by gap junction coupling with principal cells. *Nature Neuroscience* **16**, 1764–1772 (2013).

8. Apostolides, P. F. & Trussell, L. O. Control of Interneuron Firing by Subthreshold Synaptic Potentials in Principal Cells of the Dorsal Cochlear Nucleus. *Neuron* **83**, 324–330 (2014).

9. Apps, R. & Garwicz, M. Anatomical and physiological foundations of cerebellar information processing. *Nat Rev Neurosci* **6**, 297–311 (2005).

10. Arai, I. & Jonas, P. Nanodomain coupling explains Ca2+ independence of transmitter release time course at a fast central synapse. *eLife* **3**, e04057 (2014).

11. Azouz, R. Physiological properties of inhibitory interneurons in cat striate cortex. *Cerebral Cortex* **7**, 534–545 (1997).

12. Bao, J., Reim, K. & Sakaba, T. Target-Dependent Feedforward Inhibition Mediated by Short-Term Synaptic Plasticity in the Cerebellum. *Journal of Neuroscience* **30**, 8171–8179 (2010).

13. Beierlein, M., Gibson, J. R. & Connors, B. W. A network of electrically coupled interneurons drives synchronized inhibition in neocortex. *Nature Neuroscience* **3**, 904–910 (2000).

14. Bell, C. C., Caputi, A., Grant, K. & Serrier, J. Storage of a sensory pattern by anti-Hebbian synaptic plasticity in an electric fish. *Proceedings of the National Academy of Sciences* **90**, 4650–4654 (1993).

15. Belluardo, N. *et al.* Expression of Connexin36 in the adult and developing rat brain. *Brain Research* **865**, 121–138 (2000).

16. Bender, V. A., Pugh, J. R. & Jahr, C. E. Presynaptically Expressed Long-Term Potentiation Increases Multivesicular Release at Parallel Fiber Synapses. *Journal of Neuroscience* **29**, 10974–10978 (2009).

17. Bennett, M. V., Pappas, G. D., Aljure, E. & Nakajima, Y. Physiology and ultrastructure of electrotonic junctions. II. Spinal and medullary electromotor nuclei in mormyrid fish. *Journal of Neurophysiology* **30**, 180–208 (1967).

18. Bennett, M. V. L. Electrical synapses, a personal perspective (or history) (2000).

19. Bennett, M. V. L. & Zukin, R. S. Electrical Coupling and Neuronal Synchronization in the Mammalian

Brain. *Neuron* **41**, 495–511 (2004).

20. Blot, A. & Barbour, B. Ultra-rapid axon-axon ephaptic inhibition of cerebellar Purkinje cells by the pinceau. *Nat Neurosci* **17**, 289–295 (2014).

21. Blot, A. *et al.* Time-invariant feed-forward inhibition of Purkinje cells in the cerebellar cortex *in vivo*: Interneurons *in vivo*. *The Journal of Physiology* **594**, 2729–2749 (2016).

22. Bosman, L. W. J. *et al.* Encoding of whisker input by cerebellar Purkinje cells: Whisker encoding by Purkinje cells. *The Journal of Physiology* **588**, 3757–3783 (2010).

23. Bostan, A. C., Dum, R. P. & Strick, P. L. Cerebellar networks with the cerebral cortex and basal ganglia. *Trends in Cognitive Sciences* **17**, 241–254 (2013).

24. Bouvier, G. *et al.* Cerebellar learning using perturbations. *Elife* 45 (2018).

25. Bracha, V. Role of the cerebellum in eyeblink conditioning. in *Progress in Brain Research* **143**, 331–339 (Elsevier, 2004).

26. Branco, T. & Häusser, M. Synaptic Integration Gradients in Single Cortical Pyramidal Cell Dendrites. *Neuron* **69**, 885–892 (2011).

27. Brock, L. G., Coombs, J. S. & Eccles, J. C. The recording of potentials from motoneurones with an intracellular electrode. *The Journal of Physiology* **117**, 431–460 (1952).

28. Brown, S. T. & Raman, I. M. Sensorimotor Integration and Amplification of Reflexive Whisking by Well-Timed Spiking in the Cerebellar Corticonuclear Circuit. *Neuron* **99**, 564-575.e2 (2018).

29. Carter, A. G. & Regehr, W. G. Quantal events shape cerebellar interneuron firing. *Nat Neurosci* **5**, 1309–1318 (2002).

30. Cayco-Gajic, N. A. & Silver, R. A. Re-evaluating Circuit Mechanisms Underlying Pattern Separation. *Neuron* **101**, 584–602 (2019).

31. Cazé, R. D., Humphries, M. & Gutkin, B. Passive Dendrites Enable Single Neurons to Compute Linearly Non-separable Functions. *PLoS Comput Biol* **9**, e1002867 (2013).

32. Chabrol, F. P., Arenz, A., Wiechert, M. T., Margrie, T. W. & DiGregorio, D. A. Synaptic diversity enables temporal coding of coincident multisensory inputs in single neurons. *Nat Neurosci* **18**, 718–727 (2015).

33. Chadderton, P., Margrie, T. W. & Häusser, M. Integration of quanta in cerebellar granule cells during sensory processing. *Nature* **428**, 856–860 (2004).

34. Chavas, J. & Marty, A. Coexistence of Excitatory and Inhibitory GABA Synapses in the Cerebellar Interneuron Network. *The Journal of Neuroscience* **23**, 2019–2031 (2003).

35. Chen, S., Wang, J. & Siegelbaum, S. A. Properties of Hyperpolarization-Activated Pacemaker Current Defined by Coassembly of Hcn1 and Hcn2 Subunits and Basal Modulation by Cyclic Nucleotide. *J Gen Physiol* **117**, 491–504 (2001).

36. Chen, S., Augustine, G. J. & Chadderton, P. The cerebellum linearly encodes whisker position during voluntary movement. *eLife* **5**, e10509 (2016).

37. Chu, C.-P., Bing, Y.-H., Liu, H. & Qiu, D.-L. Roles of Molecular Layer Interneurons in Sensory Information Processing in Mouse Cerebellar Cortex Crus II In Vivo. *PLoS ONE* **7**, e37031 (2012).

38. Condorelli, D. F. *et al.* Cloning of a new gap junction gene (Cx36) highly expressed in mammalian brain neurons: New gap junction gene expressed in CNS. *European Journal of Neuroscience* **10**, 1202–1208 (1998).

39. Cowan, W. M., Südhof, T. C. & Stevens, C. F. *Synapses*. (2001).

40. Crawley, J. N. *What's wrong with my mouse: behavioral phenotyping of transgenic and knockout mice.* (Wiley-Liss, Hoboken, USA., 2007).

41. Crepel, F., Delhaye-Bouchaud, N. & Dupont, J. L. Fate of the multiple innervation of cerebellar Purkinje cells by climbing fibers in immature control, X-irradiated and hypothyroid rats. *Developmental Brain Research* **1**, 59–71 (1981).

42. Cruikshank, S. J. *et al.* Potent block of Cx36 and Cx50 gap junction channels by mefloquine. *Proceedings of the National Academy of Sciences* **101**, 12364–12369 (2004).

43. Curti, S. Voltage-Dependent Enhancement of Electrical Coupling by a Subthreshold Sodium Current. *Journal of Neuroscience* **24**, 3999–4010 (2004).

44. Curti, S. Voltage-Dependent Enhancement of Electrical Coupling by a Subthreshold Sodium Current. *Journal of Neuroscience* **24**, 3999–4010 (2004).

45. D'Angelo, E. & Casali, S. Seeking a unified framework for cerebellar function and dysfunction: from circuit operations to cognition. *Front. Neural Circuits* **6**, (2013).

46. D'Angelo, E. & De Zeeuw, C. I. Timing and plasticity in the cerebellum: focus on the granular layer. *Trends in Neurosciences* **32**, 30–40 (2009).

47. Davis, L. M., Kanter, H. L., Beyer, E. C. & Saffitz, J. E. Distinct gap junction protein phenotypes in cardiac tissues with disparate conduction properties. *Journal of the American College of Cardiology* **24**, 1124–1132 (1994).

48. Davis, L. M., Rodefeld, M. E., Green, K., Beyer, E. C. & Saffitz, J. E. Gap Junction Protein Phenotypes of the Human Heart and Conduction System. *J Cardiovasc Electrophysiol* **6**, 813–822 (1995).

49. Deans, M. R., Gibson, J. R., Sellitto, C., Connors, B. W. & Paul, D. L. Synchronous Activity of Inhibitory Networks in Neocortex Requires Electrical Synapses Containing Connexin36. *Neuron* **31**, 477–485 (2001).

50. del Castillo, J. & Katz, B. Quantal components of the end-plate potential. *The Journal of Physiology* **124**, 560–573 (1954).

51. DiGregorio, D. A., Nusser, Z. & Silver, R. A. Spillover of Glutamate onto Synaptic AMPA Receptors Enhances Fast Transmission at a Cerebellar Synapse. *Neuron* **35**, 521–533 (2002).

52. Dizon, M. J. & Khodakhah, K. The Role of Interneurons in Shaping Purkinje Cell Responses in the Cerebellar Cortex. *Journal of Neuroscience* **31**, 10463–10473 (2011).

53. Dorgans, K. *et al.* Short-term plasticity at cerebellar granule cell to molecular layer interneuron synapses expands information processing. *eLife* **8**, e41586 (2019).

54. Draguhn, A., Traub, R. D., Schmitz, D. & Jefferys, J. G. R. Electrical coupling underlies high-frequency oscillations in the hippocampus in vitro. *Nature* **394**, 189–192 (1998).

55. Dugué, G. P. *et al.* Electrical Coupling Mediates Tunable Low-Frequency Oscillations and Resonance in the Cerebellar Golgi Cell Network. *Neuron* **61**, 126–139 (2009).

56. Eccles, J. C., Ito, M. & Szentagothai, J. *The Cerebellum as a Neuronal Machine*. (Springer Science + Business Media New York, 1967).

57. Eccles, J. C., Llinás, R. & Sasaki, K. The excitatory synaptic action of climbing fibres on the Purkinje cells of the cerebellum. *The Journal of Physiology* **182**, 268–296 (1966).

58. Feldmeyer, D., Qi, G., Emmenegger, V. & Staiger, J. F. Inhibitory Interneurons and their Circuit Motifs in the Many Layers of the Barrel Cortex. *Neuroscience* **368**, 132–151 (2018).

59. Flores, C. E., Li, X., Bennett, M. V. L., Nagy, J. I. & Pereda, A. E. Interaction between connexin35 and zonula occludens-1 and its potential role in the regulation of electrical synapses. *Proceedings of the National Academy of Sciences* **105**, 12545–12550 (2008).

60. Flourens, P. *Recherches expérimentales sur les propriétés et les fonctions du système nerveux dans les animaux vertébrés*. (Crevot, 1824).

61. Fortier, P. A. & Bagna, M. Estimating conductances of dual-recorded neurons within a network of coupled cells. *Journal of Theoretical Biology* **240**, 501–510 (2006).

62. Frisch, C. *et al.* Stimulus complexity dependent memory impairment and changes in motor performance after deletion of the neuronal gap junction protein connexin36 in mice. *Behavioural Brain Research* **157**, 177–185 (2005).

63. Furshpan, E. J. 'Electrical Transmission' at an Excitatory Synapse in a Vertebrate Brain. *Science* **144**, 878–880 (1964).

64. Furshpan, E. J. & Potter, D. D. Transmission at the giant motor synapses of the crayfish. *The Journal of Physiology* **145**, 289–325 (1959).

65. Galarreta, M. & Hestrin, S. Electrical synapses between Gaba-Releasing interneurons. *Nature Reviews Neuroscience* **2**, 425–433 (2001).

66. Gao, Z., van Beugen, B. J. & De Zeeuw, C. I. Distributed synergistic plasticity and cerebellar learning. *Nature Reviews Neuroscience* **13**, 619–635 (2012).

67. Geiger, J. R. P., Lübke, J., Roth, A., Frotscher, M. & Jonas, P. Submillisecond AMPA Receptor-Mediated Signaling at a Principal Neuron–Interneuron Synapse. *Neuron* **18**, 1009–1023 (1997).

68. Gibson, J. R., Beierlein, M. & Connors, B. W. Functional Properties of Electrical Synapses Between Inhibitory Interneurons of Neocortical Layer 4. *Journal of Neurophysiology* **93**, 467–480 (2005).

69. Grangeray-Vilmint, A., Valera, A. M., Kumar, A. & Isope, P. Short-Term Plasticity Combines with Excitation–Inhibition Balance to Expand Cerebellar Purkinje Cell Dynamic Range. *The Journal of Neuroscience* **38**, 5153–5167 (2018).

70. Gutierrez, G. J., O'Leary, T. & Marder, E. Multiple Mechanisms Switch an Electrically Coupled, Synaptically Inhibited Neuron between Competing Rhythmic Oscillators. *Neuron* **77**, 845–858 (2013).

71. Haas, J. S., Zavala, B. & Landisman, C. E. Activity-Dependent Long-Term Depression of Electrical Synapses. *Science* **334**, 389–393 (2011).

72. Hamelin, R., Allagnat, F., Haefliger, J.-A. & Meda, P. Connexins, Diabetes and the Metabolic Syndrome. *CPPS* **10**, 18–29 (2009).

73. Harris, A. L., Spray, D. C. & Bennett, M. V. L. Kinetic properties of a voltage-dependent junctional conductance. *The Journal of General Physiology* **77**, 95–117 (1981).

74. Harting, J. K. *The Global Cerebellum*. (University of Wisconsin Medical School, 1997).

75. Harvey, R. J. & Napper, R. M. A. Quantitative studies on the mammalian cerebellum. (1991).

76. Hausser, M. Differential Shunting of EPSPs by Action Potentials. *Science* **291**, 138–141 (2001).

77. Häusser, M. & Mel, B. Dendrites: bug or feature? *Current Opinion in Neurobiology* **13**, 372–383 (2003).

78. He, Q. *et al.* Interneuron- and GABAA receptor-specific inhibitory synaptic plasticity in cerebellar Purkinje cells. *Nature Communications* **6**, 7364 (2015).

79. Heiney, S. A., Kim, J., Augustine, G. J. & Medina, J. F. Precise Control of Movement Kinematics by

Optogenetic Inhibition of Purkinje Cell Activity. *Journal of Neuroscience* **34**, 2321–2330 (2014).

80. Hille, B. *Ion Channels of Excitable Membranes*. (Sinauer Associates, Inc, 2001).

81. Hines, M. L. & Carnevale, N. T. The NEURON Simulation Environment. *Neural Computation* **9**, 1179–1209 (1997).

82. Hjorth, J., Blackwell, K. T. & Hellgren Kotaleski, J. Gap Junctions between Striatal Fast-Spiking Interneurons Regulate Spiking Activity and Synchronization as a Function of Cortical Activity. *Journal of Neuroscience* **29**, 5276–5286 (2009).

83. Hodgkin, A. L. & Huxley, A. F. A quantitative description of membrane current and its application to conduction and excitation in nerve. *The Journal of Physiology* **117**, 500–544 (1952).

84. Hormuzdi, S. G., Filippov, M. A., Mitropoulou, G., Monyer, H. & Bruzzone, R. Electrical synapses: a dynamic signaling system that shapes the activity of neuronal networks. *Biochimica et Biophysica Acta (BBA) - Biomembranes* **1662**, 113–137 (2004).

85. Hormuzdi, S. G. *et al.* Impaired Electrical Signaling Disrupts Gamma Frequency Oscillations in Connexin 36-Deficient Mice. *Neuron* **31**, 487–495 (2001).

86. Hu, H., Gan, J. & Jonas, P. Fast-spiking, parvalbumin+ GABAergic interneurons: From cellular design to microcircuit function. *Science* **345**, 1255263–1255263 (2014).

87. Hu, H., Martina, M. & Jonas, P. Dendritic Mechanisms Underlying Rapid Synaptic Activation of Fast-Spiking Hippocampal Interneurons. *Science* **327**, 52–58 (2010).

88. Hu, H. & Agmon, A. Properties of precise firing synchrony between synaptically coupled cortical interneurons depend on their mode of coupling. *Journal of Neurophysiology* **114**, 624–637 (2015).

89. Huang, C.-C. *et al.* Convergence of pontine and proprioceptive streams onto multimodal cerebellar granule cells. *eLife* **2**, e00400 (2013).

90. Isaacson, J. S. & Scanziani, M. How Inhibition Shapes Cortical Activity. *Neuron* **72**, 231–243 (2011).

91. Ishikawa, T., Shimuta, M. & Häusser, M. Multimodal sensory integration in single cerebellar granule cells in vivo. *eLife* **4**, e12916 (2015).

92. Ito, M. *The Cerebellum and Neural Control*. (Raven Press, 1984).

93. Ito, M. Control of mental activities by internal models in the cerebellum. *Nature Reviews Neuroscience* **9**, 304–313 (2008).

94. Ito, M. & Kano, M. Long-lasting depression of parallel Fiber-Purkinje cell transmission induced by conjunctive stimulation of parallel fibers and climbing fibers in the cerebellar cortex. *Neuroscience Letters* 253–258 (1982).

95. Jack, J. J. B., Noble, D. & Tsien, R. W. *Electric current flow in excitable cells*. (Oxford University Press, 1975).

96. Jaeger, D., De Schutter, E. & Bower, J. M. The Role of Synaptic and Voltage-Gated Currents in the Control of Purkinje Cell Spiking: A Modeling Study. *J. Neurosci.* **17**, 91–106 (1997).

97. Jarsky, T. *et al.* A Synaptic Mechanism for Retinal Adaptation to Luminance and Contrast. *Journal of Neuroscience* **31**, 11003–11015 (2011).

98. Johnston, D. & Wu, S. M.-S. *Foundations of Cellular Neurophysiology*. (MIT Press, 1995).

99. Jörntell, H. & Ekerot, C.-F. Reciprocal Bidirectional Plasticity of Parallel Fiber Receptive Fields in Cerebellar Purkinje Cells and Their Afferent Interneurons. *Neuron* **34**, 797–806 (2002).

100. Kano, M., Rexhausen, U., Dreessen, J. & Konnerth, A. Synaptic excitation produces a long-lasting rebound potentiation of inhibitory synaptic signals in cerebellar Purkinje cells. *Nature* **356**, 601–604 (1992).

101. Kanold, P. O., Davis, K. A. & Young, E. D. Somatosensory context alters auditory responses in the cochlear nucleus. *Journal of Neurophysiology* **105**, 1063–1070 (2011).

102. Kanold, P. O. & Young, E. D. Proprioceptive Information from the Pinna Provides Somatosensory Input to Cat Dorsal Cochlear Nucleus. *J. Neurosci.* **21**, 7848–7858 (2001).

103. Kennedy, A. A temporal basis for predicting the sensory consequences of motor commands in an electric fish. *nature NEUROSCIENCE* **17**, 9 (2014).

104. Kim, J. *et al.* Optogenetic Mapping of Cerebellar Inhibitory Circuitry Reveals Spatially Biased Coordination of Interneurons via Electrical Synapses. *Cell Reports* **7**, 1601–1613 (2014).

105. Koehler, S. D., Pradhan, S., Manis, P. B. & Shore, S. E. Somatosensory inputs modify auditory spike timing in dorsal cochlear nucleus principal cells: Somatosensory inputs alter auditory spike timing. *European Journal of Neuroscience* **33**, 409–420 (2011).

106. Koehler, S. D. & Shore, S. E. Stimulus-Timing Dependent Multisensory Plasticity in the Guinea Pig Dorsal Cochlear Nucleus. *PLoS ONE* **8**, e59828 (2013).

107. Kondo, S. & Marty, A. Synaptic currents at individual connections among stellate cells in rat cerebellar slices. *Journal of Physiology* (1998).

108. Kuo, S. P., Schwartz, G. W. & Rieke, F. Nonlinear Spatiotemporal Integration by Electrical and Chemical Synapses in the Retina. *Neuron* **90**, 320–332 (2016).

109. Landisman, C. E. & Connors, B. W. Long-Term Modulation of Electrical Synapses in the Mammalian Thalamus. *Science* **310**, 1809–1813 (2005).

110. Landisman, C. E. *et al.* Electrical Synapses in the Thalamic Reticular Nucleus. *J. Neurosci.* **22**, 1002–1009 (2002).

111. Leiner, H. C., Leiner, A. L. & Dow, R. S. Does the Cerebellum Contribute to Mental Skills? 12 (1986).

112. Lev-Ram, V., Wong, S. T., Storm, D. R. & Tsien, R. Y. A new form of cerebellar long-term potentiation is postsynaptic and depends on nitric oxide but not cAMP. *Proceedings of the National Academy of Sciences* **99**, 8389–8393 (2002).

113. Lin, J. & Faber, D. Synaptic transmission mediated by single club endings on the goldfish Mauthner cell. I. Characteristics of electrotonic and chemical postsynaptic potentials. *J. Neurosci.* **8**, 1302–1312 (1988).

114. London, M. & Hausser, M. DENDRITIC COMPUTATION. 32 (2005).

115. Long, M. A., Landisman, C. E. & Connors, B. W. Small Clusters of Electrically Coupled Neurons Generate Synchronous Rhythms in the Thalamic Reticular Nucleus. *Journal of Neuroscience* **24**, 341–349 (2004).

116. Luján, R., Albasanz, J. L., Shigemoto, R. & Juiz, J. M. Preferential localization of the hyperpolarization-activated cyclic nucleotide-gated cation channel subunit HCN1 in basket cell terminals of the rat cerebellum. *European Journal of Neuroscience* **21**, 2073–2082 (2005).

117. Lüthi, A. & McCormick, D. H-Current: Properties of a Neuronal and Network Pacemaker. *Neuron* (1998).

118. Maccaferri, G., Mangoni, M., Lazzari, A. & DiFrancesco, D. Properties of the hyperpolarization-activated current in rat hippocampal CA1 pyramidal cells. *Journal of Neurophysiology* **69**, 2129–2136 (1993).

119. Maex, R. & De Schutter, E. Mechanism of spontaneous and self-sustained oscillations in networks connected through axo-axonal gap junctions: Dynamics of axo-axonally coupled networks. *European Journal of Neuroscience* **25**, 3347–3358 (2007).

120. Maex, R. & Gutkin, B. Temporal integration and 1/ *f* power scaling in a circuit model of cerebellar interneurons. *Journal of Neurophysiology* **118**, 471–485 (2017).

121. Magee, J. C. Dendritic integration of excitatory synaptic input. *Nat Rev Neurosci* **1**, 181–190 (2000).

122. Major, G., Larkum, M. E. & Schiller, J. Active Properties of Neocortical Pyramidal Neuron Dendrites. *Annual Review of Neuroscience* **36**, 1–24 (2013).

123. Mann-Metzer, P. & Yarom, Y. Electrotonic Coupling Interacts with Intrinsic Properties to Generate Synchronized Activity in Cerebellar Networks of Inhibitory Interneurons. *The Journal of Neuroscience* **19**, 3298–3306 (1999).

124. Mapelli, L., Pagani, M., Garrido, J. A. & D'Angelo, E. Integrated plasticity at inhibitory and excitatory synapses in the cerebellar circuit. *Frontiers in Cellular Neuroscience* **9**, (2015).

125. Marcaggi, P. & Attwell, D. Endocannabinoid signaling depends on the spatial pattern of synapse activation. *Nature Neuroscience* **8**, 776–781 (2005).

126. Marcaggi, P. & Attwell, D. Short- and long-term depression of rat cerebellar parallel fibre synaptic transmission mediated by synaptic crosstalk: Cerebellar parallel fibre synaptic plasticity and synaptic crosstalk. *The Journal of Physiology* **578**, 545–550 (2007).

127. Marek, R. *et al.* Hippocampus-driven feed-forward inhibition of the prefrontal cortex mediates relapse of extinguished fear. *Nat Neurosci* **21**, 384–392 (2018).

128. Marr, D. A theory of cerebellar cortex. *The Journal of Physiology* **202**, 437–470 (1969).

129. Mathias, R. T., Kistler, J. & Donaldson, P. The Lens Circulation. *J Membrane Biol* **216**, 1–16 (2007).

130. Mathy, A., Clark, B. A. & Häusser, M. Synaptically Induced Long-Term Modulation of Electrical Coupling in the Inferior Olive. *Neuron* **81**, 1290–1296 (2014).

131. McBain, C. J. & Fisahn, A. Interneurons unbound. *Nat Rev Neurosci* **2**, 11–23 (2001).

132. McCormick, D. & Thompson, R. Cerebellum: essential involvement in the classically conditioned eyelid response. *Science* **223**, 296–299 (1984).

133. Medina, J. F. & Lisberger, S. G. Variation, Signal, and Noise in Cerebellar Sensory-Motor Processing for Smooth-Pursuit Eye Movements. *Journal of Neuroscience* **27**, 6832–6842 (2007).

134. Medina, J. F. The multiple roles of Purkinje cells in sensori-motor calibration: to predict, teach and command. *Current Opinion in Neurobiology* **21**, 616–622 (2011).

135. Medina, J. F. & Lisberger, S. G. Links from complex spikes to local plasticity and motor learning in the cerebellum of awake-behaving monkeys. *Nat Neurosci* **11**, 1185–1192 (2008).

136. Medina, J. F., Nores, W. L., Ohyama, T. & Mauk, M. D. Mechanisms of cerebellar learning suggested by eyelid conditioning. *Current Opinion in Neurobiology* 8 (2000)

137. Medina, J. F. & Mauk, M. D. Computer simulation of cerebellar information processing. *Nature Neuroscience* **3**, 1205–1211 (2000).

138. Meier, C. & Dermietzel, R. Electrical Synapses – Gap Junctions in the Brain. in *Cell Communication in Nervous and Immune System* (eds. Gundelfinger, E. D., Seidenbecher, C. I. & Schraven, B.) **43**, 99–128 (Springer Berlin Heidelberg, 2006).

139. Mejia-Gervacio, S. *et al.* Axonal Speeding: Shaping Synaptic Potentials in Small Neurons by the Axonal Membrane Compartment. *Neuron* **53**, 843–855 (2007).

140. Mercer, A., Bannister, A. P. & Thomson, A. M. Electrical coupling between pyramidal cells in adult cortical

regions. *Brain Cell Biology* **35**, 13–27 (2007).

141. Mittmann, W., Koch, U. & Häusser, M. Feed-forward inhibition shapes the spike output of cerebellar Purkinje cells: Feed-forward inhibition in the cerebellar cortex. *The Journal of Physiology* **563**, 369–378 (2005).

142. Moberget, T. & Ivry, R. B. Cerebellar contributions to motor control and language comprehension: searching for common computational principles: Cerebellar contributions to motor control and language. *Annals of the New York Academy of Sciences* **1369**, 154–171 (2016).

143. Motanis, H., Seay, M. J. & Buonomano, D. V. Short-Term Synaptic Plasticity as a Mechanism for Sensory Timing. *Trends in Neurosciences* **41**, 701–711 (2018).

144. Nagy, J. I., Pereda, A. E. & Rash, J. E. Electrical synapses in mammalian CNS: Past eras, present focus and future directions. *Biochimica et Biophysica Acta* 22 (2018).

145. Napper, R. M. A. & Harvey, R. J. Number of parallel fiber synapses on an individual Purkinje cell in the cerebellum of the rat. *The Journal of Comparative Neurology* **274**, 168–177 (1988).

146. Neher, E. & Sakmann, B. Single-channel currents recorded from membrane of denervated frog muscle fibers. (1976).

147. Nielsen, M. S. *et al.* Gap Junctions. in *Comprehensive Physiology* (ed. Terjung, R.) c110051 (John Wiley & Sons, Inc., 2012). doi:10.1002/cphy.c110051

148. Norenberg, A., Hu, H., Vida, I., Bartos, M. & Jonas, P. Distinct nonuniform cable properties optimize rapid and efficient activation of fast-spiking GABAergic interneurons. *Proceedings of the National Academy of Sciences* **107**, 894–899 (2010).

149. Ohyama, T., Nores, W. L., Murphy, M. & Mauk, M. D. What the cerebellum computes. *Trends in Neurosciences* **26**, 222–227 (2003).

150. Otsuka, T. & Kawaguchi, Y. Common excitatory synaptic inputs to electrically connected cortical fast-spiking cell networks. *Journal of Neurophysiology* **110**, 795–806 (2013).

151. Palay, S. L. & Chan-Palay, V. *Cerebellar Cortex: Cytology and Organization*. (Springer-Verlag, 1974).

152. Patel, L. S., Mitchell, C. K., Dubinsky, W. P. & O'Brien, J. Regulation of Gap Junction Coupling Through the Neuronal Connexin Cx35 by Nitric Oxide and cGMP. *Cell Communication & Adhesion* **13**, 41–54 (2006).

153. Peinado, A., Yuste, R. & Katz, L. C. Extensive Dye Coupling behween Rat Neocortical Neurons during the Period of Circuit Formation. *Neuron* **10**, 103–114 (1993).

154. Pereda, A. & Faber, D. Activity-dependent short-term enhancement of intercellular coupling. *The Journal of Neuroscience* **16**, 983–992 (1996).

155. Pereda, A. E. Electrical synapses and their functional interactions with chemical synapses. *Nature Reviews Neuroscience* **15**, 250–263 (2014).

156. Phelan, P. *et al.* Molecular Mechanism of Rectification at Identified Electrical Synapses in the Drosophila Giant Fiber System. *Current Biology* **18**, 1955–1960 (2008).

157. Pian, P., Bucchi, A., Robinson, R. B. & Siegelbaum, S. A. Regulation of Gating and Rundown of HCN Hyperpolarization-activated Channels by Exogenous and Endogenous PIP $_2$. *J Gen Physiol* **128**, 593–604 (2006).

158. Poirazi, P., Brannon, T. & Mel, B. W. Pyramidal Neuron as Two-Layer Neural Network. *Neuron* **37**, 989–999 (2003).

159. Poirazi, P. & Mel, B. W. Impact of Active Dendrites and Structural Plasticity on the Memory Capacity of Neural Tissue. *Neuron* **29**, 779–796 (2001).

160. Pouille, F. Enforcement of Temporal Fidelity in Pyramidal Cells by Somatic Feed-Forward Inhibition. *Science* **293**, 1159–1163 (2001).

161. Pouille, F., Marin-Burgin, A., Adesnik, H., Atallah, B. V. & Scanziani, M. Input normalization by global feedforward inhibition expands cortical dynamic range. *nature NEUROSCIENCE* **12**, 11 (2009).

162. Pouille, F., Watkinson, O., Scanziani, M. & Trevelyan, A. J. The contribution of synaptic location to inhibitory gain control in pyramidal cells. *Physiological Reports* **1**, (2013).

163. Pulido, C., Trigo, F. F., Llano, I. & Marty, A. Vesicular Release Statistics and Unitary Postsynaptic Current at Single GABAergic Synapses. *Neuron* **85**, 159–172 (2015).

164. Rall, W., Burke, R. E., Smith, T. G., Nelson, P. G. & Frank, K. Dendritic location of synapses and possible mechanisms for the monosynaptic EPSP in motoneurons. *Journal of Neurophysiology* **30**, 1169–1193 (1967).

165. Rall, W. Distributions of Potential in Cylindrical Coordinates and Time Constants for a Membrane Cylinder. **9**, 33 (1969).

166. Rall, W. Time Constants and Electrotonic Length of Membrane Cylinders and Neurons. *Biophysical Journal* 26 (1969).

167. Rall, W., Koch, U. & Segev, I. Cable theory for dendritic neurons. in *Methods in neuronal modeling.* (MIT Press, 1989).

168. Rasmussen, A. & Hesslow, G. Feedback Control of Learning by the Cerebello-Olivary Pathway. in *Progress in Brain Research* **210**, 103–119 (Elsevier, 2014).

169. Rieubland, S., Roth, A. & Häusser, M. Structured Connectivity in Cerebellar Inhibitory Networks. *Neuron* **81**, 913–929 (2014).

170. Roberts, M. T. & Trussell, L. O. Molecular Layer Inhibitory Interneurons Provide Feedforward and Lateral Inhibition in the Dorsal Cochlear Nucleus. *Journal of Neurophysiology* **104**, 2462–2473 (2010).

171. Roberts, P. D. & Portfors, C. V. Design principles of sensory processing in cerebellum-like structures: Early stage processing of electrosensory and auditory objects. *Biol Cybern* **98**, 491–507 (2008).

172. Rössert, C., Dean, P. & Porrill, J. At the Edge of Chaos: How Cerebellar Granular Layer Network Dynamics Can Provide the Basis for Temporal Filters. *PLOS Computational Biology* **11**, e1004515 (2015).

173. Russo, G., Nieus, T. R., Maggi, S. & Taverna, S. Dynamics of action potential firing in electrically connected striatal fast-spiking interneurons. *Frontiers in Cellular Neuroscience* **7**, (2013).

174. Sakurai, M. Synaptic modification of parallel fibre-Purkinje cell transmission in in vitro guinea-pig cerebellar slices. *The Journal of Physiology* **394**, 463–480 (1987).

175. Santamaria, F., Tripp, P. G. & Bower, J. M. Feedforward Inhibition Controls the Spread of Granule Cell–Induced Purkinje Cell Activity in the Cerebellar Cortex. *Journal of Neurophysiology* **97**, 248–263 (2007).

176. Sawtell, N. B. Multimodal Integration in Granule Cells as a Basis for Associative Plasticity and Sensory Prediction in a Cerebellum-like Circuit. *Neuron* **66**, 573–584 (2010).

177. Schilling, K. & Oberdick, J. The Treasury of the Commons: Making Use of Public Gene Expression Resources to Better Characterize the Molecular Diversity of Inhibitory Interneurons in the Cerebellar Cortex. *Cerebellum* **8**, 477–489 (2009).

178. Schneiderman, N. & Gormezano, I. CONDITIONING OF THE NICTITATING MEMBRANE OF THE

RABBIT AS A FUNCTION OF CS-US INTERVAL. *Journal of comparative and physiological psychology* **57**, 188–195 (1964).

179. Shepherd, G. M. *The Synaptic Organization of the Brain*. (Oxford University Press, 1994).

180. Shepherd, G. M. & Grillner, S. *Handbook of Brain Microcircuits*. (Oxford University Press, 2010).

181. Shiroma, A. *et al.* Cerebellar Contribution to Pattern Separation of Human Hippocampal Memory Circuits. *The Cerebellum* **15**, 645–662 (2016).

182. Silver, R. A. Estimation of nonuniform quantal parameters with multiple-probability fluctuation analysis: theory, application and limitations. *Journal of Neuroscience Methods* **130**, 127–141 (2003).

183. Smith, M. & Pereda, A. E. Chemical synaptic activity modulates nearby electrical synapses. *Proceedings of the National Academy of Sciences* **100**, 4849–4854 (2003).

184. Söhl, G., Degen, J., Teubner, B. & Willecke, K. The murine gap junction gene connexin36 is highly expressed in mouse retina and regulated during brain development. *FEBS Letters* **428**, 27–31 (1998).

185. Soler-Llavina, G. J. & Sabatini, B. L. Synapse-specific plasticity and compartmentalized signaling in cerebellar stellate cells. *Nat Neurosci* **9**, 798–806 (2006).

186. Southan, A. P., Morris, N. P., Stephens, G. J. & Robertson, B. Hyperpolarization-activated currents in presynaptic terminals of mouse cerebellar basket cells. *The Journal of Physiology* **526**, 91–97 (2000).

187. Spencer, W. A. & Kandel, E. R. ELECTROPHYSIOLOGY OF HIPPOCAMPAL NEURONS: IV. FAST PREPOTENTIALS. *Journal of Neurophysiology* **24**, 272–285 (1961).

188. Spray, D. C. & Bennett, M. V. L. Physiology and Pharmacology of Gap Junctions. *Annual Review of Physiology* 23 (1985).

189. Srinivas, M. *et al.* Functional Properties of Channels Formed by the Neuronal Gap Junction Protein Connexin36. *The Journal of Neuroscience* **19**, 9848–9855 (1999).

190. Stasheff, S. F., Hines, M. & Wilson, W. A. Axon terminal hyperexcitability associated with epileptogenesis in vitro. I. Origin of ectopic spikes. *Journal of Neurophysiology* **70**, 961–975 (1993).

191. Steinmetz, J. E., Lavond, D. G. & Thompson, R. F. Classical conditioning in rabbits using pontine nucleus stimulation as a conditioned stimulus and inferior olive stimulation as an unconditioned stimulus. *Synapse* **3**, 225–233 (1989).

192. Strick, P. L., Dum, R. P. & Fiez, J. A. Cerebellum and Nonmotor Function. *Annual Review of Neuroscience* **32**, 413–434 (2009).

193. Stuart, G., Spruston, N. & Häusser, M. *Dendrites*. (Oxford University Press, 2008).

194. Sudhakar, S. K. *et al.* Spatiotemporal network coding of physiological mossy fiber inputs by the cerebellar granular layer. *PLOS Computational Biology* **13**, e1005754 (2017).

195. Sultan, F. & Bower, J. M. Quantitative Golgi study of the rat cerebellar molecular layer interneurons using principal component analysis. *The Journal of Comparative Neurology* 21 (1998).

196. Szapiro, G. & Barbour, B. Multiple climbing fibers signal to molecular layer interneurons exclusively via glutamate spillover. *Nature Neuroscience* **10**, 735–742 (2007).

197. Szoboszlay, M. *et al.* Functional Properties of Dendritic Gap Junctions in Cerebellar Golgi Cells. *Neuron* **90**, 1043–1056 (2016).

198. Takeuchi, T., Duszkiewicz, A. J. & Morris, R. G. M. The synaptic plasticity and memory hypothesis: encoding, storage and persistence. *Phil. Trans. R. Soc. B* **369**, 20130288 (2014).

199. Tamás, G., Buhl, E. H., Lörincz, A. & Somogyi, P. Proximally targeted GABAergic synapses and gap junctions synchronize cortical interneurons. *Nat Neurosci* **3**, 366–371 (2000).

200. Thompson, R. F. & Steinmetz, J. E. The role of the cerebellum in classical conditioning of discrete behavioral responses. *Neuroscience* **162**, 732–755 (2009).

201. Todd, K. L., Kristan, W. B. & French, K. A. Gap Junction Expression Is Required for Normal Chemical Synapse Formation. *Journal of Neuroscience* **30**, 15277–15285 (2010).

202. Tran-Van-Minh, A., Abrahamsson, T., Cathala, L. & DiGregorio, D. A. Differential Dendritic Integration of Synaptic Potentials and Calcium in Cerebellar Interneurons. *Neuron* **91**, 837–850 (2016).

203. Tran-Van-Minh, A. *et al.* Contribution of sublinear and supralinear dendritic integration to neuronal computations. *Frontiers in Cellular Neuroscience* **9**, (2015).

204. Turecek, J. *et al.* NMDA Receptor Activation Strengthens Weak Electrical Coupling in Mammalian Brain. *Neuron* **81**, 1375–1388 (2014).

205. Tzounopoulos, T., Kim, Y., Oertel, D. & Trussell, L. O. Cell-specific, spike timing–dependent plasticities in the dorsal cochlear nucleus. *Nat Neurosci* **7**, 719–725 (2004).

206. Ueno, S., Bracamontes, J., Zorumski, C., Weiss, D. S. & Steinbach, J. H. Bicuculline and Gabazine Are Allosteric Inhibitors of Channel Opening of the GABA $_{A}$ Receptor. *J. Neurosci.* **17**, 625–634 (1997).

207. Urschel, S. *et al.* Protein Kinase A-mediated Phosphorylation of Connexin36 in Mouse Retina Results in Decreased Gap Junctional Communication between AII Amacrine Cells. *J. Biol. Chem.* **281**, 33163–33171 (2006).

208. Valera, A. M. *et al.* Stereotyped spatial patterns of functional synaptic connectivity in the cerebellar cortex. *eLife* **5**, e09862 (2016).

209. van Welie, I., Roth, A., Ho, S. S. N., Komai, S. & Häusser, M. Conditional Spike Transmission Mediated by Electrical Coupling Ensures Millisecond Precision-Correlated Activity among Interneurons In Vivo. *Neuron* **90**, 810–823 (2016).

210. Vervaeke, K., Lorincz, A., Nusser, Z. & Silver, R. A. Gap Junctions Compensate for Sublinear Dendritic Integration in an Inhibitory Network. *Science* **335**, 1624–1628 (2012).

211. Vervaeke, K. *et al.* Rapid Desynchronization of an Electrically Coupled Interneuron Network with Sparse Excitatory Synaptic Input. *Neuron* **67**, 435–451 (2010).

212. Vincent, P. & Marty, A. Fluctuations of inhibitory postsynaptic currents in Purkinje cells from rat cerebellar slices. *The Journal of Physiology* **494**, 183–199 (1996).

213. Vyklicky, V. *et al.* Structure, Function, and Pharmacology of NMDA Receptor Channels. **63**, 13 (2014).

214. Wang, B. *et al.* Firing Frequency Maxima of Fast-Spiking Neurons in Human, Monkey, and Mouse Neocortex. *Front. Cell. Neurosci.* **10**, (2016).

215. Wang, S. S.-H., Kloth, A. D. & Badura, A. The Cerebellum, Sensitive Periods, and Autism. *Neuron* **83**, 518–532 (2014).

216. Wang, Z., Neely, R. & Landisman, C. E. Activation of Group I and Group II Metabotropic Glutamate Receptors Causes LTD and LTP of Electrical Synapses in the Rat Thalamic Reticular Nucleus. *Journal of Neuroscience* **35**, 7616–7625 (2015).

217. Warren, R. & Sawtell, N. B. A comparative approach to cerebellar function: insights from electrosensory systems. *Current Opinion in Neurobiology* **41**, 31–37 (2016).

218. Wigderson, E., Nelken, I. & Yarom, Y. Early multisensory integration of self and source motion in the

auditory system. *Proc Natl Acad Sci USA* **113**, 8308–8313 (2016).

219. Wilms, C. D. & Häusser, M. Reading out a spatiotemporal population code by imaging neighbouring parallel fibre axons in vivo. *Nat Commun* **6**, 6464 (2015).

220. Yamazaki, T. & Tanaka, S. A spiking network model for passage-of-time representation in the cerebellum: Cerebellar passage-of-time representation. *European Journal of Neuroscience* **26**, 2279–2292 (2007).

221. Yanagihara, K. & Irisawa, H. Inward current activated during hyperpolarization in the rabbit sinoatrial node cell. *Pflügers Arch.* **385**, 11–19 (1980).

222. Yao, X.-H. *et al.* Electrical coupling regulates layer 1 interneuron microcircuit formation in the neocortex. *Nat Commun* **7**, 12229 (2016).

223. Zhang, J. & Hill, C. E. Differential connexin expression in preglomerular and postglomerular vasculature: Accentuation during diabetes. *Kidney International* **68**, 1171–1185 (2005).

224. Zolnik, T. A. & Connors, B. W. Electrical synapses and the development of inhibitory circuits in the thalamus: Electrical synapses and thalamic development. *J Physiol* **594**, 2579–2592 (2016).

225. Zsiros, V., Aradi, I. & Maccaferri, G. Propagation of postsynaptic currents and potentials via gap junctions in GABAergic networks of the rat hippocampus: Propagation of synaptic activity via gap junctions. *The Journal of Physiology* **578**, 527–544 (2007).

Appendices:

I - 1) Coupling Coefficients and input resistances:

In the main text, I referred to this parameter as if it was unique, in the sense that it would have the same value if it was calculated from cell A to cell B, or the other way around. However, when an electrical circuit is drawn to model two electrically connected cells, it is possible to derive the equations of steady-state currents and voltages which are relevant for calculating the coupling coefficients. A description of these method can be found in (Fortier and Bagna, 2006). I will show here the simplified model, and the solutions of steady-state voltages in the two cells, to reveal that coupling coefficient calculations, when performed in one direction or the other, usually return two different values, and that this result is expected from a simple model (Figure A-1).

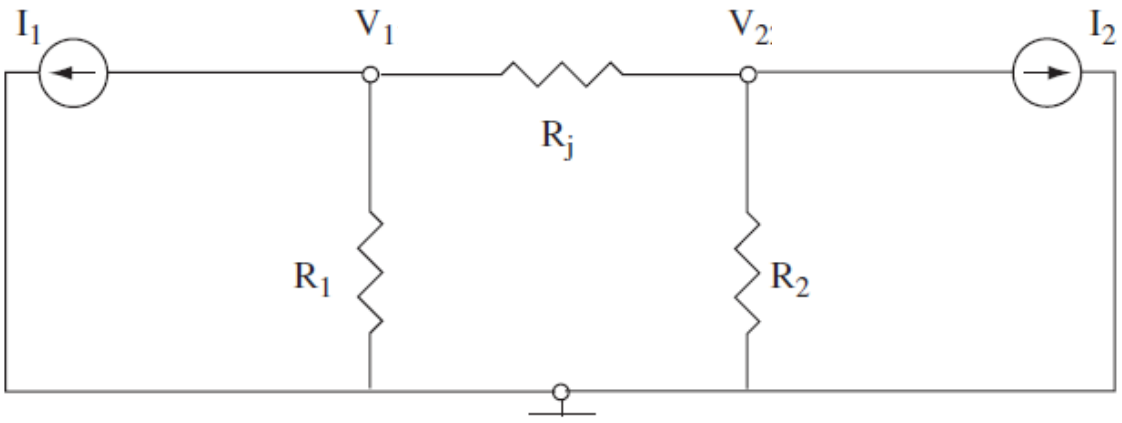

Figure A-1: Simplified model of two cells connected by an electrical synapse: V_1 and V_2 represent the holding membrane potential of cell 1 and 2, respectively; I_1 and I_2 represent the two current sources introduced by the patch pipettes in current-clamp configuration - one for each cell. R_1 and R_2 are the *intrinsic* input resistances of cell 1 and 2, respectively, while R_j denotes the resistance due to the electrical synapse connecting them.

From Fortier and Bagna, 2006

The steady-state responses are given by:

$V_{11} = I_1 * R_1 \frac{(R_2+R_j)}{(R_1+R_j+R_2)}$, the voltage response in cell 1 when current I_1 is injected in cell 1;

$V_{12} = I_1 * R_1 \frac{R_2}{(R_1+R_j+R_2)}$, the voltage response in cell 2 when current I_1 is injected in cell 1;

$V_{22} = I_2 * R_2 \frac{(R_1+R_j)}{(R_1+R_j+R_2)}$, the voltage response in cell 2 when current I_2 is injected in cell 2;

$V_{21} = I_2 * R_2 \frac{R_1}{(R_1+R_j+R_2)}$, the voltage response in cell 1 when current I_2 is injected in cell 2;

These equations are terribly annoying to read, but the key point is to relate them to coupling coefficients, which I will do now:

$$C_{12} = \frac{V_{12}}{V_{11}} = \frac{R_2}{(R_2+R_j)} \quad \text{and} \quad C_{21} = \frac{V_{21}}{V_{22}} = \frac{R_1}{(R_1+R_j)}$$

And now, one can observe that the calculation of the coupling coefficient ***does*** depend on the cell in which current is injected: if the two cells have different input resistances, then there is a difference in the coupling coefficients, despite the unique value of the junctional resistance. This explains why coupling coefficients can sometimes provide quite different values when calculated in one direction or the other. More importantly, these calculations reveal that the asymmetry of coupling goes along with the asymmetry in input resistance. As a consequence, although we usually think of electrical synapses as linking two different cells of a similar population of neurons, it is known that they can be made between different subtypes of neurons. In the extreme case, they can also be found between interneurons and principal cells, as it is the case in the Dorsal Cochlear Nucleus (DCN) (Apostolides and Trussel, 2013): in this cerebellum-like structure, fusiform cells (principal cells) make electrical synapses with stellate cells (interneurons), and the coupling coefficients are systematically higher in the fusiform -> stellate direction, because interneurons have higher input resistances than principal cells.

I - 2) Evidence for indirect coupling in paired recordings:

In this short section I merely wish to reveal one representative recording indicating an indirect coupling between two BCs patched simultaneously (Figure A-2).

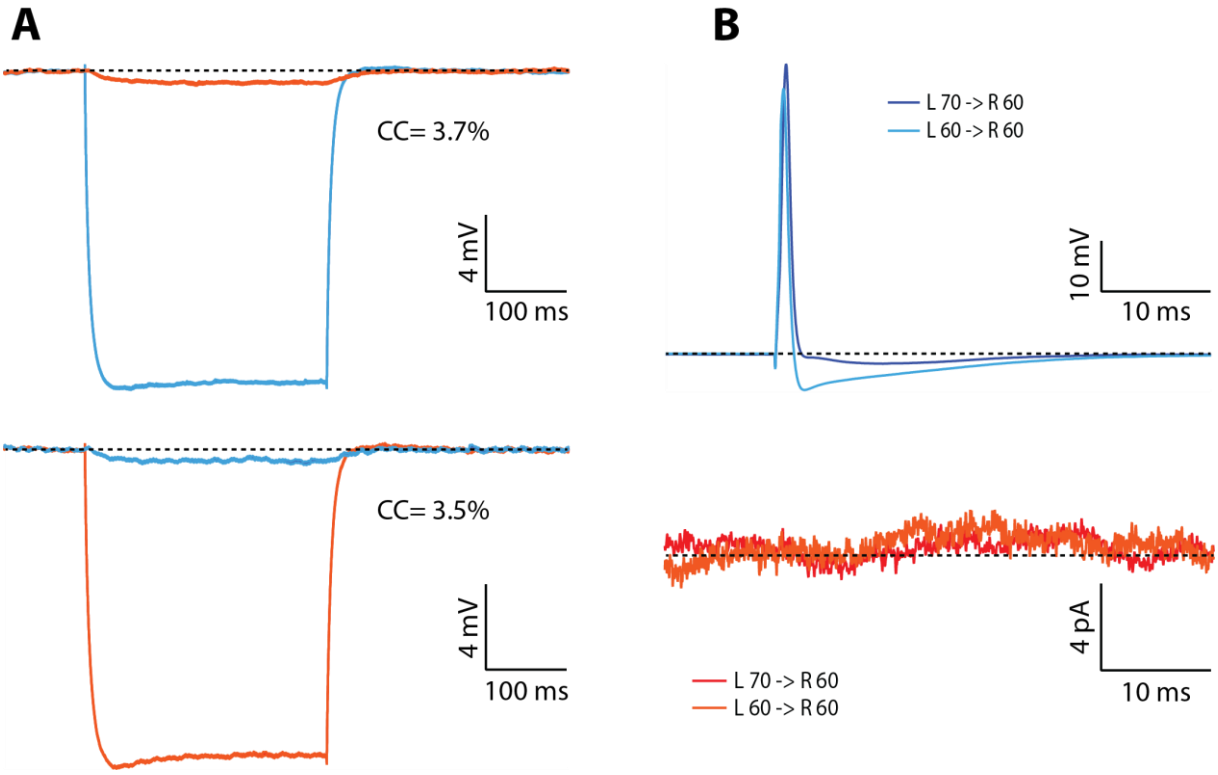

Figure A-2: Evidence for indirect coupling in paired recordings: A) Long current pulse injection in one cell (blue) causes a small but detectable hyperpolarization of the second cell (red). This behaviour is observed in the reversed direction; **B)** AP firing in cell blue doesn't cause a spikelet response, no matter the presynaptic AP waveform.

Here, long current pulse injection caused a significant hyperpolarisation of the non-injected cell, and this phenomenon was bidirectional (Figure A-2A), indicative of electrical coupling. However, AP firing from one cell to the other doesn't lead to a significant post-synaptic response, regardless of the shape of the pre-synaptic AP, suggesting that the coupling is not direct.

I - 3) Simultaneous recruitment of EPSP and spikelets narrows half-width of EPSPs:

In this section, I simply provide more results obtained when performing double-stimulation (ON-beam + OFF-beam, as in Chapter 3 - Figure 6). Here, we demonstrate that spikelets do narrow EPSPs' half-width when the two types of signals are coincident, as it would happen when EPSP and spikelet are recruited with a single stimulation pipette. The results shown here may be later incorporated in the manuscript as a supplementary figure, but for now, we have not found necessary to do so.

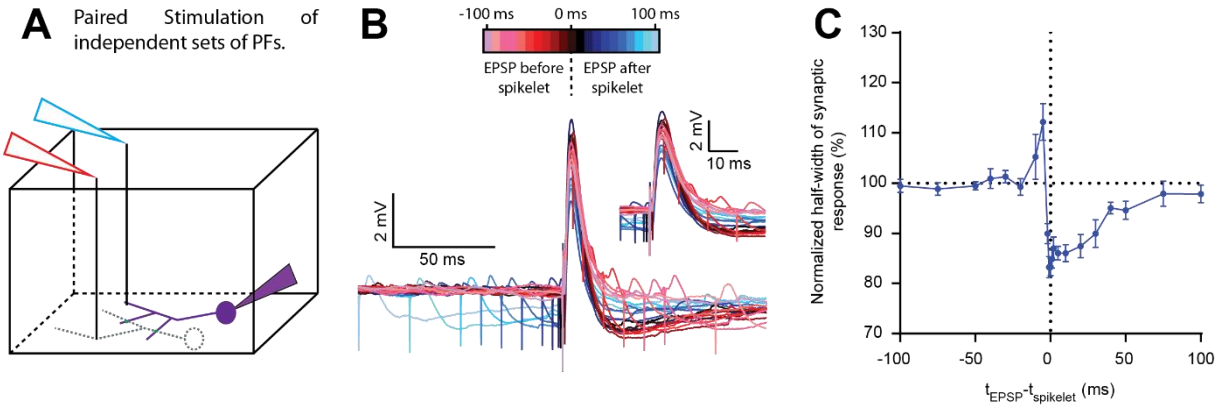

Figure A-2: Spikelet reduce the half-width of coincident EPSP: A) block diagram representing the experimental paradigm **B)** Compound synaptic responses (EPSP + spikelet), depending on the time delay between the two stimulations, aligned on EPSP onset **C)** Population averages of the half-width of synaptic responses versus time-delay.

These results show that when EPSP and spikelets are recruited simultaneously, the half-width of the compound synaptic response is minimal (83 ± 2%). Note that the increase in half width for short negative time delays (-10 to -5ms) are caused by the depolarizing peaks of the spikelets arriving during the falling phase of the EPSP.

I - 4) Impact of stimulation intensity of PFs on the temporal summation of EPSPs:

Here, I will briefly show the results I obtained when comparing recordings of 50Hz train of five PF stimulations, in minimal stimulation intensity and high stimulation intensity, for the same set of PFs. These data were recorded from n = 13 cells, and the statistical test employed to quantify the influence of the pulse and the stimulation intensity factors was a two-way repeated measure ANOVA, *with pairing for both factors*. Indeed, in a given train, the EPSP amplitudes are matched in time (because the same synapses are stimulated all throughout the train) and more importantly, each point in the train of minimal stimulation can be matched to the same point in the train of high stimulation. Figure A-3 shows a representative example, along with the corresponding statistical analysis at the population level. It can be seen that the stimulation regime has a significant impact on the temporal summation of EPSPs. These results therefore show that changing the stimulation intensity is ill-suited to examine the contribution of spikelets on temporal summation, because the experimental manipulation alone already impacts temporal summation.

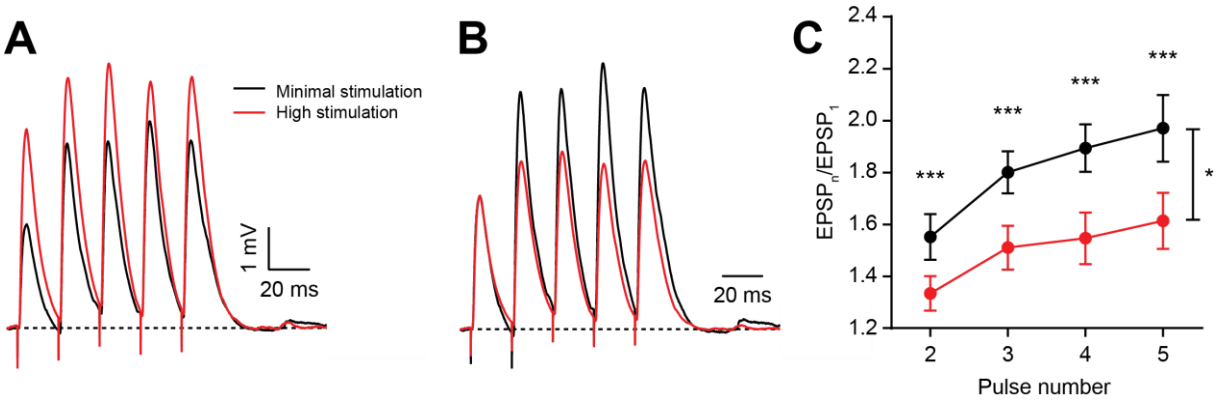

Figure A-3: Impact of stimulation intensity on temporal summation of PF-mediated EPSPs: A) 50 train stimulation of PFs, in minimal stimulation intensity (black) and high stimulation intensity (red) regimes. Both recordings come from the same stimulation site, in the same cell; **B)** Same as in A, but traces have been normalized to the peak amplitude of the first responses, to clearly reveal the differences in temporal summation; **C)** Population averages of EPSP peak amplitude throughout the train (two-way repeated measure ANOVA, with pairing information for both factors.

These results are consistent with a sublinear dendritic integration regime, because an increase in AMPAR conductance (caused by increasing the stimulation intensity) would lead to smaller and smaller EPSP amplitudes, *when normalized to the first peak amplitude* (Figure A-4).

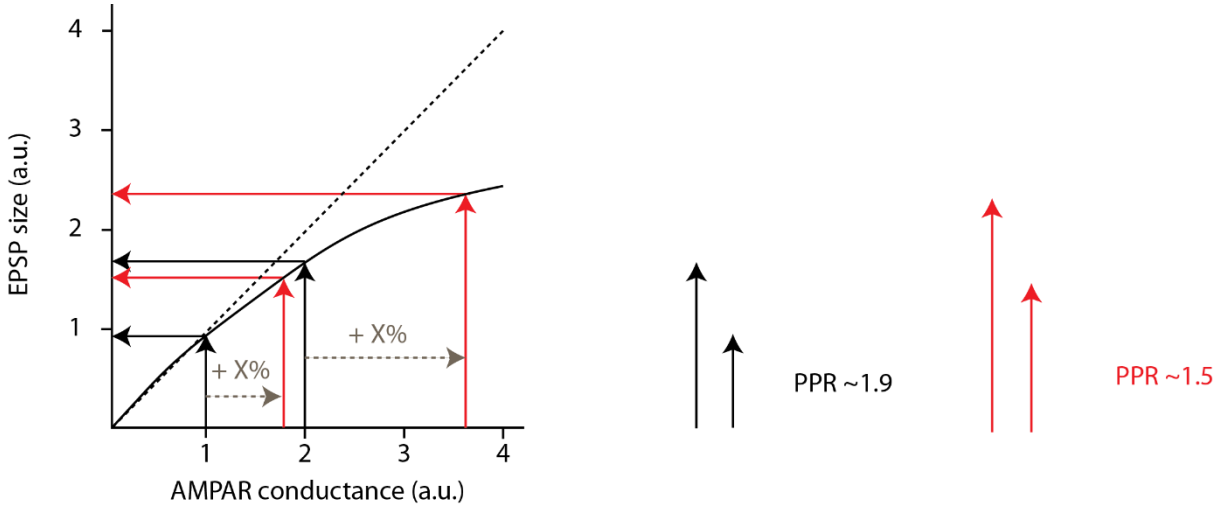

Figure A-4: Indirect indication of sublinear dendritic integration behaviour by increasing stimulation intensity of PFs: left) Sublinear I/O relationship predicts that increasing AMPAR conductance (X-axis), leads to sublinear EPSP amplitude (Y-axis). Schematic up-right arrows represent EPSP amplitude in minimal (black) or high (red) stimulation regime. For each color, the small arrow represents the peak amplitude of the 1st EPSP in a train, and the high one the fifth EPSP. When stimulation intensity is increased, both black arrows are moved by a similar percentage along the X-axis; **right)** In the end, the ratio of arrows' amplitudes indicates a PPR, and the black one is higher than the red one as a consequence of sublinearity.

If we assume a sublinear behaviour in dendritic integration because of local saturation, then the relationship between AMPAR conductance and the corresponding EPSPs falls below the linearity line. Consequently, if stimulation of PFs causes an average increase in AMPAR twice as large in the second pulse compared to the first one, the PPR will invariably be smaller than 2. Moreover, if more and more AMPAR are opened by increasing stimulation intensity, then the PPR will fall closer to 1, because the sublinearity is more pronounced.

I - 5) Testing the hypothesis that HCN channels can shape transmitted spikelets: inconclusive but insightful experiments:

In an initial set of experiment, I performed OFF-beam stimulation of PFs to force electrical neighbours to fire an AP, and examine the difference in spikelet waveforms before and after application of ZD-7288, a potent blocker of HCN channels. For reasons which will be explained in the next paragraph, and exemplified by the representative case shown in Figure A-5, I did not perform many experiments of this type, and later moved to another strategy to test my hypothesis.

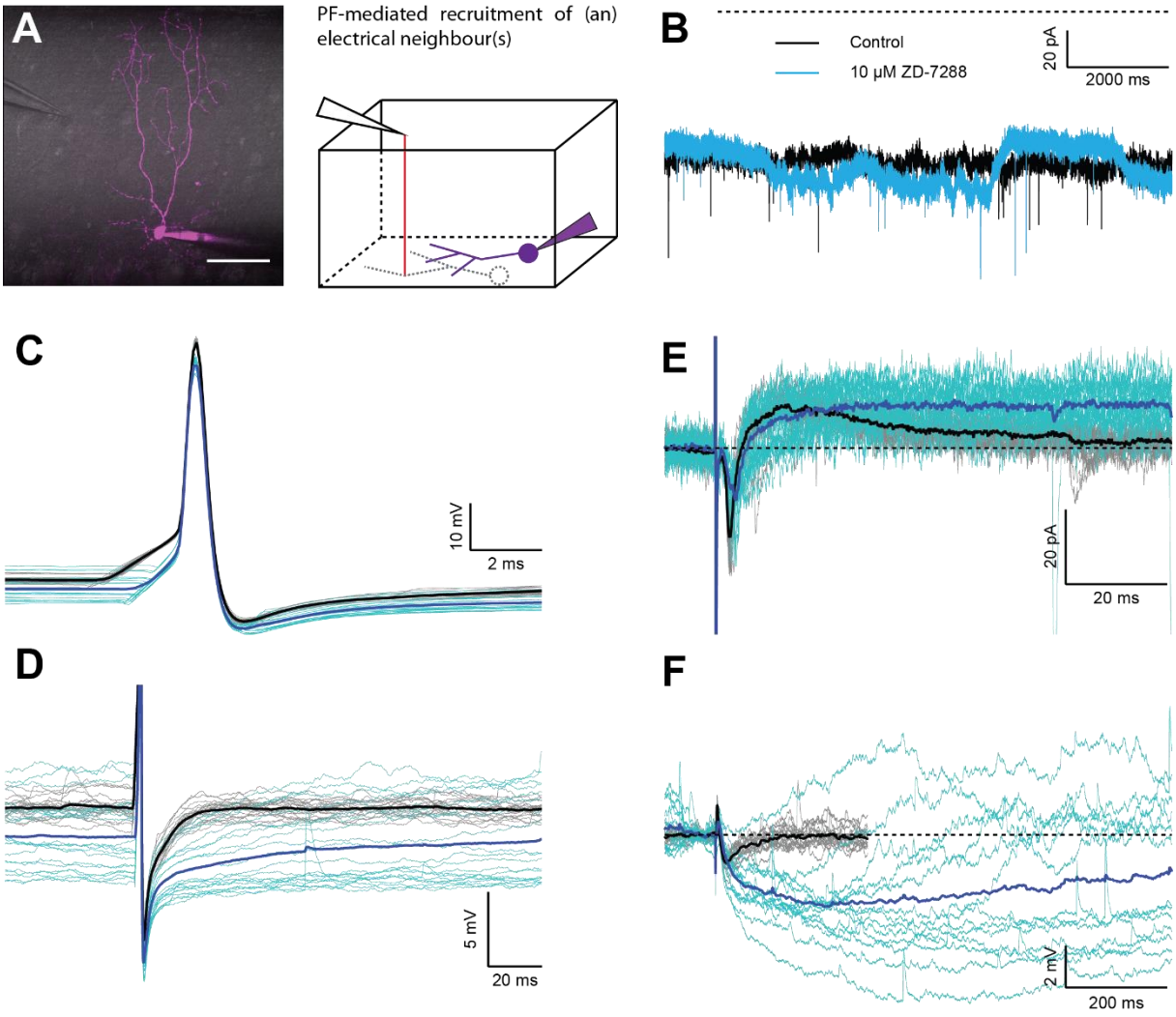

Figure A-5: Blockade of HCN channels causes large fluctuations of membrane potentials and holding currents: A) Representative experiment (left) and its corresponding diagram (right); **B)** 10s recording of spontaneous activity, before (black) and after (blue) application of 10 µM ZD-7288). Note the large fluctuations in holding current after ZD application; **C)** AP waveform of the patched cell, before and after application of ZD-7288; **D)** Same as in C, but for the steady-state resting membrane potential around the AP. Note here the larger range within which Vm fluctuates after drug application; **E)** Spikelets recorded in voltage-clamp in the patched cell, before and after application of ZD; **F)** Same as in E, but for spikelets recorded in current-clamp.

As it can be seen clearly in this example, application of ZD-7288 in the whole tissue causes erratic and large fluctuations of the holding current (in VC) or resting membrane potential (in CC). This is best revealed in panel B, where I show the holding current for 10s in the patched cell, between the two conditions. This first observation is very important to keep in mind, as it indicates that the resting state of the patched cell is highly "impaired" after application of the drug. This is further confirmed in subsequent protocols: when APs are fired in the patched cell, the resting membrane potential fluctuates within a range of at least 5mV after application of the drug (Panel B). As I have already shown, the resting membrane potential of the patched cell is critical in shaping the AP waveform (Chapter III, Figure 3). Therefore, it is unwise to make any claim about the specific effect of ZD on shaping AP waveform, because it already has a striking impact on the resting state of the cell. Furthermore, when I aimed to force electrical neighbours to spike, and record the corresponding spikelets in voltage-clamp (panel E) or current-clamp (panel F), I observed that the peak amplitude of the depolarizing current was reduced (in this experiment, at least), and that the hyperpolarizing component could become so long that the recording time of the protocol was not long enough to capture its full return to baseline. However, here again, one can note the high fluctuations in voltage trajectories of the spikelet responses, especially when they are recorded in current-clamp.

I did not perform many experiments of this type for the following reasons: 1) application of ZD causes strong fluctuations of the resting state of the patched cells. Consequently, further analysis of signal-to-noise ratio of any type of signal (AP or AHP peaks, inward or outward currents of spikelets, etc...) is highly impaired; 2) since I was interested in examining the role of HCN channels in shaping AP waveform *along with* the transmitted spikelet, I reasoned that this question was better answered in paired recordings configuration, where it is possible to examine AP waveform changes in a pre-synaptic cell, along with the corresponding changes of spikelet waveforms in the post-synaptic cell.

These preliminary experiments (for which only a representative case is shown) still provided some evidence for the role of HCN channels in BCs. First, it can be observed on panels C and D that, on average, the resting membrane potential of the patched cell is lower after application of ZD, for a similar injected current from the amplifier. This indicates that, at rest, HCN channels are open and reduce the input resistance of the cells, thus providing a depolarizing current. After their blockade, input resistance is higher, and the depolarizing current is gone, so it is not surprising to observe a decrease in the resting membrane potential of the cell. Secondly, it *appears* that my hypothesis was "correct" (or at the very least, it was supported by the observations I could draw so far): when electrical neighbours are forced to fire

an AP, they *seem* to deliver spikelets which have longer-lasting outward currents, indicating that the presynaptic AHP has indeed been made longer-lasting after blockade of HCN channels. Finally, if one applies this reasoning to the whole MLI circuit (remember that HCN blockade is applied to the whole slice), then the large fluctuations in holding current observed in panel B may be caused by spontaneously spiking MLIs forming electrical synapses with the patched cell, which would fire APs with strikingly long AHPs, requiring hundreds of milliseconds to return to baseline. It is indeed known that in vitro, MLIs are spontaneously active (Häusser and Clark, 1997), and throughout my PhD, I often encountered cases where whole-cell patch-clamp recordings of BCs displayed regular "spikelets".

I - 6) Testing the hypothesis that spikelets influence EPSPs' kinetics - inconclusive but insightful experiments:

In Chapter III, I showed that additional spikelet recruitment in high stimulation intensity regime of ON-beam stimulations narrows the half-width of EPSPs, while the sole increase in stimulation intensity doesn't display any significant effect (Chapter III, Figure 5). This experiment was the updated version of a prior protocol which I will briefly describe here, and which did not produce any conclusive results because of an unwanted off-side effect of the experimental manipulation I employed at the beginning. I still wish to present this original protocol, as it gave some insights as to the general method to be employed in testing spikelets' ability to change the kinetics of concomitant EPSPs.

At the beginning of my PhD, I had performed electrophysiological experiments aiming to see how the spikelet-mediated outward current was sensitive to the holding membrane potential of the patched cell. I systematically examined the outward current peak amplitude of PF-mediated synaptic responses (EPSC + spikelets), as the holding membrane potential was varied from -90mV to 0mV, in 10mV increments. These experiments were conducted with a Cs^+-based internal solution, as otherwise, depolarisation of the patched cells beyond -50mV would have caused deleterious effects due to the opening of K^+ channels (Figure IV-6).

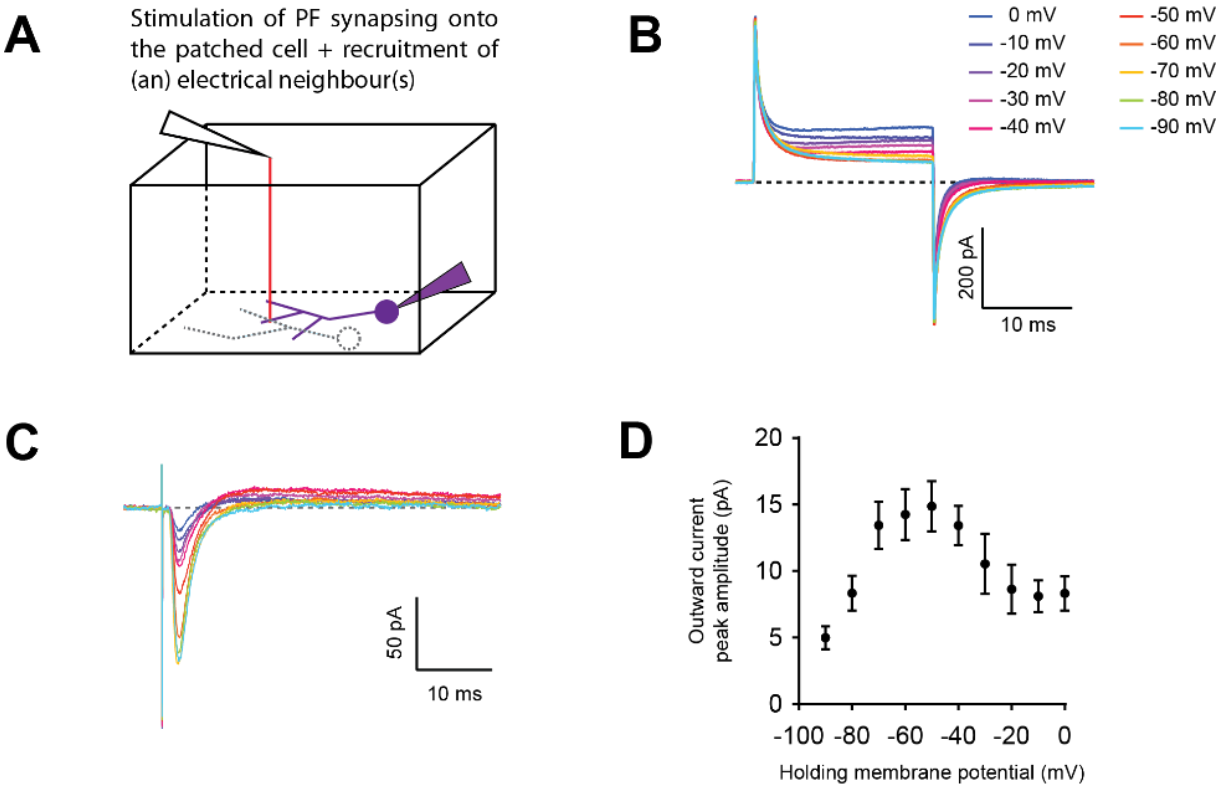

Figure IV-6: Voltage-dependence of the spikelet-mediated outward current: **A)** Schematic of the experimental configuration; **B)** Seal-test responses versus holding membrane potential of the patched cell; **C)** Compound synaptic responses versus holding membrane potential; **D)** Outward current peak amplitude versus holding membrane potential (n= 9 cells)

First of all, one can observe that the seal test responses reveal an expected decrease in input resistance of the cell, beyond -50mV (Figure IV-6B). This means that any spikelet current recorded in these conditions will display a lesser amplitude than in control conditions (-50mV and below), due to changes in coupling strength (Fortier and Bagna, 2006 - see Appendices for a discussion on how changes in input resistances of two electrically connected cells changes their coupling coefficients). I found that the peak amplitude of the spikelet-mediated outward current was maximal at -50mV holding membrane potential, and negligible (if detectable) at -90mV.

This result can be explained by two (non-exclusive) possibilities: when the patched cell is hyperpolarized, a bias current flows across the electrical synapse(s) and hyperpolarizes the electrical neighbour(s) delivering the spikelet(s), which can:

- decrease its/their likelihood to fire an AP because of "tonic hyperpolarisation";

- decrease the amplitude of the recorded outward current when (an) AP(s) is/are fired, because the AHP(s) in the presynaptic cell(s) is/are now smaller than in baseline conditions (Chapter III, Figure 3).

I therefore reasoned at that time that changing the holding membrane potential of the patched cell (between -70 and -90mV) was one way to test the hypothesis that spikelet can reduce the half-width of PF-induced EPSPs. I therefore performed experiments where BCs were patched with a K^+-based internal solution, and compared PF-mediated synaptic responses recorded at -70 and -90mV, between two groups: one where an outward current could be detected at -70mV, and one where no outward current could be detected at -70mV. Two representative examples (one from each group), along with population averages, are shown in Figure IV-7.

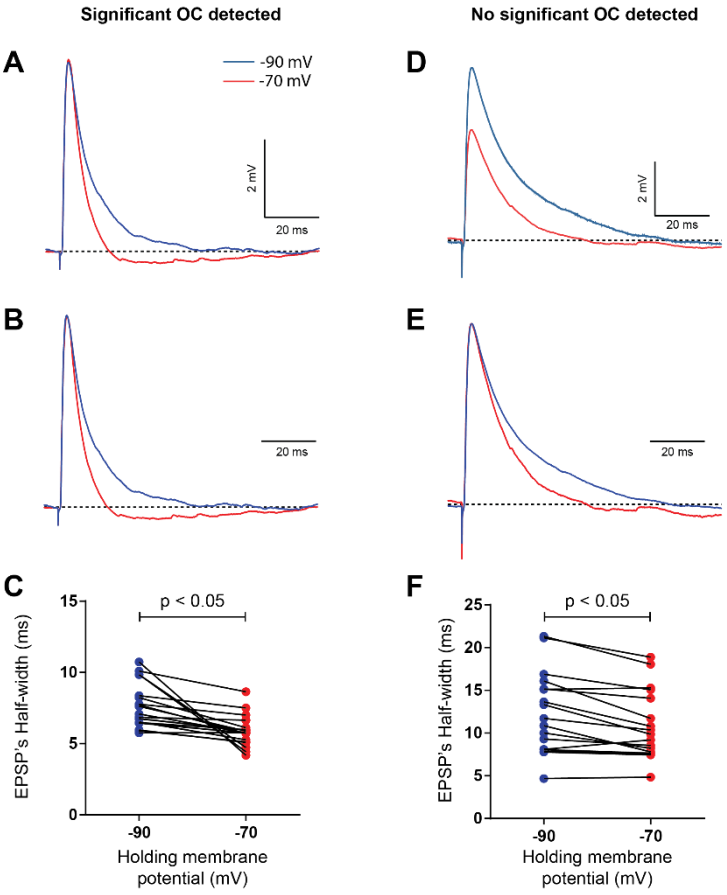

Figure IV-7: EPSPs half-width is increased by spikelet recruitment, but also by sole hyperpolarisation of the patched cell : A) Representative traces of one cell, where a significant hyperpolarisation is detected after the EPSP; **B)** Same as in A, but responses are normalized to the EPSP peak amplitude - the traces look very similar to A, because they originally had very comparable amplitudes; **C)** EPSP half-width is smaller at -70mV (n=20 cells, Wilcoxon matched-pairs); **D)** Same as in A, but when no significant hyperpolarisation is detected after the initial EPSP; **E)** Same as in D, but the traces are here again normalized to their peak amplitudes; **F)** EPSP half-width is also significantly reduced at -70mV (n = 17 cells, Wilcoxon matched-pairs), and this effect is readily detected even though no spikelet is recorded at -70mV.

It can be seen here that recruitment of spikelets at -70mV in the first group *correlates with* a signficant decrease in the half-width of the EPSPs (Figure IV-7C, -1.67± 0.41 ms; mean ± SEM, $p < 0.05$, Wilcoxon matched pairs). However, we cannot conclude that spikelet recruitment is responsible for this phenomenon, because the sole experimental manipulation of changing the holding membrane potential of the patched cell is sufficient to cause a significant decrease in the EPSP half-width (Figure IV-7F, -1.51 ± 0.37 ms; mean ± SEM, Wilcoxon matched pairs). Importantly, the latter change is detected thanks to pairing information of compairing the same synaptic responses, at two holding membrane potentials. If the statistical

test employed is only a Mann-Whitney test (*i.e.*, equivalent of the Wilcoxon matched-pairs, without the pairing information), then no significant effect is detected ($p = 0.32$). This particular point is emphasized here, and explains why in Chapter III, I performed experiments of changing the stimulation intensity to keep the pairing information. I was indeed affraid to miss a real a non-specific effect of changing the stimulation intensity on the half-width of EPSPs, and be potentially left with only a correlation and not a causal relationship between "additional spikelet recruitment" and "decrease in EPSP half-width".

To conclude here, it was important to observe that the significant effect observed in Figure IV-10-C was merely a correlation, and not a causality. Therefore, these results were inconclusive with regard to testing the hypothesis that spikelet recruitment has any effect on EPSP kinetics, let alone on temporal summation. However, they were important to set up the protocol presented in Chapter III on two key aspects: examining the influence of the experimental manipulation on the kinetics of the synaptic responses (1); and establishing a protocol where pairing information could be employed for statistical analysis (2).

Supplementary methods:

This section summarizes methodological procedures which I employed during this PhD. Some of the content presented here may be later incorporated in the supplementary methods section of our manuscript.

I - 1) Testing electrical and chemical connectivity:

When recordings are performed in presence of blockers of chemical synapses, any post-synaptic response following AP firing in a pre-synaptic cell can only be due to electrical synapses, and the recorded spikelet waveform will qualitatively match the waveform of the pre-synaptic "action current". It is then possible to correlate the peak amplitudes of these responses with coupling coefficients.

Alternatively, when the coupling coefficients are below a few percent, it is almost impossible to record a significant spikelet-mediated inward current in the post-synaptic cell. Therefore, any detectable post-synaptic response consequent to AP firing indicates the presence of a GABAergic synapse. Comparing post-synaptic responses at different holding membrane potentials of the post-synaptic cell (in order to change the electromotive force for Cl^- ions), or before and after application of gabazine, can provide further confirmation that the post-synaptic current is indeed due to a GABAergic synapse.

However, the most delicate cases to treat are of course the mixed presence of chemical and electrical synapses within the same pair, especially when electrical synapses are strong (*e.g.*, CC > 10%) and the chemical synapses are relatively weak. In this case, the post-synaptic response is a mixture of a spikelet and a GABAergic current. In order to disentangle the relative contribution of each input, and uncover a putative chemical synapse, one should ideally perform recordings were presynaptic APs do not display any AHP (*e.g.*, -80mV in my case), so that spikelet responses only cause an inward current, and no outward current. If the post-synaptic cell is held at -60 mV, then GABAergic inputs will display an outward current. Therefore, an electrical synapse can be reliably detected by the presence of a post-synaptic inward current, while a chemical synapse can be reliably detected based on the presence of an outward current. It is important to note that when applying the method proposed here, care must be taken in keeping a similar presynaptic AP waveform before comparing post-synaptic responses and infer the presence of a chemical synapse, if an electrical synapse is already detected (based on CC). Indeed, if the AHP of the presynaptic neuron decreases significantly (for example, before and

after application of gabazine) due to a non-specific effect (*e.g.*, slow drift of access resistance or holding currents during drug application), then a decrease in outward current peak amplitude will be observed in the post-synaptic cell. However, this change cannot be attributed to a blockade of a GABAergic synapse, but simply to a non-specific change in presynaptic AP waveform.

The protocol suggested above should be well-suited to estimate the presence or absence of either type of synaptic connections, but one potential drawback is that the relative weight of chemical input may be underestimated, due to pre-synaptic mechanisms influencing vesicular release (Christie et al., 2011; Jarsky et al., 2011). However, if the resting membrane potential of the MLIs is known, then a subsequent set of recordings can be performed to estimate parameters for chemical transmission: both the pre- and post-synaptic cells should be held at their resting membrane potential (*e.g.*, -60mV), and post-synaptic responses should be compared before and after application of gabazine, in order to subtract the spikelet component of the post-synaptic response.

I - 2) Retrieving the resting membrane potential of electrically connected cells:

I propose that the method shown in Figure 3 of Chapter III can be applied to retrieve the resting membrane potential of any type of neurons forming electrical synapses. For this method to provide the most accurate (*i.e.*, precise and unbiased) result, I propose that the relationship between post-synaptic state and spikelets waveform is first established (by performing paired recordings), in order to ensure that in subsequent experiments, the holding membrane potential of the cell receiving the spikelets (*i.e.*, the "probe") doesn't influence the waveform of the recorded signal. Indeed, without prior knowledge of a particular cell-type, one cannot tell if spikelets can recruit active conductances in the post-synaptic cells. Secondly, the "probe" should ideally be held close to the value towards which the estimate of the resting membrane potential of unperturbed neighbours converges, in order to minimize the bias current flowing across the electrical synapse. Thirdly, I hypothesize that additional knowledge about the location of the electrical synapse in the dendritic tree could be used to estimate the extent to which the fast depolarizing component and the slower hyperpolarizing component would be differentially filtered by the two electrically-connected cells. Owing to the low-pass filtering properties of the cellular membrane, I expect that for a given coupling coefficient (which only provides an information for steady-state currents to cross the synapse - like the filtered AHP), the variability of the fast depolarizing component will be higher than that of the slow

hyperpolarizing component. Fourthly, a "proper" range of coupling coefficients would be best to retrieve the resting membrane potential of unperturbed cells. Indeed, if the CC is too small, a negligible bias current is introduced to the unperturbed electrical neighbour, but the corresponding spikelet might be too small to be reliably detected. In line with this idea, I provided evidence that small CCs can be due to indirect couplings, as they correlate with an inability to observe a spikelet after AP firing in the presynaptic element. On the other hand, if the CC is too high, then a large bias current will be injected in the unpatched cell, and significantly alter its resting membrane potential. In first approximation, the "best spikelets" should ideally indicate a coupling coefficient lying between 5 and 10%, but this intuition may be further refined by considering how differences in input resistances between two connected cells differentially influences the ability of currents to cross them in either direction (Fortier and Bagna, 2006; Yihe and Timofeeva, 2016). Finally, when aiming to trigger APs in electrically connected cells by stimulating their presynaptic afferents, being able to distinguish if a spikelets-like response comes from one, two, or even more electrical neighbours would be ideal; and one should ensure that the recorded "spikelet-like" signals are not a mixture of "pure spikelets" and indirect EPSCs/IPSCs concomitantly experienced by the presynaptic electrical partner, by using appropriate blockers.